Survival lessons from stress assemblies

Angelica Aguilera Gomez

Utrecht, 2017

For happiness, how little suffices for happiness! ...
The least thing precisely, the gentlest thing, the lightest thing,
a lizard's rustling, a breath, a whisper, an eye glance,
little makes up the best happiness.

Nietzche

The research described in this thesis was performed at the Hubrecht Institute for Developmental Biology and Stem Cell Research, within the framework of the research school Cancer Stem cells and Developmental biology, which is part of the Utrecht Graduate School of Life Sciences (Utrecht University).

Cover: depicting stress assemblies. Design by the author and based on the drawing "Andreas Cellarius, The Harmonia Macrocosmica (frontispiece), 1680" for which a license was obtained via Alamy Limited under number OY15410655 to use this image for this thesis.

Printing: Ipskamp Printing, Enschede

ISBN: 978-94-028-0572-7

Survival lessons from stress assemblies

Overlevingslessen van stres assemblages
(met een samenvatting in het Nederlands)

Proefschrift

ter verkrijging van de graad van doctor aan de Universiteit Utrecht op gezag van de rector magnificus, prof.dr. G.J. van der Zwaan, ingevolge het besluit van het college voor promoties in het openbaar te verdedigen op donderdag 13 april 2017 des ochtends te 10.30 uur

door

Angelica Aguilera Gomez

geboren op 20 oktober 1980 te *Bogotá*, *Colombia*

Promotoren:

prof.dr. A. van Oudenaarden
prof.dr. C. Rabouille

Table of contents

Chapter 1

General Introduction

Introduction Part C

Angelica Aguilera-Gomez and Catherine Rabouille (2017)

Submitted to Dev. Biology

General Introduction

Part A: The early secretory pathway

I. The secretory pathway.

The secretory pathway is where proteins are synthesized, folded and delivered to their corresponding cellular space in a process known as protein secretion. This pathway is conformed by the rough endoplasmic reticulum (rough ER), ER exit sites (ERESs) the ER-to-Golgi intermediate compartment (ERGIC), the Golgi complex and post-Golgi carriers. The endoplasmic reticulum (ER) is an interconnected network of tubules and cisternae throughout the cytoplasm and represents the entry point into the secretory pathway (Voeltz et al., 2002). Protein synthesis takes place at the ER. After translation and translocation of secretory proteins into the ER lumen, rapid folding occurs and correctly folded proteins are transported towards the Golgi apparatus in a process known as anterograde transport. The anterograde transport of correctly folded secretory cargo is mediated by the production of COPII-coated vesicles that bud from the ER (Barlowe et al., 1994). COPII vesicles are delivered to the early Golgi via tethering and fusion machineries. In contrast, ER residents and other cycling transport machinery components are returned to the ER via COPI-coated vesicles. COPI vesicles undergo similar tethering and fusion reactions as COPII vesicles (**Figure 1**).

Importantly, organelle structure, function, and cell homeostasis are maintained by modulating protein transport through the secretory pathway. In the last decade, several studies have added greatly to the understanding of the complexity of this conserved and fundamental process.

II. ERES and COPII vesicle formation.

COPII vesicle formation takes place in specialized regions of the ERES, also known as transitional ER (tER) (Bannykh et al., 1996; Orci et al., 1991; Palade, 1975; Tang et al., 2005). The ERES is part of a larger structure known as the export complexes (Bannykh et al., 1996). These complexes are formed by one or more transitional ER elements facing towards a central cavity containing a number of vesicles and tubules (Balch et al., 1994; Schweizer et al., 1991). They are surrounded by rough ER (Bannykh and Balch, 1997; Palade, 1975), and in many eukaryotes they are functionally and physically linked to Golgi stacks. In this regard, ERES organization studies have clarified the mechanisms of Golgi biogenesis (Budnik and Stephens, 2009; Glick and Nakano, 2009). Therefore, there is a possibility of membrane connectivity between the ERES and Golgi (Ladinsky et al., 1999; Stinchcombe et al., 1995). ERES are ribosome-free, relatively stable and immobile

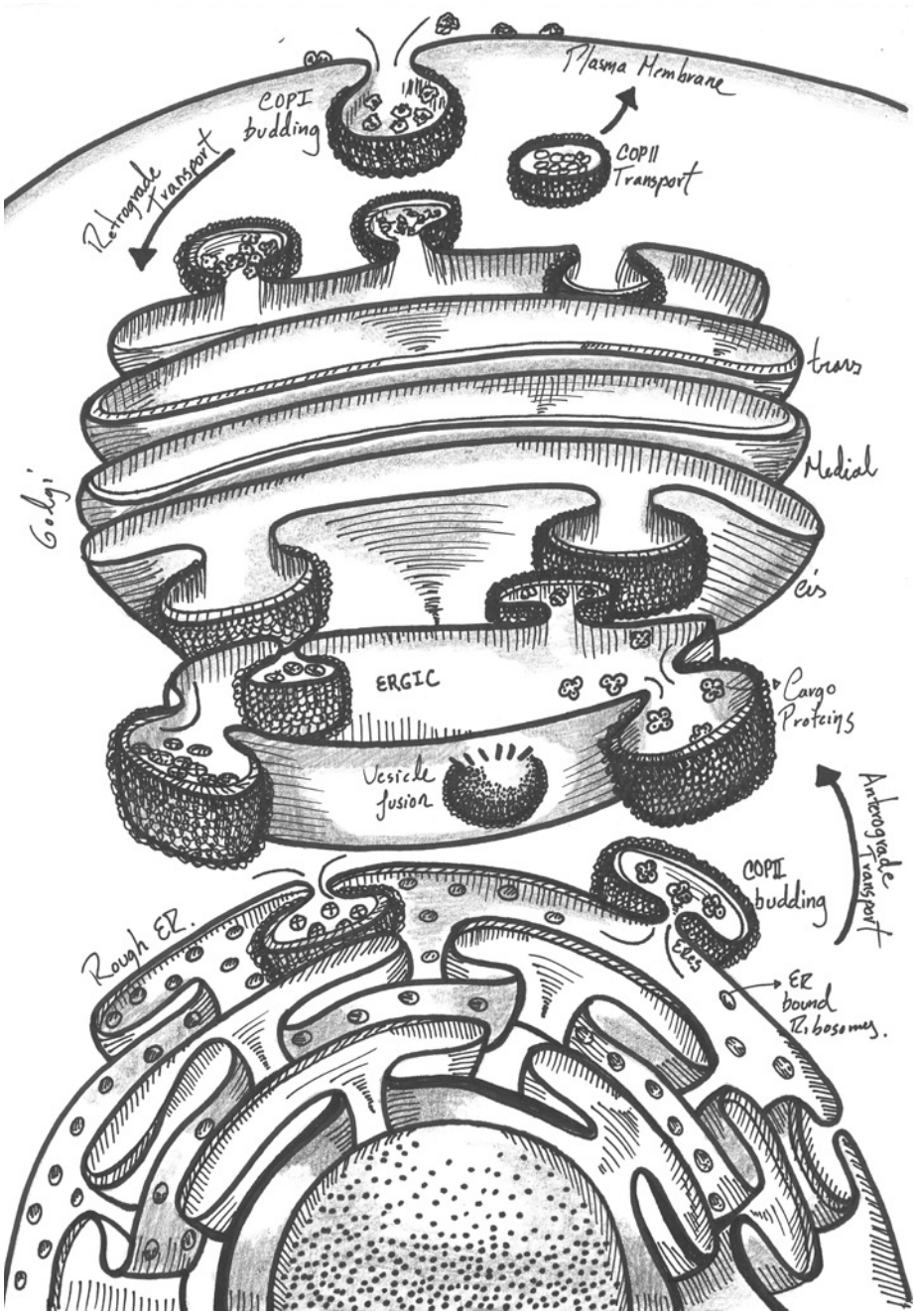

Figure 1. The Secretory pathway. Proteins are translated at the rough ER in ER-bound ribosomes. Cargo proteins leave the ER packed in COPII vesicles that are budding at the ER exit side (ERES). Cargo proteins pass through the ER-Golgi intermediated compartment (ERGIC) to reach the cis, medial and trans Golgi where they are further modified to be dispatched to their final destinations. COPI coated vesicles mediated retrograde transport of cycling proteins back to the ER.

structures as determined in studies using time-lapse imaging (Hammond and Glick, 2000; Stephens et al., 2000). Observed by light microscopy and immunoelectron microscopy the classical distribution of COPII-coated ERES is throughout the cell cytoplasm, clustering in the juxtanuclear area of cell types with a juxtanuclear Golgi (Bannykh et al., 1996; Hammond and Glick, 2000; Martinez-Menarguez et al., 1999; Orci et al., 1991; Stephens et al., 2000). The juxtanuclear ERES population accounts for 50-60% of ERES within the cell. The majority of ERES move only a short distance that often goes together with the movement of the underlying ER network itself, but also ERES can move using kinesin-1 and dynein-1 (Gupta et al., 2009).

The mechanism for transport vesicle formation is highly conserved in many clades of life ranging from yeast to humans (Barlowe and Miller, 2013). This process is initiated by Sec12 a guanine-nucleotide exchange factor (GEF) that activates the small GTPase Sar1 (Barlowe and Schekman, 1993; Weissman et al., 2001). The GDP/GTP exchange leads to the exposure of an N-terminal amphipathic helix of Sar1, with which it is inserted into the ER membrane (Bi et al., 2002; Bielli et al., 2005). This insertion causes membrane deformation that is required for membrane fission (Bielli et al., 2005; Lee et al., 2005). Through direct interaction with Sec23, Sar1 recruits the heterodimer Sec23/Sec24 (Yoshihisa et al., 1993), to form the pre-budding complex (Aridor et al., 1998; Tabata et al., 2009). Thus, this primary complex is conformed by the inner coat complex Sec23/Sec24 (Miller et al., 2002; Pagant et al., 2015). The majority of cargo is captured through interaction with Sec24, which exhibits multiple independent cargo binding sites (Miller et al., 2003; Mossessova et al., 2003). After the incorporation of cargo, the outer layer of the coat is recruited to the ER membrane. This outer layer is composed of the heterotetramer Sec13/Sec31, which consists of two Sec13 and two Sec31 subunits (Lederkremer et al., 2001). Binding of the outer coat enhances the activity of the GTPase-protein Sec23 that completes the coat assembly (Figure 2) (Matsuoka et al., 1998; Yoshihisa et al., 1993).

After budding, COPII vesicles are uncoated via accelerated Sar1 GTP hydrolysis (Oka and Nakano, 1994). The Sar1 GTP hydrolysis rate is accelerated in two steps, first by its interaction with Sec23 (Yoshihisa et al., 1993), and second through the binding of Sec13/Sec31, which increases Sec23 mediated GAP activity (Antonny et al., 2003). Inherent instability could present a problem with regard to stabilization of the COPII coat, but the constant presence of Sec12 provides a continuing supply of Sar1 GTP (Futai et al., 2004) and cargo coat interactions stabilize the pre-budding complex even in the presence of ongoing GTP hydrolysis by Sar1 (Sato and Nakano, 2005). In summary, Sar1, Sec23/Sec24, and Sec13/Sec31 are the minimal machinery required to reconstitute COPII-dependent budding *in vitro* (Matsuoka et al., 1998). However, GTP-dependent budding requires in addition also Sec12 (Futai

et al., 2004). *In vivo*, multiple other factors are likely to play key roles. For instance, COPII budding in mammalian cells is ATP-dependent and sensitive to protein kinase inhibitors (Aridor and Balch, 2000). Sec16 is another factor that is essential in COPII biogenesis and functions as a scaffold protein interacting in particular with coat proteins (Connerly et al., 2005; Whittle and Schwartz, 2010) **(Figure 2)**.

III. Sec16

Sec16 is a large protein that is essential for the transport of cargo from the ER to the Golgi *in vivo*. It is localized at the ERES where it is less abundant than the COPII coat proteins (Bhattacharyya and Glick, 2007; Connerly et al., 2005; Ivan et al., 2008; Watson et al., 2006). It has been shown using yeast-two-hybrid and biochemical assays that Sec16 interacts with the COPII coat proteins Sec23, Sec24, Sec31 (Espenshade et al., 1995; Gimeno et al., 1996; Shaywitz et al., 1997), Sec12 (Montegna et al., 2012), the Sec12 homologue, Sed4 (Gimeno et al., 1995), Sec13 (Hughes et al., 2009; Whittle and Schwartz, 2010) and Sar1 (Ivan et al., 2008; Nakano and Muramatsu, 1989; Supek et al., 2002; Yorimitsu and Sato, 2012). Because of these multiple interaction partners and their large size, Sec16 has been proposed to be an ERES scaffold protein that concentrates COPII components at the ERES for COPII vesicle formation (Hughes et al., 2009; Ivan et al., 2008; Shaywitz et al., 1997; Shindiapina and Barlowe, 2010).

Several models have been proposed for this scaffolding activity. In one of these models Sec16 establishes a link between COPII coat and accessory proteins. This model is supported by the results observed in *P. pastoris*, where Sec16 concentrates Sec12 at the ERES, and this also likely occurs in mammalian cells (Montegna et al., 2012; Soderholm et al., 2004). Additionally, Sec16 also binds the ER export factor TFG-1 (Witte et al., 2011). An alternative model for the scaffold function proposes that Sec16 organizes COPII assembly, as it has been demonstrated that the Sec16-P1092L mutation results in ERES fragmentation (Connerly et al., 2005). It also has been suggested that Sec16 binds to newly synthesized COPII vesicles and cross-links them to form the ERES (Connerly et al., 2005); or that Sec16 associates with the ER membrane upstream of Sar1 (Ivan et al., 2008; Watson et al., 2006). Furthermore, Sec16 has been proposed to be a template for assembling the COPII coat (Whittle and Schwartz, 2010).

In general, the notion that Sec16 somehow organizes COPII has become broadly accepted (Barlowe and Miller, 2013; Budnik and Stephens, 2009; Lord et al., 2013). However in the absence of Sec16 COPII vesicle budding can be reconstituted *in vitro* (Matsuoka et al., 1998). Furthermore, it has been demonstrated that Sec16 delays Sar1 GTP hydrolysis, resulting in a slower COPII turnover and stabilizing the COPII coat, suggesting that Sec16 serves rather as a regulator (Kung et al., 2012; Supek et al., 2002; Yorimitsu and Sato, 2012). In this regard, *in vivo* evidence in *P. pastoris* demonstrated this negative regulatory function for Sec16. Overall, these

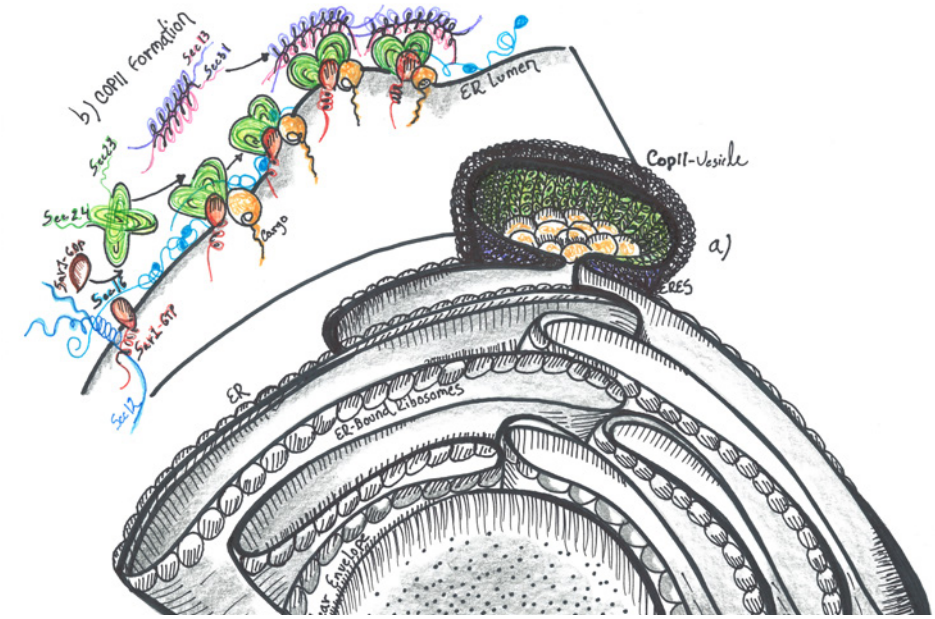

Figure 2. ER exit side (ERES) and COPII vesicle formation. a. Newly synthesized proteins that are not destined to be ER residents exit the ER in COPII coated vesicles at specialized ribosome free, cup shape ER domains (ERES). **b. COPII vesicles formation.** The transmembrane GEF, Sec12 mediates GTP loading of Sar1, which in the GTP-bound form inserts an amphipathic helix in the ER-membrane and initiates vesicle formation. The inner coat (Sec23/24) is assembled, leading to the binding of cargo proteins and recruiting the outer coat (Sec13/31). Coat polymerization mediates COPII coated budding. Sec16 interacts with all the COPII components and acts as an organizer.

findings could explain why Sec16 is not essential for COPII vesicle budding *in vitro* (Bharucha et al., 2013; Matsuoka et al., 1998; Supek et al., 2002). Taken together, Sec16 has been proposed to have two distinct functions; organizing COPII assembly at ERES and negatively regulating COPII turnover.

In humans two genes encode Sec16 orthologs; Sec16A and Sec16B. Sec16A can be seen as the primary ortholog as it is the most similar to Sec16 present in other species, and its localization to the ERES is dictated by a short, and rather poorly conserved region upstream of the central conserved domain (CCD), named ERES localization domain (ELD) (Ivan et al., 2008; Sprangers and Rabouille, 2015). The CCD shows quite a high level of conservation between species (Bhattacharyya and Glick, 2007). In contrast, in *Drosophila* Sec16 both the ELD, as well as the CCD are necessary for correct ERES localization (Ivan et al., 2008). Another Sec16 domain is the C-terminal conserved domain (CTCD), most Sec16 homologs have this domain with exception of human Sec16B (Bhattacharyya and Glick, 2007; Sprangers and Rabouille, 2015).

Part B: The cellular stress response

Living organisms have a very complex biochemistry and metabolism. Therefore in order to survive life challenges, each biological process needs to be tightly organized in time and space. This organization is normally achieved via compartmentalization. The general consensus is that compartmentalization is exclusively mediated by membrane-bound organelles. However, during the last decade a novel concept of cellular architecture and organization has emerged with the recognition of high-order membrane-less macromolecular structures. Although these membrane-less structures exist in basal conditions, most of them are the result of stress.

I. Different types of stress.

Oxidative stress

One of the major types of stress is oxidative stress, which is the result of a perturbation in the equilibrium between the antioxidant systems and Reactive oxygen species (ROS). ROS are unavoidable products of aerobic metabolism and they activate signaling pathways such as cell proliferation, growth, differentiation and eventually cell death (Orom et al., 2008). Calcium and ROS signaling mutually interplay: calcium can increase ROS production, and ROS can significantly affect intracellular calcium levels (Gorlach et al., 2015). In addition to physiological ROS production/levels, several pathological conditions display a major increase in ROS such as ischemia (Kalogeris et al., 2014), exposure to UV (Rinnerthaler et al., 2015) diabetes and aging (Butterfield et al., 2014; Magenta et al., 2014). In addition, ROS can decrease cytosolic pH via inhibition of Na+/H+ exchange (Kaufman et al., 1993).

ER stress

Another well-studied response to stress is the ER stress response, which is induced by accumulation of unfolded proteins at the ER. This stress is a classical feature of secretory cells because the ER is very large and challenged to cope with the secretory load. ER stress it is observed in many human diseases including cancer, obesity and neurodegeneration (Hetz et al., 2011). ER stress is triggered by many conditions, such as altered protein maturation leading to accumulation of misfolded proteins in the ER lumen, modification of chaperone function, expression of disease related mutant proteins, decrease in the ER calcium content, and redox alterations (Balch et al., 2008; Schroder and Kaufman, 2005).

The adaptive response to ER stress is the unfolded protein response (UPR). The UPR is initiated by three ER transmembrane proteins; Inositol Requiring 1 (IRE1), PKR-like ER kinase (PERK), and Activating Transcription Factor 6 (ATF6). In steady conditions, the ER chaperone, immunoglobin binding protein (BiP) binds to the luminal domains of these three master regulators keeping them inactive. Upon

ER stress, BiP dissociates from them, allowing their activation (Oslowski and Urano, 2011). Thus, BiP assists the folding of misfolded proteins and also helps the COPII subunits to increase the ER exit potential and decrease the ER cargo load (Richter et al., 2010).

IRE1, is an ER transmembrane kinase, that upon ER stress dimerizes and autophosphorylates to become active. Activated IRE1α splices X-box binding protein 1 (XBP1) mRNA (Calfon et al., 2002; Yoshida et al., 2003), which encodes a basic leucine zipper (bZIP) transcription factor that upregulates UPR target genes. PERK is also a trans-membrane kinase, that oligomerizes and autophosphorylates to become active. Once it is active, it phosphorylates Ser51 on the α subunit of eukaryotic initiation factor 2 (eIF2α) (Harding et al., 1999). Phosphorylated eIF2α prevents formation of ribosomal initiation complexes leading to mRNA translational attenuation. The third regulator of ER stress signaling is the type II ER transmembrane transcription factor, ATF6 (Yoshida et al., 1998). Upon ER stress, ATF6α translocates to the Golgi where it is cleaved by site 1 and site 2 proteases, generating an activated bZIP-factor (Rawson, 2003). Cleaved ATF6α moves into the nucleus to activate UPR genes involved in protein folding, processing, and degradation (Yoshida et al., 2000).

DNA damage response

Nuclear DNA is also affected by stresses such as genotoxic stress and radiation. The DNA damage response (DDR) refers to the intracellular pathways that sense and resolve damaged DNA. This stress can be a major cause of genomic instability, in particular when cell death pathways have been deactivated (Halazonetis et al., 2008). It has been proposed that when a DNA lesion occurs, it is accompanied by relaxation of chromatin through a series of post-translational histone modifications that include ADP-Ribosylation, phosphorylation and acetylation (Lukas et al., 2011). These modifications "freeze" transcription and replication around the DNA lesion site to facilitate repair (Marechal and Zou, 2013). ATM and ATR kinases bind to damaged DNA and trigger the recruitment of several proteins, many of which are phosphorylated and activated to further orchestrate DNA replication, cell cycle control, transcription repair damage and/or survival. Such as tumor suppressor p53, which regulates cell survival versus death (Kim et al., 1999), the BASC complex containing DNA damage repair proteins (Wang et al., 2000), FOXO3 (Tran et al., 2002), and the senescence regulator ARF (Velimezi et al., 2013).

Small RNAs also respond to DNA damage, such as LincRNA-p21 that represses apoptosis (Huarte et al., 2010), Pint and TUG1 that facilitate the epigenetic silencing of cell-cycle factors by inhibiting cell proliferation until genomic integrity has been restored (Khalil et al., 2009; Marin-Bejar et al., 2013). Accumulating evidence suggests that autophagy can be activated by DNA damage (Eapen and Haber, 2013; Orlotti et al., 2012; Robert et al., 2011). In this regard, in response to genotoxic and oxidative stress, ATM is linked to DDR and the induction of autophagy by activating

AMPK, which in turn phosphorylates TSC2 and removes the inhibitory effect of the target of Rapamycin Complex 1 (TORC1), inducing autophagy (Alexander et al., 2010; Tripathi et al., 2013). Interestingly, PARP1, a NAD+ dependent chromatin associated poly-ADP ribose enzyme, is another DDR protein involved in autophagy regulation (de Murcia et al., 1997). Thus, DNA damage induced PARP1 activation is associated with a reduction in the NAD+ and ATP pool, resulting in an elevated level of AMP that is sensed by AMPK, leading to its activation and autophagy induction (Rodriguez-Vargas et al., 2012). In addition, ATM forms a nuclear complex with PARP1 and NEMO that leads to its nuclear export (Mabb et al., 2006; Wu et al., 2006).

Nutrient stress

It has been demonstrated from yeast to humans that TORC1 regulates the sensing of nutrient stress and cell metabolism (Laplante and Sabatini, 2012; Loewith and Hall, 2011). In the presence of enough nutrients, TORC1 is actively stimulating protein synthesis and cell growth through phosphorylation of downstream effectors such as protein kinase S6 beta 1 (S6K) and eukaryotic initiation factor (4E-BP), while simultaneously inhibiting catabolic metabolism and autophagy (Hay and Sonenberg, 2004; Wullschleger et al., 2006). Conversely, upon nutrient deprivation, TORC1 is inactivated, resulting in cell growth inhibition and activation of catabolic metabolism (He and Klionsky, 2009; Jung et al., 2010). Its activity can contribute to numerous pathologies, including cancer, diabetes and neurodegenerative disorders such as Parkinson's (Johnson et al., 2013; Laplante and Sabatini, 2012). Therefore, TORC1 modulation allows the cells to adjust their metabolic state in response to intra- and extra-cellular nutrient changes.

Autophagy is the conserved pathway that helps the cell cope with nutrient starvation. The house keeping function of autophagy is essential for maintaining cellular homeostasis and cell survival during nutrient stress (Chen et al., 2014). This pathway starts with the engulfment of parts of the cytoplasm, either randomly or in a targeted fashion by a double membrane organelle called the phagophore that matures and fuses with the lysosome for degradation so that the components can be recycled (Codogno et al., 2011).

Autophagy is under the control of TORC1. Amino-acid starvation induces a robust autophagy response, comparable with the response that is induced by pharmacological mTORC1 inhibition (Wong et al., 2015). Starvation is known to activate AMP-activated protein kinase (AMPK) signaling (Ghislat et al., 2012) by decreasing the activity of mTORC1 components such as Rag-GTPases (Meijer and Codogno, 2008).

Interestingly, COPII vesicle budding mutants and other mutants that affect ER-Golgi traffic can disrupt autophagy (Hamasaki et al., 2003). Multiple COPII coat subunits, such as Sec23 and Sec24, are phosphorylated by Hrr25 (Bhandari et al., 2013; Lord et al., 2011). This is a kinase required for ER-Golgi traffic and autophagy

(Lord et al., 2011; Wang et al., 2015). Furthermore, the phosphorylation of the distal surface of Sec24 promotes its interaction with the c-terminus of Atg9, which is required for autophagy (Davis et al., 2016). This suggests that COPII function and by extension protein transport out of the ER through this machinery is necessary for the initiation of autophagy.

II. Pathways in Cellular Stress response.

Life is constantly challenged by adverse environmental stimuli, such as oxidation, low oxygen availability, extreme temperatures, acidosis, chemical exposures, aging and nutrient deprivation. Each of these stresses trigger a decision making process in cells; they can either attempt to survive until the stress is resolved, or die to prevent further damage to the whole organism. Over the last decade apoptosis, or programmed cell death, has been considered a major cellular stress response. Recently, accumulating evidence has demonstrated that in response to stress cells have many adaptive responses that allow them to survive and probably evolve.

The main goal of an adaptive stress response is to conserve energy and divert cellular resources towards survival and eventual recovery. Therefore, cells exposed to environmental stress prefer to change from a growth to a quiescent/slowdown state rather than undergo apoptosis (Cmielova et al., 2012). Importantly, under appropriated conditions quiescent/slowdown cells are capable to recover and re-enter cell cycle.

The HSP

In order to survive acute stress, heat shock proteins (HSPs) are essential for all organisms. They were first identified as key chaperones helping to refold proteins that have been damaged during heat shock. They now are the best-known inducible transcriptional regulators of genes encoding molecular chaperones and other stress proteins. Some members of this family are also important for development and lifespan. Thus, expanding their functions beyond heat shock genes, and uncovered complex layers of heat HSPs post-translational regulation (Akerfelt et al., 2007). Elements that are present upstream of the Heat Shock Factor (HSF) genes regulate the heat shock response at the transcriptional level (Pelham, 1982). The mammalian HSF family consists of four members: HSF1, HSF2, HSF3 and HSF4. Each of them possesses distinct and overlapping functions, they are tissue-specific, have multiple post-translational modifications, and interacting protein partners (Akerfelt et al., 2007; Fujimoto et al., 2010).

Upregulation of HSPs is a hallmark of stressed cells and organisms. Their main function in this regard is as molecular chaperones to maintain protein homeostasis, also called proteostasis (Powers et al., 2009). The transcriptional activation of HSPs is mediated by HSFs, of which HSF1 is the master regulator in vertebrates as it maintains cellular integrity during stress and development of thermo tolerance

(McMillan et al., 1998; Zhang et al., 2002b). HSF1 is constitutively expressed in most tissues and cell types (Fiorenza et al., 1995), where it is kept inactive in the absence of stress stimuli. HSF1 is regulated through multiple post-translational modifications, protein–protein interactions and subcellular localization. HSF1 also has an intrinsic stress-sensing capacity, as it can be converted from a monomer to a homotrimer *in vitro* in response to thermal or oxidative stress, this is observed in both *D. melanogaster* and mammals (Goodson and Sarge, 1995; Zhong et al., 1998).

eIF2α phosphorylation

However, stress does not necessarily lead to protein misfolding. In fact, one of the mean features to stress responses is to slow down energy consuming processes and one of the most consuming is ribosome biogenesis and protein translation. To inhibit/stall protein synthesis, the initiation factor eIF2a is phosphorylated by kinases such as BiP.

The stress response that is the most studied so far, is that under diverse stress conditions, the α subunit of eukaryotic translation factor 2 (eIF2α) is phosphorylated (Wek et al., 2006). eIF2α phosphorylation, causes attenuation of the translation initiation of most mRNAs and induces the transcription of downstream transcription factors. This activation induces signaling programs that allow cells to adapt to the various stress conditions. Overall this is referred to as the Integrated Stress Response (ISR) (Harding et al., 2003; Ron, 2002). ISR plays physiological roles in the regulation of intermediary metabolism (Baird and Wek, 2012; Oyadomari et al., 2008), tumorigenesis (Dey et al., 2015) and immunity (Munn et al., 2005).

Some of the eIF2α kinases that have been identified in vertebrates are for example, heme-regulated inhibitor (HRI/EIF2AK1) that is activated during heme deficiency (Chen and London, 1995; Chen et al., 1991), protein kinase R (PKR/EIF2AK2) that is activated during viral infection by the binding of double stranded RNA (Levin et al., 1980; Meurs et al., 1990). Further; PKR-like endoplasmic reticulum (ER) kinase (PERK/EIF2AK3) that is activated during ER stress by the release of binding immunoglobulin protein from its ER luminal domains (Bertolotti et al., 2000; Harding et al., 1999). Last, the general control non-depressible 2 (GCN2/EIF2AK4) that is activated under amino acid deprivation by the binding of uncharged tRNA to the regulatory domains (Dever et al., 1992; Zhang et al., 2002a).

III. Membrane-less assemblies.

Eukaryotic cells have evolved strategies to overcome almost every type of cellular stress. Recently, it has become more and more evident that cells have developed specific and sophisticated mechanisms to preserve their homeostasis and have a survival chance upon detrimental conditions. In this regard, during the last decade membrane-less assemblies induced by stress conditions have emerged as key players for the adaptive stress response.

It is easy to understand how membrane bound compartments can coexist inside the cell, but in the case of non-membrane bound compartments it becomes more complicated. Membrane-less assemblies can be formed by condensation of protein and nucleic acid components into liquid phases that aggregate from the bulk aqueous phase of the cell (Mitrea and Kriwacki, 2016). The lack of membrane and liquid-like composition of stress assemblies allows them to remain inside the cell in a dynamic equilibrium with their surrounding and rapidly rearrange in response to intra and extra cellular clues (Wang et al., 2014; Wippich et al., 2013). Current data demonstrate that membrane-less assemblies are many; they come in different size, and morphologies and have different, specific functions (such as, response to various stresses or cell cycle). Below a few examples of the most studied non-membrane bound, liquid-like assemblies that exist in basal conditions and those generated by stress are introduced.

III. 1 Assemblies that exist at steady state.

Germline P granules:
One of the first identified examples of a liquid-like assembly was the P granule from *Caenorhabditis elegans* (Strome and Wood, 1983; Wolf et al., 1983). P granules are assembled from RNA and RNA-binding proteins that mediate germ cell specification. Their main function is the storage of maternal mRNAs from early development (Barbarese et al., 2013). These P granules are observed to fuse and rapidly exchange components with the cytoplasm and their size is spatiotemporally controlled (Brangwynne et al., 2009). Furthermore, the polarity proteins MEX-5 and PAR-1 are implicated in the degradation of P granule components and P granule stability respectively. Thus, MEX-5 levels correlate with P granule dissolution and PAR-1 with their condensation (Cheeks et al., 2004; Spike and Strome, 2003).

P bodies.
P bodies are cytoplasmic domains that contain proteins involved in diverse posttranscriptional processes, such as translational repression, RNA mediated gene silencing, nonsense mediated mRNA decay and mRNA degradation (Eulalio et al., 2007). Stress induced mRNA stabilization involves the inactivation of mRNA decay pathways (Decker and Parker, 2002), such as the 3'-5' exosome dependent pathway (Chen et al., 2001; Mukherjee et al., 2002) and the DCP1-DCP2 complex (Jacobson, 2004; Long and McNally, 2003). Yeast genetic studies have revealed that mRNA decay intermediates accumulate at P bodies when the decay is blocked, suggesting that P bodies are sites of decapping and 5'-3' degradation (Sheth and Parker, 2003). In line with this, studies in mammalian cells have revealed similar structures that contain DCP1/2, XRN1, GW182, and Lsm1-7 heptamers (Eystathioy et al., 2003; Yang et al., 2004).

Interestingly, metabolic inhibitors that promote or inhibit stress granule

formation such as Puromycin or emetine have similar effects on the assembly of yeast and mammalian P bodies. This indicates that both stress granules and P bodies are sites at which mRNA accumulates after polysome disassembly (Kedersha et al., 2005). In this regard, stress granules and P bodies can harbor the same species of mRNA and physically associate *in vivo*, an interaction that is promoted by TTP and BRF. Furthermore, it has been proposed that mRNA released from disassembled polysomes is sorted and remodeled at stress granules, and that from there selected transcripts are delivered to P bodies for degradation (Kedersha et al., 2005).

Nuclear Granules.

The dynamic spatial organization of the nucleus plays a primary role in genome function and maintenance (Misteli, 2007; Rajapakse and Groudine, 2011). The nucleus is densely crowded, and possesses a three-dimensional architecture. Therefore it is crucial to establish efficient transport and reaction rates, that co-regulate genes and enhancer elements (Branco and Pombo, 2006; Nicodemi and Pombo, 2014). In this regard, the nucleus contains a large amount of non-membrane bound bodies that play an important role by organizing the spatially patterning of concentrations of molecules at the nucleoplasma (Zhu and Brangwynne, 2015). Thus, nuclear bodies locally increase the concentration of molecules involved in chromatin remodeling, transcription initiation and RNA processing (Matsuda et al., 2014).

These nuclear granules could also play a role as biological switches responding to local signals, as they are frequently associated with specific active gene loci (Zhu and Brangwynne, 2015). Examples of nuclear bodies include Cajal bodies, speckles, Histone Locus Bodies, PML bodies and nucleoli (Dundr and Misteli, 2010). These structures can remain stable over time scales of minutes to hours, and their components are in constant state of dynamic flux with the surrounding nucleoplasm (Phair and Misteli, 2000).

III. 2: Stress assemblies.

Stress Granules

Stress granules are the best-studied stress assemblies that form in response to many different stresses. One of the key elements in their formation is the accumulation of untranslated messenger ribonucleoproteins (mRNPs) that form from mRNAs stalled in translation inhibition. The best evidence demonstrating that stress granules are the result/consequence of translation inhibition is that stress granules fail to form when mRNAs are trapped in polysomes (Jevtov et al., 2015). This suggests that mRNAs associated with full ribosomes are unable to enter stress granules (Buchan and Parker, 2009).

Stress granules are known to contain translation initiation factors and specific mRNAs that are stalled in steps of translation initiation and RNA binding proteins that specifically bind RNAs that are not covered by ribosomes presumably because

they expose binding motifs (Damgaard and Lykke-Andersen, 2011). Some stress granule components do not bind RNAs, such as post-translational modification enzymes, metabolic enzymes, proteins (with some exceptions bind RNA) and may be recruited through protein-protein interactions (Jain et al., 2016). Stress granules can also contain key components of signaling pathways (Buchan, 2014) and they are shown to sequester pro-apoptotic components thus leading to an inhibition of apoptosis during stress. They also recruit TORC1 (Wippich et al., 2013).

Stress granule assembly can be influenced by protein methylation, phosphorylation and glycosylation, probably because these processes have the capability of altering protein-protein interactions (Tourriere et al., 2003). Importantly, several experimental data suggest that stress granule composition can vary and that this variation depends on the different stress conditions, revealing that they are variable and complex (Buchan and Parker, 2009).

However, the functionality of stress granules and how their conformation affects the regulation of mRNA function or other aspects of cell physiology remains to be established (Protter and Parker, 2016). For instance many virus infections employ mechanisms to block stress granule assembly, such as proteolytic cleavage of G3BP, mainly because stress granules have the capacity to recruit numerous antiviral proteins and stimulate their activation, enhancing the induction of the innate immune response and viral resistance. (Onomoto et al., 2012; Reineke and Lloyd, 2015).

Another way stress granules affect biological functions is by limiting the interactions of sequestered components. For instance it has been proposed that they can modulate signaling pathways by sequestering pro-apoptotic components of TOR, RACK1 or TRAF2 (Arimoto et al., 2008; Thedieck et al., 2013). Overall, stress granules have been shown to sequester numerous factors involved in RNA physiology and metabolism, and therefore they most likely have broad effects on the physiology of cells.

Proteasome storage granules

Protein degradation in the cell is tightly regulated; the main protein degradation system is the 26S proteasome (Peters et al., 2013). The proteasome is primarily composed out of regulatory and core particles with protease activity. Ubiquitination is the modification that targets proteins that are misfolded or damaged for proteasomal degradation (Hershko and Ciechanover, 1998). Proteasomes are generally abundant and massive complexes, which are very costly for cells to assemble (Russell et al., 1999). Therefore, during cellular stresses such as quiescence or glucose starvation, cells use proteasome storage granules (PSGs) in order to preserve this degradation system (Laporte et al., 2008). For instance in yeast, PSGs are a proteasome protective mechanism from autophagy degradation. The cellular use of PSGs saves a lot of cellular energy, as it avoids a *de novo* rebuilding of active proteasome subunits. This makes the entrance of the cell into a proliferative state quicker and more efficient.

Metabolic granules

Protein assemblies can also have functional roles. Yeast subjected to external fluctuations, such as the response of budding yeast to starvation, leads to the formation of higher-order protein assemblies. During starvation an immediate slowdown of the yeast metabolism makes it very difficult to maintain ATP levels. Consequently, starved yeast undergoes extreme fluctuations in ion concentration, osmotic conditions and pH levels. These fluctuations cause changes in the solubility and macromolecules interactions, leading to the formation of stress adaptive assemblies. In line with this, when yeast cells are depleted of energy, several proteins form structures (Munder et al., 2016; Narayanaswamy et al., 2009; Petrovska et al., 2014). These structures can be polymers or crystals (Noree et al., 2010). Other assemblies can be more irregular and heterogeneous, and they seem to be like gels or glasses (Munder et al., 2016; Narayanaswamy et al., 2009). Recent studies show that the cytoplasm of an energy starved cell transitions from a fluid to a solid-like state (Munder et al., 2016). However, there is some debate as to whether these higher-order structures are functional, even though they reverse very quickly. Furthermore, when they are prevented to form, the survival of yeast cell upon starvation is severely compromised.

Amyloid bodies

Amyloids are protein aggregates associated with human neuropathies, such as Alzheimer, Parkinson, and Huntington. These amyloids are believed to convert native folded proteins into irreversible b-sheet-rich protein aggregates (Knowles et al., 2014). In mammals, functional amyloidogenesis has been associated with hormone storage (Maji et al., 2009), melanin production (Fowler et al., 2006), kinase activity regulation (Li et al., 2012a) and protein synthesis (Berchowitz et al., 2015). Most proteins seem to possess the capacity to adopt an amyloid state (Goldschmidt et al., 2010). Researchers have proposed the existence of suppressor programs to prevent the conversion of proteins to a toxic amyloid state (Dobson, 1999). Therefore, it seems that the amyloidogenic propensity of proteins is essentially undesirable for the cell. However this view has been challenged by the recent discovery of the formation of Amyloid bodies (A-bodies), in tumorigenic human cells and tissues. It has been reported that in response to stress, cells activate amyloidogenesis in order to store large quantities of proteins into this novel body to consequently enter in a state of dormancy. A-bodies store in subnuclear foci a different array of proteins that adopt an amyloid like state. Importantly, A-bodies are inducible and reversible (Audas et al., 2016).

Sec bodies

Upon amino-acid starvation of Drosophila S2 cells, protein transport is inhibited. As a consequence the COPII subunits, Sec16 and perhaps many more proteins that remain to be identified are incorporated into the membrane-less stress assembly,

the Sec body. Sec bodies have many of the properties attributed to liquid droplets, they are reversible and pro-survival, acting as a reservoir for COPII subunits and Sec16 in order to rapidly resume protein transport upon re-feeding **(Chapter 2)**. Sec body formation relies on the post-translational modification mono-ADP ribosylation, which is in this case executed by the mono-ADP ribose, dPARP16. In this regard, dPARP16 modifies the Sec body component Sec16 at a specific region at its C-terminal domain **(Chapter 3)**.

IV. Properties and Mechanism behind the formation of stress assemblies.

What sort of structure or organization could a cell use to build and maintain membrane-less compartments? Despite the broad diversity of non-membrane bound stress assemblies that have been described so far, there is still a lot to be investigated regarding the properties and mechanisms behind their formation. Recently, they have become studied more in-depth and some models have been described to propose how they are formed.

Physical properties

In general, non-membrane bound assemblies will most likely have the properties of a liquid droplet (Brangwynne et al., 2009; Elbaum-Garfinkle et al., 2015). Because of the rapid motion found in liquids, different components can mix easily. But then the questions remains; how can liquids stay separated inside the cell without a membrane, and why is the system not driven towards a mixed state of higher entropy? One clear possibility is that liquids such as complex fluids, gels, and colloidal systems achieve higher entropy when they are de-mixed in phases (Hyman et al., 2014). The components forming an assembly must become rapidly concentrated in one specific part of the cell and they achieve this by phase separation. An example of this principle is depicted in P granules, as the components of P granules have higher affinity for each other than they do with cytoplasmic molecules (Bray, 1994; Doi, 2013).

Phase separation in non-membrane bound assemblies is also achieved via interaction between proteins and biomolecules. To achieve this, the proteins are most likely associated by attracting but still loose interactions (Asherie et al., 1996). These attracting interactions are characterized by moderate valency and long-range interactions. In this regard, it has been shown that multivalent weak interactions between signaling proteins can drive liquid droplet formation (Li et al., 2012b). Li et al, demonstrated that the concentration of N-WASP proteins in the droplet was hundredfold higher than in the surrounding medium.

The main characteristics of a liquid-like state in cells of granules, bodies and assemblies in cells are:

- They can fuse after touching, and reverse back to a spherical shape that is driven by the surface tension.
- They can deform in shear flow.
- They can exchange material with the cytoplasm. Therefore, they recover after photobleaching, albeit sometimes at a low rate.
- After photobleaching half of a granule, it will recover very quickly through rapid exchange of materials within the droplet.

Liquid-liquid demixing phase separation is one of the sides of protein condensation, as it results in the formation of liquid droplets enriched in a specific set of proteins. In general this process is highly controlled, completely reversible, and strongly condition-dependent (Uversky, 2017). In this regard, phase separation does not occur until specific conditions are reached. Therefore, small changes can easily lead to the complete disintegration of the condensed phase, as they depend of the thermodynamic forces that define the equilibrium of a system and manifest themselves in a form of a switch-like formation of large-scale molecular organization.

Importantly, membrane-less compartments like stress assemblies should be dynamic, so that chemical reactions can take place. In order to achieve this dynamic state they need to allow diffusion. Both diffusion and chemical reactions are driven by the differences in the chemical potential of each one of the molecular species or components. Thus, individual species of molecules move in or out of a concentrated system depending on their own chemical potential (Hyman et al., 2014).

On the other hand, despite the fluid nature of membrane less compartments, they can contain morphologically, physically and functionally distinct regions (Schmidt and Rohatgi, 2016). This might be a common characteristic of several membrane-less assemblies. For instance, electron dense-regions micrographs have revealed that stress granules contain internal substructures (Souquere et al., 2009). These sub-regions also referred to as cores, are characterized by higher concentrations of proteins and mRNAs and they can be biochemically isolated (Jain et al., 2016). Overall, this suggests that they may have two regions, one at the outer layer and another at the inner core with weak and stronger interactions respectively. Furthermore, P granules exhibit a spatial orientation when bound to the nuclear pore forming a "Tripartite sandwich" like structure (Sheth et al., 2010). Drosophila germiline granules also have foci of specific mRNAs, implying sub-organization (Little et al., 2015). At last, the nucleolus contains also substructures of fibrillarin cores (Brangwynne et al., 2011).

The role of intrinsically disordered proteins

A very important feature of membrane-less compartments is their enrichment with intrinsically disordered proteins (Uversky, 2017). Those are proteins that

have the capability to function in the absence of a fixed or unique 3D structure (Zimmerman and Trach, 1991). They constitute a large proportion of any proteome and their amount increases with the increase in organism complexity (Walsh et al., 2012; Xue et al., 2012). Several intrinsically disordered proteins have been found in many assemblies; for instance eIF4B and TDP43 in stress granules (Isabelle et al., 2012), TTP in P-bodies (Bhullar et al., 2016), RNG105 in RNA granules, centrins in centrosomes, NOPP140 in nucleoli, SRSF4 in nuclear speckles, Saf-B in nuclear stress bodies, CBP in PML nuclear bodies, SOX9 in paraspeckles, KSRP in perinucleolar compartment and hnRNPG and Sam68 in Sam68 nuclear bodies (Zhu and Brangwynne, 2015).

This indicates that the formation of these phase-separated droplets is crucially dependent on intrinsic disordered proteins, that is, regions containing low complexity polypeptide (Kato et al., 2012). These sequences are known to be regions/domains in proteins with little diversity in their amino acid composition. Extensive studies have shown that these low complexity sequences exist in a disordered state when the protein is soluble (Huntley and Golding, 2002; Uversky, 2002). Kato and collaborators demonstrated that by expressing the disordered domain of the fused in sarcoma (FUS) RNA-binding protein, they were able to induce the reversible formation of hydrogel droplets. This FUS hydrogel resembles morphologically uniform amyloid-like fibers, consistent with the notion that phase transition from soluble to hydrogel state is a simple reflection of polymer formation (Kato et al., 2012).

Post-translational modifications drive phase transitions

Post-translational modifications like phosphorylation, acetylation and ADP-ribosylation have also a large influence during the stress response. Recently, it has been proposed that Adenosine-diphosphate-ADP-ribosylation (ADP-ribosylation) and more specifically Poly-ADP ribosylation plays a role during the formation of mRNPs granules (Leung, 2014). ADP-ribosylation is a reversible post-translational modification of proteins that is catalyzed by ADP-ribosyltransferases and certain members of the Sirtuin family (Feijs et al., 2013; Gibson and Kraus, 2012). During ADP-ribosylation, nicotinamide adenine dinucleotide NAD is used to covalently attach residues of ADP-ribose to specific amino acids of substrate proteins. PARPs, also known as ARTs, share a structurally conserved catalytic domain. They are intracellular enzymes that are able to transfer either a single ADP-ribose residue to an amino-acid/acceptor, in a process referred to as mono-ADP-ribosylation (MARylation), or they are able to attach several ADP-ribose residues with ADP-ribose being the acceptor, resulting in either linear or branched chains of ADP-ribose (poly-ADP-ribosylation or PARylation) (Kleine et al., 2008)**(Figure 3)**.

The founding member of the PARP family, poly-ADP-ribose polymerase 1 (PARP1), can PARylate itself as well as substrate proteins. The capability of PARPs to form ADP-ribose polymers depends on the H-Y-E amino acid signature in their catalytic center. Enzymes with this signature transfer multiple ADP-ribose units to

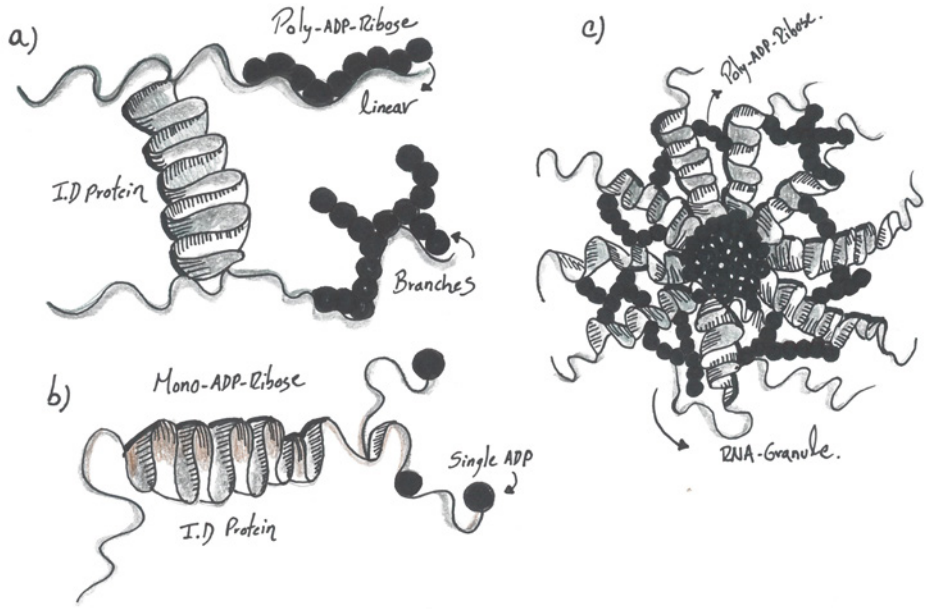

Figure 3. a. Poly-ADP ribosylation. Cartoon depicting PARylation of an intrinsically disordered protein (I.D protein), at the upper side a linear ADP polymer, and at the lower side a branched polymer **b. Mono-ADP ribosylation**. Cartoon depicting MARylation of an I.D protein, note that there is the addition of single ADP ribose**. c. Role of Parylation in mRNPs formation as described in (Leung, 2014).** Cartoon depticting the formation of an mRNP granules, note that I.D proteins are kept together via ADP-ribose polymers (PARylation).

their substrates using glutamate to activate NAD. This catalytic glutamate residue is replaced in enzymes of the mono- PARP group, defined as variants of the active site. These enzymes instead employ a glutamate residue of the substrate for the transfer of ADP-ribose, therefore this residue is no longer available for the activation of additional NAD molecules (Kleine et al., 2008).

There are several enzymes that have been identified and classified according to their catalytic activity, PARP1 (Artd1), PARP2 (Artd2), PARP5A (Tankyrase 1) and PARP6 (Tankyrase 2) which all synthesize poly-ADP-ribose chains. PARP15, PARP14 (Artd7/8), PARP10–12 (Artd10–12), and PARP8, 7,16,6 (Artd14–17) are classified as mono-ADP-ribosyltransferases (Hottiger et al., 2010; Kleine et al., 2008). Additional amino acid substitutions in the catalytic domain of PARP9 and PARP13 (Artd9 and Artd13) prohibit NAD-binding and render these proteins catalytically inactive (Karlberg et al., 2015; Kleine et al., 2008). At last, although PARP3 and PARP4 (Artd3 and Artd4) were initially proposed to have PARylation activity based on their classical H-Y-E signature, MARylation activity has been reported for both enzymes (Loseva et al., 2010; Vyas et al., 2014), suggesting that additional features in the active center are responsible for the lack of PARylation activity or that the substrate specificity can restrict these enzymes to MARylation (Isabelle et al., 2012).

Overall, the cellular environment appears to be crowded with biological macromolecules, numerous cellular bodies and membrane-less assemblies that can be exclusively formed by proteins and/or RNAs. These assemblies can be found in the cytoplasm and nucleoplasm. They are formed as a consequence of highly regulated and reversible liquid-liquid demixing phase separation, represented by condensed liquid droplets, which are very often enriched in intrinsically disordered proteins. Phase transitions formation is controlled by many factors, such as concentrations of intrinsically disordered proteins, their multivalency and their ability to have specific but weak interactions. Furthermore phase transition formation is influenced by post-translational modifications and local environmental challenges.

In summary, in order to survive changing environmental conditions, the cell response should not only be quick but also efficient. Upon several of the above-described stresses, the first cellular response is to slow down and/or activate key anabolic pathways. One of the main consequences of this response is the accumulation/stalling of key factors that are normally used to maintain cellular homeostasis in steady conditions. As the production and maintenance of these key factors are very costly for the cell, not only in terms of time but also energy, one of the cellular mechanisms to achieve a quick and efficient recovery is through the storage of key factors inside of non-membrane bound, reversible and pro-survival structures known as stress assemblies.

Part C: Membrane-bound organelles, membrane-less compartments and the control of anabolic pathways

Abstract

Classically, we think of cell compartmentalization as achieved by membrane-bound organelles. It has emerged that membrane-less assemblies also largely contribute to this compartmentalization. Here, we compare the characteristics of both types of compartmentalization in term of maintenance of functional identities. Furthermore, as membrane-bound organelles, membrane less-compartments are critical for developmental and cell biology as they control major metabolic pathways. We describe two examples related to this issue, the P-bodies in the translational control of *gurken* in the Drosophila oocyte, and Sec bodies in relation of protein transport in the early secretory pathway.

Introduction

Cell compartmentalization is paramount for sustaining key cell biological events and programmes of developmental biology. It is classically achieved by membrane-bound organelles, such as those forming the secretory pathway, the endosomal/

lysosomal pathway, mitochondria, peroxisomes, lipid droplets, autophagosomes. It is nevertheless emerging that cytoplasm compartmentalization is also achieved by steady-state membrane-less assemblies, such as nucleoli, Cajal bodies, P-granule in the C-elegans oocyte, P-bodies, risobomes (all of them RNA based), as well as others that do not contain RNA, such as centrosome, proteasome, aggresome (Rajan et al., 2001) and even the cytoskeleton (see references in (Hyman et al., 2014)). Interestingly, the formation of many additional membrane-less assemblies (whether RNA based or not) is triggered by cellular stress. This is the case for stress granules (Anderson and Kedersha, 2002), Sec bodies (Aguilera-Gomez et al., 2017; Zacharogianni et al., 2014), filamentous high order assemblies in yeast under energy deprivation (Munder et al., 2016; Petrovska et al., 2014), A-bodies in the nucleus (Audas et al., 2016). Below, we compare both types of compartmentalization and discuss them in term of acquisition and maintenance of functional identities. In a third part, we describe how two membrane less-compartments are critical for two developmental and cell biological events in controlling major metabolic pathways.

I. Membrane-bound organelles.

Most cell biologists use the term organelle for a specialized subunit within a cell that has a specific function and that is usually separately enclosed by their own lipid bilayers. Organelles are identified by microscopy, with emphasis of electron microscopy (to be able to visualize the membrane) and can usually be isolated and/or purified by cell fractionation. Membrane-bound organelles are a characteristic of eukaryotic cells. Mitochondria, the endoplasmic reticulum, the Golgi apparatus, the endosomal/lysosomal system are all micro-meter large membrane-bound organelles. On the other hand, prokaryotes do contain protein-based micro-compartments (what we refer to here as membrane-less assemblies, which are thought to act as primitive organelles (Kerfeld et al., 2005) (see below).

One important characteristic of cell organelles is that intensely communicate with one another. They do so by signaling (Bard and Chia, 2016; Farhan and Rabouille, 2011; Villasenor et al., 2016), but they also directly exchange materials via small vesicular carriers, such as the COPI coated vesicles budding mostly from the Golgi (Aguilera-Gomez and Rabouille, 2014), the COPII coated budding from the ER exit site (ERES) (Miller and Schekman, 2013), and the clathrin coated vesicles budding from the Trans Golgi Network (TGN) and the plasma membrane (Robinson, 2015). Yet, despite this intense vesicular trafficking, the organelles maintain their identity.

How do organelles achieve this? Organelle identity is defined by the acquisition of a set of markers that often defines and carries the organelle function. These markers can be luminal, transmembrane and peripheral proteins. For instance, lysosomes contain cathepsins in their interior (Erickson, 1989), LAMPs integral to their membrane (Saftig and Klumperman, 2009), and Rab7 as a peripheral protein.

The Golgi apparatus displays oligosaccharide transferases integral to its membrane (Fisher and Ungar, 2016; Gill et al., 2011) as well as numerous peripheral proteins, such as the large coiled coil Golgins (Gillingham and Munro, 2016), GRASP65/55 (Rabouille and Linstedt, 2016), the COPI subunits (Jackson, 2014). Furthermore, ERESs are characterized by the concentration of the transmembrane protein Sec12, the COPII subunits (Miller and Schekman, 2013) and Sec16 (Sprangers and Rabouille, 2015).

Luminal and transmembrane organelle markers are synthesized in the ER together with all the newly synthesized cargos that are secreted. Both markers and cargos are transported through the ER>Golgi>PM secretory pathway. However, markers are sorted from cargos to be sent to their correct locations (endosome/lysosomes), retained in the organelle where they exert their function (ER/Golgi), and retrieved from un-correct locations. Sorting and retrieval is mediated by a number of signals in their cytoplasmic tails such as the KKXX motif for the ER transmembrane proteins (Nilsson and Warren, 1994), their transmembrane domains (Banfield, 2011; Nilsson and Warren, 1994) and their C terminus, such as the KDEL present in luminal ER proteins.

II. Membrane-less compartments.

Next to membrane-bound organelles, a number of cell compartments are membrane-less. They are micron large multi-component assemblies that contain many different types of biomolecules. Examples range from the nucleolus, where ribosomes are made inside the nucleus (Boisvert et al., 2007; Falahati et al., 2016); centrosomes that nucleate the interphase microtubule network (Mahen and Venkitaraman, 2012); nuclear Cajal bodies where spliceosomes are generated (Gall, 2003); P-bodies where basal RNA metabolism takes place (Parker and Sheth, 2007), P-granules during the development of the C.elegans embryo (Saha et al., 2016) and many RNA granules (Leung, 2014; Moser and Fritzler, 2010). As membrane-bound organelles, these membrane-less compartments are also defined by specific set of markers, such as fibrilarin for the nucleolus, pericentrin and AKAP450 for centrosome (Bornens, 2002); DCP2, Ago and Me31B for P-bodies, and PGL and GLH in P-granules of C elegans, cajal bodies (Machyna et al., 2013).

Furthermore, many membrane-less compartments are formed during stress (Rabouille and Alberti, 2017), such as stress granules (Anderson and Kedersha, 2008; Protter and Parker, 2016); DNA repair foci (Gibson and Kraus, 2012); Sec bodies (Aguilera-Gomez et al., 2016; Zacharogianni et al., 2014); higher order assemblies of metabolic enzymes in energy deprived yeast (Narayanaswamy et al., 2009) (Munder et al., 2016; Petrovska et al., 2014). Importantly, these stress assemblies are reversible and contribute to cell survival during stress and cell fitness upon stress relief.

How are the components kept together to form identifiable assemblies without a

membrane? Essentially membrane-less compartments are formed by the collective behavior of macromolecules and can adopt at least three material properties: Liquid droplets, gels and solid/polymers. Liquid droplets are formed by liquid-liquid phase separation whereby an initially homogeneous solution of macromolecules demixes into two distinct liquid phases that then stably coexist (Brangwynne et al., 2009; Hyman et al., 2014). Gels are formed by gelation, and solid by nucleated polymerization. Altogether, this creates compartments that are enriched in certain active biomolecules while others are repelled (Su et al., 2016). Furthermore, they function as storage, protection and release assemblies for macromolecules.

Phase separation/transition occurs as cellular systems continuously seek a state with minimal free energy also known as "droplet" phase (Hyman and Simons, 2012). This mediates the formation of finite size complexes through low valency followed by multivalency promoting the formation of physically separate phases. Here, valency is used to define the number of possible interactions that each molecule has. Both low and multivalency can be generated through multi-domain proteins or RNA (Banani et al., 2016; Protter and Parker, 2016).

The question is therefore which type of proteins promote this behavior? Phase transition is usually triggered by an increase in local concentration of certain types of proteins, particularly those with multidomains and/or with intrinsically disordered, low complexity sequences (Huntley and Golding, 2002). These proteins are not globular and exhibit regions of poor amino-acid diversity (Low complexity sequences) that can be prion-like proteins (Q, N, S, G, Y) (Alberti et al., 2009), or repeats of alternating charges, such as RGG (Nott et al., 2015). Importantly, these sequences show a high degree of flexibility in their conformation. Electrostatic interactions play an important role (Nott et al., 2015), which make them strongly sensitive to ionic conditions. Interestingly, assemblies can be reconstituted from single proteins in vitro (Elbaum-Garfinkle et al., 2015; Lin et al., 2015; Molliex et al., 2015; Patel et al., 2015). However, it is also clear that post-translational modifications, such as phosphorylation, methylation, ADP-ribosylation (Han et al., 2012) (Aguilera-Gomez et al., 2016; Banani et al., 2016; Kato et al., 2012) are important for the formation of these membrane-less compartments. These post-translational modifications appear to be specific for certain stresses, such as poly-ADP ribosylation for arsenite triggered stress granules (Leung et al., 2011) and ubiquitination for proteasome storage granules (Peters et al., 2013).

Therefore, intrinsically disordered proteins seem to be ideal for stress adaptation: They can sense and respond to changes in the environment by forming platforms where a large number of proteins can be recruited through non-covalent interactions thus generating stress assemblies, sometimes in a time scale of minutes (Halfmann, 2016).

Do membrane less-assemblies communicate with other parts of the cell? A number

of stress assemblies are formed in response to signaling elicited by stress, such as stress granules, Sec bodies (see below) and A bodies (Audas et al., 2016). Conversely, stress granules have been proposed to modulate signaling pathways, such as apoptosis by sequestering key pro-apoptotic components (Arimoto et al., 2008; Kim et al., 2005) and the TOR pathway (Takahara and Maeda, 2012) (Thedieck et al., 2013; Wippich et al., 2013). Second, P-bodies and stress granules communicate. mRNAs that are stored in stress granule can be sorted in P-bodies for degradation if they are damaged (Buchan et al., 2008) (Buchan and Parker, 2009; Kedersha et al., 2005). Interestingly, P-bodies and stress granules are found in close proximity (Aguilera-Gomez et al., 2017; Souquere et al., 2009). Last, membrane-less compartments also communicate with membrane-bound *organelles*. For instance, yeast P-bodies communicate with the ER that modulate their formation (Weidner et al., 2014) and prion based membrane-less assemblies can form in the lumen of an organelle: (Ritz et al., 2014).

How is this communication achieved remains to be better investigated. Is it through the controlled diffusion of their components as it is the case of damaged RNA between stress granule and P-bodies? Or is there a more dynamic relationship, like the active shuttling of TIA-1 from stress granules to polysomes in order to selectively enhance or repress mRNA expression (Kedersha et al., 1999). Last, as mentioned above, many stress assemblies are the result of activated stress signaling pathways, but do they initiate signaling?

III. Similarities/differences between membrane-bound and membrane-less compartments.

The first obvious difference is the presence of a membrane. The membrane is not only a physical barrier that regulates the exchange between the cytoplasm and the lumen, but it also act as a platform for many signaling pathways and recruitment of peripheral proteins. However, the exchange between the core of a membrane-less compartment and the surrounding space is also regulated, not by transporters but by the strength of interactions between the components. This not only allows their diffusion out but also prevents cytoplasmic components to reach the inside.

The second is their biogenesis. Many membrane-bound organelles are not formed *de novo*. When needed (for instance during mitosis when two daughter cells form), most of the organelles undergo fission that generates templates onto which membrane and protein components are recruited. This allows their fusion and growth. This follows the principle of self-organization that involves the physical interaction of molecules to form a steady-state structure (Prigogine et al., 1974) (Misteli, 2001). This is not to be confused with self-assembly that involves the physical association of molecules into an equilibrium structure (Misteli, 2001), such as those existing in virus. Many membrane-less assemblies are also self-organized and are steady-state

structures rather than equilibrium structures. This is not only true for the structures that form under stress and that rapidly dissolve upon stress relief, but also for those that exist in basal conditions, such as nucleolus (Lewis and Tollervey, 2000) and the cajal bodies (Dundr et al., 2004) that constantly and rapidly exchange molecules with the nucleoplasm.

The third is the time scale of their response to (environmental) signaling/ perturbations. Perhaps the most dramatic difference is the formation within minutes of stress assemblies from seemingly diffuse (or nanoscopic) components upon stress signaling, as well as their dissolution upon stress relief, as opposed to the rather stable presence of membrane-bound organelles. However, addition of drugs, such as Brefeldin A, leads to the complete fragmentation and re-absorption of the Golgi in the ER in a matter of minutes (Lippincott-Schwartz et al., 1989), and stress also leads to rapid changes in its architecture (Cancino et al., 2013; Farhan and Rabouille, 2011).

The fourth is the type of proteins that are found in these two types of compartments. As mentioned above, membrane-less compartments appear to be enriched of intrinsically disordered proteins whose properties mediate their formation. This does appear to be the case for membrane-bound organelles but these proteins have not yet been all well-studied and they might also contribute to the organelle proteomes. In this regard, it is interesting to note the presence of membrane-anchored prion-like proteins that act as retention mechanism in the yeast TGN through their formation of small aggregates (Ritz et al., 2014).

We therefore propose that the similarities between membrane-bound and membrane-less compartments outweigh their differences and they both should be called "organelles". In this regard, membrane-less compartments, as their membrane-bound counterparts, are also known to control anabolic pathways. This is the case for the production of ribosomes and spliceosomes in the nucleolus and cajal bodies, respectively. Below, we present further illustrations of this notion with implications in developmental and cell biology.

IV. Membrane-less compartments and anabolic pathways.

IV. 1: P-bodies and translational control in the developing Drosophila oocyte.

Translation in compartmentalized P-bodies

As mentioned above, P-bodies are the crucible in which most of the RNA metabolism takes place, including degradation through decapping, endonucleases, RNAi mediated pathway as well as microRNA (Parker and Sheth, 2007).

However, some translationally silent mRNAs have also been shown to be stored in P-bodies (Aizer et al., 2014), so attention has been given to their role in the translational control during development, for instance in plants (Xu and Chua, 2011), but also in the Drosophila oocyte (Snee and Macdonald, 2009) (Weil et

al., 2012). In this respect, sponge bodies (named so because of their appearance) (Wilsch-Brauninger et al., 1997) (Nakamura et al., 2001) (Delanoue et al., 2007) were later characterized as the oocyte P-bodies as they contain many translational control components (Snee and Macdonald, 2009) (Weil et al., 2012). Furthermore the oocyte P-bodies were shown to be key for the targeted localization of the developmentally critical mRNAs *gurken* and *bicoid* (Delanoue et al., 2007) (Weil et al., 2012). Indeed, the localization of both *gurken* mRNA at the oocyte dorsal anterior corner at stage 7-9, and of *bicoid* mRNA around the entire anterior cortex is largely mediated by their association to the oocyte P-bodies. *gurken* and *bicoid* transcripts are even localized to the same P-bodies at the dorsal anterior corner. However, *gurken* tends to be enriched at the edge of these structures whereas *bicoid* in enriched in their core, thus reflecting a potential functional sub-compartmentalisation of the P-bodies (Weil et al., 2012).

The core is further defined by the absence of ribosomes and the enrichment of the translational repressors, whereas the edge is enriched in the cytoplasmic polyadenylation element binding protein Orb and ribosomes are present. The edge of oocyte P-bodies is therefore proposed to be translational active whereas their core is translationally silent**.** Interestingly, this organization completely reflects the translational status of both mRNAs. *gurken* mRNA is translated at stage 8-9, *whereas* bicoid mRNA is stored and will only be translated at stage 14 of oogenesis (Weil et al., 2012) (**Figure 4**).

Orb modulates gurken translation

Does this P-body sub-compartmentalization explain why *gurken* RNA is not translated in the adjacent nurse cells where it is transcribed? Indeed, *gurken* mRNA is synthesized in the nurse cell nucleus (Caceres and Nilson, 2005). It is then transported through ring canals along microtubules to the dorsal anterior corner of the oocyte (Clark et al., 2007). There, it is anchored to oocyte P-bodies and translated (Delanoue et al., 2007) (Weil et al., 2012). However, what prevents it to be translated in the nurse cells was till recently not clear.

There were two possibilities: *gurken* mRNA could be bound to repressors and buried in the core of the nurse cell P-bodies. This hypothesis is sustained by the identification of *gurken* repressors, such as Bruno (Filardo and Ephrussi, 2003; Reveal et al., 2011; Yan and Macdonald, 2004), and the dead end helicase Me31B (Kugler et al., 2009; Nakamura et al., 2001). Alternatively, the composition of the nurse cell P-bodies could be different and unable to support *gurken* translation.

The MS2 tagging system based upon the natural interaction of the MS2 bacteriophage coat protein with a stem-loop structure from the phage genome (Bertrand et al., 1998) (Jaramillo et al., 2008) was employed to visualize *gurken* mRNA in the Drosophila egg chamber and to show that in the nurse cells it does not associate to

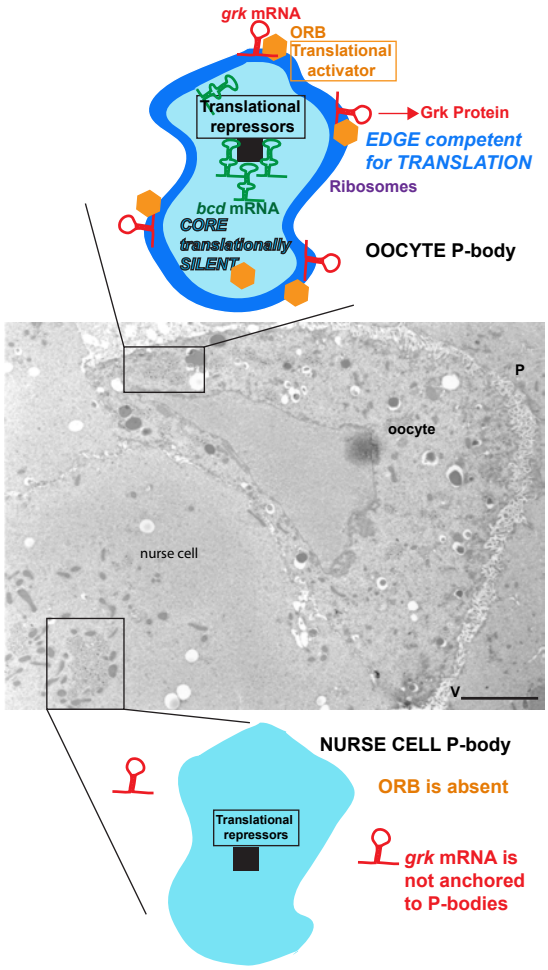

Figure 4: Orb control of gurken translation at the edge of the Drosophila oocyte P-bodies. Electron micrograph of a frozen ultrathin section of stage 8/9 Drosophila egg chamber labeled for Me31B (10 nm gold) to mark P-bodies. Note that the labeling is similarly restricted to P-bodies in the oocyte and the nurse cells (examples are boxed). Scale bar: 10um The schematics above the micrograph represents a sub-compartmentalized oocyte P-body at the dorsal- anterior corner with its translational silent core containing bicoid mRNA and its translational competent edge to which gurken mRNA, Orb and ribosomes are associated, thus allowing Gurken synthesis. The schematics below the micrograph represents a nurse cell P-body to which gurken mRNA is not associated due to the absence of Orb.

P-bodies either in their core or at their edge (Davidson et al., 2016). It is therefore possible that *gurken* transcripts are not able to properly anchor to the nurse cell P-bodies. This was investigated by assessing the differences in proteins associated to nurse cells and oocyte P-bodies. The most critical difference was the amount of Orb that was significantly lower in the nurse cells and its absence in the nurse cell P-bodies (Davidson et al., 2016).

Orb is the Drosophila homologue of cytoplasmic polyadenylation element binding protein (CPEB) that is a key translational activator of *gurken.* Consequently, *gurken* is not translated in an Orb mutant (Chang et al., 2001). Furthermore, Orb forms a complex with poly(A) polymerase Wispy and this is required for *grk* hyper-adenylation as well as its translation (Norvell et al., 2015) (Wong et al., 2011).

To test whether Orb is the key factor regulating *gurken* translation, Orb was overexpressed in the nurse cells, and this resulted in the clear ectopic expression of Gurken protein in these cells. Critically, upon Orb expression, *gurken* mRNA was found associated to nurse cells P-bodies together with Orb (Davidson et al., 2016). This indicates that Orb is a determining factor controlling *gurken* anchoring to P-bodies where it is translated. Where Orb is absent or low, *gurken* mRNA is not anchored and not translated. When Orb is high, *gurken* is anchored and translated (Davidson et al., 2016; Derrick and Weil, 2016).

Taken together, this shows a critical role for the membrane-less assembly P-body in the control of translation of *gurken* translation.

IV. 2: Sec bodies and protein transport in the early secretory pathway.

Sec bodies form to protect ERES components

The secretory pathway is another major anabolic pathway formed by a series of morphologically and functionally defined membrane-bound compartments. It is used to deliver proteins to the plasma membrane, all membrane compartments (except mitochondria), and extracellular medium. Newly synthesized proteins exit the ER in COPII coated vesicles at the ER exit sites (ERES). COPII coat vesicles are formed by Sar1, its GEF Sec12, the heterodimer Sec23/24 at the inner layer (Antonny et al., 2001; Bi et al., 2007; Lord et al., 2011), the dimer Sec 13/31 at the outer layer (Stagg et al., 2008). Another factor necessary for ER exit and protein transport is the non-COPII component and scaffold protein Sec16 (Kaiser and Schekman, 1990; Sprangers and Rabouille, 2015). Newly synthesized proteins then reach to the Golgi where they are processed, sorted and dispatched. Together, the ERES and the Golgi form the early secretory pathway.

Cellular stress, such as heat stress (Petrosyan and Cheng, 2014), oxidative stress, and genotoxic stress leading to DNA damage (Farber-Katz et al., 2014), all affect the functional organization of the early secretory pathway, especially the Golgi apparatus, and protein transport is inhibited. In Drosophila cells, the stress of serum starvation also inhibits protein transport through the secretory pathway (Zacharogianni et al., 2011) and amino-acid starvation leads to the remodeling of the ERES components into a novel membrane-less stress assembly, the Sec body (Zacharogianni et al., 2014).

During the period of stress, Sec bodies store and protect most of the COPII components as well as Sec16 from degradation. They are round, membrane-less and display liquid droplet properties. Importantly, they are pro survival and rapidly disassemble upon stress relief, where their components are recovered and functional in order to resume protein transport (Zacharogianni et al., 2014). As such, Sec bodies are part of the adaptive response to stress (**Figure 5**).

Interestingly, amino-acid starvation also leads to the formation of another stress assemblies, the stress granules that form in response to the inhibition/stalling of protein synthesis elicited by the stress (Zacharogianni et al., 2014). Both Sec bodies and stress granules form very close to one another in S2 cells but they do not seem to mix and they display a high specificity in their composition. Sec body stores COPII components and Sec16 but they do not appear to contain RNA. In contrast, stress granules are RNA and translation machinery rich structures (**Figure 5**).

Sec16 mono-ADP-ribosylation by ER-localized dPARP16 is required for Sec body formation.

As mentioned in Part IV.I, an emerging concept in cellular organization is that non-membranous structures are formed through phase transition (Hyman and Simons, 2012) (Weber and Brangwynne, 2012), gelation or nuclear polymerization (Protter and Parker, 2016), resulting in liquid, gel and solid assemblies, respectively. A key question is what triggers this process. How is stress sensed by the cell interior to lead to the formation of these higher-order assemblies? The traditional view is that stress stimulate signaling pathways that transmit fluctuations from the cell environment to the cell interior, for instance by promoting proteins post-translational modifications. In this regard, Leung and colleagues (Leung et al., 2012) have proposed Poly-ADP-ribosylation (PARylation) as an organizer of macromolecular architecture and a mediator for RNA granule formation by facilitating the local concentration of proteins and promoting their oligomerization (Leung, 2014). PARylation is a post-translational modification consisting in the addition of two or more ADP-ribose units to a protein substrate by ADP-ribosyltrasferases (PARPs) (Gibson and Kraus, 2012; Hottiger et al., 2010). Importantly, its is reversible and the primary enzyme that involves PARP degradation is known as poly(ADP-ribose) glycohydrolase (PARG) (Hatakeyama et al., 1986).

The role for PARylation in reorganizing cellular architecture has also been demonstrated during genotoxic stress where it is required for subnuclear localization of RNA-binding proteins in nuclear speckles (Jungmichel et al., 2013). The funding member of ADP-ribosylation, the nuclear PARP1 is required for DNA repair during DNA damage (Gibson and Kraus, 2012) where it hyper-PARylates itself as well as surrounding histones (Gibbs-Seymour et al., 2016). PARylation is also associated with stress granule formation in mammalian cells. First, stress granule components are PARylated upon arsenate treatment (Leung et al., 2011). Second stress granules

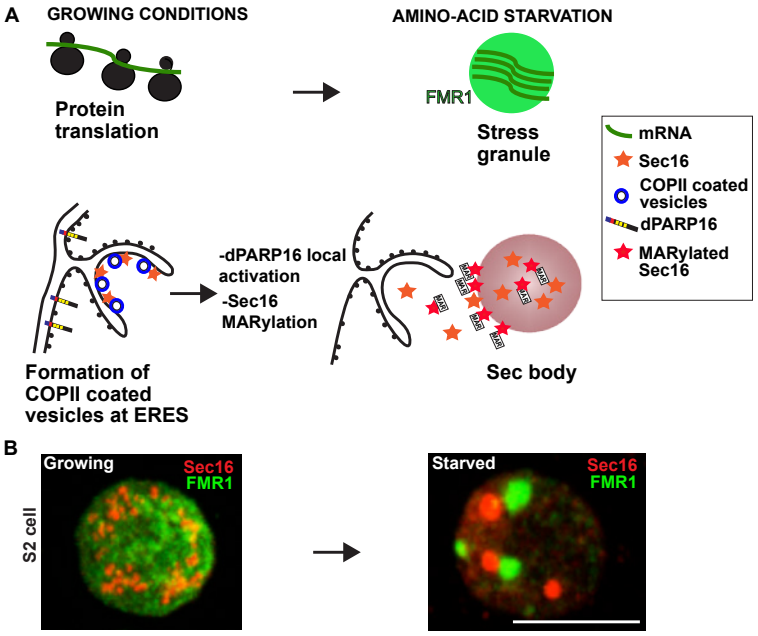

Figure 5: The amino-acid stress response in Drosophila S2 cells. A: Schematics of protein translation and protein transport out of the ER at ER exit sites (ERES, where COPII coated vesicles formed) that are both active in growing conditions. Upon amino-acid starvation, translation initiation is inhibited. Untranslated mRNAs accumulate and are bound by RNA binding proteins, such as FMR1, leading to the formation of membrane-less stress granules. Amino-acid starvation also inhibits protein transport out of the ER. ER localized dPARP16 is activated and MARylates Sec16 on its C-terminus leading to the formation of Sec bodies that protect COPII components and Sec16 from degradation. **B:** Immunofluorescence visualization of FMR1 (green) and Sec16 (red) in growing cells. FMR1 is cytoplasmic and Sec16 is localized at the ERES. Amino-acid starvation leads to the formation of stress granules (marked by FMR1) and Sec bodies (marked by Sec16). Scale bar: 10 μm.

contain PARPs, especially PARP13 (Leung et al., 2011) (Leung et al., 2012) and PARP12 (Welsby et al., 2014). Overexpression of these PARPs induces stress granule formation, even in the absence of stress. Third, the PARylation inhibitor 3-aminobenzamide completely inhibits stress granule formation (Leung et al., 2011). Last, stress granules also contain PARG (Gagne et al., 2005) and its overexpression also inhibits their formation (Leung et al., 2012). Together, this has led to the model that stress-induced PARylation of RNA binding proteins leads to their coalescence into cytoplasmic assemblies containing RNAs, PARPs and PARGs (Leung, 2014).

In line with this, we have found that Sec body formation also requires ADP-ribosylation. However, it is not PARylation but Mono-ADP-ribosylation (MARylation) catalyzed by the mono-ADP ribose, ER localized dPARP16 (Aguilera-Gomez et al., 2016). dPARP16 over-expression drives Sec body formation even in the absence of stress and conversely dPARP16 depletion prevents their formation upon amino-acid starvation. dPARP16 is expressed at very low level in the cell but when depleted, the cells are more sensitive to amino-acid starvation and they do not

recover well after stress relief. As such dPARP16 is a novel stress survival factor.

Interestingly, using a probe that we designed to specifically detect MARylation events in vivo (Aguilera-Gomez et al., 2016), we showed that amino-acid starvation triggers a strong wave of cytoplasmic MARylation events that take place in the same time frame as Sec body formation and localizes in close proximity to these assemblies. Using this probe, the Sec body component Sec16 has been demonstrated to be one of the dPARP16 substrates upon amino-acid starvation and we identified the small sequence in the Sec16 C-terminus that is MARylated. Altogether, dPARP16 dependent Sec16 MARylation is necessary and sufficient for Sec body assembly (Aguilera-Gomez et al., 2016).

These findings show that MARylation of one substrate by a specific enzyme can drive a major remodeling of the cellular architecture, including one related to membrane-bound components. Moreover, this finding not only establishes an unprecedented role for MARylation in the formation of membrane-less assemblies, but also links this post-translational modification to a specific metabolic stress and cell survival pathway.

Conclusion and perspectives.

The field of membrane-bound organelles has been intensely studied in the last half century and they are fairly well understood. However, new fields are emerging, such as: membrane contact sites (Gatta and Levine, 2016), including their role in the formation of organellar structures like mitochondrial cristae (van der Laan et al., 2016); the role of membrane-bound compartments as signaling platforms, receiving and sending signals (Cancino et al., 2013; Farhan and Rabouille, 2011); their functional and morphological response to stress for instance Golgi stress (Machamer, 2015); and new developments for old pathways, such as Arf1 in mitochondria morphology (Ackema et al., 2014) and O-linked glycosylation (Bard and Chia, 2016).

Membrane-less compartments have also been described for a long time but they only recently have become the focus on intense research in term of their dynamics (formation, maintenance and dissolution), their composition, and their role in surviving stress in different models. Furthermore, as described above, specific biochemical reactions are uniquely taking place in these compartments and this will need to be further deciphered. Last, their de-regulation could have deleterious consequences. For instance, it is now clear that faulty stress granule dynamics is linked to neurodegeneration (Li et al., 2013), and it will be important to understand how other of these high-order assemblies can contribute to pathologies.

Finally, it will be interesting to understand how membrane-bound and membrane-less compartments interact with one another. It seems for instance that P-bodies are assembled at the surface of the ER in yeast, thus presumably controlling translation there (Weidner et al., 2014). Is it the case for other membrane-less compartments? In

this regard, it is interesting to note that prion-based membrane-less small aggregates appears to form in the lumen of the yeast TGN and mediate retention of a specific class of proteins (Ritz et al., 2014). The next step will be to investigate whether fragments of membrane-bound organelles could be incorporated in membrane-less compartments.

Acknowledgements

We thank our colleagues for many discussions on several aspects of this review, especially from the Davis lab (Oxford, UK) on Drosophila P-bodies, and Bram Herpers (Leiden University, the Netherlands) for the micrograph shown in Figure 1. The work in the Rabouille lab is funded by NWO and the KNAW.

Scope of the thesis

During the last decade, a novel concept of cellular architecture and organization has re-emerged with the recognition of high-order compartmentalization via non membrane-bound macromolecular structures. These membrane-less structures are in most of the cases the result of several stress conditions.

The aim of this thesis is to depict the mechanisms behind the formation of Sec bodies and Stress granules in Drosophila S2 cells upon amino-acid starvation. These stress assemblies are formed as a result of the stalled of protein transport and protein translation respectively.

In chapter 2, we investigate the behavior of ERES components upon amino-acid starvation. This nutrient stress leads to the stalling of protein secretion, which results in the formation of a novel membrane-less stress assembly that we have named the Sec body. This assembly is mainly composed of COPII proteins as well as the large scaffold protein Sec16. We demonstrate that Sec bodies are reversible, pro-survival structures with liquid droplets properties. Sec bodies act as reservoir for ERES components for the duration that this nutrient stress is taking place. Therefore, upon the relief of the stress the secretory pathway is rapidly reconstituted and functional.

In chapter 3, we study the post-translational modifications Mono and Poly-ADP-ribosylation as they have been proposed to be involved in the formation of aggregates and RNA granules. For this purpose, we designed and build specific fluorescent probes, Marylation detection (MAD) and Parylation detection (PAD) that allow us to follow these post-translational modifications *in vivo*. We discover that mono-ADP-ribosylation by the mono-ADP-ribose dPARP16 plays a crucial role in Sec body formation, as it modifies the Sec body component Sec16 on a very specific sequence in its C–terminus. In summary, we demonstrate that dPARP16 catalytic activity on Sec16 is a necessary and sufficient step to induce Sec body assembly

and cell survival. Furthermore, we propose that Sec16 is a key factor for the stress response to amino acid starvation.

In chapter 4, our focus moves towards the post-translation mechanism behind the formation of stress granules upon amino-acid starvation. We report that mono-ADP-ribosylation by dPARP16 is necessary but not sufficient for their formation. Our experimental data points also towards a role for Poly-ADP-ribosylation. In this regard, we show that the nuclear resident, poly-ADP-ribose dPARP1 plays a crucial role. Interestingly, in order to induce stress granule formation dPARP1 has to localize at the cytoplasm. Critically, dPARP1 localization out of the nucleus depends on dPARP16, possibly through the mono-ADP-ribosylation of the nuclear exporter Karyopherin beta 3. These findings provide a link between the stress responses exerted at the secretory pathway, nuclear export and the translation turnover upon nutrient stress.

In chapter 5, we approach the role of Sec16 in the formation of the stress granules upon amino-acid starvation. We have identified that Sec16 plays a crucial role in stress granule formation upon this nutrient stress. Using mass spectrometry and a plasma membrane anchor-away technique, we show that Sec16 specifically interacts with the phosphorylated-Ser-142 of Rasputin, the form that is exclusively required for stress granule formation upon this nutrient stress. These results reinforce the notion of Sec16 as a stress response protein upon amino-acid starvation.

At last, going back to the study of the secretory pathway, **in chapter 6**, we outline different current models that have been proposed in the field in order to describe anterograde transport through the secretory pathway. However, there is still no clear consensus on how newly synthesized proteins traverse the Golgi apparatus while keeping the structural integrity of the organelle.

In **chapter 7,** we discuss our findings, and suggest further research directions.

References:

Ackema, K.B., Hench, J., Bockler, S., Wang, S.C., Sauder, U., et al., 2014. The small GTPase Arf1 modulates mitochondrial morphology and function. The EMBO journal 33, 2659-2675.
Aguilera-Gomez, A., Rabouille, C., 2014. Intra-Golgi Transport. In: Ralph A Bradshaw and Philip D Stahl (Editors-in-Chief), Encyclopedia of Cell Biology, Waltham, MA: Academic Press, Vol 2,, 354-362.
Aguilera-Gomez, A., van Oorschot, M.M., Veenendaal, T., Rabouille, C., 2016. In vivo vizualisation of mono-ADP-ribosylation by dPARP16 upon amino-acid starvation. Elife 5.
Aguilera-Gomez, A., Zacharogianni, M., van Oorschot, M.M., Genau, H.M., Veenendaal, T., et al., 2017. Phospho-Rasputin stabilization by Sec16 is required for stress granules formation upon amino-acid starvation. . Submitted.
Aizer, A., Kalo, A., Kafri, P., Shraga, A., Ben-Yishay, R., et al., 2014. Quantifying mRNA targeting to P-bodies in living human cells reveals their dual role in mRNA decay and storage. J Cell Sci 127, 4443-4456.
Akerfelt, M., Trouillet, D., Mezger, V., Sistonen, L., 2007. Heat shock factors at a crossroad between stress and development. Ann N Y Acad Sci 1113, 15-27.
Alberti, S., Halfmann, R., King, O., Kapila, A., Lindquist, S., 2009. A systematic survey identifies prions and illuminates sequence features of prionogenic proteins. Cell 137, 146-158.
Alexander, A., Cai, S.L., Kim, J., Nanez, A., Sahin, M., et al., 2010. ATM signals to TSC2 in the cytoplasm to

regulate mTORC1 in response to ROS. Proc Natl Acad Sci U S A 107, 4153-4158.
Anderson, P., Kedersha, N., 2002. Stressful initiations. J Cell Sci 115, 3227-3234.
Anderson, P., Kedersha, N., 2008. Stress granules: the Tao of RNA triage. Trends Biochem Sci 33, 141-150.
Antonny, B., Gounon, P., Schekman, R., Orci, L., 2003. Self-assembly of minimal COPII cages. EMBO Rep 4, 419-424.
Antonny, B., Madden, D., Hamamoto, S., Orci, L., Schekman, R., 2001. Dynamics of the COPII coat with GTP and stable analogues. Nat Cell Biol 3, 531-537.
Aridor, M., Balch, W.E., 2000. Kinase signaling initiates coat complex II (COPII) recruitment and export from the mammalian endoplasmic reticulum. J Biol Chem 275, 35673-35676.
Aridor, M., Weissman, J., Bannykh, S., Nuoffer, C., Balch, W.E., 1998. Cargo selection by the COPII budding machinery during export from the ER. J Cell Biol 141, 61-70.
Arimoto, K., Fukuda, H., Imajoh-Ohmi, S., Saito, H., Takekawa, M., 2008. Formation of stress granules inhibits apoptosis by suppressing stress-responsive MAPK pathways. Nat Cell Biol 10, 1324-1332.
Asherie, N., Lomakin, A., Benedek, G.B., 1996. Phase Diagram of Colloidal Solutions. Phys Rev Lett 77, 4832-4835.
Audas, T.E., Audas, D.E., Jacob, M.D., Ho, J.J., Khacho, M., et al., 2016. Adaptation to Stressors by Systemic Protein Amyloidogenesis. Dev Cell 39, 155-168.
Baird, T.D., Wek, R.C., 2012. Eukaryotic initiation factor 2 phosphorylation and translational control in metabolism. Adv Nutr 3, 307-321.
Balch, W.E., McCaffery, J.M., Plutner, H., Farquhar, M.G., 1994. Vesicular stomatitis virus glycoprotein is sorted and concentrated during export from the endoplasmic reticulum. Cell 76, 841-852.
Balch, W.E., Morimoto, R.I., Dillin, A., Kelly, J.W., 2008. Adapting proteostasis for disease intervention. Science 319, 916-919.
Banani, S.F., Rice, A.M., Peeples, W.B., Lin, Y., Jain, S., et al., 2016. Compositional Control of Phase-Separated Cellular Bodies. Cell 166, 651-663.
Banfield, D.K., 2011. Mechanisms of protein retention in the Golgi. Cold Spring Harb Perspect Biol 3, a005264.
Bannykh, S.I., Balch, W.E., 1997. Membrane dynamics at the endoplasmic reticulum-Golgi interface. J Cell Biol 138, 1-4.
Bannykh, S.I., Rowe, T., Balch, W.E., 1996. The organization of endoplasmic reticulum export complexes. J Cell Biol 135, 19-35.
Barbarese, E., Ifrim, M.F., Hsieh, L., Guo, C., Tatavarty, V., et al., 2013. Conditional knockout of tumor overexpressed gene in mouse neurons affects RNA granule assembly, granule translation, LTP and short term habituation. PLoS One 8, e69989.
Bard, F., Chia, J., 2016. Cracking the Glycome Encoder: Signaling, Trafficking, and Glycosylation. Trends Cell Biol 26, 379-388.
Barlowe, C., Orci, L., Yeung, T., Hosobuchi, M., Hamamoto, S., et al., 1994. COPII: a membrane coat formed by Sec proteins that drive vesicle budding from the endoplasmic reticulum. Cell 77, 895-907.
Barlowe, C., Schekman, R., 1993. SEC12 encodes a guanine-nucleotide-exchange factor essential for transport vesicle budding from the ER. Nature 365, 347-349.
Barlowe, C.K., Miller, E.A., 2013. Secretory protein biogenesis and traffic in the early secretory pathway. Genetics 193, 383-410.
Berchowitz, L.E., Kabachinski, G., Walker, M.R., Carlile, T.M., Gilbert, W.V., et al., 2015. Regulated Formation of an Amyloid-like Translational Repressor Governs Gametogenesis. Cell 163, 406-418.
Bertolotti, A., Zhang, Y., Hendershot, L.M., Harding, H.P., Ron, D., 2000. Dynamic interaction of BiP and ER stress transducers in the unfolded-protein response. Nat Cell Biol 2, 326-332.
Bertrand, E., Chartrand, P., Schaefer, M., Shenoy, S.M., Singer, R.H., et al., 1998. Localization of ASH1 mRNA particles in living yeast. Mol Cell 2, 437-445.
Bhandari, D., Zhang, J., Menon, S., Lord, C., Chen, S., et al., 2013. Sit4p/PP6 regulates ER-to-Golgi traffic by controlling the dephosphorylation of COPII coat subunits. Mol Biol Cell 24, 2727-2738.
Bharucha, N., Liu, Y., Papanikou, E., McMahon, C., Esaki, M., et al., 2013. Sec16 influences transitional ER sites by regulating rather than organizing COPII. Mol Biol Cell 24, 3406-3419.
Bhattacharyya, D., Glick, B.S., 2007. Two mammalian Sec16 homologues have nonredundant functions in endoplasmic reticulum (ER) export and transitional ER organization. Mol Biol Cell 18, 839-849.
Bhullar, D.S., Sheahan, M.B., Rose, R.J., 2016. RNA processing body (P-body) dynamics in mesophyll protoplasts re-initiating cell division. Protoplasma.
Bi, X., Corpina, R.A., Goldberg, J., 2002. Structure of the Sec23/24-Sar1 pre-budding complex of the COPII vesicle coat. Nature 419, 271-277.
Bi, X., Mancias, J.D., Goldberg, J., 2007. Insights into COPII coat nucleation from the structure of Sec23.Sar1 complexed with the active fragment of Sec31. Dev Cell 13, 635-645.
Bielli, A., Haney, C.J., Gabreski, G., Watkins, S.C., Bannykh, S.I., et al., 2005. Regulation of Sar1 NH2 terminus by GTP binding and hydrolysis promotes membrane deformation to control COPII vesicle fission. J Cell Biol 171, 919-924.
Boisvert, F.M., van Koningsbruggen, S., Navascues, J., Lamond, A.I., 2007. The multifunctional nucleolus. Nat Rev Mol Cell Biol 8, 574-585.
Bornens, M., 2002. Centrosome composition and microtubule anchoring mechanisms. Curr Opin Cell Biol 14, 25-34.
Branco, M.R., Pombo, A., 2006. Intermingling of chromosome territories in interphase suggests role in translocations and transcription-dependent associations. PLoS Biol 4, e138.
Brangwynne, C.P., Eckmann, C.R., Courson, D.S., Rybarska, A., Hoege, C., et al., 2009. Germline P granules are

liquid droplets that localize by controlled dissolution/condensation. Science 324, 1729-1732.
Brangwynne, C.P., Mitchison, T.J., Hyman, A.A., 2011. Active liquid-like behavior of nucleoli determines their size and shape in Xenopus laevis oocytes. Proc Natl Acad Sci U S A 108, 4334-4339.
Bray, A.J., 1994. Theory of phase-ordering kinetics. Adv Phys 43, 357-459.
Buchan, J.R., 2014. mRNP granules. Assembly, function, and connections with disease. RNA Biol 11, 1019-1030.
Buchan, J.R., Muhlrad, D., Parker, R., 2008. P bodies promote stress granule assembly in Saccharomyces cerevisiae. J Cell Biol 183, 441-455.
Buchan, J.R., Parker, R., 2009. Eukaryotic stress granules: the ins and outs of translation. Mol Cell 36, 932-941.
Budnik, A., Stephens, D.J., 2009. ER exit sites--localization and control of COPII vesicle formation. FEBS Lett 583, 3796-3803.
Butterfield, D.A., Di Domenico, F., Barone, E., 2014. Elevated risk of type 2 diabetes for development of Alzheimer disease: a key role for oxidative stress in brain. Biochim Biophys Acta 1842, 1693-1706.
Caceres, L., Nilson, L.A., 2005. Production of gurken in the nurse cells is sufficient for axis determination in the Drosophila oocyte. Development 132, 2345-2353.
Calfon, M., Zeng, H., Urano, F., Till, J.H., Hubbard, S.R., et al., 2002. IRE1 couples endoplasmic reticulum load to secretory capacity by processing the XBP-1 mRNA. Nature 415, 92-96.
Cancino, J., Capalbo, A., Luini, A., 2013. Golgi-dependent signaling: self-coordination of membrane trafficking. Methods Cell Biol 118, 359-382.
Chang, J.S., Tan, L., Wolf, M.R., Schedl, P., 2001. Functioning of the Drosophila orb gene in gurken mRNA localization and translation. Development 128, 3169-3177.
Cheeks, R.J., Canman, J.C., Gabriel, W.N., Meyer, N., Strome, S., et al., 2004. C. elegans PAR proteins function by mobilizing and stabilizing asymmetrically localized protein complexes. Curr Biol 14, 851-862.
Chen, C.Y., Gherzi, R., Ong, S.E., Chan, E.L., Raijmakers, R., et al., 2001. AU binding proteins recruit the exosome to degrade ARE-containing mRNAs. Cell 107, 451-464.
Chen, J.J., London, I.M., 1995. Regulation of protein synthesis by heme-regulated eIF-2 alpha kinase. Trends Biochem Sci 20, 105-108.
Chen, J.J., Throop, M.S., Gehrke, L., Kuo, I., Pal, J.K., et al., 1991. Cloning of the cDNA of the heme-regulated eukaryotic initiation factor 2 alpha (eIF-2 alpha) kinase of rabbit reticulocytes: homology to yeast GCN2 protein kinase and human double-stranded-RNA-dependent eIF-2 alpha kinase. Proc Natl Acad Sci U S A 88, 7729-7733.
Chen, R., Zou, Y., Mao, D., Sun, D., Gao, G., et al., 2014. The general amino acid control pathway regulates mTOR and autophagy during serum/glutamine starvation. J Cell Biol 206, 173-182.
Clark, A., Meignin, C., Davis, I., 2007. A Dynein-dependent shortcut rapidly delivers axis determination transcripts into the Drosophila oocyte. Development 134, 1955-1965.
Cmielova, J., Havelek, R., Soukup, T., Jiroutova, A., Visek, B., et al., 2012. Gamma radiation induces senescence in human adult mesenchymal stem cells from bone marrow and periodontal ligaments. Int J Radiat Biol 88, 393-404.
Codogno, P., Mehrpour, M., Proikas-Cezanne, T., 2011. Canonical and non-canonical autophagy: variations on a common theme of self-eating? Nat Rev Mol Cell Biol 13, 7-12.
Connerly, P.L., Esaki, M., Montegna, E.A., Strongin, D.E., Levi, S., et al., 2005. Sec16 is a determinant of transitional ER organization. Curr Biol 15, 1439-1447.
Damgaard, C.K., Lykke-Andersen, J., 2011. Translational coregulation of 5'TOP mRNAs by TIA-1 and TIAR. Genes Dev 25, 2057-2068.
Davidson, A., Parton, R.M., Rabouille, C., Weil, T.T., Davis, I., 2016. Localized Translation of gurken/TGF-alpha mRNA during Axis Specification Is Controlled by Access to Orb/CPEB on Processing Bodies. Cell Rep 14, 2451-2462.
Davis, S., Wang, J., Zhu, M., Stahmer, K., Lakshminarayan, R., et al., 2016. Sec24 phosphorylation regulates autophagosome abundance during nutrient deprivation. Elife 5.
de Murcia, J.M., Niedergang, C., Trucco, C., Ricoul, M., Dutrillaux, B., et al., 1997. Requirement of poly(ADP-ribose) polymerase in recovery from DNA damage in mice and in cells. Proc Natl Acad Sci U S A 94, 7303-7307.
Decker, C.J., Parker, R., 2002. mRNA decay enzymes: decappers conserved between yeast and mammals. Proc Natl Acad Sci U S A 99, 12512-12514.
Delanoue, R., Herpers, B., Soetaert, J., Davis, I., Rabouille, C., 2007. Drosophila Squid/hnRNP helps Dynein switch from a gurken mRNA transport motor to an ultrastructural static anchor in sponge bodies. Dev Cell 13, 523-538.
Derrick, C.J., Weil, T.T., 2016. Translational control of gurken mRNA in Drosophila development. Cell Cycle, 0.
Dever, T.E., Feng, L., Wek, R.C., Cigan, A.M., Donahue, T.F., et al., 1992. Phosphorylation of initiation factor 2 alpha by protein kinase GCN2 mediates gene-specific translational control of GCN4 in yeast. Cell 68, 585-596.
Dey, S., Sayers, C.M., Verginadis, II, Lehman, S.L., Cheng, Y., et al., 2015. ATF4-dependent induction of heme oxygenase 1 prevents anoikis and promotes metastasis. J Clin Invest 125, 2592-2608.
Dobson, C.M., 1999. Protein misfolding, evolution and disease. Trends Biochem Sci 24, 329-332.
Doi, M., 2013. Soft matter physics. New York: Oxford Univ Press, 257pp.
Dundr, M., Hebert, M.D., Karpova, T.S., Stanek, D., Xu, H., et al., 2004. In vivo kinetics of Cajal body components. The Journal of cell biology 164, 831-842.
Dundr, M., Misteli, T., 2010. Biogenesis of nuclear bodies. Cold Spring Harb Perspect Biol 2, a000711.
Eapen, V.V., Haber, J.E., 2013. DNA damage signaling triggers the cytoplasm-to-vacuole pathway of autophagy to regulate cell cycle progression. Autophagy 9, 440-441.
Elbaum-Garfinkle, S., Kim, Y., Szczepaniak, K., Chen, C.C., Eckmann, C.R., et al., 2015. The disordered P granule protein LAF-1 drives phase separation into droplets with tunable viscosity and dynamics. Proc Natl Acad Sci U

S A 112, 7189-7194.
Erickson, A.H., 1989. Biosynthesis of lysosomal endopeptidases. J Cell Biochem 40, 31-41.
Espenshade, P., Gimeno, R.E., Holzmacher, E., Teung, P., Kaiser, C.A., 1995. Yeast SEC16 gene encodes a multidomain vesicle coat protein that interacts with Sec23p. J Cell Biol 131, 311-324.
Eulalio, A., Behm-Ansmant, I., Schweizer, D., Izaurralde, E., 2007. P-body formation is a consequence, not the cause, of RNA-mediated gene silencing. Mol Cell Biol 27, 3970-3981.
Eystathioy, T., Jakymiw, A., Chan, E.K., Seraphin, B., Cougot, N., et al., 2003. The GW182 protein colocalizes with mRNA degradation associated proteins hDcp1 and hLSm4 in cytoplasmic GW bodies. RNA 9, 1171-1173.
Falahati, H., Pelham-Webb, B., Blythe, S., Wieschaus, E., 2016. Nucleation by rRNA Dictates the Precision of Nucleolus Assembly. Current biology : CB 26, 277-285.
Farber-Katz, S.E., Dippold, H.C., Buschman, M.D., Peterman, M.C., Xing, M., et al., 2014. DNA damage triggers Golgi dispersal via DNA-PK and GOLPH3. Cell 156, 413-427.
Farhan, H., Rabouille, C., 2011. Signalling to and from the secretory pathway. J Cell Sci 124, 171-180.
Feijs, K.L., Forst, A.H., Verheugd, P., Luscher, B., 2013. Macrodomain-containing proteins: regulating new intracellular functions of mono(ADP-ribosyl)ation. Nat Rev Mol Cell Biol 14, 443-451.
Filardo, P., Ephrussi, A., 2003. Bruno regulates gurken during Drosophila oogenesis. Mech Dev 120, 289-297.
Fiorenza, M.T., Farkas, T., Dissing, M., Kolding, D., Zimarino, V., 1995. Complex expression of murine heat shock transcription factors. Nucleic Acids Res 23, 467-474.
Fisher, P., Ungar, D., 2016. Bridging the Gap between Glycosylation and Vesicle Traffic. Front Cell Dev Biol 4, 15.
Fowler, D.M., Koulov, A.V., Alory-Jost, C., Marks, M.S., Balch, W.E., et al., 2006. Functional amyloid formation within mammalian tissue. PLoS Biol 4, e6.
Fujimoto, M., Hayashida, N., Katoh, T., Oshima, K., Shinkawa, T., et al., 2010. A novel mouse HSF3 has the potential to activate nonclassical heat-shock genes during heat shock. Mol Biol Cell 21, 106-116.
Futai, E., Hamamoto, S., Orci, L., Schekman, R., 2004. GTP/GDP exchange by Sec12p enables COPII vesicle bud formation on synthetic liposomes. EMBO J 23, 4146-4155.
Gagne, J.P., Bonicalzi, M.E., Gagne, P., Ouellet, M.E., Hendzel, M.J., et al., 2005. Poly(ADP-ribose) glycohydrolase is a component of the FMRP-associated messenger ribonucleoparticles. Biochem J 392, 499-509.
Gall, J.G., 2003. The centennial of the Cajal body. Nat Rev Mol Cell Biol 4, 975-980.
Gatta, A.T., Levine, T.P., 2016. Piecing Together the Patchwork of Contact Sites. Trends in cell biology.
Ghislat, G., Patron, M., Rizzuto, R., Knecht, E., 2012. Withdrawal of essential amino acids increases autophagy by a pathway involving Ca2+/calmodulin-dependent kinase kinase-beta (CaMKK-beta). J Biol Chem 287, 38625-38636.
Gibbs-Seymour, I., Fontana, P., Rack, J.G., Ahel, I., 2016. HPF1/C4orf27 Is a PARP-1-Interacting Protein that Regulates PARP-1 ADP-Ribosylation Activity. Mol Cell 62, 432-442.
Gibson, B.A., Kraus, W.L., 2012. New insights into the molecular and cellular functions of poly(ADP-ribose) and PARPs. Nat Rev Mol Cell Biol 13, 411-424.
Gill, D.J., Clausen, H., Bard, F., 2011. Location, location, location: new insights into O-GalNAc protein glycosylation. Trends Cell Biol 21, 149-158.
Gillingham, A.K., Munro, S., 2016. Finding the Golgi: Golgin Coiled-Coil Proteins Show the Way. Trends Cell Biol.
Gimeno, R.E., Espenshade, P., Kaiser, C.A., 1995. SED4 encodes a yeast endoplasmic reticulum protein that binds Sec16p and participates in vesicle formation. J Cell Biol 131, 325-338.
Gimeno, R.E., Espenshade, P., Kaiser, C.A., 1996. COPII coat subunit interactions: Sec24p and Sec23p bind to adjacent regions of Sec16p. Mol Biol Cell 7, 1815-1823.
Glick, B.S., Nakano, A., 2009. Membrane traffic within the Golgi apparatus. Annu Rev Cell Dev Biol 25, 113-132.
Goldschmidt, L., Teng, P.K., Riek, R., Eisenberg, D., 2010. Identifying the amylome, proteins capable of forming amyloid-like fibrils. Proc Natl Acad Sci U S A 107, 3487-3492.
Goodson, M.L., Sarge, K.D., 1995. Heat-inducible DNA binding of purified heat shock transcription factor 1. J Biol Chem 270, 2447-2450.
Gorlach, A., Bertram, K., Hudecova, S., Krizanova, O., 2015. Calcium and ROS: A mutual interplay. Redox Biol 6, 260-271.
Gupta, K.K., Paulson, B.A., Folker, E.S., Charlebois, B., Hunt, A.J., et al., 2009. Minimal plus-end tracking unit of the cytoplasmic linker protein CLIP-170. J Biol Chem 284, 6735-6742.
Halazonetis, T.D., Gorgoulis, V.G., Bartek, J., 2008. An oncogene-induced DNA damage model for cancer development. Science 319, 1352-1355.
Halfmann, R., 2016. A glass menagerie of low complexity sequences. Current opinion in structural biology 38, 18-25.
Hamasaki, M., Noda, T., Ohsumi, Y., 2003. The early secretory pathway contributes to autophagy in yeast. Cell Struct Funct 28, 49-54.
Hammond, A.T., Glick, B.S., 2000. Dynamics of transitional endoplasmic reticulum sites in vertebrate cells. Mol Biol Cell 11, 3013-3030.
Han, T.W., Kato, M., Xie, S., Wu, L.C., Mirzaei, H., et al., 2012. Cell-free formation of RNA granules: bound RNAs identify features and components of cellular assemblies. Cell 149, 768-779.
Harding, H.P., Zhang, Y., Ron, D., 1999. Protein translation and folding are coupled by an endoplasmic-reticulum-resident kinase. Nature 397, 271-274.
Harding, H.P., Zhang, Y., Zeng, H., Novoa, I., Lu, P.D., et al., 2003. An integrated stress response regulates amino acid metabolism and resistance to oxidative stress. Mol Cell 11, 619-633.
Hatakeyama, K., Nemoto, Y., Ueda, K., Hayaishi, O., 1986. Purification and characterization of poly(ADP-ribose) glycohydrolase. Different modes of action on large and small poly(ADP-ribose). J Biol Chem 261, 14902-14911.

Hay, N., Sonenberg, N., 2004. Upstream and downstream of mTOR. Genes Dev 18, 1926-1945.
He, C., Klionsky, D.J., 2009. Regulation mechanisms and signaling pathways of autophagy. Annu Rev Genet 43, 67-93.
Hershko, A., Ciechanover, A., 1998. The ubiquitin system. Annu Rev Biochem 67, 425-479.
Hetz, C., Martinon, F., Rodriguez, D., Glimcher, L.H., 2011. The unfolded protein response: integrating stress signals through the stress sensor IRE1alpha. Physiol Rev 91, 1219-1243.
Hottiger, M.O., Hassa, P.O., Luscher, B., Schuler, H., Koch-Nolte, F., 2010. Toward a unified nomenclature for mammalian ADP-ribosyltransferases. Trends Biochem Sci 35, 208-219.
Huarte, M., Guttman, M., Feldser, D., Garber, M., Koziol, M.J., et al., 2010. A large intergenic noncoding RNA induced by p53 mediates global gene repression in the p53 response. Cell 142, 409-419.
Hughes, H., Budnik, A., Schmidt, K., Palmer, K.J., Mantell, J., et al., 2009. Organisation of human ER-exit sites: requirements for the localisation of Sec16 to transitional ER. J Cell Sci 122, 2924-2934.
Huntley, M.A., Golding, G.B., 2002. Simple sequences are rare in the Protein Data Bank. Proteins 48, 134-140.
Hyman, A.A., Simons, K., 2012. Cell biology. Beyond oil and water--phase transitions in cells. Science 337, 1047-1049.
Hyman, A.A., Weber, C.A., Julicher, F., 2014. Liquid-liquid phase separation in biology. Annu Rev Cell Dev Biol 30, 39-58.
Isabelle, M., Gagne, J.P., Gallouzi, I.E., Poirier, G.G., 2012. Quantitative proteomics and dynamic imaging reveal that G3BP-mediated stress granule assembly is poly(ADP-ribose)-dependent following exposure to MNNG-induced DNA alkylation. J Cell Sci 125, 4555-4566.
Ivan, V., de Voer, G., Xanthakis, D., Spoorendonk, K.M., Kondylis, V., et al., 2008. Drosophila Sec16 mediates the biogenesis of tER sites upstream of Sar1 through an arginine-rich motif. Mol Biol Cell 19, 4352-4365.
Jackson, L.P., 2014. Structure and mechanism of COPI vesicle biogenesis. Curr Opin Cell Biol 29C, 67-73.
Jacobson, A., 2004. Regulation of mRNA decay: decapping goes solo. Mol Cell 15, 1-2.
Jain, S., Wheeler, J.R., Walters, R.W., Agrawal, A., Barsic, A., et al., 2016. ATPase-Modulated Stress Granules Contain a Diverse Proteome and Substructure. Cell 164, 487-498.
Jaramillo, A.M., Weil, T.T., Goodhouse, J., Gavis, E.R., Schupbach, T., 2008. The dynamics of fluorescently labeled endogenous gurken mRNA in Drosophila. J Cell Sci 121, 887-894.
Jevtov, I., Zacharogianni, M., van Oorschot, M.M., van Zadelhoff, G., Aguilera-Gomez, A., et al., 2015. TORC2 mediates the heat stress response in Drosophila by promoting the formation of stress granules. J Cell Sci 128, 2497-2508.
Johnson, S.C., Rabinovitch, P.S., Kaeberlein, M., 2013. mTOR is a key modulator of ageing and age-related disease. Nature 493, 338-345.
Jung, C.H., Ro, S.H., Cao, J., Otto, N.M., Kim, D.H., 2010. mTOR regulation of autophagy. FEBS Lett 584, 1287-1295.
Jungmichel, S., Rosenthal, F., Altmeyer, M., Lukas, J., Hottiger, M.O., et al., 2013. Proteome-wide identification of poly(ADP-Ribosyl)ation targets in different genotoxic stress responses. Mol Cell 52, 272-285.
Kaiser, C.A., Schekman, R., 1990. Distinct sets of SEC genes govern transport vesicle formation and fusion early in the secretory pathway. Cell 61, 723-733.
Kalogeris, T., Bao, Y., Korthuis, R.J., 2014. Mitochondrial reactive oxygen species: a double edged sword in ischemia/reperfusion vs preconditioning. Redox Biol 2, 702-714.
Karlberg, T., Klepsch, M., Thorsell, A.G., Andersson, C.D., Linusson, A., et al., 2015. Structural basis for lack of ADP-ribosyltransferase activity in poly(ADP-ribose) polymerase-13/zinc finger antiviral protein. J Biol Chem 290, 7336-7344.
Kato, M., Han, T.W., Xie, S., Shi, K., Du, X., et al., 2012. Cell-free formation of RNA granules: low complexity sequence domains form dynamic fibers within hydrogels. Cell 149, 753-767.
Kaufman, D.S., Goligorsky, M.S., Nord, E.P., Graber, M.L., 1993. Perturbation of cell pH regulation by H2O2 in renal epithelial cells. Arch Biochem Biophys 302, 245-254.
Kedersha, N., Stoecklin, G., Ayodele, M., Yacono, P., Lykke-Andersen, J., et al., 2005. Stress granules and processing bodies are dynamically linked sites of mRNP remodeling. J Cell Biol 169, 871-884.
Kedersha, N.L., Gupta, M., Li, W., Miller, I., Anderson, P., 1999. RNA-binding proteins TIA-1 and TIAR link the phosphorylation of eIF-2 alpha to the assembly of mammalian stress granules. J Cell Biol 147, 1431-1442.
Kerfeld, C.A., Sawaya, M.R., Tanaka, S., Nguyen, C.V., Phillips, M., et al., 2005. Protein structures forming the shell of primitive bacterial organelles. Science 309, 936-938.
Khalil, A.M., Guttman, M., Huarte, M., Garber, M., Raj, A., et al., 2009. Many human large intergenic noncoding RNAs associate with chromatin-modifying complexes and affect gene expression. Proc Natl Acad Sci U S A 106, 11667-11672.
Kim, G.D., Choi, Y.H., Dimtchev, A., Jeong, S.J., Dritschilo, A., et al., 1999. Sensing of ionizing radiation-induced DNA damage by ATM through interaction with histone deacetylase. J Biol Chem 274, 31127-31130.
Kim, W.J., Back, S.H., Kim, V., Ryu, I., Jang, S.K., 2005. Sequestration of TRAF2 into stress granules interrupts tumor necrosis factor signaling under stress conditions. Mol Cell Biol 25, 2450-2462.
Kleine, H., Poreba, E., Lesniewicz, K., Hassa, P.O., Hottiger, M.O., et al., 2008. Substrate-assisted catalysis by PARP10 limits its activity to mono-ADP-ribosylation. Mol Cell 32, 57-69.
Knowles, T.P., Vendruscolo, M., Dobson, C.M., 2014. The amyloid state and its association with protein misfolding diseases. Nat Rev Mol Cell Biol 15, 384-396.
Kugler, J.M., Chicoine, J., Lasko, P., 2009. Bicaudal-C associates with a Trailer Hitch/Me31B complex and is required for efficient Gurken secretion. Dev Biol 328, 160-172.
Kung, L.F., Pagant, S., Futai, E., D'Arcangelo, J.G., Buchanan, R., et al., 2012. Sec24p and Sec16p cooperate to regulate the GTP cycle of the COPII coat. EMBO J 31, 1014-1027.

Ladinsky, M.S., Mastronarde, D.N., McIntosh, J.R., Howell, K.E., Staehelin, L.A., 1999. Golgi structure in three dimensions: functional insights from the normal rat kidney cell. J Cell Biol 144, 1135-1149.
Laplante, M., Sabatini, D.M., 2012. mTOR signaling in growth control and disease. Cell 149, 274-293.
Laporte, D., Salin, B., Daignan-Fornier, B., Sagot, I., 2008. Reversible cytoplasmic localization of the proteasome in quiescent yeast cells. J Cell Biol 181, 737-745.
Lederkremer, G.Z., Cheng, Y., Petre, B.M., Vogan, E., Springer, S., et al., 2001. Structure of the Sec23p/24p and Sec13p/31p complexes of COPII. Proc Natl Acad Sci U S A 98, 10704-10709.
Lee, M.C., Orci, L., Hamamoto, S., Futai, E., Ravazzola, M., et al., 2005. Sar1p N-terminal helix initiates membrane curvature and completes the fission of a COPII vesicle. Cell 122, 605-617.
Leung, A., Todorova, T., Ando, Y., Chang, P., 2012. Poly(ADP-ribose) regulates post-transcriptional gene regulation in the cytoplasm. RNA Biol 9, 542-548.
Leung, A.K., 2014. Poly(ADP-ribose): an organizer of cellular architecture. J Cell Biol 205, 613-619.
Leung, A.K., Vyas, S., Rood, J.E., Bhutkar, A., Sharp, P.A., et al., 2011. Poly(ADP-ribose) regulates stress responses and microRNA activity in the cytoplasm. Mol Cell 42, 489-499.
Levin, D.H., Petryshyn, R., London, I.M., 1980. Characterization of double-stranded-RNA-activated kinase that phosphorylates alpha subunit of eukaryotic initiation factor 2 (eIF-2 alpha) in reticulocyte lysates. Proc Natl Acad Sci U S A 77, 832-836.
Lewis, J.D., Tollervey, D., 2000. Like attracts like: getting RNA processing together in the nucleus. Science 288, 1385-1389.
Li, J., McQuade, T., Siemer, A.B., Napetschnig, J., Moriwaki, K., et al., 2012a. The RIP1/RIP3 necrosome forms a functional amyloid signaling complex required for programmed necrosis. Cell 150, 339-350.
Li, P., Banjade, S., Cheng, H.C., Kim, S., Chen, B., et al., 2012b. Phase transitions in the assembly of multivalent signalling proteins. Nature 483, 336-340.
Li, Y.R., King, O.D., Shorter, J., Gitler, A.D., 2013. Stress granules as crucibles of ALS pathogenesis. J Cell Biol 201, 361-372.
Lin, Y., Protter, D.S., Rosen, M.K., Parker, R., 2015. Formation and Maturation of Phase-Separated Liquid Droplets by RNA-Binding Proteins. Mol Cell 60, 208-219.
Lippincott-Schwartz, J., Yuan, L.C., Bonifacino, J.S., Klausner, R.D., 1989. Rapid redistribution of Golgi proteins into the ER in cells treated with brefeldin A: evidence for membrane cycling from Golgi to ER. Cell 56, 801-813.
Little, S.C., Sinsimer, K.S., Lee, J.J., Wieschaus, E.F., Gavis, E.R., 2015. Independent and coordinate trafficking of single Drosophila germ plasm mRNAs. Nat Cell Biol 17, 558-568.
Loewith, R., Hall, M.N., 2011. Target of rapamycin (TOR) in nutrient signaling and growth control. Genetics 189, 1177-1201.
Long, R.M., McNally, M.T., 2003. mRNA decay: x (XRN1) marks the spot. Mol Cell 11, 1126-1128.
Lord, C., Bhandari, D., Menon, S., Ghassemian, M., Nycz, D., et al., 2011. Sequential interactions with Sec23 control the direction of vesicle traffic. Nature 473, 181-186.
Lord, C., Ferro-Novick, S., Miller, E.A., 2013. The highly conserved COPII coat complex sorts cargo from the endoplasmic reticulum and targets it to the golgi. Cold Spring Harb Perspect Biol 5.
Loseva, O., Jemth, A.S., Bryant, H.E., Schuler, H., Lehtio, L., et al., 2010. PARP-3 is a mono-ADP-ribosylase that activates PARP-1 in the absence of DNA. J Biol Chem 285, 8054-8060.
Lukas, J., Lukas, C., Bartek, J., 2011. More than just a focus: The chromatin response to DNA damage and its role in genome integrity maintenance. Nat Cell Biol 13, 1161-1169.
Mabb, A.M., Wuerzberger-Davis, S.M., Miyamoto, S., 2006. PIASy mediates NEMO sumoylation and NF-kappaB activation in response to genotoxic stress. Nat Cell Biol 8, 986-993.
Machamer, C.E., 2015. The Golgi complex in stress and death. Frontiers in neuroscience 9, 421.
Machyna, M., Heyn, P., Neugebauer, K.M., 2013. Cajal bodies: where form meets function. Wiley Interdiscip Rev RNA 4, 17-34.
Magenta, A., Greco, S., Capogrossi, M.C., Gaetano, C., Martelli, F., 2014. Nitric oxide, oxidative stress, and p66Shc interplay in diabetic endothelial dysfunction. Biomed Res Int 2014, 193095.
Mahen, R., Venkitaraman, A.R., 2012. Pattern formation in centrosome assembly. Curr Opin Cell Biol 24, 14-23.
Maji, S.K., Perrin, M.H., Sawaya, M.R., Jessberger, S., Vadodaria, K., et al., 2009. Functional amyloids as natural storage of peptide hormones in pituitary secretory granules. Science 325, 328-332.
Marechal, A., Zou, L., 2013. DNA damage sensing by the ATM and ATR kinases. Cold Spring Harb Perspect Biol 5.
Marin-Bejar, O., Marchese, F.P., Athie, A., Sanchez, Y., Gonzalez, J., et al., 2013. Pint lincRNA connects the p53 pathway with epigenetic silencing by the Polycomb repressive complex 2. Genome Biol 14, R104.
Martinez-Menarguez, J.A., Geuze, H.J., Slot, J.W., Klumperman, J., 1999. Vesicular tubular clusters between the ER and Golgi mediate concentration of soluble secretory proteins by exclusion from COPI-coated vesicles. Cell 98, 81-90.
Matsuda, H., Putzel, G.G., Backman, V., Szleifer, I., 2014. Macromolecular crowding as a regulator of gene transcription. Biophys J 106, 1801-1810.
Matsuoka, K., Orci, L., Amherdt, M., Bednarek, S.Y., Hamamoto, S., et al., 1998. COPII-coated vesicle formation reconstituted with purified coat proteins and chemically defined liposomes. Cell 93, 263-275.
McMillan, D.R., Xiao, X., Shao, L., Graves, K., Benjamin, I.J., 1998. Targeted disruption of heat shock transcription factor 1 abolishes thermotolerance and protection against heat-inducible apoptosis. J Biol Chem 273, 7523-7528.
Meijer, A.J., Codogno, P., 2008. Nutrient sensing: TOR's Ragtime. Nat Cell Biol 10, 881-883.
Meurs, E., Chong, K., Galabru, J., Thomas, N.S., Kerr, I.M., et al., 1990. Molecular cloning and characterization of the human double-stranded RNA-activated protein kinase induced by interferon. Cell 62, 379-390.
Miller, E., Antonny, B., Hamamoto, S., Schekman, R., 2002. Cargo selection into COPII vesicles is driven by the

Sec24p subunit. EMBO J 21, 6105-6113.
Miller, E.A., Beilharz, T.H., Malkus, P.N., Lee, M.C., Hamamoto, S., et al., 2003. Multiple cargo binding sites on the COPII subunit Sec24p ensure capture of diverse membrane proteins into transport vesicles. Cell 114, 497-509.
Miller, E.A., Schekman, R., 2013. COPII - a flexible vesicle formation system. Curr Opin Cell Biol 25, 420-427.
Misteli, T., 2001. The concept of self-organization in cellular architecture. The Journal of cell biology 155, 181-185.
Misteli, T., 2007. Beyond the sequence: cellular organization of genome function. Cell 128, 787-800.
Mitrea, D.M., Kriwacki, R.W., 2016. Phase separation in biology; functional organization of a higher order. Cell Commun Signal 14, 1.
Molliex, A., Temirov, J., Lee, J., Coughlin, M., Kanagaraj, A.P., et al., 2015. Phase Separation by Low Complexity Domains Promotes Stress Granule Assembly and Drives Pathological Fibrillization. Cell 163, 123-133.
Montegna, E.A., Bhave, M., Liu, Y., Bhattacharyya, D., Glick, B.S., 2012. Sec12 binds to Sec16 at transitional ER sites. PLoS One 7, e31156.
Moser, J.J., Fritzler, M.J., 2010. Cytoplasmic ribonucleoprotein (RNP) bodies and their relationship to GW/P bodies. Int J Biochem Cell Biol 42, 828-843.
Mossessova, E., Bickford, L.C., Goldberg, J., 2003. SNARE selectivity of the COPII coat. Cell 114, 483-495.
Mukherjee, D., Gao, M., O'Connor, J.P., Raijmakers, R., Pruijn, G., et al., 2002. The mammalian exosome mediates the efficient degradation of mRNAs that contain AU-rich elements. EMBO J 21, 165-174.
Munder, M.C., Midtvedt, D., Franzmann, T., Nuske, E., Otto, O., et al., 2016. A pH-driven transition of the cytoplasm from a fluid- to a solid-like state promotes entry into dormancy. Elife 5.
Munn, D.H., Sharma, M.D., Baban, B., Harding, H.P., Zhang, Y., et al., 2005. GCN2 kinase in T cells mediates proliferative arrest and anergy induction in response to indoleamine 2,3-dioxygenase. Immunity 22, 633-642.
Nakamura, A., Amikura, R., Hanyu, K., Kobayashi, S., 2001. Me31B silences translation of oocyte-localizing RNAs through the formation of cytoplasmic RNP complex during Drosophila oogenesis. Development 128, 3233-3242.
Nakano, A., Muramatsu, M., 1989. A novel GTP-binding protein, Sar1p, is involved in transport from the endoplasmic reticulum to the Golgi apparatus. J Cell Biol 109, 2677-2691.
Narayanaswamy, R., Levy, M., Tsechansky, M., Stovall, G.M., O'Connell, J.D., et al., 2009. Widespread reorganization of metabolic enzymes into reversible assemblies upon nutrient starvation. Proc Natl Acad Sci U S A 106, 10147-10152.
Nicodemi, M., Pombo, A., 2014. Models of chromosome structure. Curr Opin Cell Biol 28, 90-95.
Nilsson, T., Warren, G., 1994. Retention and retrieval in the endoplasmic reticulum and the Golgi apparatus. Curr Opin Cell Biol 6, 517-521.
Noree, C., Sato, B.K., Broyer, R.M., Wilhelm, J.E., 2010. Identification of novel filament-forming proteins in Saccharomyces cerevisiae and Drosophila melanogaster. J Cell Biol 190, 541-551.
Norvell, A., Wong, J., Randolph, K., Thompson, L., 2015. Wispy and Orb cooperate in the cytoplasmic polyadenylation of localized gurken mRNA. Dev Dyn 244, 1276-1285.
Nott, T.J., Petsalaki, E., Farber, P., Jervis, D., Fussner, E., et al., 2015. Phase transition of a disordered nuage protein generates environmentally responsive membraneless organelles. Mol Cell 57, 936-947.
Oka, T., Nakano, A., 1994. Inhibition of GTP hydrolysis by Sar1p causes accumulation of vesicles that are a functional intermediate of the ER-to-Golgi transport in yeast. J Cell Biol 124, 425-434.
Onomoto, K., Jogi, M., Yoo, J.S., Narita, R., Morimoto, S., et al., 2012. Critical role of an antiviral stress granule containing RIG-I and PKR in viral detection and innate immunity. PLoS One 7, e43031.
Orci, L., Ravazzola, M., Meda, P., Holcomb, C., Moore, H.P., et al., 1991. Mammalian Sec23p homologue is restricted to the endoplasmic reticulum transitional cytoplasm. Proc Natl Acad Sci U S A 88, 8611-8615.
Orlotti, N.I., Cimino-Reale, G., Borghini, E., Pennati, M., Sissi, C., et al., 2012. Autophagy acts as a safeguard mechanism against G-quadruplex ligand-mediated DNA damage. Autophagy 8, 1185-1196.
Orom, U.A., Nielsen, F.C., Lund, A.H., 2008. MicroRNA-10a binds the 5'UTR of ribosomal protein mRNAs and enhances their translation. Mol Cell 30, 460-471.
Oslowski, C.M., Urano, F., 2011. Measuring ER stress and the unfolded protein response using mammalian tissue culture system. Methods Enzymol 490, 71-92.
Oyadomari, S., Harding, H.P., Zhang, Y., Oyadomari, M., Ron, D., 2008. Dephosphorylation of translation initiation factor 2alpha enhances glucose tolerance and attenuates hepatosteatosis in mice. Cell Metab 7, 520-532.
Pagant, S., Wu, A., Edwards, S., Diehl, F., Miller, E.A., 2015. Sec24 is a coincidence detector that simultaneously binds two signals to drive ER export. Curr Biol 25, 403-412.
Palade, G., 1975. Intracellular aspects of the process of protein synthesis. Science 189, 347-358.
Parker, R., Sheth, U., 2007. P bodies and the control of mRNA translation and degradation. Mol Cell 25, 635-646.
Patel, A., Lee, H.O., Jawerth, L., Maharana, S., Jahnel, M., et al., 2015. A Liquid-to-Solid Phase Transition of the ALS Protein FUS Accelerated by Disease Mutation. Cell 162, 1066-1077.
Pelham, H.R., 1982. A regulatory upstream promoter element in the Drosophila hsp 70 heat-shock gene. Cell 30, 517-528.
Peters, L.Z., Hazan, R., Breker, M., Schuldiner, M., Ben-Aroya, S., 2013. Formation and dissociation of proteasome storage granules are regulated by cytosolic pH. J Cell Biol 201, 663-671.
Petrosyan, A., Cheng, P.W., 2014. Golgi fragmentation induced by heat shock or inhibition of heat shock proteins is mediated by non-muscle myosin IIA via its interaction with glycosyltransferases. Cell Stress Chaperones 19, 241-254.
Petrovska, I., Nuske, E., Munder, M.C., Kulasegaran, G., Malinovska, L., et al., 2014. Filament formation by metabolic enzymes is a specific adaptation to an advanced state of cellular starvation. Elife.

Phair, R.D., Misteli, T., 2000. High mobility of proteins in the mammalian cell nucleus. Nature 404, 604-609.
Powers, E.T., Morimoto, R.I., Dillin, A., Kelly, J.W., Balch, W.E., 2009. Biological and chemical approaches to diseases of proteostasis deficiency. Annu Rev Biochem 78, 959-991.
Prigogine, I., Nicolis, G., Babloyantz, A., 1974. Nonequilibrium problems in biological phenomena. Annals of the New York Academy of Sciences 231, 99-105.
Protter, D.S., Parker, R., 2016. Principles and Properties of Stress Granules. Trends Cell Biol 26, 668-679.
Rabouille, C., Alberti, S., 2017. Cell adaptation upon stress: the emerging role of membrane-less compartments. Current opinion in cell biology in press.
Rabouille, C., Linstedt, A.D., 2016. GRASP: A Multitasking Tether. Front Cell Dev Biol 4, 1.
Rajan, R.S., Illing, M.E., Bence, N.F., Kopito, R.R., 2001. Specificity in intracellular protein aggregation and inclusion body formation. Proc Natl Acad Sci U S A 98, 13060-13065.
Rajapakse, I., Groudine, M., 2011. On emerging nuclear order. J Cell Biol 192, 711-721.
Rawson, R.B., 2003. The SREBP pathway--insights from Insigs and insects. Nat Rev Mol Cell Biol 4, 631-640.
Reineke, L.C., Lloyd, R.E., 2015. The stress granule protein G3BP1 recruits protein kinase R to promote multiple innate immune antiviral responses. J Virol 89, 2575-2589.
Reveal, B., Garcia, C., Ellington, A., Macdonald, P.M., 2011. Multiple RNA binding domains of Bruno confer recognition of diverse binding sites for translational repression. RNA Biol 8, 1047-1060.
Richter, M., Bosnali, M., Carstensen, L., Seitz, T., Durchschlag, H., et al., 2010. Computational and experimental evidence for the evolution of a (beta alpha)8-barrel protein from an ancestral quarter-barrel stabilised by disulfide bonds. J Mol Biol 398, 763-773.
Rinnerthaler, M., Bischof, J., Streubel, M.K., Trost, A., Richter, K., 2015. Oxidative stress in aging human skin. Biomolecules 5, 545-589.
Ritz, A.M., Trautwein, M., Grassinger, F., Spang, A., 2014. The prion-like domain in the exomer-dependent cargo Pin2 serves as a trans-Golgi retention motif. Cell Rep 7, 249-260.
Robert, T., Vanoli, F., Chiolo, I., Shubassi, G., Bernstein, K.A., et al., 2011. HDACs link the DNA damage response, processing of double-strand breaks and autophagy. Nature 471, 74-79.
Robinson, M.S., 2015. Forty Years of Clathrin-coated Vesicles. Traffic 16, 1210-1238.
Rodriguez-Vargas, J.M., Ruiz-Magana, M.J., Ruiz-Ruiz, C., Majuelos-Melguizo, J., Peralta-Leal, A., et al., 2012. ROS-induced DNA damage and PARP-1 are required for optimal induction of starvation-induced autophagy. Cell Res 22, 1181-1198.
Ron, D., 2002. Translational control in the endoplasmic reticulum stress response. J Clin Invest 110, 1383-1388.
Russell, S.J., Steger, K.A., Johnston, S.A., 1999. Subcellular localization, stoichiometry, and protein levels of 26 S proteasome subunits in yeast. J Biol Chem 274, 21943-21952.
Saftig, P., Klumperman, J., 2009. Lysosome biogenesis and lysosomal membrane proteins: trafficking meets function. Nat Rev Mol Cell Biol 10, 623-635.
Saha, S., Weber, C.A., Nousch, M., Adame-Arana, O., Hoege, C., et al., 2016. Polar Positioning of Phase-Separated Liquid Compartments in Cells Regulated by an mRNA Competition Mechanism. Cell 166, 1572-1584 e1516.
Sato, K., Nakano, A., 2005. Dissection of COPII subunit-cargo assembly and disassembly kinetics during Sar1p-GTP hydrolysis. Nat Struct Mol Biol 12, 167-174.
Schmidt, H.B., Rohatgi, R., 2016. In Vivo Formation of Vacuolated Multi-phase Compartments Lacking Membranes. Cell Rep 16, 1228-1236.
Schroder, M., Kaufman, R.J., 2005. ER stress and the unfolded protein response. Mutat Res 569, 29-63.
Schweizer, A., Matter, K., Ketcham, C.M., Hauri, H.P., 1991. The isolated ER-Golgi intermediate compartment exhibits properties that are different from ER and cis-Golgi. J Cell Biol 113, 45-54.
Shaywitz, D.A., Espenshade, P.J., Gimeno, R.E., Kaiser, C.A., 1997. COPII subunit interactions in the assembly of the vesicle coat. J Biol Chem 272, 25413-25416.
Sheth, U., Parker, R., 2003. Decapping and decay of messenger RNA occur in cytoplasmic processing bodies. Science 300, 805-808.
Sheth, U., Pitt, J., Dennis, S., Priess, J.R., 2010. Perinuclear P granules are the principal sites of mRNA export in adult C. elegans germ cells. Development 137, 1305-1314.
Shindiapina, P., Barlowe, C., 2010. Requirements for transitional endoplasmic reticulum site structure and function in Saccharomyces cerevisiae. Mol Biol Cell 21, 1530-1545.
Snee, M.J., Macdonald, P.M., 2009. Dynamic organization and plasticity of sponge bodies. Dev Dyn 238, 918-930.
Soderholm, J., Bhattacharyya, D., Strongin, D., Markovitz, V., Connerly, P.L., et al., 2004. The transitional ER localization mechanism of Pichia pastoris Sec12. Dev Cell 6, 649-659.
Souquere, S., Mollet, S., Kress, M., Dautry, F., Pierron, G., et al., 2009. Unravelling the ultrastructure of stress granules and associated P-bodies in human cells. J Cell Sci 122, 3619-3626.
Spike, C.A., Strome, S., 2003. Germ plasm: protein degradation in the soma. Curr Biol 13, R837-839.
Sprangers, J., Rabouille, C., 2015. SEC16 in COPII coat dynamics at ER exit sites. Biochem Soc Trans 43, 97-103.
Stagg, S.M., LaPointe, P., Razvi, A., Gurkan, C., Potter, C.S., et al., 2008. Structural basis for cargo regulation of COPII coat assembly. Cell 134, 474-484.
Stephens, D.J., Lin-Marq, N., Pagano, A., Pepperkok, R., Paccaud, J.P., 2000. COPI-coated ER-to-Golgi transport complexes segregate from COPII in close proximity to ER exit sites. J Cell Sci 113 (Pt 12), 2177-2185.
Stinchcombe, J.C., Nomoto, H., Cutler, D.F., Hopkins, C.R., 1995. Anterograde and retrograde traffic between the rough endoplasmic reticulum and the Golgi complex. J Cell Biol 131, 1387-1401.
Strome, S., Wood, W.B., 1983. Generation of asymmetry and segregation of germ-line granules in early C. elegans embryos. Cell 35, 15-25.
Su, X., Ditlev, J.A., Hui, E., Xing, W., Banjade, S., et al., 2016. Phase separation of signaling molecules promotes T cell receptor signal transduction. Science 352, 595-599.

Supek, F., Madden, D.T., Hamamoto, S., Orci, L., Schekman, R., 2002. Sec16p potentiates the action of COPII proteins to bud transport vesicles. J Cell Biol 158, 1029-1038.
Tabata, K.V., Sato, K., Ide, T., Nishizaka, T., Nakano, A., et al., 2009. Visualization of cargo concentration by COPII minimal machinery in a planar lipid membrane. EMBO J 28, 3279-3289.
Takahara, T., Maeda, T., 2012. Transient sequestration of TORC1 into stress granules during heat stress. Mol Cell 47, 242-252.
Tang, B.L., Wang, Y., Ong, Y.S., Hong, W., 2005. COPII and exit from the endoplasmic reticulum. Biochim Biophys Acta 1744, 293-303.
Thedieck, K., Holzwarth, B., Prentzell, M.T., Boehlke, C., Klasener, K., et al., 2013. Inhibition of mTORC1 by astrin and stress granules prevents apoptosis in cancer cells. Cell 154, 859-874.
Tourriere, H., Chebli, K., Zekri, L., Courselaud, B., Blanchard, J.M., et al., 2003. The RasGAP-associated endoribonuclease G3BP assembles stress granules. J Cell Biol 160, 823-831.
Tran, H., Brunet, A., Grenier, J.M., Datta, S.R., Fornace, A.J., Jr., et al., 2002. DNA repair pathway stimulated by the forkhead transcription factor FOXO3a through the Gadd45 protein. Science 296, 530-534.
Tripathi, D.N., Chowdhury, R., Trudel, L.J., Tee, A.R., Slack, R.S., et al., 2013. Reactive nitrogen species regulate autophagy through ATM-AMPK-TSC2-mediated suppression of mTORC1. Proc Natl Acad Sci U S A 110, E2950-2957.
Uversky, V.N., 2002. Natively unfolded proteins: a point where biology waits for physics. Protein Sci 11, 739-756.
Uversky, V.N., 2017. How to Predict Disorder in a Protein of Interest. Methods Mol Biol 1484, 137-158.
van der Laan, M., Horvath, S.E., Pfanner, N., 2016. Mitochondrial contact site and cristae organizing system. Current opinion in cell biology 41, 33-42.
Velimezi, G., Liontos, M., Vougas, K., Roumeliotis, T., Bartkova, J., et al., 2013. Functional interplay between the DNA-damage-response kinase ATM and ARF tumour suppressor protein in human cancer. Nat Cell Biol 15, 967-977.
Villasenor, R., Kalaidzidis, Y., Zerial, M., 2016. Signal processing by the endosomal system. Curr Opin Cell Biol 39, 53-60.
Voeltz, G.K., Rolls, M.M., Rapoport, T.A., 2002. Structural organization of the endoplasmic reticulum. EMBO Rep 3, 944-950.
Vyas, S., Matic, I., Uchima, L., Rood, J., Zaja, R., et al., 2014. Family-wide analysis of poly(ADP-ribose) polymerase activity. Nat Commun 5, 4426.
Walsh, I., Martin, A.J., Di Domenico, T., Tosatto, S.C., 2012. ESpritz: accurate and fast prediction of protein disorder. Bioinformatics 28, 503-509.
Wang, J.T., Smith, J., Chen, B.C., Schmidt, H., Rasoloson, D., et al., 2014. Regulation of RNA granule dynamics by phosphorylation of serine-rich, intrinsically disordered proteins in C. elegans. Elife 3, e04591.
Wang, Y., Cortez, D., Yazdi, P., Neff, N., Elledge, S.J., et al., 2000. BASC, a super complex of BRCA1-associated proteins involved in the recognition and repair of aberrant DNA structures. Genes Dev 14, 927-939.
Wang, Z.H., Rabouille, C., Geisbrecht, E.R., 2015. Loss of a Clueless-dGRASP complex results in ER stress and blocks Integrin exit from the perinuclear endoplasmic reticulum in Drosophila larval muscle. Biol Open 4, 636-648.
Watson, P., Townley, A.K., Koka, P., Palmer, K.J., Stephens, D.J., 2006. Sec16 defines endoplasmic reticulum exit sites and is required for secretory cargo export in mammalian cells. Traffic 7, 1678-1687.
Weber, S.C., Brangwynne, C.P., 2012. Getting RNA and protein in phase. Cell 149, 1188-1191.
Weidner, J., Wang, C., Prescianotto-Baschong, C., Estrada, A.F., Spang, A., 2014. The polysome-associated proteins Scp160 and Bfr1 prevent P body formation under normal growth conditions. J Cell Sci 127, 1992-2004.
Weil, T.T., Parton, R.M., Herpers, B., Soetaert, J., Veenendaal, T., et al., 2012. Drosophila patterning is established by differential association of mRNAs with P bodies. Nat Cell Biol 14, 1305-1313.
Weissman, J.T., Plutner, H., Balch, W.E., 2001. The mammalian guanine nucleotide exchange factor mSec12 is essential for activation of the Sar1 GTPase directing endoplasmic reticulum export. Traffic 2, 465-475.
Wek, R.C., Jiang, H.Y., Anthony, T.G., 2006. Coping with stress: eIF2 kinases and translational control. Biochem Soc Trans 34, 7-11.
Welsby, I., Hutin, D., Gueydan, C., Kruys, V., Rongvaux, A., et al., 2014. PARP12, an interferon-stimulated gene involved in the control of protein translation and inflammation. J Biol Chem 289, 26642-26657.
Whittle, J.R., Schwartz, T.U., 2010. Structure of the Sec13-Sec16 edge element, a template for assembly of the COPII vesicle coat. J Cell Biol 190, 347-361.
Wilsch-Brauninger, M., Schwarz, H., Nusslein-Volhard, C., 1997. A sponge-like structure involved in the association and transport of maternal products during Drosophila oogenesis. J Cell Biol 139, 817-829.
Wippich, F., Bodenmiller, B., Trajkovska, M.G., Wanka, S., Aebersold, R., et al., 2013. Dual specificity kinase DYRK3 couples stress granule condensation/dissolution to mTORC1 signaling. Cell 152, 791-805.
Witte, K., Schuh, A.L., Hegermann, J., Sarkeshik, A., Mayers, J.R., et al., 2011. TFG-1 function in protein secretion and oncogenesis. Nat Cell Biol 13, 550-558.
Wolf, N., Priess, J., Hirsh, D., 1983. Segregation of germline granules in early embryos of Caenorhabditis elegans: an electron microscopic analysis. J Embryol Exp Morphol 73, 297-306.
Wong, L.C., Costa, A., McLeod, I., Sarkeshik, A., Yates, J., 3rd, et al., 2011. The functioning of the Drosophila CPEB protein Orb is regulated by phosphorylation and requires casein kinase 2 activity. PLoS One 6, e24355.
Wong, P.M., Feng, Y., Wang, J., Shi, R., Jiang, X., 2015. Regulation of autophagy by coordinated action of mTORC1 and protein phosphatase 2A. Nat Commun 6, 8048.
Wu, C.J., Conze, D.B., Li, T., Srinivasula, S.M., Ashwell, J.D., 2006. Sensing of Lys 63-linked polyubiquitination by NEMO is a key event in NF-kappaB activation [corrected]. Nat Cell Biol 8, 398-406.
Wullschleger, S., Loewith, R., Hall, M.N., 2006. TOR signaling in growth and metabolism. Cell 124, 471-484.

Xu, J., Chua, N.H., 2011. Processing bodies and plant development. Curr Opin Plant Biol 14, 88-93.
Xue, B., Dunker, A.K., Uversky, V.N., 2012. Orderly order in protein intrinsic disorder distribution: disorder in 3500 proteomes from viruses and the three domains of life. J Biomol Struct Dyn 30, 137-149.
Yan, N., Macdonald, P.M., 2004. Genetic interactions of Drosophila melanogaster arrest reveal roles for translational repressor Bruno in accumulation of Gurken and activity of Delta. Genetics 168, 1433-1442.
Yang, Z., Jakymiw, A., Wood, M.R., Eystathioy, T., Rubin, R.L., et al., 2004. GW182 is critical for the stability of GW bodies expressed during the cell cycle and cell proliferation. J Cell Sci 117, 5567-5578.
Yorimitsu, T., Sato, K., 2012. Insights into structural and regulatory roles of Sec16 in COPII vesicle formation at ER exit sites. Mol Biol Cell 23, 2930-2942.
Yoshida, H., Haze, K., Yanagi, H., Yura, T., Mori, K., 1998. Identification of the cis-acting endoplasmic reticulum stress response element responsible for transcriptional induction of mammalian glucose-regulated proteins. Involvement of basic leucine zipper transcription factors. J Biol Chem 273, 33741-33749.
Yoshida, H., Matsui, T., Hosokawa, N., Kaufman, R.J., Nagata, K., et al., 2003. A time-dependent phase shift in the mammalian unfolded protein response. Dev Cell 4, 265-271.
Yoshida, H., Okada, T., Haze, K., Yanagi, H., Yura, T., et al., 2000. ATF6 activated by proteolysis binds in the presence of NF-Y (CBF) directly to the cis-acting element responsible for the mammalian unfolded protein response. Mol Cell Biol 20, 6755-6767.
Yoshihisa, T., Barlowe, C., Schekman, R., 1993. Requirement for a GTPase-activating protein in vesicle budding from the endoplasmic reticulum. Science 259, 1466-1468.
Zacharogianni, M., Aguilera Gomez, A., Veenendaal, T., Smout, J., Rabouille, C., 2014. A stress assembly that confers cell viability by preserving ERES components during amino-acid starvation. Elife 3.
Zacharogianni, M., Kondylis, V., Tang, Y., Farhan, H., Xanthakis, D., et al., 2011. ERK7 is a negative regulator of protein secretion in response to amino-acid starvation by modulating Sec16 membrane association. EMBO J 30, 3684-3700.
Zhang, Q., Ragnauth, C., Greener, M.J., Shanahan, C.M., Roberts, R.G., 2002a. The Nesprins Are Giant Actin-Binding Proteins, Orthologous to Drosophila melanogaster Muscle Protein MSP-300. Genomics 80, 473-481.
Zhang, Y., Huang, L., Zhang, J., Moskophidis, D., Mivechi, N.F., 2002b. Targeted disruption of hsf1 leads to lack of thermotolerance and defines tissue-specific regulation for stress-inducible Hsp molecular chaperones. J Cell Biochem 86, 376-393.
Zhong, M., Orosz, A., Wu, C., 1998. Direct sensing of heat and oxidation by Drosophila heat shock transcription factor. Mol Cell 2, 101-108.
Zhu, L., Brangwynne, C.P., 2015. Nuclear bodies: the emerging biophysics of nucleoplasmic phases. Curr Opin Cell Biol 34, 23-30.
Zimmerman, S.B., Trach, S.O., 1991. Estimation of macromolecule concentrations and excluded volume effects for the cytoplasm of Escherichia coli. J Mol Biol 222, 599-620.

Chapter 2

A reversible non-membrane bound stress assembly that confers cell viability by preserving ERES components during amino-acid starvation

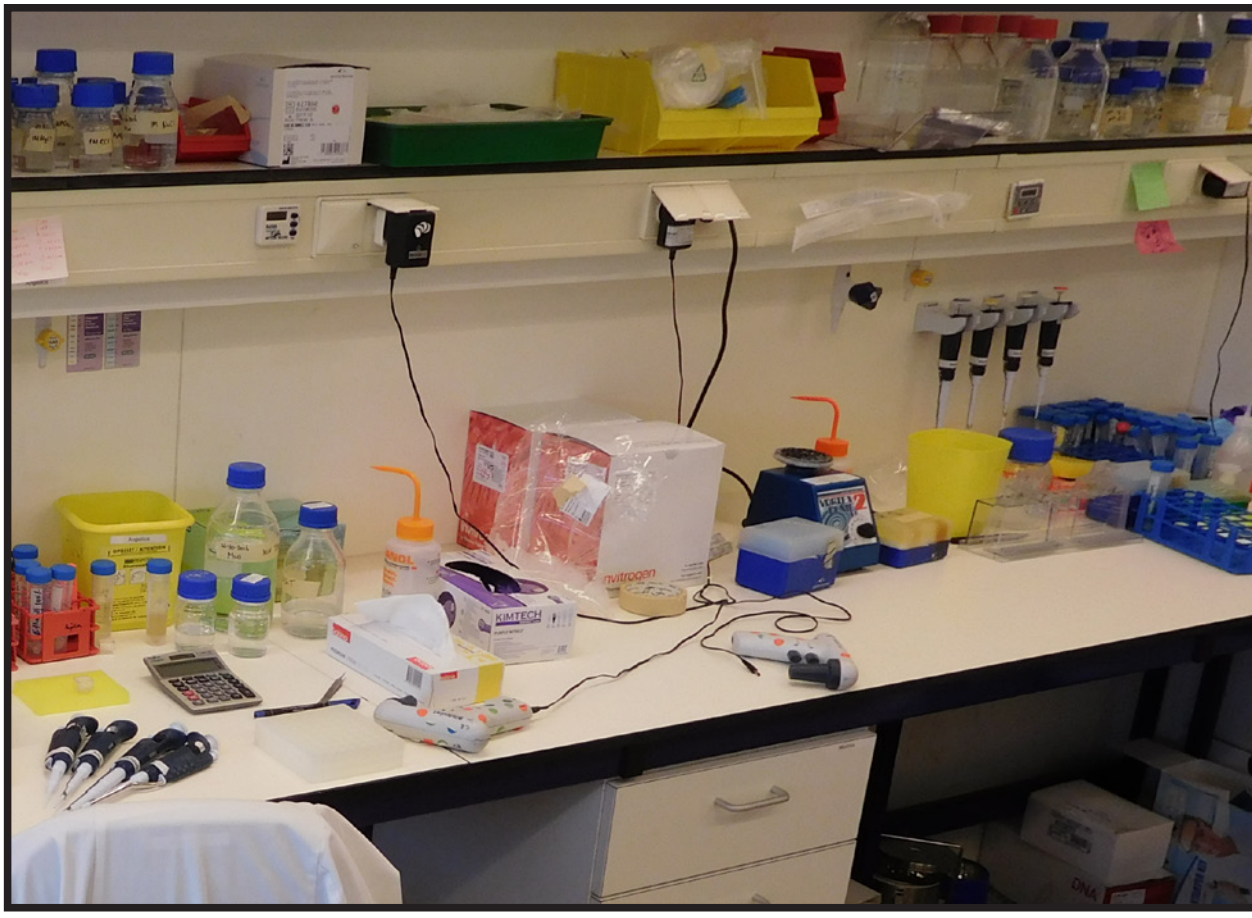

Margarita Zacharogianni, **Angelica Aguilera Gomez**, Tineke Veenendaal, Jan Smout, and Catherine Rabouille (2014)
eLife 2014;3:e04132

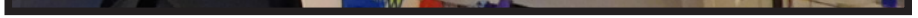

A reversible non-membrane bound stress assembly that confers cell viability by preserving ERES components during amino-acid starvation

Abstract

Nutritional restriction leads to protein translation attenuation that results in the storage and degradation of free mRNAs in cytoplasmic assemblies. Here, we show in Drosophila S2 cells that amino-acid starvation also leads to the inhibition of another major anabolic pathway, the protein transport through the secretory pathway, and to the formation of a novel reversible non-membrane bound stress assembly, the Sec body that incorporates components of the ER exit sites. Sec body formation does not depend on membrane traffic in the early secretory pathway, yet requires both Sec23 and Sec24AB. Sec bodies have liquid droplet-like properties and they act as a protective reservoir for ERES components to rebuild a functional secretory pathway after re-addition of amino-acids acting as a part of a survival mechanism. Taken together, we propose that the formation of these structures is a novel stress response mechanism to provide cell viability during and after nutrient stress.

Introduction

Cell response to nutritional restriction includes stimulation of degradation pathways, such as autophagy as well as attenuating anabolic pathways, such as protein translation (Castilho et al., 2014).

Another key anabolic pathway is protein transport through the secretory pathway. In mammals, one third of the proteome encounters this pathway (Almen et al., 2009; Stevens and Arkin, 2000), such as the proteins delivered to the extracellular medium, the plasma membrane or to other cellular membrane compartments with the exception of mitochondria and the nucleus. After their synthesis at the endoplasmic reticulum, proteins exit the ER at specialized ER exit sites (ERES) defined by a cup-shaped ER overlaying COPII coated vesicles in which newly synthesized proteins are packaged. They then reach the Golgi apparatus where they are further modified, sorted and dispatched to their correct final localization. The COPII coat assembly requires 6 proteins, including the transmembrane protein Sec12 that acts as a GEF for the small GTPase Sar1. GTP-bound Sar1 recruits Sec23/Sec24, the inner COPII coat that in turn recruits Sec13/31, the outer coat (Bard et al., 2006; d'Enfert et al., 1991; Oka et al., 1991; Rothman and Wieland, 1996; Schekman and Orci, 1996). In addition, the large hydrophilic protein Sec16 has been found to play a major role in the COPII assembly and regulation (Hughes et al., 2009; Ivan et al., 2008) (Bharucha et al., 2013; Connerly et al., 2005; Kung et al., 2012) and Sec16 mutation or loss of function leads to a severe impairment trafficking through the secretory pathway.

Stress strongly affects the functional organization of the secretory pathway. For instance, energy deprivation and osmotic shock also block secretion at the level of the ER exit and the cis Golgi, a response mostly triggered by impaired dynamics of the COPI coat, which mediates retrograde transport (Cluett et al., 1993; Jamieson and Palade, 1968; Lee and Linstedt, 1999). Interestingly, GBF1, the GEF of Arf, the small GTPase required for COPI assembly, is phosphorylated and consequently inactivated by AMPK under conditions of nutrient starvation and energy depletion, leading to a block in secretion (Miyamoto et al., 2008). Furthermore, biosynthesis of PI4P in yeast that was shown to play a key role in coordinating trafficking from the Golgi with cell growth seems to also be sensitive to nutrient conditions (Piao et al., 2012). Last, ER stress that elicits the so-called "unfolded protein response" (Shamu et al., 1994) directly impedes on the functional organization of ERES in Drosophila S2 cells (Kondylis et al., 2011) and reduces COPII subunits assembly in human cells (Amodio et al., 2009). Furthermore, we have recently reported that serum starvation of Drosophila S2 cells also results in a distinct change in the ERES organization, namely Sec16 cytoplasmic dispersion away from ERES, in a conserved ERK7 dependent mechanism (Zacharogianni et al., 2011) that leads to protein secretion inhibition.

Here, we focus on amino-acid starvation that leads to the formation of a novel, non-membrane bound cytoplasmic stress assembly that contains ERES components and that we call "Sec bodies" [**Figure 1A** and (Zacharogianni et al., 2011)]. Sec bodies do not represent terminal aggregates. They are reversible, act as a reservoir for ERES components to reconstruct a functional secretory pathway upon re-feeding and are critical for cell survival during stress and upon stress relief. Furthermore, they display properties similar to those of Stress Granules, which place them in the rapidly growing class of cytoplasmic mesoscale assemblies and more specifically, the category of liquid droplets.

Results

Amino-acid starvation of Drosophila S2 cells induces the remodeling of ERES components into Sec bodies.

Amino-acid starvation of Drosophila S2 cells (i.e cell incubation in Krebs Ringers Bicarbonate buffer, KRB, (Gaccioli et al., 2006) leads to inhibition of protein transport through the secretory pathway, as shown by monitoring the plasma membrane localization of the transmembrane reporter Delta (Kondylis et Rabouille, 2003). In cells grown in Schneider's, Delta reaches the plasma membrane, whereas in KRB, it is retained intracellularly (**Figure 1A**). Amino-acid starvation also results in the formation of novel Sec16 positive spherical structures (**Figure 1B**). In addition to Sec16, these structures also contain COPII subunits Sec23, the two Sec24 orthologs Sec24AB (CG1472, Hau) (Norum et al., 2010) and Sec24CD (CG10882,

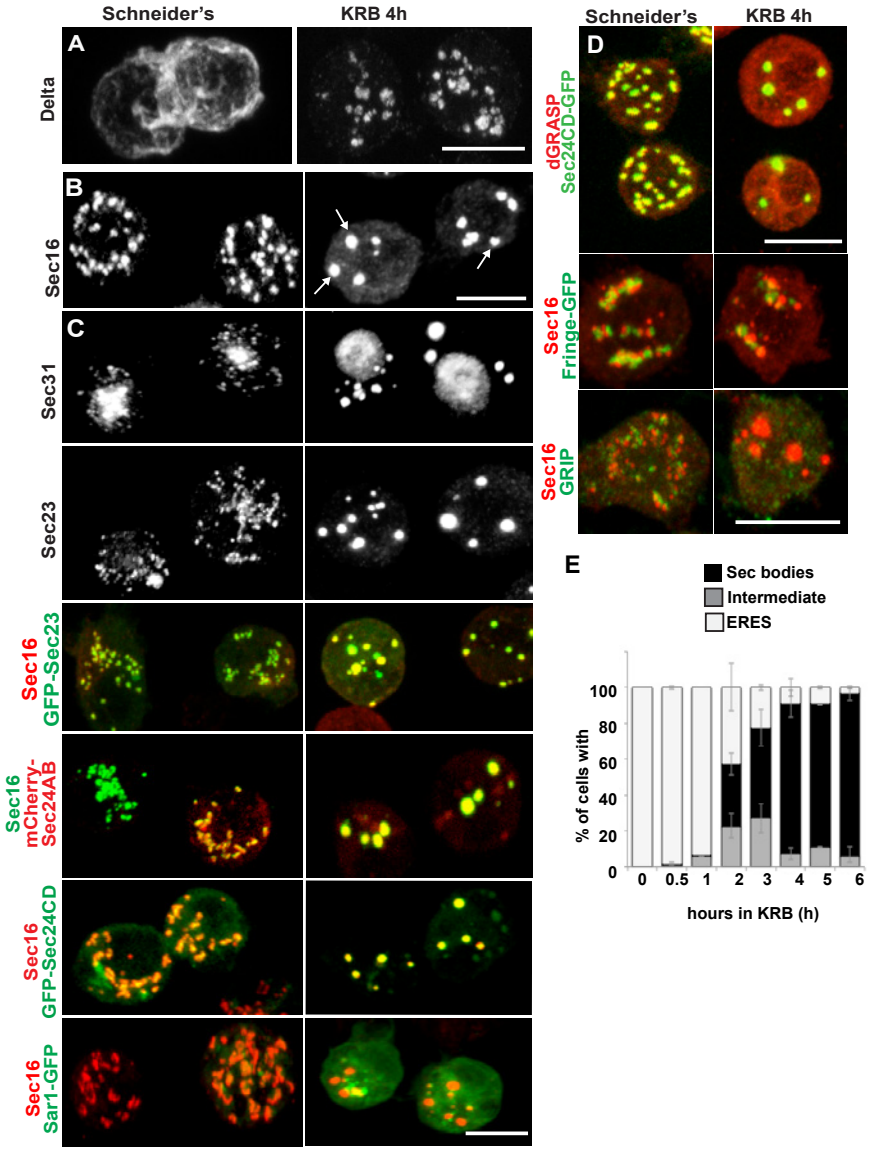

Figure 1: Amino-acid starvation induces the formation of a novel stress assembly in Drosophila S2 cells. A: Immunofluoresence (IF) visualization of Delta-myc (using an anti-Delta antibody) in S2 cells in Schneider's (normal growth conditions) or incubated with Krebs Ringer Bicarbonate buffer (KRB) for 4 h (amino-acid starvation). Note that in Schneider's Delta reaches the plasma membrane whereas it is retained intracellularly in starved cells. B: IF visualization of endogenous Sec16 in Drosophila S2 cells grown in Schneider's and incubated in KRB for 4 h. Note the formation of Sec bodies (arrows). C: IF visualization of Sec31, Sec23 and co-visualization of GFP-Sec23, mCherry-Sec24AB, Sec24CD-GFP, Sar1-GFP with Sec16 in S2 cells in Schneider's and KRB for 4 h. D: IF co-visualization of dGRASP/Sec24CD-GFP, GRIP/Sec16 and Fringe-GFP/Sec16 in S2 cells grown in Schneider's and incubated in KRB for 4 h. E: Kinetics of Sec body formation in S2 cells incubated in KRB over indicated time (up to 6 h) expressed as the percentage of cells exhibiting ERES, intermediates (see materials and methods) and Sec bodies. Scale bars: 10 μm (A-D).

Sten) (Forster et al., 2010) and Sec31 and we therefore name them "Sec bodies". Conversely, Sec bodies do not contain Sar1 (**Figure 1C**), COPI components and clathrin (not shown). They also do not contain dGRASP (that amino-acid starvation drives to complete dispersion in the cytoplasm), the TGN GRIP-domain protein dGCC185, and the Golgi integral membrane protein, Fringe-GFP (**Figure 1D**), although these two latter proteins are often found in close proximity to Sec bodies. The morphology of the ER, on the other hand, does not seem affected by amino-acid starvation (not shown).

Quantitation of this starvation phenotype reveals that although Sec bodies are present in 20% of cells after 1h of amino-acid starvation, it takes between 4 and 6 h to get 90% of the cells displaying the typical Sec body pattern **(Figure 1E)**, that is 7 ± 3 Sec bodies/cell, including 1 to 5 with a diameter comprised between 0.6 and 0.8 μm. Interestingly. 4-6 h corresponds to the end of the autophagy peak, a degradative pathway stimulated by starvation (Klionsky et al., 2012) **(***Figure 1-figure supplement 1A'*) as assessed by appearance of Atg5 punctae (*Figure 1-figure supplement 1A,A'*). In this regard, pharmacological inhibition of autophagy (by wortmanin or bafilomycin) results in a premature formation of Sec bodies (*Figure 1-figure supplement 1B, B'*), consistent with the notion that Sec bodies form in response to a reduced level of intracellular amino-acid concentration.

Given the Sec body content in COPII subunits, we used immuno-electron microscopy (IEM) to test whether they are not simply a collection of COPII vesicles. Sec bodies are electron dense structures and non-membrane bound, although small membrane profiles can occasionally be observed in their core, and often ER is in close proximity (**Figure 2A,** arrows). Sec body formation is associated with the loss of the typical early secretory pathway morphology (Kondylis and Rabouille, 2009). ERES and Golgi stacks are no longer visible.

Sec body formation is specific for amino-acid starvation as heat shock, ER stress (tunicamycin and DTT treatment), glucose starvation, oxidative stress (arsenate treatment), hypoxia (1% O_2 for 19 h) and respiration uncoupling (CCCP for 4 h) do not lead to this response (not shown). Furthermore, to assess whether Sec bodies form in response to the withdrawal of specific amino-acids, cells were incubated in KRB in the presence of individual amino-acids. Histidine, aspartate and asparagine (at 15 mM) strongly prevent Sec body formation but others also do so, albeit more mildly (*Figure 1-figure supplement 2*)**,** suggesting that the signaling pathway is complex. Taken together, we demonstrate that amino-acid starvation leads to the remodeling of ERES components into Sec bodies.

Sec bodies seemingly also form *in vivo*, for instance in ovaries starved either ex vivo or dissected from starved female flies (*Figure 1-figure supplement 3*). We also asked whether they form in mammalian cells. Although we do observe some degrees of remodeling of COPII components upon mammalian cell starvation, it remains unclear whether the resulting structures are Sec bodies (*Figure 1-figure supplement 4*). However, when human Sec16A is transfected in S2 cells, it is efficiently recruited to

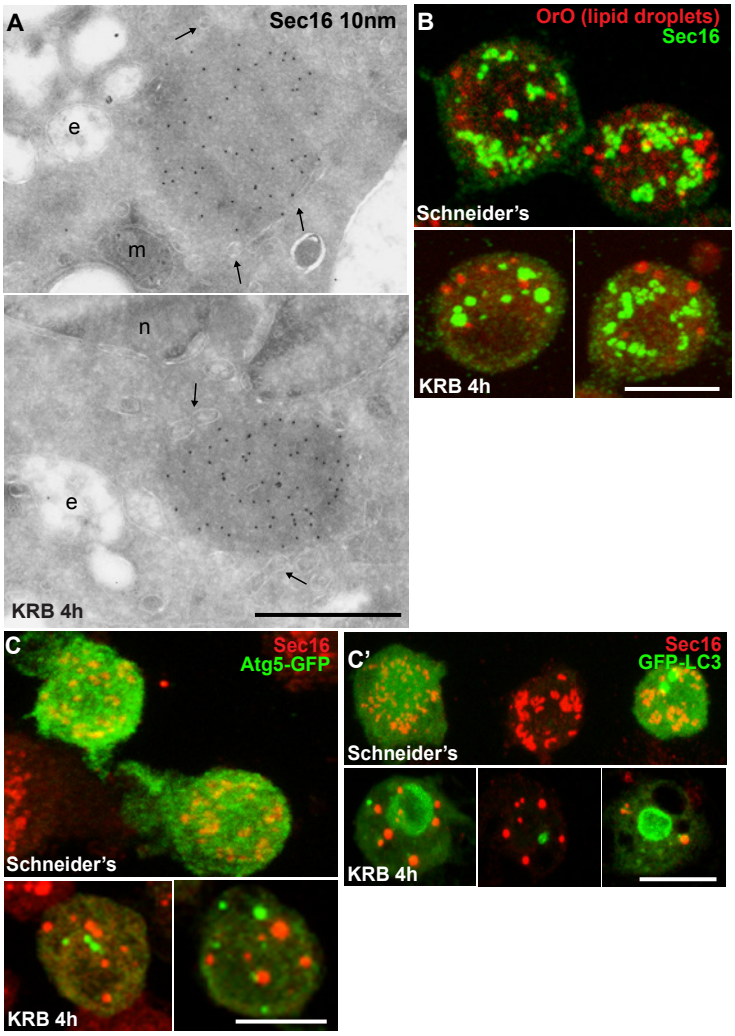

Figure 2: Sec bodies are non-membrane bound structures. **A**: Immuno-electron microscopy (IEM) visualization of Sec16 (10 nm colloidal gold) in Sec bodies in ultrathin sections of S2 cells incubated in KRB for 4 h. Arrows point to membrane in close proximity of Sec bodies. E, endosomes; n, nucleus; m, mitochondria. **B**: Visualization of Sec bodies (Sec16, green) and lipid droplets (marked by oil-red-O, red). Note that 95% of Sec bodies do not co-localize with lipid droplets. **C-C'**: Visualization of Sec bodies (Sec16, red) and Atg5-GFP punctae (C) and GFP-Atg8 (C') after 4 h starvation. Note that 82% of Sec bodies do not co-localize with Atg5 or Atg8 punctae. Scale bars: 500 nm (A); 10 μm (B, C).

Sec bodies along with the endogenous components (*Figure 1-figure supplement 5*). This suggests that in mammalian cells, Sec body formation is perhaps less pronounced due to different signaling events, and not to the properties of the ERES components themselves (at least Sec16).

Sec bodies are a novel stress assembly.

The IEM analysis shows that Sec bodies are not endosomes or lipid droplets, as their ultrastructure is very different from these organelles [see (Teixeira et al., 2003), for lipid droplet ultrastructure in Drosophila]. This is confirmed by the fact that Sec bodies are negative for neutral lipids stained by oil red O that stains lipid droplet content (**Figure 2B**).

As mentioned above, amino-acid starvation is known to induce autophagy, but we demonstrate that Sec bodies are not autophagosomes, as they do not co-localize with Atg5 or Atg8 (**Figure 2C**). Furthermore, as Sec bodies do not contain dGRASP, they are clearly different from the recently described yeast "compartment for unconventional protein secretion" (CUPS) (Bruns et al., 2011).

Amino-acid starvation also results in protein translation inhibition/stalling that leads to the accumulation of untranslated mRNAs. Those are stored in Stress Granules (Anderson and Kedersha, 2008; Kedersha et al., 1999), or degraded in Processing Bodies (P-Bodies), both cytoplasmic ribonucleoprotein particles (RNPs) comprising mRNAs, RNA binding proteins, RNA processing machineries (P-bodies), and translation initiation factors (Stress Granules). We therefore tested whether Sec bodies are related to these structures. We visualized Stress Granules using endogenous FMR1 (Fragile X mental retardation protein 1), an RNA binding protein, and elF4E, a translation initiation factor, and P-bodies with Tral (Trailer Hitch), a like-SM protein. In normal growth conditions, FMR1, elF4E, and Tral are largely diffuse in the cytoplasm and Tral is also found in small punctae representing steady state P-bodies **(Figure 3A)** (Eulalio et al., 2007). Upon amino-acid starvation, as expected, Stress Granules form and P-Bodies enlarge (**Figure 3A**) (Shimada et al., 2011) in agreement with reported phenotypes in many cell types, (Buchan et al., 2008; Stoecklin and Kedersha, 2013). In S2 cells, they form a dual structure, Stress Granule/P-Bodies (SG/PB), in which FMR1 strictly co-localizes with Tral (**Figure 3A**).

Sec bodies and SG/PBs form under the same conditions and in the same time frame, and although they have a spatial relationship and are often found adjacent to each other, Sec bodies are clearly distinct from SG/PBs (**Figure 3B**). To confirm that they are indeed different structures, we also performed IEM of FMR1 and Tral in starved cells (**Figure 3C)** and compared them to Sec bodies **(Figure 2A)**. The FMR1/Tral positive structures are less electron dense, round and regular, and they appear to be often surrounded by mitochondria, which is not the case for Sec bodies.

Taken together, these results show that Sec bodies are a novel stress assembly triggered by amino-acid starvation that is distinct from compartments and structures that are also formed upon this condition.

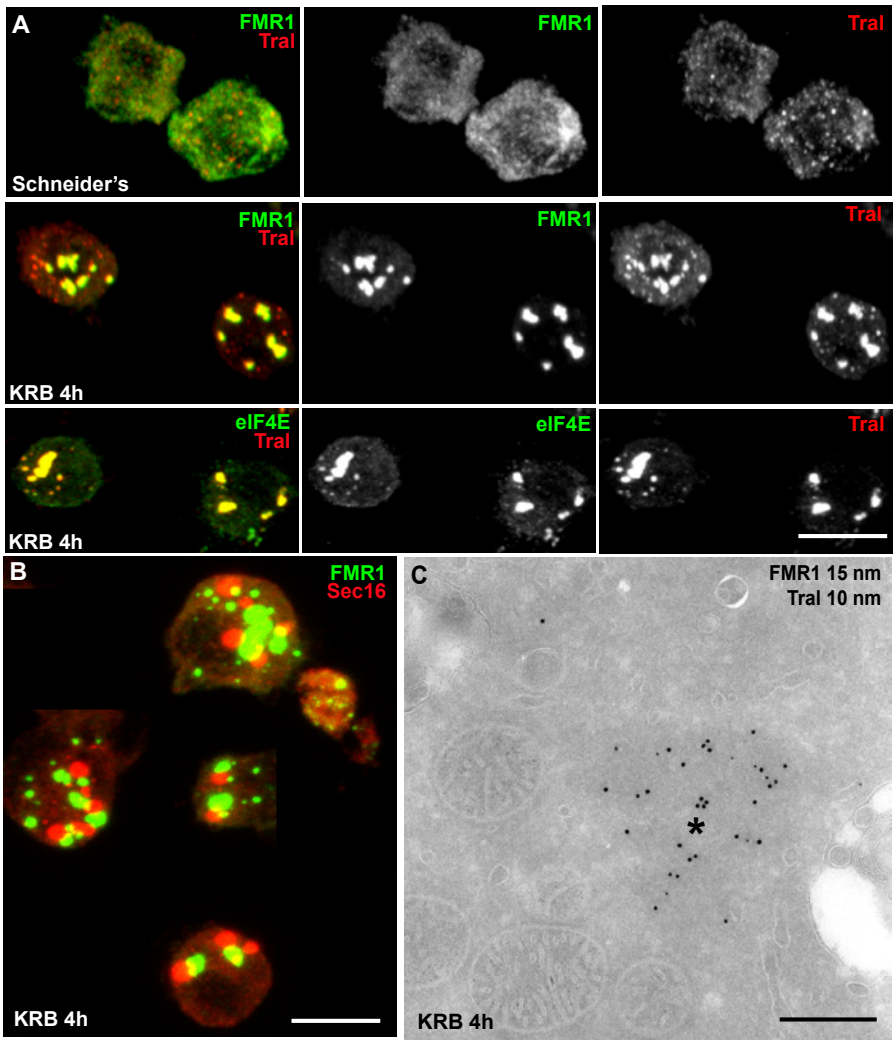

Figure 3: Sec bodies are distinct from Stress Granules and P-bodies. A: IF visualization of endogenous FMR1, eIF4E (green) and Tral (red) in cells growing in Schneider's and incubated in KRB for 4 h. Note upon starvation, Stress Granules (FMR1, eIF4E) form and P-Bodies (Tral) enlarge to co-localize in SG/PBs. **B**: IF visualization of Sec16 (Sec bodies) and FMR1 (SG/PB) in cells incubated in KRB for 4 h. Sec bodies and SG/PBs are distinct structures but have a spatial relationship. **C**: IEM visualization of FRM1 and Tral in ultrathin sections of S2 cell incubated with KRB for 4 h. Note that the Tral and FMR1 positive SG/PBs (asterisk) are clearly different from Sec bodies (Figure 2A). Scale bars: 10 μm (A, B); 500 nm (C, C').

Sec bodies form at ERES.

We then asked how Sec bodies form. Time-lapse imaging of live cells using GFP-Sec23 reveals that once the cells sense amino-acid depletion, a pool of ERES rapidly disappears by releasing their components in the cytoplasm, and the remaining ones

are rapidly transformed into smaller round structures. These small structures do not seem to efficiently fuse with one another. Instead, they seem to act as a seed and grow by recruiting ERES components from the cytoplasm where they were released to reach the typical Sec body size **(Figure 4A, and** *Video supplement 1***).**

To assess, as suggested by the time-lapse, whether Sec bodies form at ERES, we used a truncated version of Sec16, miniSec16 (690-1954), which comprises the minimal Sec16 sequence required for ERES localization (Ivan et al., 2008) (**Figure 4B**) but is not incorporated into Sec bodies upon amino-acid starvation (**Figure 4B').** Instead, miniSec16 remains associated to the cup-shaped ER of the ERES and seems to cradle the forming Sec bodies (marked by endogenous Sec16; **Figure 4B'**). This indicates that Sec bodies form where ERES were present, in line with their observed proximity to ER membrane (arrows in **Figure 2A**).

The time-lapse also suggested that the Sec body enlargement is mediated by recruitment of ERES components that have been dispersed in the cytoplasm. To test this further, we used a Sec16 deletion mutant (NC2-3) that does not localize to ERES and is mostly cytoplasmic (**Figure 4B**) because it lacks the region that mediates its recruitment to ERES (NC2-3) (Ivan et al., 2008). We found that it is efficiently recruited to Sec bodies, showing that Sec16 can be recruited from the cytoplasm and contributes to Sec body enlargement **(Figure 4B")**. Furthermore, this result indicates that the localization to ERES prior to starvation is not necessary for incorporation to Sec bodies. Importantly, the recruitment of this cytosolic mutant is not due to its interaction with endogenous Sec16 as the NC2-3 also contains the Sec16 oligomerization domain (Ivan et al., 2008). This suggests that a distinct Sec16 domain responds to amino-acid starvation.

Taken together, these results show that Sec bodies form (at least initially) where ERES were located and increase in size by recruiting ERES components dispersed in the cytoplasm.

Sec body assembly does not require active transport through the early secretory pathway but depends on specific ERES components.

We then ask whether membrane traffic through the early secretory pathway is required for Sec body formation. To test if COPII vesicle formation is required, we depleted Sar1 by RNAi before starvation. Sar1 depletion is evidenced by a strong reduction (40 ± 5%) in cell proliferation and ERES enlargement (Ivan et al., 2008) (**Figure 4C,** arrows). However, Sec body formation was found to be as efficient as in control (mock depleted) cells (**Figure 4C**). Second, we pharmacologically inhibited protein trafficking with Brefeldin A (**Figure 4D**) and found that this treatment before and during starvation does not affect Sec body formation (**Figure 4E**). This demonstrates that transport in the early secretory pathway via COPI and COPII vesicle formation is not required for the formation of Sec bodies.

Given the Sec body content in ERES components (**Figure 1**), we then tested using

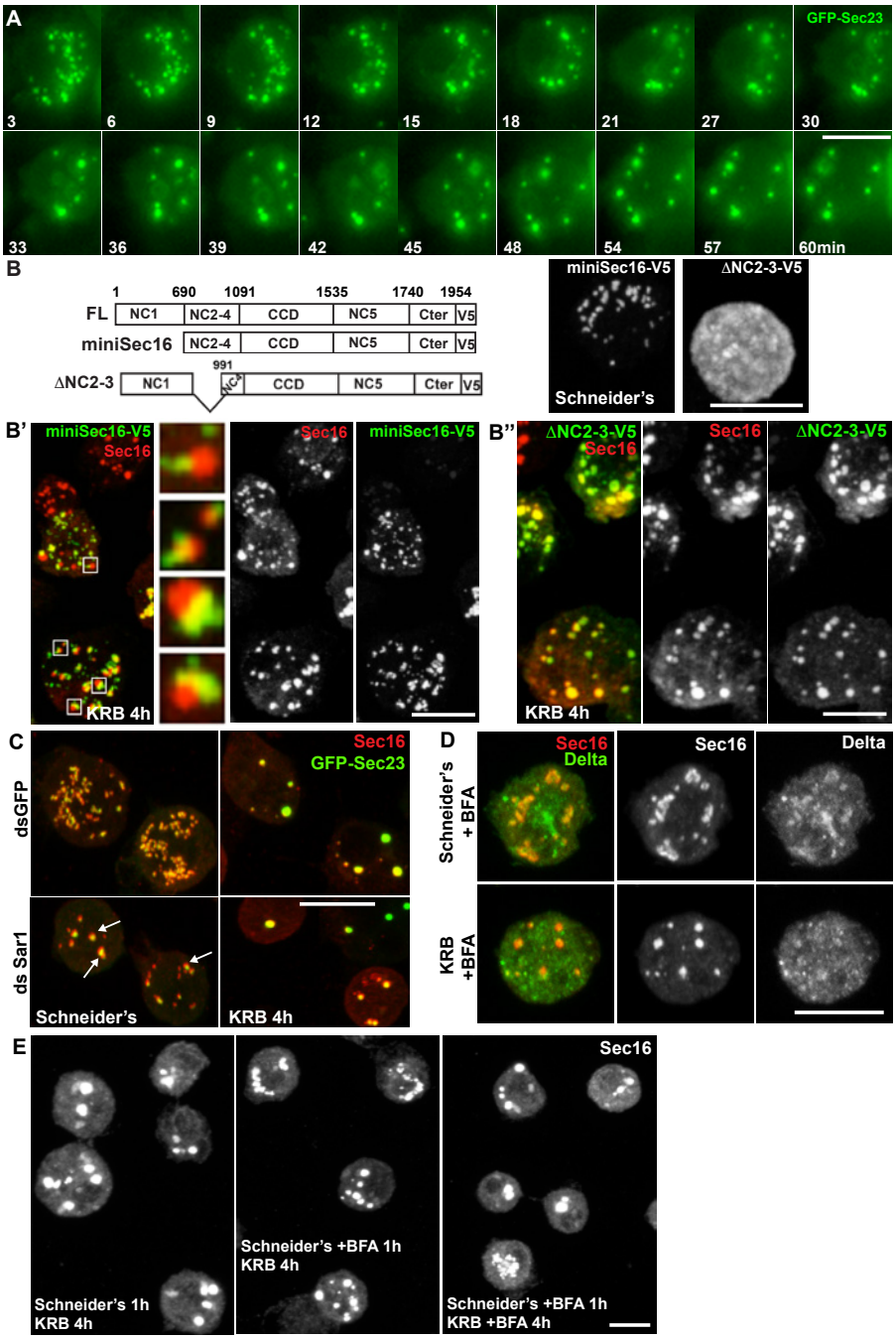

Figure 4: Sec bodies form at ERES but COPII and COPI coated vesicle formation is not required. **A:** Stills of a GFP-Sec23 time-lapse movie of a cell incubated in KRB (t=0) for 60 min showing Sec body formation. **B-B":** IF visualization of miniSec16-V5 (B, B') and ΔNC2-3-Sec16-V5 (B, B") in S2 cells incubated in Schneider's (B) and KRB for 4 h. Endogenous Sec16 is in red. Note that the cup

shaped ER forms a cradle for Sec bodies (B', insert). **C**: IF visualization of Sec16 and GFP-Sec23 in mock and Sar1 depleted S2 cells grown in Schneider's and incubated in KRB for 4 h. Note that the ERES are enlarged in Sar1 depleted cells (arrows) and Sec bodies form in both conditions to the same extent. **D**: IF visualizations of Sec16 and Delta-myc in S2 cells incubated with brefeldin A (BFA) in Schneider's and KRB for 3 h. Note that Delta transport is inhibited in both cases as Delta is retained intracellularly. **E**: IF visualization of Sec16 in S2 cells grown in Schneider's and incubated in KRB for 4 h in the presence or absence of brefeldin A (BFA). Note that pre-incubation with the drug does not affect Sec body formation during starvation. Scale bars: 10 μm.

RNAi if they are necessary for Sec body formation. Depleting Sec16 did not yield satisfactory conclusions as we have shown that Sec16 is critical for the organization of ERES in Drosophila S2 cells (Ivan et al., 2008) and Sec16 depletion led to the aggregation of most of the COPII components even in cells grown in full medium (see Figure 2A-C" of Ivan et al, 2008). However, in the few depleted cells where an observation could be made, Sec bodies did not form (**not shown**).

We then depleted the two Sec24 gene products that are both are expressed in S2 cells (see DRSC, Drosophila RNAi screening center, http://www.flyrnai.org/) (see materials and methods for depletion controls). When Sec24AB depleted cells are starved, the normal Sec body formation (marked by Sec16, **Figure 5A**) is impaired (**Figure 5B**). The distribution of diameters of the resulting structures shows that they are 2 fold smaller and twice as many, when compared to Sec bodies in mock depleted cells (**Figure 5E**). In agreement with Sec24 forming a complex with Sec23, Sec23 depletion also results in the same phenotype (**Figure 5C, E**). These smaller structures are not classical Sec bodies. By IF, some of them appear to have a horseshoe shape. By IEM, they appear as a collection of Sec16 positive vesicular and tubular membrane profiles, some small, some large probably corresponding to ERES mixed with Golgi fragments, and a third category that we name "intermediates" as they are reminiscent of Sec bodies by their round shape but that contain membrane and are smaller in size when compared to Sec bodies found in mock-depleted cells (*Figure 5-figure supplement 1*).

Interestingly, Sec24CD depletion (**Figure 5D, E**) does not lead to the same phenotype as Sec24AB depletion and Sec bodies form seemingly normally, showing specificity for one Sec24 homologue.

Taken together, this indicates a key and novel role for Sec23, Sec24AB (and perhaps Sec16) in Sec body formation, which is distinct from their classical role in ER exit via COPII vesicle formation that is not required (**Figure 4C-E**).

Sec bodies display liquid droplet-like properties: Role of Low complexity sequences.

Given that the Sec bodies are non-membrane bound, we then asked how their components are prevented from freely diffusing in the cytoplasm. One class of stress related cytoplasmic structures are liquid droplets that are described to result from phase separation-induced liquid demixing in the cytoplasm (Brangwynne et al.,

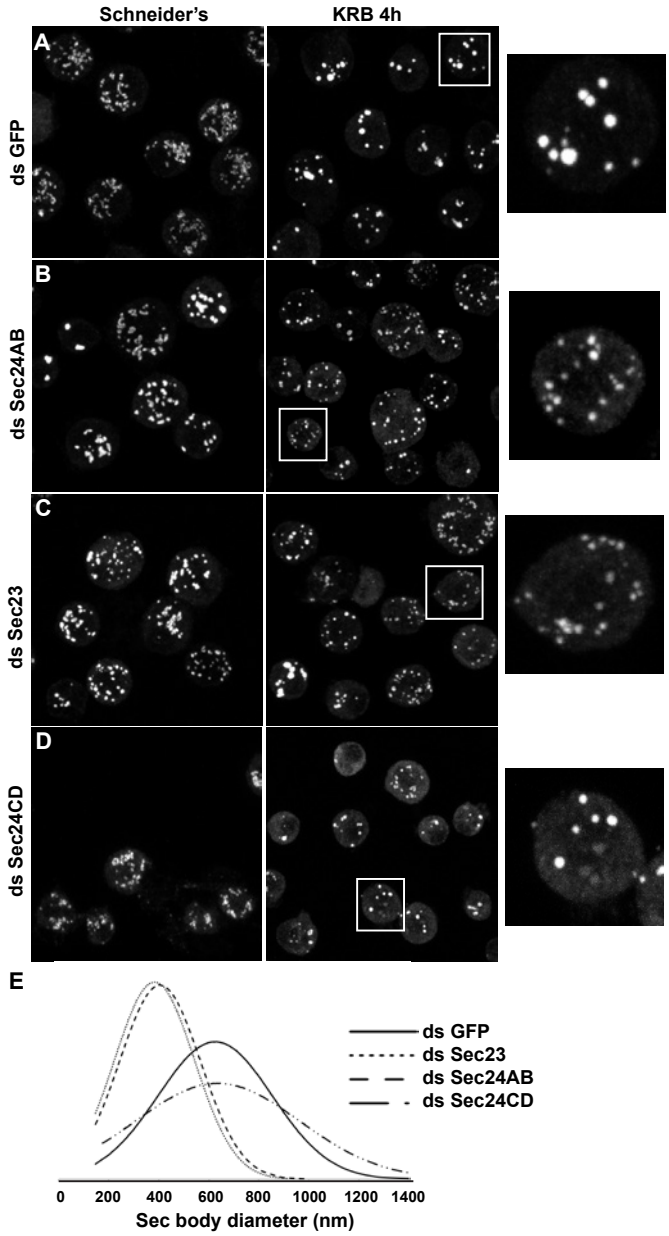

Figure 5: Sec23 and Sec24AB are key factors for Sec body formation. A-D: IF visualization of Sec16 in mock (A), Sec24AB (B), Sec23 (C) and Sec24CD (D) depleted S2 cells in Schneider's and incubated in KRB for 4 h. Note that Sec body formation is inhibited upon Sec24AB and Sec23, but not upon Sec24CD depletion. Boxed areas are shown at higher magnification. **E**: Distribution of Sec body size (shown as frequency of observed Sec body diameter) in mock, Sec24AB, Sec24CD and Sec23 depleted and starved cells (as in A) (dsGFP: 45 cells, 341 Sec bodies; dsSec24AB: 43 cells, 585 Sec bodies; dsSec24CD: 35 cells, 245 Sec bodies; dsSec23: 36 cells, 504 Sec bodies). Note that the Sec body's mean diameter decreases by 1.8 fold upon Sec24AB and Sec23 depletion and that Sec bodies are twice as many. Scale bars: 10 μm.

2009; Brangwynne et al., 2011; Hyman and Simons, 2012). They are defined as non-membrane bound, spherical, reversible structures, the components of which diffuse easily within the droplet but are in slower exchange with the cytoplasm. Furthermore, liquid droplets are known to contain proteins that are prone to engage in weak protein-RNA or protein-protein interactions as their components display a high level of low complexity sequences (LCS, defined as regions of low amino-acid diversity) (Kato et al., 2012) (*Figure 6-Source data 1*)**.** P-granules in *C. elegans*, nucleoli, but also Stress Granules and P-bodies have been shown to have liquid droplet properties (Brangwynne et al., 2009; Brangwynne et al., 2011; Hyman and Simons, 2012). We therefore set out to assess whether Sec bodies are also liquid droplets.

First, we used SEG, a bioinformatics tool that determines the LCS content of proteins recruited to the Sec bodies. Interestingly, we found that Sec16 and the two Sec24 gene products, Sec24AB, Sec24CD (**Figure 6A**) display a significantly higher LCS content when compared to other proteins related to the early secretory pathway and to the entire Drosophila proteome (our analysis, see Materials and Methods, **Figure 6A'**; *Figure 6-Source data 1*). Sec16 LCSs are situated throughout its sequence with the notable exception of its conserved central domain (CCD, aa 1090-1590) (**Figure 6A)**. On the other hand, Sec24AB and Sec24CD LCSs are mostly situated at the N-terminus of the protein sequence in a manner that is partially conserved throughout evolution (*Figure 6-figure supplement 1)*. Furthermore, as recently suggested (Das et al., 2014), LCSs correspond to a high level of unstructured sequences and we show that it is indeed the case for Sec24AB, Sec24CD and Sec16 (using HHpred, http://toolkit.tuebingen.mpg.de/hhpred/), *Figure 6-figure supplement 2* and not shown, respectively).

Remarkably, two of the LCS enriched proteins Sec24AB and Sec16 are also required for Sec body assembly, suggesting that this feature might be necessary. However, not all ERES residing and LCS rich proteins are necessary for Sec body formation as Sec24CD that contains the same amount of LCS is not.

We then tested whether LCSs were necessary for protein recruitment to Sec bodies and/or sufficient for their formation. We focused on Sec24AB as the LCSs are clustered to the first 415 amino-acids at the N-terminus (Sec24AB LCS) and compared their Sec body recruitment to this of its nonLCS region (aa 416-1184) (**Figure 6B**). LCS-sfGFP is largely recruited to ERES under normal growth conditions although not as efficiently as full length Sec24AB. Under starvation conditions, it localizes to Sec bodies as full length Sec24AB and seems to lead to their enlargement. This demonstrates that the LCS rich region of Sec24AB is sufficient to mediate recruitment to Sec bodies. Conversely, the nonLCS region is mostly cytoplasmic and remains largely so upon starvation, although a small pool is recruited to the Sec bodies. This shows that the LCS rich N-terminus region of Sec24AB plays a key role, in recruitment of Sec24 to the Sec body.

We then tested whether the Sec24AB LCS was sufficient to drive Sec body

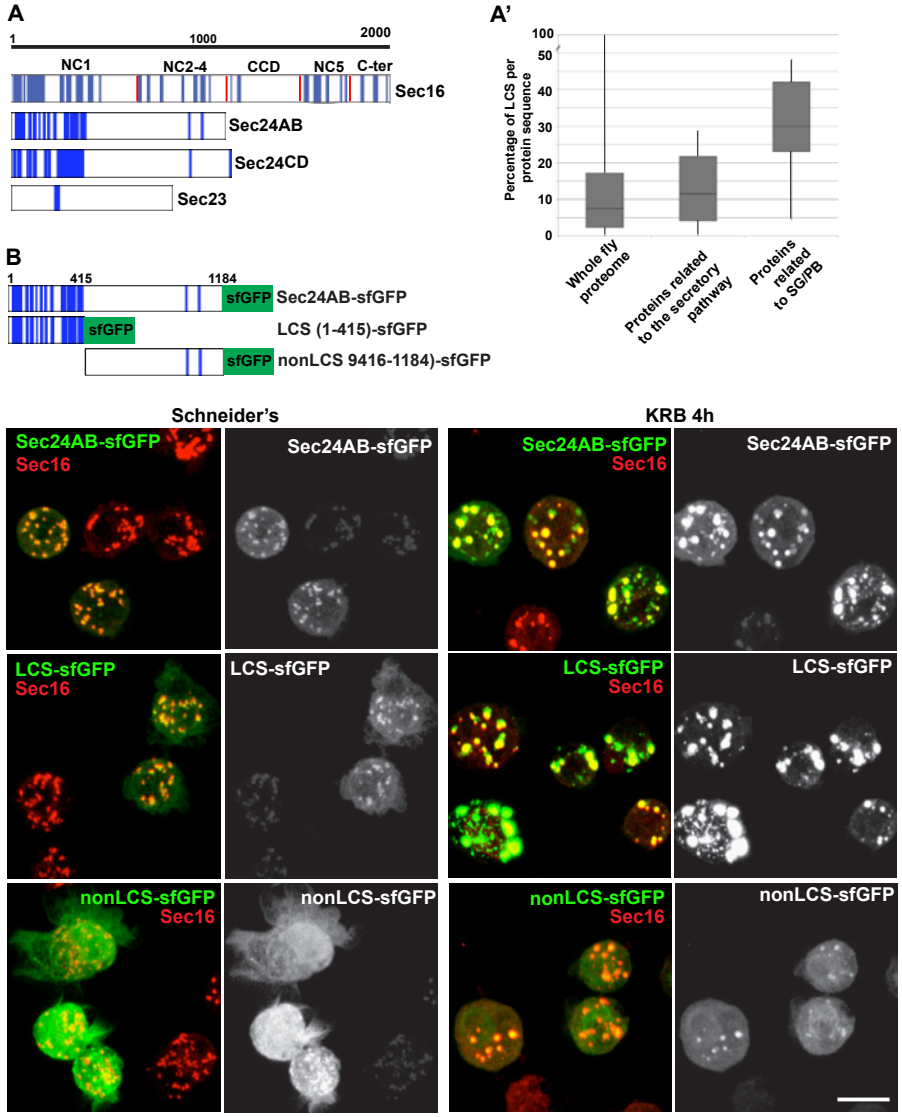

Figure 6: Sec body proteins contain low complexity sequences that are necessary for Sec body recruitment. A-A': Schematic representation of the Low Complexity Sequences (blue bars) in Sec16, Sec24AB, Sec24CD and Sec23 (A). The red bars mark the boundaries of the Sec16 domains. Genome wide analysis of Low Complexity Sequence (LCS) in the Drosophila proteome, in proteins related to the secretory pathway and proteins related to Stress Granules/P-bodies (A'). **B**: IF localization of sfGFP tagged full length Sec24B, Sec24AB LCS and Sec24AB nonLCS in S2 cells in Schneider's and KRB for 4 h, together with endogenous Sec16 (red). Scale bars: 10 μm.

formation. To do so, cells were depleted of endogenous Sec24AB (resulting in the formation of Sec16 positive smaller structures) followed by the expression of Sec24AB LCS. If this is sufficient, we expect that Sec bodies would form. However, although Sec24AB LCS is recruited to the smaller structures, Sec bodies did not

significantly form (*Figure 6-figure supplement 3*). This suggests that either the non LCS region of Sec24AB participates to Sec body formation, even though on its own, it is only slightly recruited, or that one or multiple other factors are involved in driving Sec body formation.

Sec bodies have FRAP properties compatible with liquid droplets.

Second, we assessed whether the FRAP properties of Sec bodies are compatible with liquid droplets, that is, assemblies made through phase separation. When a fraction of such an assembly (GFP marked) is photobleached, the recovery is quick as the molecules within mix instantaneously. However, when entirely photobleached, the recovery is slower as the exchange with the surrounding cytoplasm is not as efficient. We used Sec16-sfGFP and GFP-Sec23 that are efficiently incorporated to Sec bodies. When Sec bodies are partially bleached, the recovery is very fast for both GFP-Sec23 and Sec16-sfGFP and the maximum intensity is approximately 50% of the original one. After complete photobleaching, however, Sec bodies recover more slowly and only to 10% of the initial fluorescence intensity, showing an inefficient exchange with the surrounding cytoplasm (**Figure 7A, A';** *Video supplement 2,3*). This is comparable to FRAP properties of Stress Granules that are well-documented liquid droplets. When entirely bleached, Stress Granules recover more that Sec bodies and when partially bleached, they recover slightly less (**Figure 7B, B';** *Video supplement 4,5*). This indicates that the Sec23 and Sec16 diffuse more quickly within Sec bodies than FMR1 in Stress Granules, but that their phase transition barrier is higher.

Taken together, the spherical morphology, specific FRAP properties and presence of LCSs are features compatible with Sec bodies being liquid droplets.

Sec bodies are reversible.

Third, we assessed the Sec body reversibility, a key feature of liquid droplets and we tested it using cells that were starved for 4 h and further incubated in Schneider's. This results in the full recovery of their typical ERES pattern in less than 30 min **(Figure 8A;** *Video supplement 6*; *Figure 8-figure supplement 1***; Figure 8E**). This convincingly shows that Sec bodies are not terminal aggregates. Furthermore, these ERES are functional as they support efficient transport in the secretory pathway (**Figure 8B**) to allow proliferation (**Figure 9B,** solid dark blue line). Overall, although we have not been able to determine with certainty whether Sec bodies contain RNAs as all liquid droplets so far characterized do, we propose that amino-acid starvation leads to the formation of a novel stress assembly with liquid droplets features, the Sec bodies.

Sec bodies act as a reservoir for COPII components and are necessary for cell viability during amino-acid starvation and recovery after stress relief.

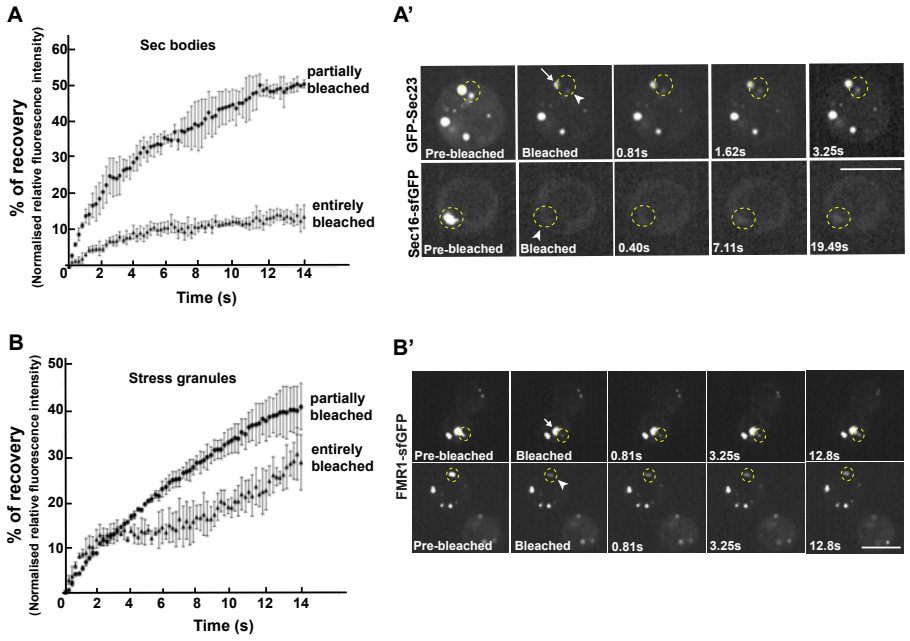

Figure 7: Sec bodies have FRAP properties consistent with liquid droplets. A-A': Percentage of fluorescence recovery after photobleaching (FRAP) over time of individual Sec bodies, marked by GFP-Sec23 (Video supplement 2), and ΔNC1-Sec16-sfGFP (Video supplement 3) in S2 cells incubated in KRB for 4 h. The triangles in B show the FRAP of Sec bodies that have been entirely bleached (n=3, arrowheads in B'). The circles show the FRAP of Sec bodies (n=3, arrows in B') that have been partially bleached. The dashed circles in B' indicate the Sec bodies that have been entirely bleached and assessed in stills taken from Video supplement 2 and 3. **B-B'**: Percentage of fluorescence recovery after photobleaching (FRAP) over time of individual Stress Granules marked by FMR1-sfGFP (Video supplement 4 and 5) in S2 cells incubated in KRB for 4 h. The triangles in C show the FRAP of Stress Granules that have been entirely bleached (n=3, arrowheads in C'). The circles show the FRAP of Stress Granules (n=3, arrows in B') that have been partially bleached. The dashed circles in B' indicate the Stress Granules that have been bleached and assessed in stills taken from Video supplement 4 and 5**.** Scale bars: 10 μm.

Remarkably, addition of protein translation inhibitor cycloheximide during the reversal does not affect the ERES re-building (**Figure 8D', E**). This suggests that Sec bodies act as a reservoir for ERES components allowing their re-mobilization upon stress relief to rebuild a functional secretory pathway. Of note, cycloheximide addition during starvation also does not affect Sec body formation (**Figure 8D'**). To test further whether Sec bodies act as a mechanism for ERES components during starvation preventing their degradation, we first monitored the level of ERES components during starvation. Remarkably, amino-acid starvation leads to an increased level of Sec16, Sec23 and Sec31 (**Figure 9A; Figure 9A',** compare lanes 1 and 2). We can rule out that this is due to an increase in protein translation during starvation as it is efficiently inhibited after 20 min (not shown). It is therefore likely that Sec body formation leads to a stabilization of the ERES components and therefore protect them against degradation.

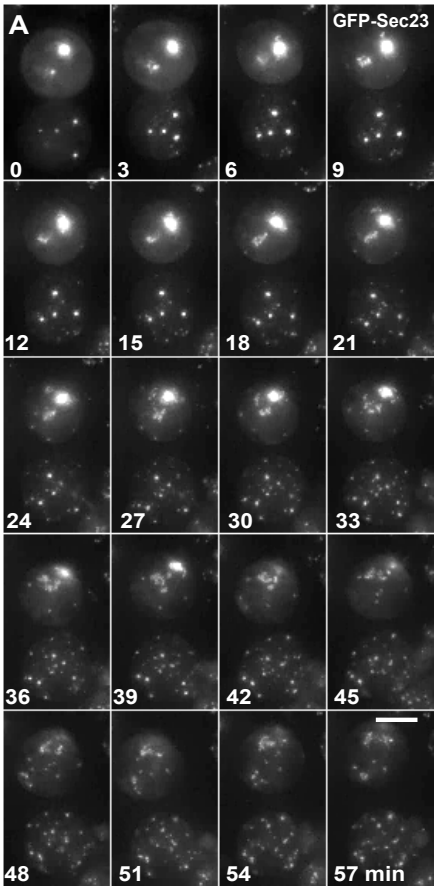

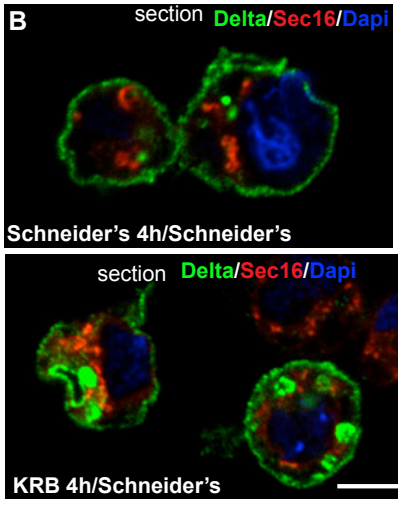

C

Reversed in Schneider's (min)	Percentage of cells with Delta at the PM: KRB 4h	Schneider's 4h
30	16±5	13±4
60	35±10	22±11
90	66±7	81±12
120	95±2	98±3

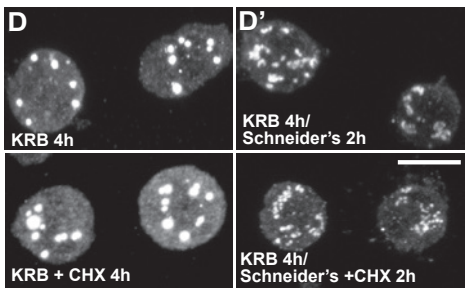

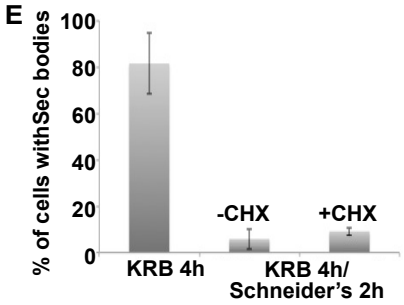

Figure 8: Sec bodies are functionally reversible and acts as reservoir for ERES components during starvation. A: Stills of a GFP-Sec23 time-lapse movie (Video supplement 6) of two cells recovering in Schneider's after 4 h in KRB (t=0, up to 60 min). Note that Sec bodies are reversed into ERES. **B:** IF localization of Delta in cells that were starved (KRB) or not (Schneider's) followed further incubation in Schneider's for 2 h. **C:** Quantification of the percentage of cells with Delta at the plasma membrane in cells that were either starved (KRB) or not (Schneider's) followed by reversion in Schneider's. Delta was induced for 30, 60, 90 and 120 min while cells were reverted in Schneider's. **D-D':** IF visualization of Sec16 in cells starved in KRB supplemented or not with cycloheximide (CHX, B), and in starved cells further incubated in Schneider's supplemented or not with CHX (C'). Note that neither Sec body formation nor reversal is affected by the presence of CHX. **E**: Quantification of the Sec body reversal as described in B' expressed as the percentage of cells exhibiting Sec bodies.

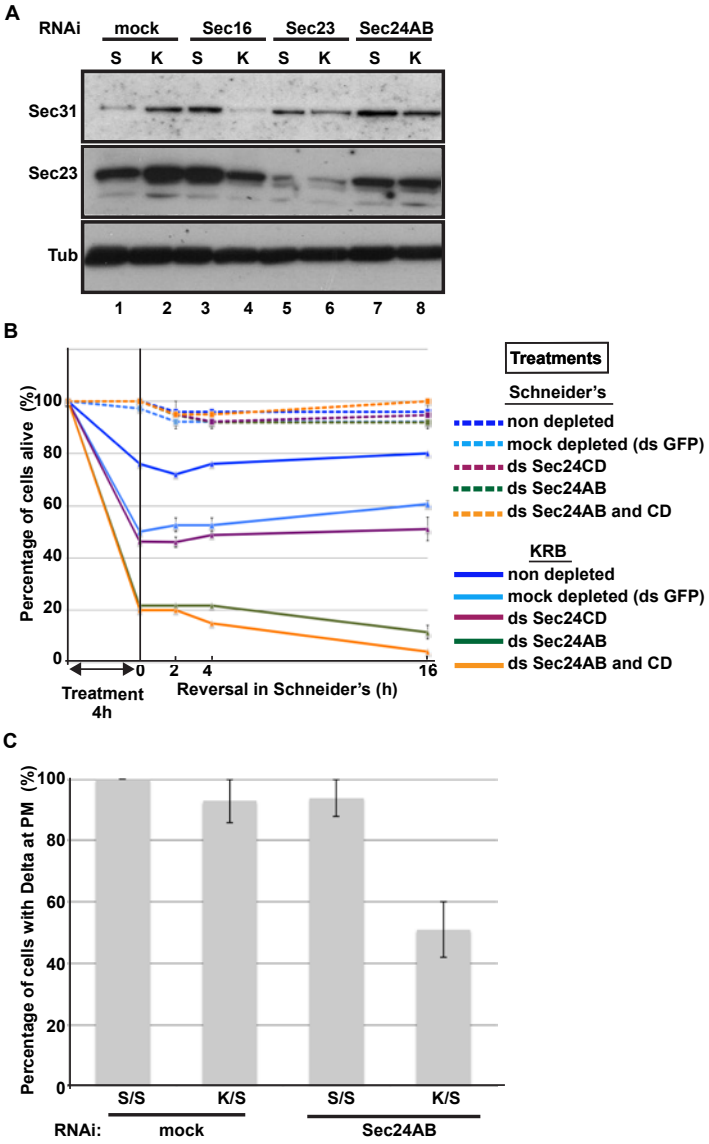

Figure 9: Sec body formation is a pro-survival mechanism. A: Western blot of Sec31, Sec23 and tubulin (loading control) of lysates from GFP, Sec16, Sec23 and Sec24AB depleted cells grown in Schneider's (S) and incubated with KRB for 4 h (K). **B**: Graph of cell viability (expressed as percentage of alive cells). The number of starting cells at t=0, either non- (control, dark blue lines), mock- (dsGFP, light blue lines), Sec24AB (green lines), Sec24CD (violet lines) and double Sec24 AB and CD (orange lines) depleted, is set at 100%. These cells are incubated in Schneider's (dashed lines) and KRB (solid lines) for 4 h and further incubated in Schneider's up to 16 h. Note that the mock depletion (dsGFP, light blue dashed lines) is slightly detrimental to cell survival upon amino-acid starvation when compared to non-depleted (control, dark blue dashed line). **C:** Quantification of the percentage of cells with Delta at the plasma membrane in mock-, Sec23 and Sec24AB depleted cells that were either starved (KRB) or not (Schneider's) followed by reversion in Schneider's. Delta was induced for 90min while cells were reverted in Schneider's. Error bars in B represent standard error of the mean and in C standard deviation.

We then asked whether this protection is inhibited when Sec bodies do not form. Upon Sec16, Sec23 and Sec 24AB depletion, we observed two things: The first is that under normal growth conditions, the level of Sec31 is higher than in mock-depleted cells (**Figure 9A,** compare lanes 3, 5 and 7 to lane 1). The second is that in depleted cells, this level is not maintained upon starvation. Sec31 level is decreased instead of being stabilized as in mock-depleted cells. Sec23 behaves similarly to Sec31. In Sec24AB depleted cells, however, its level is reduced even in cells incubated in full medium, suggesting that Sec23 turnover depends on the presence of Sec24AB.

Altogether, this experiment suggests that starvation leads to ERES component stabilization that is inhibited when Sec bodies do not form. This supports the notion that Sec bodies act as a reservoir for ERES components to rebuild a functional secretory pathway upon stress relief.

In this context, we investigated the relevance of Sec body formation in cell survival upon starvation and fitness upon stress relief. To do so, we exploited the fact that only one of the two Sec24 proteins is required for Sec body formation. Indeed, Sec bodies do not form in starved Sec24AB depleted cells, whereas they do in Sec24CD depleted cells (see **Figure 5**). As mentioned above, depletion of either of the Sec24 isoforms is effective but does not affect proliferation very much when cells are grown in normal medium (**Figure 9B**, dashed lines and see Materials and methods). However, upon amino-acid starvation, the number of Sec24AB depleted cells decreases twice as much as the mock- (ds GFP) and Sec24CD- depleted cells (**Figure 9B,** compare solid green to light blue, violet lines). As expected, the double depleted Sec24AB and CD cells also decline more quickly (**Figure 9B**, solid orange line). When reverted to full medium, control and Sec24CD depleted cells started to proliferate again, whereas the number of Sec24AB depleted cells continue to diminish (**Figure 9B**).

As the absence of Sec bodies leads to a decreased stabilization of COPII components, one reason behind the cell lethality upon re-feeding could be the inefficient protein transport through the secretory pathway. To test this, we monitored the transport of Delta to the plasma membrane of starved mock-, and Sec24AB-depleted cells upon re-feeding for 90 min (**Figure 9C**). Mock-depleted cells efficiently transport Delta whether starved or not (**Figure 9C; Figure 8C)**. Conversely, the efficiency of transport of Sec24AB depleted cells after starvation is largely compromised, suggesting that formation of Sec bodies is critical for proper transport resumption. However, this result could simply be due to the depleted Sec24AB whose absence compromises transport even in cells kept in Schneider's.

Nevertheless, Delta transport in Sec24AB depleted cells kept in Schneider's was found almost as efficient as mock-depleted cells, suggesting that Sec24CD compensates Sec24AB depletion. This indicates that the inhibition of Sec body formation, not the absence of Sec24AB, is detrimental to anterograde transport resumption.

Taken together, these result show that Sec body formation is instrumental to efficient resumption of protein transport through the secretory pathway that contributes to cell survival and growth after re-feeding.

Discussion

Sec bodies: A novel stress assembly linked to secretion inhibition.

Here, we describe a novel, reversible and non-membrane bound structure, the Sec body that forms in response to nutrient stress. Sec bodies comprise proteins that in normal growth conditions function as ERES components, including subunits of the COPII coat, namely Sec23, Sec24AB, Sec24CD, and Sec31 as well as Sec16, the upstream ERES organizer. A noticeable exception is the small GTPase Sar1. One reason for this could be that Sar1 is devoid of LCS and this is currently under further investigation.

Interestingly, the components of the other coats were seemingly not incorporated into Sec bodies but also did not form other structures, suggesting that remodeling of the ERES is sufficient to ensure inhibition of protein transport through the secretory pathway. In this regard, Sec body formation constitutes also a novel mechanism for attenuation/inhibition of protein transport through the secretory pathway. Cells can disperse ERES and Golgi components into the cytoplasm, as reported during mitosis the Golgi is fragmented (Farhan et al., 2010; Lucocq and Warren, 1987; Zacharogianni et al., 2011).

The dramatic remodeling of the ERES that we describe here appears to be specific for amino-acid starvation, possibly underlining the acute and severe nature of this particular stress. It is also different from the response to serum starvation that requires ERK7 (Zacharogianni et al., 2011). ERK7 appears to be involved to a small extent in the amino-acid starvation response, possibly facilitating the initial dispersion of a fraction of the ERES into the cytoplasm, as when depleted, it prevents Sec body formation upon amino-acid starvation by about 20% (Zacharogianni et al., 2011). However, other signaling pathways, yet un-indentified, are clearly at stake.

Interestingly, one of Sec body components is Sec16, a protein with a localization that is also modulated upon serum starvation. Furthermore, Sec16 is also phosphorylated in response to EGF signaling in human cells (Farhan et al., 2010). It could therefore be emerging as one of platform integrating nutrient and growth factors availability.

Sec bodies are novel stress structures and we have shown that they are not autophagosomes (or substrates of autophagy), not lipid droplets and not CUPS as they are devoid of dGRASP that is found quantitatively re-distributed in the cytoplasm upon amino-acid starvation, suggesting a modification involving its lipid anchor or modification of its N-terminus. Sec bodies are also different from large reversible structures containing COPII components that have been described in yeast in a number of specific COPII mutants *Sec12-4* and *Sec16-2* (Shindiapina and

Barlowe, 2010). These structures are thought to result from an imbalance between cargo incorporation in COPII coated vesicles and the coat formation, and lowering the cargo load by inhibiting protein translation prevented their appearance. Sec body formation is, however, insensitive to translation inhibition by cycloheximide and are therefore different from these yeast structures. Last, we also show that Sec bodies are distinct from Stress Granules and P-bodies that also form upon amino-acid starvation. Therefore Sec bodies are novel structures.

Stress induces the formation of stress assemblies

Formation of mesoscale protein assemblies like Stress Granules, P-bodies or now Sec bodies is emerging as a general response to stress and especially nutrient stress, and is gaining increasing attention (Hyman and Brangwynne, 2011; Wilson and Gitai, 2013). For instance, in yeast under nutrient limiting conditions, metabolic enzymes and stress response proteins form reversible foci (Narayanaswamy et al., 2009), such as purinosomes containing enzymes of the purine biosynthetic pathway (An et al., 2008; O'Connell et al., 2012), proteasome storage granules upon glucose restriction (Laporte et al., 2008; Peters et al., 2013), or, as recently described, glutamine synthetase filaments (Petrovska et al., 2014).

In challenging conditions, areas of localized biochemistry in the cytoplasm can be advantageous, as reagents and possibly energy can be focused to these specific areas. The reorganization of the cytoplasm through non-membrane bound protein assemblies could confer this rapid and spatio-temporally defined compartmentalization. In this regard, we have found that Sec bodies confer a fitness advantage to the cells under starvation (see below). However, some stress assemblies (especially cytoplasmic RNP granules) can form dysfunctional RNA-protein assemblies that become irreversible and toxic for the cell. For instance, Stress Granule components have a strong relationship with degenerative diseases, such as ALS and laminopathies (Ramaswami et al., 2013). Whether Sec body components could also form such deleterious aggregates remains to be established.

Some stress assemblies have liquid droplet properties.

Some of these mesoscale assemblies have liquid-like properties. These so-called liquid droplets are generally spherical and dynamic and form via phase separation (liquid demixing) of their components from the cytoplasm like a drop of oil in water. Their components display different rates of diffusion within the assembly and in the surrounding cytoplasm (Hyman and Brangwynne, 2011). They form via transient and weak protein-protein and protein-RNA interactions mediated by low amino-acid diversity stretches (low complexity sequences, LCS), prone to engage in such interactions. Stress granules and P-bodies have been shown to be liquid droplets and we show here that Sec bodies exhibit clear liquid droplet features as underlined by their spherical morphology, their reversibility, FRAP properties and LCS content.
In this regard, the presence of LCSs both in Sec16 and Sec24 is intriguing considering

their role in cells under normal growth conditions where they act in sequence with many others to form the COPII coat. How the LCSs are shielded to make proteins competent for their function in COPII coat formation in growing cells remains to be investigated but the interaction with both cargo and Sec23 might be instrumental to their functioning as coat subunits. We show here that the LCS rich domain of Sec24AB is sufficient and necessary for Sec body incorporation upon amino-acid starvation, but not sufficient to induce Sec body formation. This has similarity to Tia1, a key protein necessary for Stress Granule formation that has an LCS-prion like domain that is necessary to form stress granules (Gilks et al., 2004).

As mentioned above, the structures that fall in the liquid droplet category have been described to form through weak protein-RNA interactions. Although Sec bodies do not appear to contain RNAs, we propose that they are nonetheless liquid droplets. The absence of RNA might account for the very low and slow recovery we observed after complete photobleaching of whole Sec bodies when compared to Stress Granules that recovers to a higher degree. Shuttling of mRNA in and out of Stress Granules could drive more exchange between the structure and the surrounding cytoplasm, and this probably does not occur in Sec bodies. However, instead of protein-RNA interactions, Sec body components could establish weak protein-protein interactions helped by molecular modifications that could trigger conformational changes and perhaps exposure of their LCS.

Sec bodies and cell survival

Importantly, one of the key features of a liquid droplet is to be efficiently reversible and we show that Sec bodies are rapidly and completely reversible upon stress relief. This shows that they act as a reservoir of the ERES components that can be quickly remobilized to re-build a functional organelle, so that protein transport through the secretory pathway can resume once stress is relieved in order to support cell proliferation. Furthermore, Sec bodies have a role in protecting ERES components from degradation during starvation. That strengthens the fact that Sec bodies are neither autophagosomes nor a substrate of autophagy, unlike Stress Granules, which are reported to be cleared by autophagy (Buchan et al., 2013). Last, we show that Sec body formation is critical for the cell viability during amino-acid starvation. It suggests a pro-survival mechanism, perhaps through the recruitment and inactivation of pro-apoptotic factors. This remains to be investigated.

Taken together, amino-acid starvation inhibits both protein translation and protein transport through the secretory pathway, and similarly for both processes, results in the concomitant formation of cytoplasmic stress assemblies where key components necessary for cell survival are stored, untranslated mRNAs in Stress Granules, and ERES components in Sec bodies.

Materials and methods

Cell culture, amino-acid starvation, RNAi, transfection and drug treatments
Drosophila S2 cells were cultured in Schneider's medium supplemented with 10% insect tested fetal bovine serum (referred to as Schneider's) at 26°C as previously described (Kondylis and Rabouille, 2003; Kondylis et al., 2007). Amino-acid starvation was carried out by incubating the cells for 4 h (or otherwise stated) in Krebs Ringers' Bicarbonate buffer (KRB, 10 mM glucose, 0.5 mM magnesium chloride, 4.53 mM potassium chloride, 120.7 mM sodium chloride, 0.7 mM dibasic sodium phosphate, 1.5 mM monobasic sodium phosphate, 15 mM sodium bicarbonate, 5.4 mM calcium chloride) at pH 7.4. We verified that simply adding 10% FBS to the buffer did not prevent the Sec body and Stress Granule formation. Single amino-acids were added at 15 mM (unless otherwise indicated).

Wild-type S2 cells or stably transfected were depleted by RNAi, as previously described (Kondylis and Rabouille, 2003; Kondylis et al., 2007). Cells were analyzed after incubation with dsRNAs for 5 days (or 4 days in the case of Sar1 depletion). Transient transfections were performed using the Effectene transfection reagent (Qiagen, 301425) according to the manufacturer's instructions. When cells were transfected with pMT constructs, expression was induced 48 hours after transfection with 1 mM $CuSO_4$ for 1.5 h. The newly synthesized proteins were allowed to localize for 1h after $CuSO_4$ washout. When cells were transfected with the pUAS constructs transfection was done 48 h prior to the experiment.

Drugs were used at the following concentrations: cycloheximide (10 μM), wortmanin (1 μM), bafilomycin (100 nM), rapamycin (2 μM) and brefeldin A (50 μM). When a drug treatment was followed by starvation, the cells were pretreated for 30 min in Schneider's following starvation in the presence of the drug.

Antibodies
The following antibodies have been used in these experiments: rabbit polyclonal anti-Sec16 (Ivan et al., 2008), 1:800 IF, 1:2000 WB; rabbit polyclonal anti-Sec23 (Pierce PA1-069A), 1:200 IF, 1:1000 WB; rabbit polyclonal anti-Sec31 (Bentley et al., 2010) 1:200 IF; mouse monoclonal anti-V5 (life technologies R960), 1:500 IF; mouse monoclonal anti-FMR1 (DSHB supernanant clone 5A11), 1:10 IF; rabbit polyclonal anti-Tral, 1:200 IF; rabbit anti-dGRASP, 1:500 IF (with methanol fixation); mouse monoclonal anti-α-spectrin (DSHB supernatant clone 3A9), 1:20 IF; rat polyclonal anti-eIF4E, 1:200 IF (with methanol fixation); mouse monoclonal anti-Delta, (DHSB clone C594.9B),1:500 IF.

DNA constructs and RNAi
The pRmeGFP-Sec23, pRmSar1-eGFP, pMTmini-Sec16 (NC2.3-CCD)-V5, pMTΔNC2.3-V5 constructs were described in (Ivan et al., 2008). The pMTΔNC1-ΔCter-Sec16-V5 and the pMTΔNC1-Δ64-Sec16-V5 were described in (Zacharogianni et al., 2011). The pMT-Atg5-V5 is a gift from Fulvio Reggiori. The pUASt-GFP-Sec24CD (Sten) and the pUASt-mCherry-Sec24AB were a kind gift from Stefan Luschnig. The Fringe-GFP construct is described in (Kondylis et al., 2007). To generate ΔNC1Sec16sfGFP, sfGFP was amplified using the forward (ggccgcggatggtgagcaagggcgagga) and reverse (gggtttaaacttacttgtacagctcgtccatg) primers and cloned into PMTV5-B-ΔNC1Sec16 (Zacharogianni et al., 2011) using SacII and PmeI restriction sites.

Human Sec16A-V5 was cloned in the pMT-V5-HisB vector using the primers forward (tagccaccggtaccatgcctgggctcgaccga) and reverse (tacggaattcaagttcagcaccaggtgcttcctctand) the KpnI and EcoRI restriction sites.To generate FMR1-sfGFP, sfGFP was first amplified using the forward (catgttcgaaatggtgagcaagggcgag) and reverse (catgaccggtcttgtacagctcgtccatgc) primers containing the restriction sites for BstBI and AgeI, respectively and cloned into PMT-V5-His to replace the V5 tag, leading to PMT-sfGFP.
To generate super folder GFP (sfGFP) tagged pMT-Sec24AB, pMT-Sec24AB LCS and pMT-Sec24AB nonLCS, Sec24Ab LCS (1-415 aa) were amplified from cDNA of Drosophila S2 cells using the forward (gatggaattccaccatgtcgacttacaat) and reverse (gtcagggccctctggagcagtggttc), and Sec24AB nonLCS (416-1184aa) regions using forward (cagtgaattcatgctaaacgtggctca) and reverse (gtcagggccctcttttgcaacacatt) primers. Fragments were cloned into pMT-sfGFP using EcoRI and ApaI restriction sites.
FMR1 cDNA was then amplified from the total cDNA of S2-cells using the forward (catgggtacccaccatggaagatctcctcgtgga) and the reverse (catggaattcaaggacgtgc cattgaccag) primers and inserted in pMT-sfGFP-His using KpnI and EcoRI restriction sites.

The following primers were used to amplify cDNA templates using for RNAi

Sec24AB-F	taatacgactcactataggggccaaccggtttcaatcag
Sec24AB-R	taatacgactcactatagggaggaggtagctggggttgac
Sec24CD-F	taatacgactcactatagggccctagagtgctccggctat
Sec24CD-R	taatacgactcactatagggcgctctccttcgctgttc
Sec16-F	ttaatacgactcactatagggagagccagaggatcagcatc
Sec16-R	ttaatacgactcactatagggagagcgatcccacagcagtc
Sec23-F	ttaatacgactcactataggggtgcaggatatgctcggaat
Sec23-R	ttaatacgactcactataggggtggagctgggattcaatgt
Sar1-F	ttaatacgactcactatagggatgttcacttgggactggttc
Sar1-R	ttaatacgactcactatagggagaatctctcgagcccacttcaa

The DNA fragments were used for in vitro transcription using the T7 Megascript kit (AMBION) to generate the dsRNAs used for RNAi. The efficiency of Sec24AB and CD depletion was estimated by transfecting mcherry-Sec24AB in Sec24AB depleted cells and Sec24CD-GFP to Sec24CD depleted cells and comparing the level of transfection (number of cells expressing the fluorescent protein) to this of non-depleted cells. In a typical experiment, 24.1 ± 2.0% non-depleted cells were transfected with mcherry-Sec24AB versus 2.5 ± 1% in Sec24AB depleted cells, and 27.3 ± 2.4% non-depleted cells were transfected with GFP-Sec24CD versus 2.6 ± 0.7% in Sec24CD depleted cells, showing that the 90% of the cells are depleted. The depletion of Sec23 and Sec16 were also 90% (as measured by Western blot, not shown).

Immunofluorescence (IF) and immuno-electron Microscopy (IEM)
S2 cells were plated on glass coverslips, treated, fixed in 4% PFA in PBS for and processed for Immunofluorescence as previously described (Kondylis and Rabouille, 2003). Alternatively (as indicated for specific antibodies and dyes), the cells were fixed in ice-cold methanol for 5min washed with PBS and processed for IF as above. Samples were viewed under a Leica SPE confocal microscope using a 63X lens and 1.5-3x zoom. 17-22 confocal planes are projected to image the whole cells. IEM was performed as described previously (Kondylis and Rabouille, 2003; van Donselaar et al., 2007).

Delta Transport assay
To monitor Delta transport through the secretory pathway in starved Delta-S2 cells (Kondylis and Rabouille, 2003). Delta expression was induced by adding 1 mM $CuSO_4$ to Schneider's medium for 30 min before incubating the cells in KRB or further in Schneider's (control) (Figure 1A). To monitor Delta transport upon reversion, cells were incubated 4h in Schneider's or KRB. After 4h, the media was changed to Schneider's supplemented with 1 mM $CuSO_4$ for 10-120 min (Figure 8B,C).

To monitor Delta transport in Delta S2 depleted cells, 0.75 million cells were mock- (dsGFP), Sec24AB-, and Sec23- depleted for 5 days in a 6-well plates cells. Cells were then were split in 2 and plated on glass coverslips in a 12-well plate. They were allowed to attach for 1h and media was changed for either Schneider's or KRB. After 4h, the media was changed to Schneider's supplemented with 1 mM $CuSO_4$ for 90min (Figure 9C).

Cells were fixed and processed for IF using Delta antibody. Transport efficiency was calculated as percentage of cells expressing Delta at the plasma membrane over the total number of cells expressing Delta. Between 30 and 60 cells were analyzed per condition.

Autophagy
S2 cells transiently expressing Drosophila Atg5-V5 and mouse GFP-Atg8 were incubated for increasing length of time in Schneider's supplemented or not with rapamycin and in KRB supplemented or not with wortmannin and bafilomycin. The percentage of cells showing Atg5-V5 punctae was determined. Experiments were done in triplicate.

Time-lapse and FRAP
Time lapse of Sec body formation and disassembly was performed on S2 cells stably expressing GFP-Sec23. For Sec body formation, cells were incubated in KRB (t=0) at 26°C. For Sec body disassembly, cells were starved for 4h and further incubated in Schneider's (t=0) at 26°C. Cells were viewed with a Leica AF7000 Fluorescence microscope. 10 z planes with a z step of 0.7 μm of were recorded every 3 min.

The FRAP experiments were performed on cells expressing either GFP-Sec23, ΔNC1-Sec16-sfGFP and FMR1-sfGFP for 1.5 h (expression induced with $CuSO_4$) followed by incubation in Schneider's for 1 h and starvation in KRB for 4 h. Sec bodies and Stress Granules were entirely or partially (half) photobleached using a 488 nm laser at 100% laser power for 750 msec. FRAP was recorded using a PerkinElmer Ultraview VoX spinning disk microscope with the volocity software. Fluorescence recovery was recorded every 10 msec for the first 14sec after bleaching, and thereafter every 10 sec for 2 min.

Low complexity sequence analysis
The amount of LCS was determined for each protein and isoform annotated in FlyBase release FB2014_02 using SEG (ftp://ftp.ncbi.nih.gov/pub/seg/) (Wootton and Federhen, 1996). The LCS content of each protein was tested for enrichment by a hypergeometric test against the whole proteome. For the proteins that have multiple isoforms the longest isoform was chosen for comparison.

Western blot
Cells were lysed in 50 mM Tris–HCl pH 7.5, 150 mM NaCl, 1% Triton X-100, 50 mM NaF, 1 mM Na_3VO_4, 25 mM Na_2-β-glycerophosphate supplemented with a protease inhibitors tablet (Roche). The lysate were cleared by centrifugation 4°C for 15 min at 14.000 rpm and proteins were separated on SDS-PAGE followed by western blot.

Mammalian cell starvation
HEK-293T, MEFs and COS7 cells were cultured in standard DMEM and incubated in KRB supplemented with 100 nM bafilomycin for 7 h (up to 16 h for Cos cells) to mimic the optimal conditions found for S2 cells.

Cell survival and fitness upon and after amino-acid starvation.
0.75 million cells were non-, mock- (dsGFP), Sec24 AB, Sec24CD and Sec24AB and CD depleted for 5 days in a 6-well plates. They proliferated to reach 2.5, 1.9, 1.8, 1,85 and 1.9 million, respectively and this was set at 100% (t=0). These cells were then either starved in KRB for 4 h or further incubated in Schneider's, their number monitored and expressed as a percentage of t=0. The medium was changed to Schneider's and their proliferation monitored further up to 16 hours. Experiments were performed in triplicates.

Flies
Oregon R+ virgin females were fattened on standard food supplemented with yeast for 3 days. They were subsequently either dissected to harvest the ovaries for the ex vivo treatments (incubation in Schneider's and KRB for 4 h) or transferred to humidified empty vials for 36 hours before dissection. IF were performed as described in (Giuliani et al., 2014).

Quantification and statistics
Three independent experiments were performed for quantification of the Sec body phenotype as scored by immunofluorescence. At least 3 fields were analyzed comprising at least 100 cells per condition. Averages and standard deviations reflect variation throughout the experiments. For Sec bodies we considered cells with at least one large, round (>0.5 µm) structure as exhibiting Sec bodies. Cells with smaller round structures and/or haze were considered intermediate. For all measurements p-values were calculated with Excel.

Sec body diameter
Sec body diameter was measured using the Leica LAS software. At least 35 cells were analyzed per condition, in each of which all fluorescent foci (at least 500) were measured. Distribution curves were made with Excel.

Acknowledgements

We thank the Rabouille's lab members and Fulvio Reggiori for their input and constructive discussions, and Peter van der Sluijs and Adam Grieve for critically reading the manuscript. We thank Akira Nakamura for Tral and elF4E antibodies, Stefan Luschnig for the tagged Sec24 constructs, and Andrew Bailey for help with the hypoxia experiment. We thank Anko de Graaff and the Hubrecht Imaging Center for supporting the imaging. The spinning disk microscope is funded by equipment grant 834.11.002 from the Dutch Organization of Scientific Research (NWO). Part of this research is funded by NWO 822-020-016 to CR.

Supplemental figures

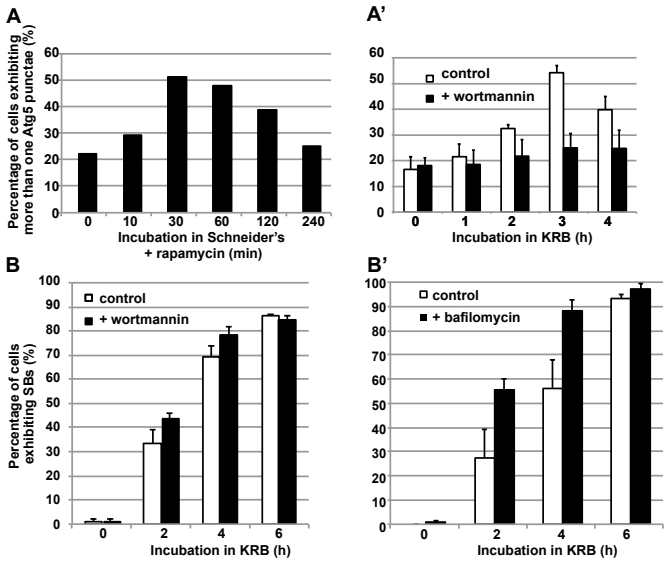

Figure 1-figure supplement 1: **Sec body formation and autophagy. A-A':** Quantification of Atg5 punctae formation in S2 cells incubated with rapamycin (A) and incubated with KRB with or without wortmannin (A') for indicated time points. Note that as expected, autophagy (marked by Atg5) is stimulated by rapamycin and starvation (KRB) and inhibited by wortmannin. **B-B'**: Quantification of Sec body formation (marked with Sec16) in cells incubated in KRB with and without wortmannin (B), and with and without bafilomycin (B').

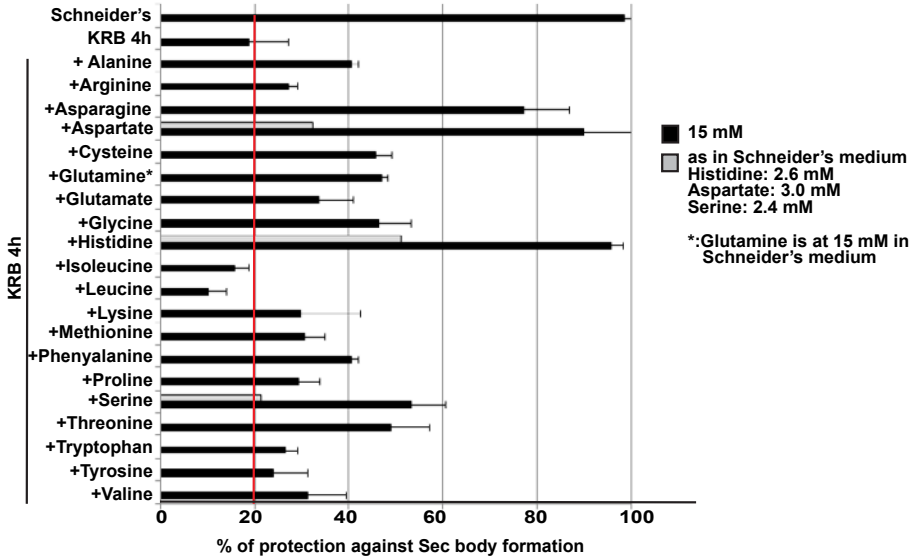

Figure 1-figure supplement 2: **Sec body formation and single amino-acids.** Quantification of the prevention of Sec body formation by specific amino-acids upon incubation in KRB for 4 h. This is expressed as the percentage of cells exhibiting the normal growth Sec16 localization at ERES. All amino-acids are added at 15 mM except for 3 (gray bars) that were also tested at their concentration in Schneider's medium. Note that at 15 mM, histidine, aspartate and asparagine significantly decreases Sec body formation.

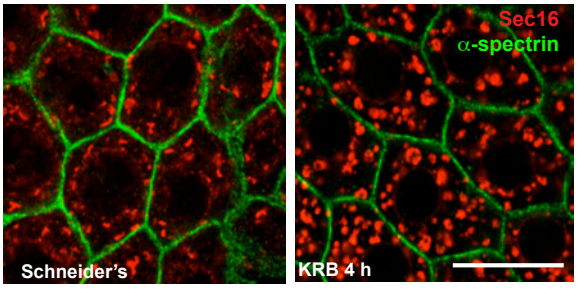

Basal view of stage 9-10 follicular epithelium from ovaries incubated ex vivo

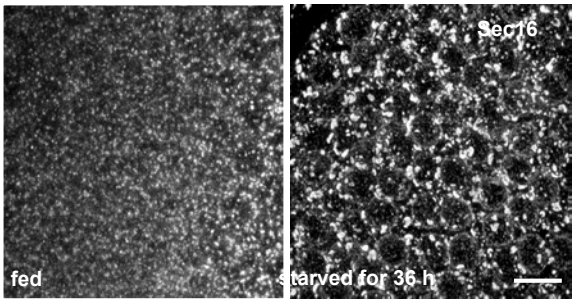

Basal view of stage 9-10 follicular epithelium

Figure 1-figure supplement 3: **Sec body formation in vivo.** Projection of 4 equatorial confocal planes of Sec16 and Spectrin (D) in the follicular epithelium covering an egg-chamber from an ovary dissected from a virgin fly fattened for 3 days and incubated ex-vivo in KRB for 4 h, and from an ovary dissected from a 36 h starved virgin female. Note that in both cases, Sec16 is found in large punctae reminiscent of Sec bodies. Scale bars: 10 μm.

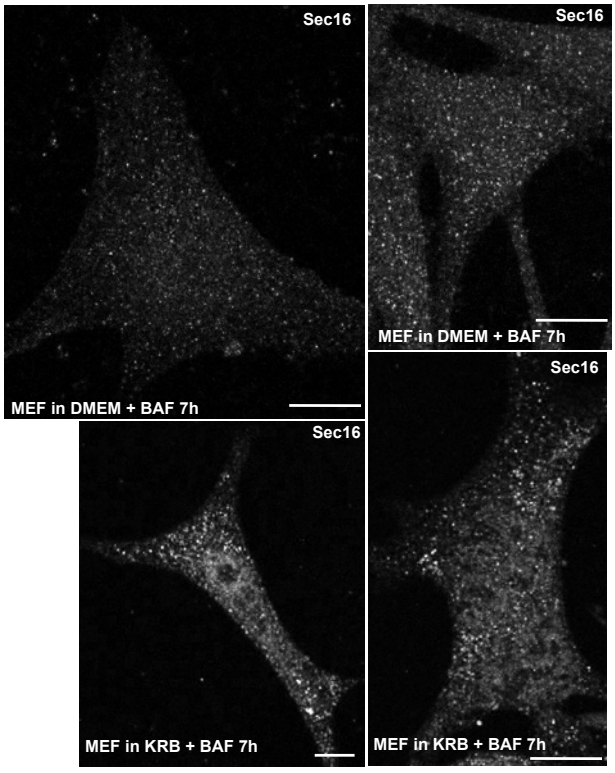

Figure 1-figure supplement 4: **Sec body formation and mammalian cells.** IF visualization of Sec16 in immortalized MEFs incubated in growth medium (DMEM) or KRB plus bafilomycin for 7 h. Note that Sec16 is remodeled into larger structures. Scale bar: 10 μm.

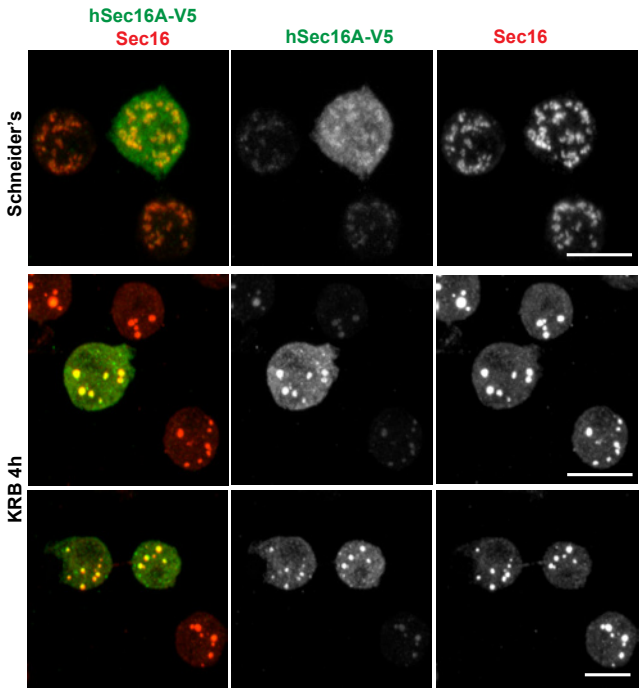

Figure 1-figure supplement 5: **Human Sec16A is incorporated to Sec bodies in starved Drosophila S2 cells.** IF visualization of human Sec16A-V5 transfected in Drosophila S2 cells. Note that it partially localizes to ERES in fed cells but is efficiently incorporated in Sec bodies upon starvation. Scale bar: 10 μm.

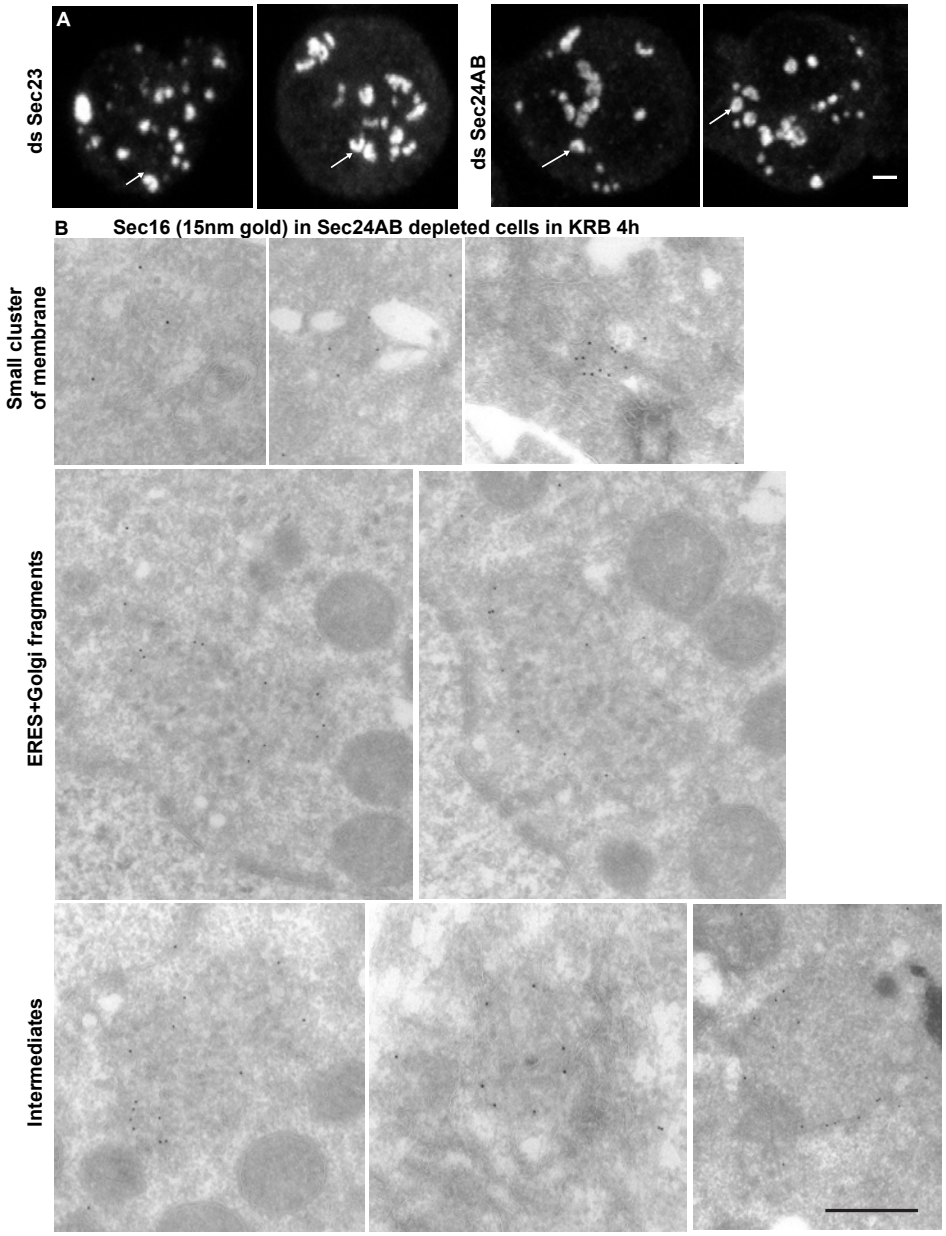

Figure 5-figure supplement 1: **The smaller structures generated in starved Sec24AB depleted cells are not Sec bodies. A**: Sec16 positive horseshoe shape structures observed by IF. **B**: Gallery of Sec16 positive IEM profiles: smaller clusters of membrane, larger ones probably corresponding to ERES mixed with Golgi fragments, intermediate structures (round shape but with membrane in their core and of smaller size than typical Sec bodies). Scale bars: 2 μm (A) and 500 nm (B).

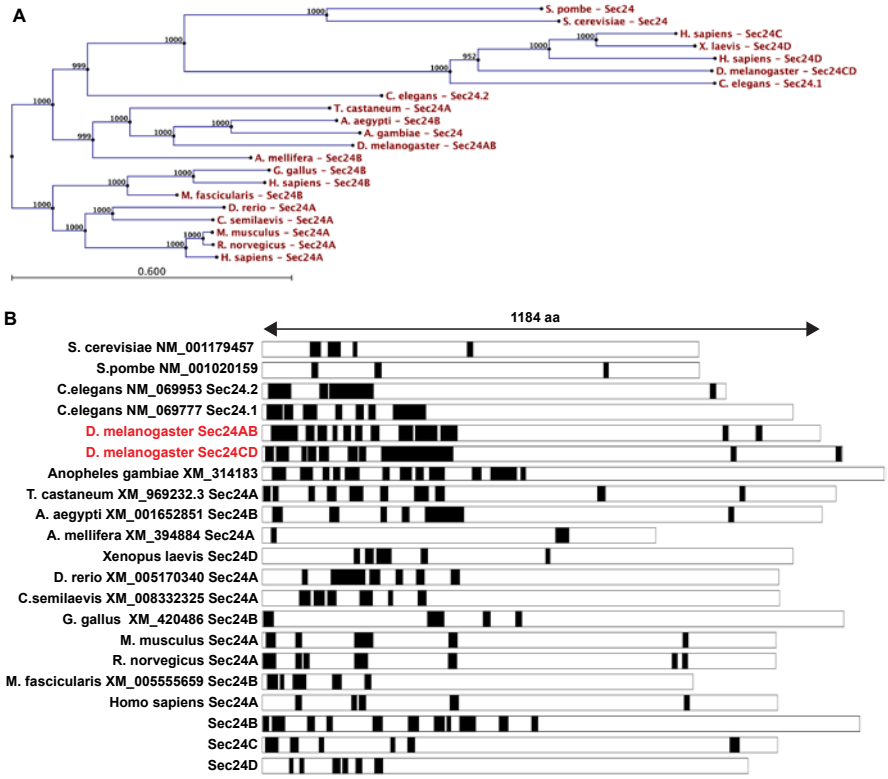

Figure 6-figure supplement 1**: LCS content of Sec24 in different species. A**: A restricted phylogenic tree of the Sec24 sequences analyzed in B. Note that S.pombe and S. cerevisiae Sec24 are similar to each other and to H. sapiens Sec24C and D, and D. melanogaster Sec24CD. However, they are distant to D. melanogaster Sec24AB, H. sapiens Sec24A and B. Furthermore, D. melanogaster Sec24AB is distant to D. melanogaster Sec24CD. **B**: LCS analysis and schematics in Sec24 sequences of different organisms. Note that most sequences contain a significant percentage of LCS in the N-terminal third of the protein with the exception of S. pombe, A. melifera and G. gallus (related to Figure 6A).

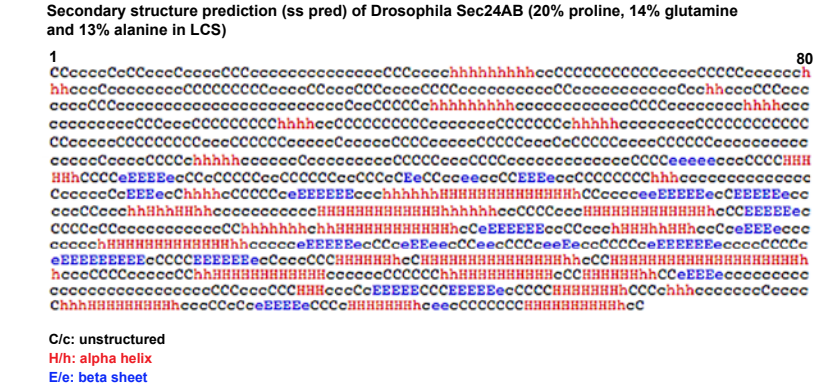

Figure 6-figure supplement 2: **Secondary structure prediction of Drosophila Sec24AB using HH pred.** C/c denotes the unstructured, H/h the alpha helices, and E/e, the beta sheets. Note their absence in the 405 amino-acids of the N-terminus corresponding to LCS.

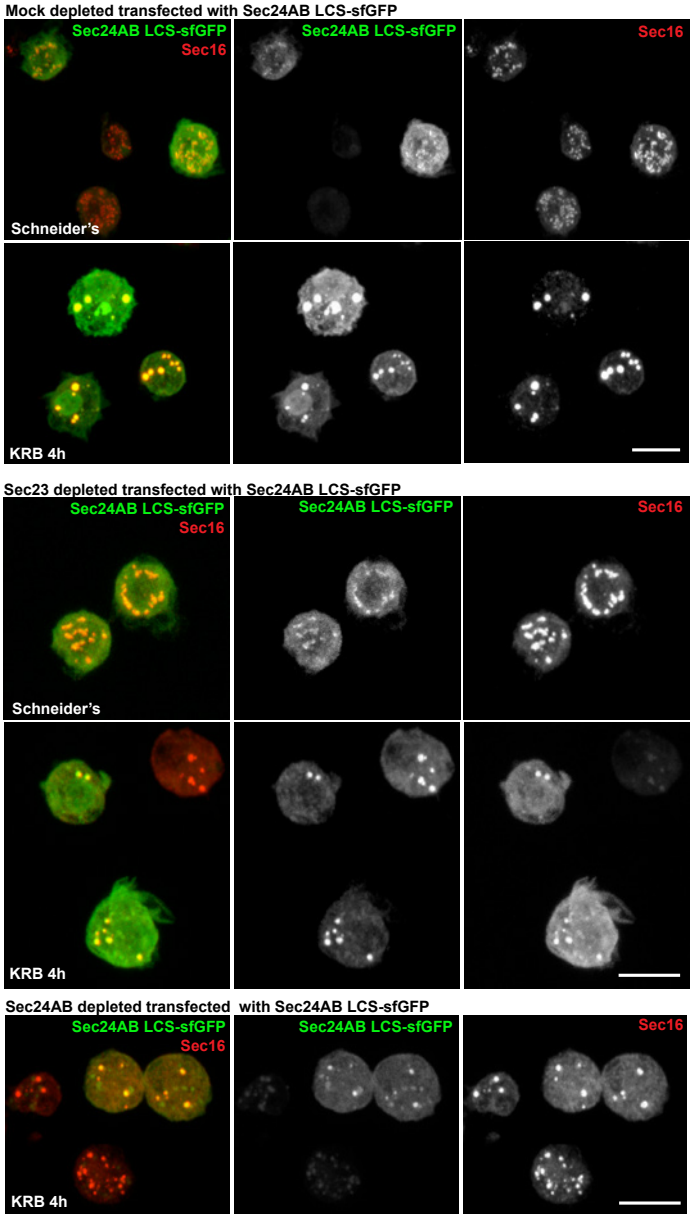

Figure 6-figure supplement 3: **Sec24AB LCS is not sufficient to drive Sec body formation.** S2 cells were depleted of endogenous Sec24AB. When starved (KRB), this resulted in the formation of small structures (as in Figure 5). The transfection of Sec24AB LCS-sfGFP in these depleted cells did not rescue the formation of Sec bodies. Scale bars: 10 μm.

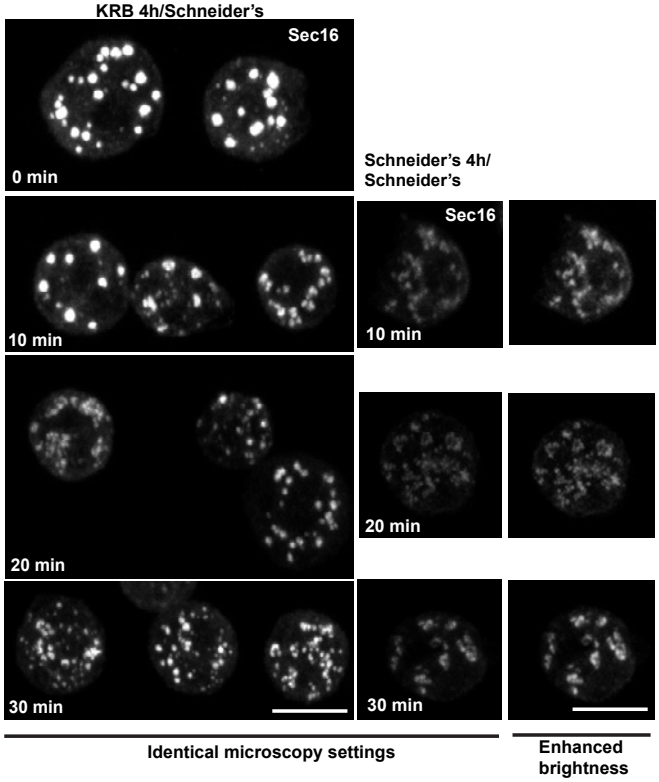

Figure 8-figure supplement 1**: IF localization of Sec16 in cells recovering in Schneider's for 10-30 min after 4h in KRB.** At 30 min, 90% of ERES are rebuilt. Note that the intensity of fluorescence of Sec16 is higher than in the cells that were maintained in Schneider's, reflecting the storage of the ERES components in Sec bodies. Scale bars: 10 μm.

Figure 6-Source data 1 and Video supplement 1-6: These supplemental data can be found in the online version of this manuscript.

References

Almen, M.S., Nordstrom, K.J., Fredriksson, R., Schioth, H.B., 2009. Mapping the human membrane proteome: a majority of the human membrane proteins can be classified according to function and evolutionary origin. BMC Biol 7, 50.

Amodio, G., Renna, M., Paladino, S., Venturi, C., Tacchetti, C., et al., 2009. Endoplasmic reticulum stress reduces the export from the ER and alters the architecture of post-ER compartments. Int J Biochem Cell Biol 41, 2511-2521.

An, S., Kumar, R., Sheets, E.D., Benkovic, S.J., 2008. Reversible compartmentalization of de novo purine biosynthetic complexes in living cells. Science 320, 103-106.

Anderson, P., Kedersha, N., 2008. Stress granules: the Tao of RNA triage. Trends Biochem Sci 33, 141-150.

Bard, F., Casano, L., Mallabiabarrena, A., Wallace, E., Saito, K., et al., 2006. Functional genomics reveals genes involved in protein secretion and Golgi organization. Nature 439, 604-607.

Bentley, M., Nycz, D.C., Joglekar, A., Fertschai, I., Malli, R., et al., 2010. Vesicular calcium regulates coat retention, fusogenicity, and size of pre-Golgi intermediates. Mol Biol Cell 21, 1033-1046.

Bharucha, N., Liu, Y., Papanikou, E., McMahon, C., Esaki, M., et al., 2013. Sec16 influences transitional ER sites by regulating rather than organizing COPII. Mol Biol Cell 24, 3406-3419.

Brangwynne, C.P., Eckmann, C.R., Courson, D.S., Rybarska, A., Hoege, C., et al., 2009. Germline P granules are liquid droplets that localize by controlled dissolution/condensation. Science 324, 1729-1732.

Brangwynne, C.P., Mitchison, T.J., Hyman, A.A., 2011. Active liquid-like behavior of nucleoli determines their size and shape in Xenopus laevis oocytes. Proc Natl Acad Sci U S A 108, 4334-4339.

Bruns, C., McCaffery, J.M., Curwin, A.J., Duran, J.M., Malhotra, V., 2011. Biogenesis of a novel compartment for autophagosome-mediated unconventional protein secretion. J Cell Biol 195, 979-992.
Buchan, J.R., Kolaitis, R.M., Taylor, J.P., Parker, R., 2013. Eukaryotic stress granules are cleared by autophagy and Cdc48/VCP function. Cell 153, 1461-1474.
Buchan, J.R., Muhlrad, D., Parker, R., 2008. P bodies promote stress granule assembly in Saccharomyces cerevisiae. J Cell Biol 183, 441-455.
Castilho, B.A., Shanmugam, R., Silva, R.C., Ramesh, R., Himme, B.M., et al., 2014. Keeping the eIF2 alpha kinase Gcn2 in check. Biochim Biophys Acta.
Cluett, E.B., Wood, S.A., Banta, M., Brown, W.J., 1993. Tubulation of Golgi membranes in vivo and in vitro in the absence of brefeldin A. J Cell Biol 120, 15-24.
Connerly, P.L., Esaki, M., Montegna, E.A., Strongin, D.E., Levi, S., et al., 2005. Sec16 is a determinant of transitional ER organization. Curr Biol 15, 1439-1447.
d'Enfert, C., Wuestehube, L.J., Lila, T., Schekman, R., 1991. Sec12p-dependent membrane binding of the small GTP-binding protein Sar1p promotes formation of transport vesicles from the ER. J Cell Biol 114, 663-670.
Das, S., Pal, U., Das, S., Bagga, K., Roy, A., et al., 2014. Sequence complexity of amyloidogenic regions in intrinsically disordered human proteins. PLoS One 9, e89781.
Eulalio, A., Behm-Ansmant, I., Schweizer, D., Izaurralde, E., 2007. P-body formation is a consequence, not the cause, of RNA-mediated gene silencing. Mol Cell Biol 27, 3970-3981.
Farhan, H., Wendeler, M.W., Mitrovic, S., Fava, E., Silberberg, Y., et al., 2010. MAPK signaling to the early secretory pathway revealed by kinase/phosphatase functional screening. J Cell Biol 189, 997-1011.
Forster, D., Armbruster, K., Luschnig, S., 2010. Sec24-dependent secretion drives cell-autonomous expansion of tracheal tubes in Drosophila. Curr Biol 20, 62-68.
Gaccioli, F., Huang, C.C., Wang, C., Bevilacqua, E., Franchi-Gazzola, R., et al., 2006. Amino acid starvation induces the SNAT2 neutral amino acid transporter by a mechanism that involves eukaryotic initiation factor 2alpha phosphorylation and cap-independent translation. J Biol Chem 281, 17929-17940.
Gilks, N., Kedersha, N., Ayodele, M., Shen, L., Stoecklin, G., et al., 2004. Stress granule assembly is mediated by prion-like aggregation of TIA-1. Mol Biol Cell 15, 5383-5398.
Giuliani, G., Giuliani, F., Volk, T., Rabouille, C., 2014. The Drosophila RNA-binding protein HOW controls the stability of dgrasp mRNA in the follicular epithelium. Nucleic Acids Res 42, 1970-1986.
Hughes, H., Budnik, A., Schmidt, K., Palmer, K.J., Mantell, J., et al., 2009. Organisation of human ER-exit sites: requirements for the localisation of Sec16 to transitional ER. J Cell Sci 122, 2924-2934.
Hyman, A.A., Brangwynne, C.P., 2011. Beyond stereospecificity: liquids and mesoscale organization of cytoplasm. Dev Cell 21, 14-16.
Hyman, A.A., Simons, K., 2012. Cell biology. Beyond oil and water--phase transitions in cells. Science 337, 1047-1049.
Ivan, V., de Voer, G., Xanthakis, D., Spoorendonk, K.M., Kondylis, V., et al., 2008. Drosophila Sec16 mediates the biogenesis of tER sites upstream of Sar1 through an arginine-rich motif. Mol Biol Cell 19, 4352-4365.
Jamieson, J.D., Palade, G.E., 1968. Intracellular transport of secretory proteins in the pancreatic exocrine cell. IV. Metabolic requirements. J Cell Biol 39, 589-603.
Kato, M., Han, T.W., Xie, S., Shi, K., Du, X., et al., 2012. Cell-free formation of RNA granules: low complexity sequence domains form dynamic fibers within hydrogels. Cell 149, 753-767.
Kedersha, N.L., Gupta, M., Li, W., Miller, I., Anderson, P., 1999. RNA-binding proteins TIA-1 and TIAR link the phosphorylation of eIF-2 alpha to the assembly of mammalian stress granules. J Cell Biol 147, 1431-1442.
Klionsky, D.J., Abdalla, F.C., Abeliovich, H., Abraham, R.T., Acevedo-Arozena, A., et al., 2012. Guidelines for the use and interpretation of assays for monitoring autophagy. Autophagy 8, 445-544.
Kondylis, V., Rabouille, C., 2003. A novel role for dp115 in the organization of tER sites in Drosophila. J Cell Biol 162, 185-198.
Kondylis, V., Rabouille, C., 2009. The Golgi apparatus: lessons from Drosophila. FEBS Lett 583, 3827-3838.
Kondylis, V., Tang, Y., Fuchs, F., Boutros, M., Rabouille, C., 2011. Identification of ER proteins involved in the functional organisation of the early secretory pathway in Drosophila cells by a targeted RNAi screen. PLoS One 6, e17173.
Kondylis, V., van Nispen tot Pannerden, H.E., Herpers, B., Friggi-Grelin, F., Rabouille, C., 2007. The golgi comprises a paired stack that is separated at G2 by modulation of the actin cytoskeleton through Abi and Scar/WAVE. Dev Cell 12, 901-915.
Kung, L.F., Pagant, S., Futai, E., D'Arcangelo, J.G., Buchanan, R., et al., 2012. Sec24p and Sec16p cooperate to regulate the GTP cycle of the COPII coat. EMBO J 31, 1014-1027.
Laporte, D., Salin, B., Daignan-Fornier, B., Sagot, I., 2008. Reversible cytoplasmic localization of the proteasome in quiescent yeast cells. J Cell Biol 181, 737-745.
Lee, T.H., Linstedt, A.D., 1999. Osmotically induced cell volume changes alter anterograde and retrograde transport, Golgi structure, and COPI dissociation. Mol Biol Cell 10, 1445-1462.
Lucocq, J.M., Warren, G., 1987. Fragmentation and partitioning of the Golgi apparatus during mitosis in HeLa cells. EMBO J 6, 3239-3246.
Miyamoto, T., Oshiro, N., Yoshino, K., Nakashima, A., Eguchi, S., et al., 2008. AMP-activated protein kinase phosphorylates Golgi-specific brefeldin A resistance factor 1 at Thr1337 to induce disassembly of Golgi apparatus. J Biol Chem 283, 4430-4438.
Narayanaswamy, R., Levy, M., Tsechansky, M., Stovall, G.M., O'Connell, J.D., et al., 2009. Widespread reorganization of metabolic enzymes into reversible assemblies upon nutrient starvation. Proc Natl Acad Sci U S A 106, 10147-10152.
Norum, M., Tang, E., Chavoshi, T., Schwarz, H., Linke, D., et al., 2010. Trafficking through COPII stabilises cell

polarity and drives secretion during Drosophila epidermal differentiation. PLoS One 5, e10802.
O'Connell, J.D., Zhao, A., Ellington, A.D., Marcotte, E.M., 2012. Dynamic reorganization of metabolic enzymes into intracellular bodies. Annu Rev Cell Dev Biol 28, 89-111.
Oka, T., Nishikawa, S., Nakano, A., 1991. Reconstitution of GTP-binding Sar1 protein function in ER to Golgi transport. J Cell Biol 114, 671-679.
Peters, L.Z., Hazan, R., Breker, M., Schuldiner, M., Ben-Aroya, S., 2013. Formation and dissociation of proteasome storage granules are regulated by cytosolic pH. J Cell Biol 201, 663-671.
Petrovska, I., Nuske, E., Munder, M.C., Kulasegaran, G., Malinovska, L., et al., 2014. Filament formation by metabolic enzymes is a specific adaptation to an advanced state of cellular starvation. Elife.
Piao, H., MacLean Freed, J., Mayinger, P., 2012. Metabolic activation of the HOG MAP kinase pathway by Snf1/AMPK regulates lipid signaling at the Golgi. Traffic 13, 1522-1531.
Ramaswami, M., Taylor, J.P., Parker, R., 2013. Altered ribostasis: RNA-protein granules in degenerative disorders. Cell 154, 727-736.
Rothman, J.E., Wieland, F.T., 1996. Protein sorting by transport vesicles. Science 272, 227-234.
Schekman, R., Orci, L., 1996. Coat proteins and vesicle budding. Science 271, 1526-1533.
Shamu, C.E., Cox, J.S., Walter, P., 1994. The unfolded-protein-response pathway in yeast. Trends Cell Biol 4, 56-60.
Shimada, Y., Burn, K.M., Niwa, R., Cooley, L., 2011. Reversible response of protein localization and microtubule organization to nutrient stress during Drosophila early oogenesis. Dev Biol 355, 250-262.
Shindiapina, P., Barlowe, C., 2010. Requirements for transitional endoplasmic reticulum site structure and function in Saccharomyces cerevisiae. Mol Biol Cell 21, 1530-1545.
Stevens, T.J., Arkin, I.T., 2000. Do more complex organisms have a greater proportion of membrane proteins in their genomes? Proteins 39, 417-420.
Stoecklin, G., Kedersha, N., 2013. Relationship of GW/P-bodies with stress granules. Adv Exp Med Biol 768, 197-211.
Teixeira, L., Rabouille, C., Rorth, P., Ephrussi, A., Vanzo, N.F., 2003. Drosophila Perilipin/ADRP homologue Lsd2 regulates lipid metabolism. Mech Dev 120, 1071-1081.
van Donselaar, E., Posthuma, G., Zeuschner, D., Humbel, B.M., Slot, J.W., 2007. Immunogold labeling of cryosections from high-pressure frozen cells. Traffic 8, 471-485.
Wilson, M.Z., Gitai, Z., 2013. Beyond the cytoskeleton: mesoscale assemblies and their function in spatial organization. Curr Opin Microbiol 16, 177-183.
Wootton, J.C., Federhen, S., 1996. Analysis of compositionally biased regions in sequence databases. Methods Enzymol 266, 554-571.
Zacharogianni, M., Kondylis, V., Tang, Y., Farhan, H., Xanthakis, D., et al., 2011. ERK7 is a negative regulator of protein secretion in response to amino-acid starvation by modulating Sec16 membrane association. EMBO J 30, 3684-3700.

Chapter 3

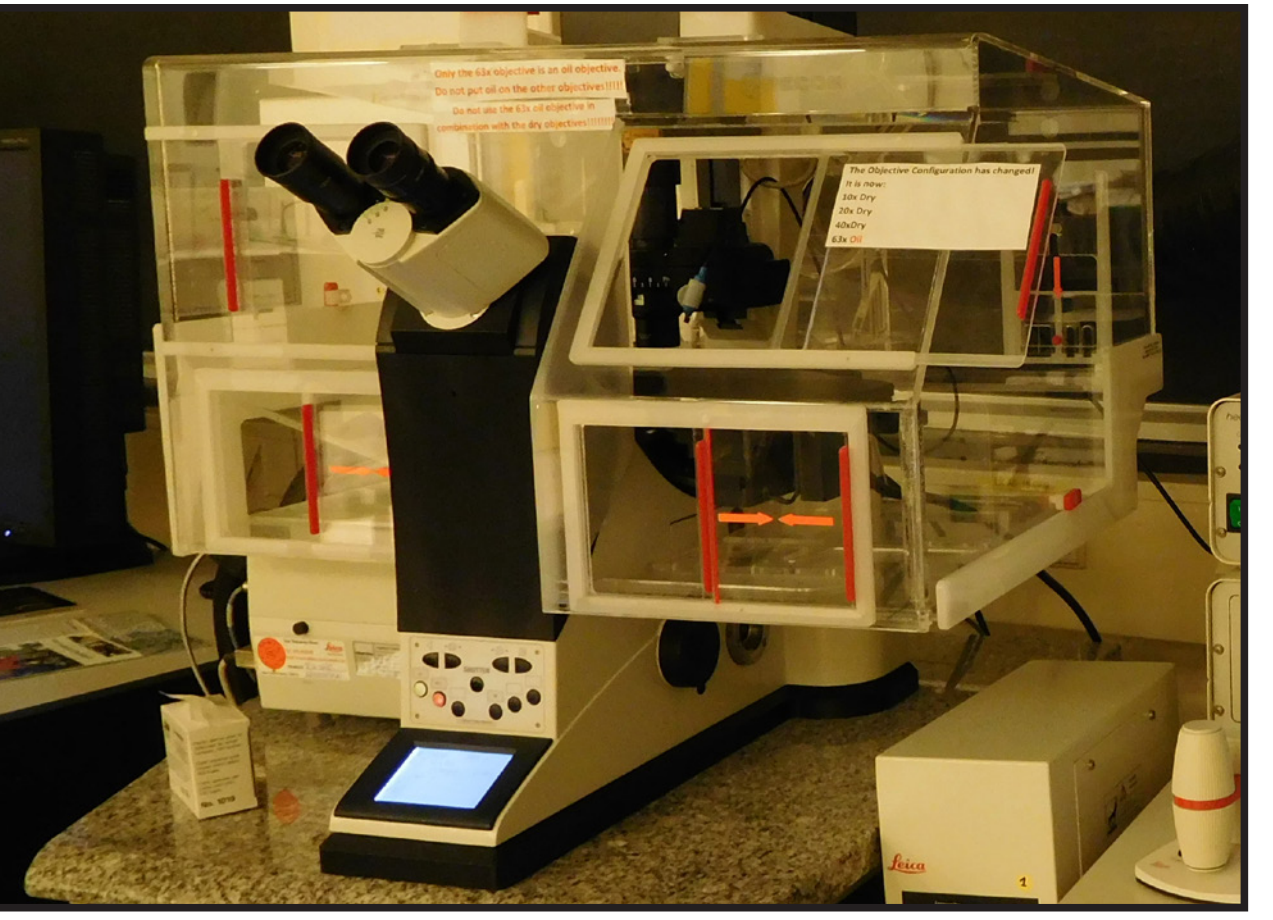
Only the 63x objective is an oil objective
Do not put oil on the other objectives!!!!!
Do not use the 63x oil objective in
combination with the dry objectives!!!!!!!
The Objective Configuration has changed!
It is now:
10x Dry
20x Dry
40xDry
63x Oil
Leica

In vivo visualization of Mono-ADP-ribosylation by dPARP16 upon amino-acid starvation

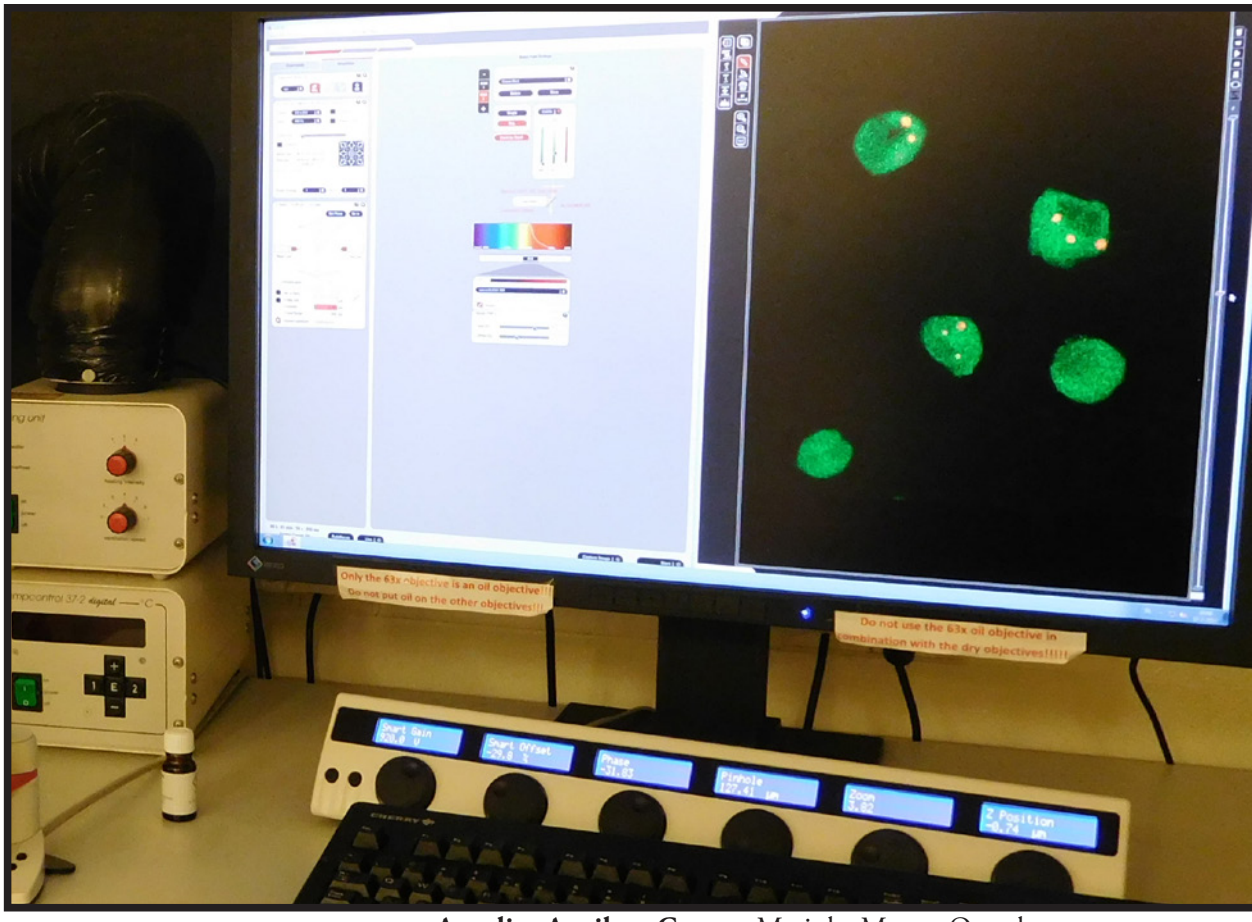

Angelica Aguilera-Gomez, Marinke M. van Oorschot, Tineke Veenendaal and Catherine Rabouille (2016)
eLife 2016;5:e21475

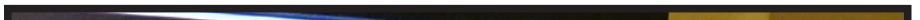

In vivo visualization of Mono-ADP-ribosylation by dPARP16 upon amino-acid starvation

Abstract

PARP catalyzed ADP-ribosylation is a post-translational modification involved in several physiological and pathological processes, including cellular stress. In order to visualize both Poly-, and Mono-, ADP-ribosylation *in vivo*, we engineered specific fluorescent probes. Using them, we show that amino-acid starvation triggers an unprecedented display of mono-ADP-ribosylation that governs the formation of Sec body, a recently identified stress assembly that forms in Drosophila cells. We show that dPARP16 catalytic activity is necessary and sufficient for both amino-acid starvation induced mono-ADP-ribosylation and subsequent Sec body formation and cell survival. Importantly, dPARP16 catalyzes the modification of Sec16, a key Sec body component, and we show that it is a critical event for the formation of this stress assembly. Taken together our findings establish a novel example for the role of mono-ADP-ribosylation in the formation of stress assemblies, and link this modification to a metabolic stress.

Introduction

ADP-ribosylation, either poly (PARylation) or mono (MARylation) is a post-translational modification that refers to the addition of one or multiple ADP-ribose units to protein substrates. It is catalyzed by PARPs (also called ADP-Ribose Transferase class D, ARTD), a family of 17 proteins in mammals (Hottiger et al., 2010; Leung, 2014; Leung et al., 2011). PARPs have emerged as major players in several physiological processes, such as transcriptional regulation, chromatin remodeling and telomere functions (Krishnakumar and Kraus, 2010), cell differentiation, proliferation, apoptosis (Hu et al., 2013) and cellular signaling (Watanabe et al., 2016) as well as pathological ones, such as cancer (Fujimori et al., 2012) and neurodegeneration (Cosi and Marien, 1999).

ADP-ribosylation has also been shown to occur during cellular stress. The founding member, the nuclear PARP1, is required for DNA repair during DNA damage (Gibson and Kraus, 2012) where it hyper-PARylates itself as well as surrounding histones (Gibbs-Seymour et al., 2016). Furthermore, MARylation is linked to ER stress via PARP16, the only membrane-anchored member of this family (Di Paola et al., 2012; Jwa and Chang, 2012).

However, the progress in understanding the role of these modifications is limited by difficulties in identifying individual targets and to validate them during specific biological processes. This is mainly due to the labile bonds between ADP-ribose to the substrate, and the low abundance of this modification in steady state conditions. So

far, chemical tools, such as NAD+ analogues, have been used for in vitro approaches, (Carter-O'Connell et al., 2016). Monitoring PARylation has been possible in vitro using the PAR affinity resin (Tulip-4301 www.tulipbiolabs.com/4301.html) and monoclonal antibodies, such as 10H and LP96-10. However, these antibodies bind poly-, not mono-ADP-ribose. This represents a serious limitation as most PARPs are predicted to be MARylation enzymes (Hottiger et al., 2010) (Leung, 2014) (Butepage et al., 2015). Yet, the role of this form of the modification in intracellular processes is largely unexplored.

Several biological modules, known as macrodomains, that specifically recognize either poly- or mono-ADP-ribose (Karras et al., 2005) (Rack et al., 2016) have also been used in pull down experiments for large scale proteomics studies (Vivelo and Leung, 2015). Accordingly, macrodomains H2A1.1 show binding specificity for PARylated proteins (Kustatscher et al., 2005; Timinszky et al., 2009). And macrodomains from human PARP14 that exclusively binds Mono-ADP-ribose have being used to pull down MARylated PARP10 (Forst et al., 2013). Importantly these macrodomains do not exhibit hydrolase activity (Jankevicius et al., 2013; Rosenthal et al., 2013).

Here, we took advantage of the specificity of these macrodomains to design, build and fine-tune stable MARylation (MAD) and PARylation (PAD) detection probes. We then used them to follow PARylation and MARylation *in vivo* during cellular stresses, with particular focus on amino-acid starvation that induces the formation of a recently described stress assembly, the Sec body (Zacharogianni et al., 2014).

Sec body formation results from the inhibition of a major anabolic pathway, the protein transport through the secretory pathway, upon amino-acid starvation of Drosophila cells (Amodio et al., 2009; Zacharogianni et al., 2014). The secretory pathway ensures the delivery of signal peptide containing proteins to the extracellular medium and the plasma membrane and to nearly all membrane-bound compartments. After the synthesis in the endoplasmic reticulum (ER), they exit this organelle in COPII coated vesicles that form and bud at defined sites on the ER, called ER exit sites (ERES). COPII formation requires Sar1, its GEF Sec12 and the structural proteins forming the coat itself, Sec23/24 and Sec13/31 (Miller and Schekman, 2013) as well as the large hydrophilic scaffold protein Sec16 (Sprangers and Rabouille, 2015). Newly synthesized proteins then reach the Golgi apparatus where they are processed, sorted and dispatch to their final destination.

The inhibition of protein transport through the secretory pathway upon amino-acid starvation is accompanied by the remodeling of ERES and the formation of a novel type of pro-survival stress assembly with liquid droplet properties, the Sec body, where COPII coat proteins and Sec16 are stored and protected from degradation during the period of stress (Zacharogianni et al., 2014).

Using PAD, we show that PARylation is not prominent during amino-acid starvation. Conversely, using MAD, we show that MARylation is strongly induced by this nutrient stress. Furthermore, we demonstrate that this modification is

required for the formation of Sec bodies. We identify dPARP16 as the enzyme necessary and sufficient to catalyze MARylation and Sec body formation during amino-acid starvation. Last, we identify the ERES component Sec16 as a novel dPARP16 substrate and show that it is MARylated on its C-terminus in an amino-acid starvation specific manner. We propose that this event initiates the formation of the Sec bodies and poses Sec16 as a stress response protein.

Taken together, our findings establish an unprecedented example for the role of mono-ADP-ribosylation in the formation of stress assemblies, and link this modification to a metabolic stress. Furthermore, this demonstrates that the macrodomain-based probes that we built are useful and specific tools to follow ADP-ribosylation taking place during biological processes *in vitro* and *in vivo.* We propose that the visualization of ADP-ribosylation will shed light on PARPs function during specific biological processes and illustrates the physiological relevance of these post-translational modifications during stress. In this regard, we have identified dPARP16 as a novel key factor in cell survival to amino-acid starvation.

Results

Visualizing PARylation and MARylation *in vivo* upon cellular stress.

To visualize whether PARylation events take place during amino-acid starvation, we engineered a PARylation detection probe (PAD) using the human Macrodomain H2A1.1 that specifically recognizes poly-ADP-ribose (Forst et al., 2013; Kustatscher et al., 2005; Timinszky et al., 2009) that we fused to YFP (YFP-PAD) (**Figure 1A**). When expressed in Drosophila S2 cells, YFP-PAD is both cytoplasmic and nuclear (**Figure 1B)**. Amino-acid starvation only elicits a weak remodeling of the probe in the cytoplasm and an increase of its nuclear pool (**Figure 1B).** To validate the functionality of the probe, we treated S2 cells with arsenite, a treatment that, in human cells, elicits PARylation known to be required for stress granules integrity (Leung et al., 2011). Accordingly, YFP-PAD forms defined cytoplasmic structures in arsenate treated S2 cells (**Figure 1C)** that partially co-localize with stress granules (marked by FMR1, **Figure 1C)**, showing that YFP-PAD is functional. Taken together, these results indicate that amino-acid starvation does not elicit detectable PARylation events.

We then asked whether amino-acid starvation elicits MARylation. To approach this, we engineered an optimized a MARylation detection (MAD) probe based upon the macrodomains 1-3 of human PARP14. Indeed, crystallography of these macrodomains has revealed a conserved fold that binds Mono-ADP-ribose. Furthermore, calorimetric affinity assays show that the affinity for mono-ADP-ribose is contributed by the three macrodomains in a cooperative manner, whereas each macrodomain taken individually does not bind the moiety. Last, PARP14 macrodomains 1-3 bind specifically MARylated, but not PARylated, substrates *in*

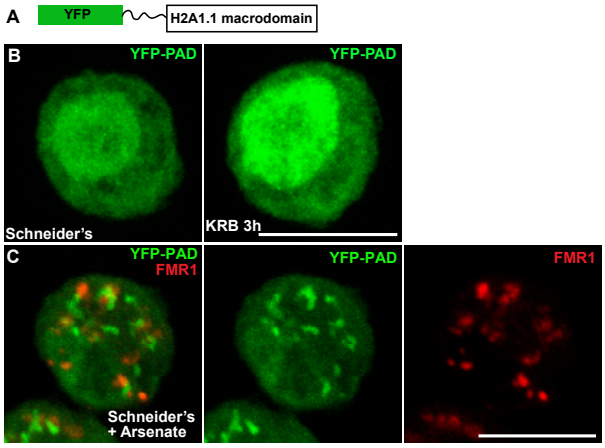

Figure 1: PAD in cellular stress. A: Schematics of YFP-PAD probe. **B**: YFP-MAD in growing (Schneider's) and amino-acid starved (KRB) cells for 3 h. Note that with the exception of an increase of the nuclear intensity, amino-acid starvation does not lead to the formation of a cytoplasmic pattern. **C:** YFP-MAD in S2 cells upon arsenate treatment. Note the formation of a robust YFP-PAD cytoplasmic pattern that co-localizes with stress granules (FMR1, red). Scale bars: 10 μm.

vitro (Forst et al., 2013). Therefore, the PARP14 macrodomains 1-3 were GFP-tagged at their N-terminus, and a linker was inserted to preserve their binding capabilities (**Figure 2A,** *Figure 2, figure supplement 1*).

When expressed in S2 cells under growing conditions, GFP-MAD is diffuse in the cytoplasm in most of the transfected cells, but in contrast to PAD is absent from the nucleus (**Figure 2B, B'**). When cells are starved of amino-acids for increasing length of time, GFP-MAD adopts a defined pattern. After 1 h, it concentrates in one spot in a low percentage of cells (arrows in **Figure 2B, B').** After 2 h, it forms 1-3 spots in a larger number of cells. Thereafter, the number of spots (some of them with a U/donut shape) (arrowheads, **Figure 2B, C, D, E**) increases and they tend to concentrate in the middle of the cell after 4 h (not shown). These results suggest that amino-acid starvation triggers cytoplasmic MARylation events that are visualized using GFP-MAD.

To demonstrate that the GFP-MAD spots forming upon amino-acid starvation correspond to the detection of MARylation events, a point mutation (G1055E) was introduced in the macrodomain 2 of GFP-MAD (**Figure 2A**). This mutation affects the ADP-ribose binding pocket and therefore interferes with the ADP-binding activity (Forst et al., 2013) and in vitro to completely abrogate its binding to mono-ADP-ribose (Dani et al., 2009; Karras et al., 2005). Strikingly, amino-acid starvation of S2 cells expressing G1055E GFP-MAD does not result in any pattern and the mutant probe remains diffuse in the cytoplasm (**Figure 2C, C').**

Next, we visualized MARylation events in live cells. This confirms that MAD spots start forming about 1h after starvation and accumulate. It also shows that they are overall stable, (**Figure 2D and** Movie 1-*Figure 2, figure supplement 2),* although

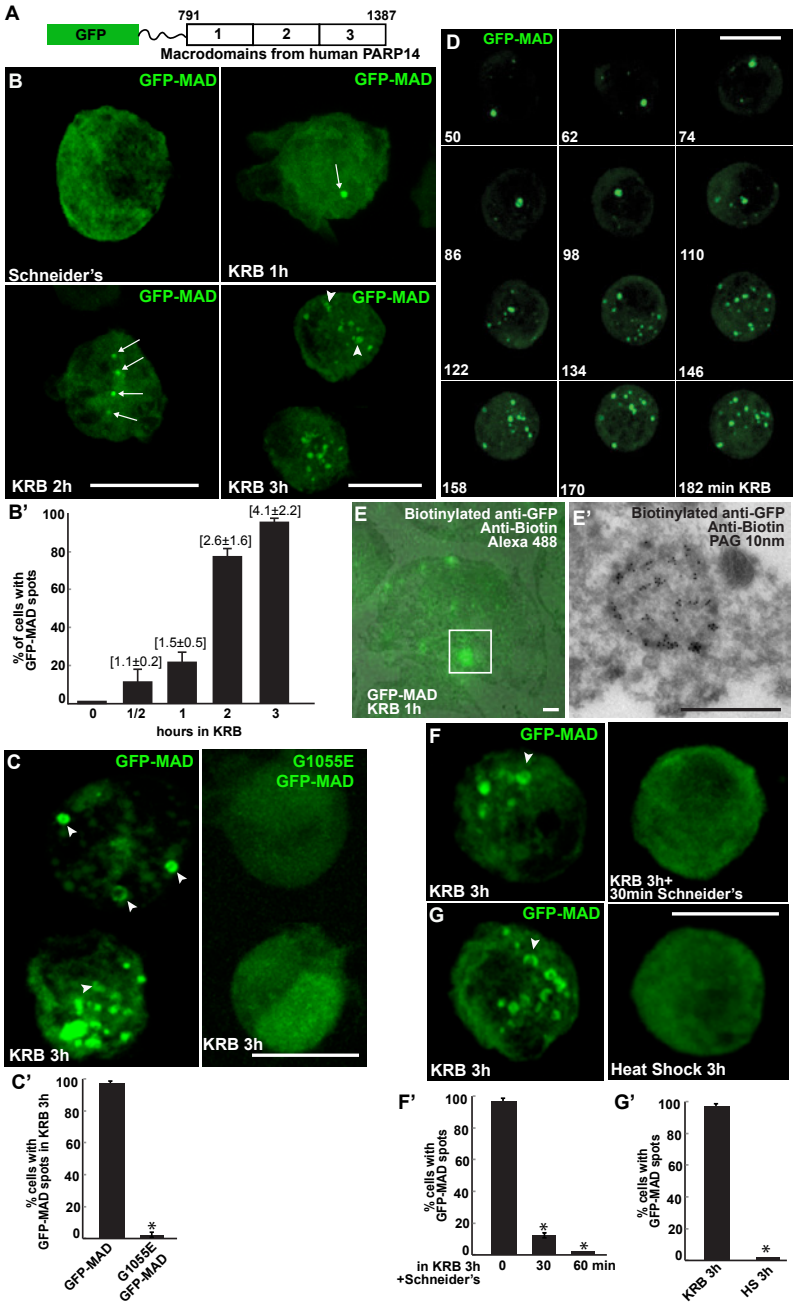

Figure 2: Amino-acid starvation leads to the formation of MARylation spots visualized with GFP-MAD. A: Schematics of the GFP-MAD probe. **B, B'**: Fluorescence of GFP-MAD in growing S2 cells (Schneider's) and upon amino-acid starvation (KRB) for increasing amount of time as indicated (B). Note the formation of GFP-MAD spots (arrows) (some in an U-shape, arrowheads in B-D). The % of cells at each time point displaying GFP-MAD spots is shown in B'. The average number of spots per cell

is indicated above each bar. **C, C'**: Fluorescence of GFP-MAD and G1095A GFP-MAD probe (that does not bind mono-ADP-ribose in vitro). Note that the mutant probe does not form spots in KRB (quantified in C'). **D**: Stills of a time-lapse movie (Figure 2, figure supplement 4) of GFP-MAD in cells incubated in KRB for 3 h. The first frame is taken after 50 min incubation. The subsequent frames are taken every 12 min. **E, E'**: Correlative Fluorescence/IEM of GFP-MAD spots in S2 cells upon amino-acid starvation (KRB, 1 h). The IEM (E') corresponds to the white rectangle in fluorescence that is overlapped with the corresponding electron micrograph (E). **F, F':** Fluorescence pattern of GFP-MAD and endogenous Sec16 (red) in KRB and in KRB followed by incubation with Schneider's for 30 min. Note that both GFP-MAD and Sec bodies are completely reverted (quantified in F') **G**, **G'**: Fluorescence pattern of GFP-MAD in KRB and upon heat shock (3 h at 37°C) Scale bars: 10 μm (B, C, D, F, G); 500 nm (E, E'). Error bars: SEM.

few appear more transient with an average lifetime of 50 min (not shown). Using a Fluorescence-to-Immuno EM correlative method (Hassink et al., 2012; Vicidomini et al., 2010), we showed that MAD spots correspond to non-membrane bound structures (**Figure 2E, E')**, ranging from 600 nm to 2 microns in diameter.

We tested their reversibility upon nutrient replenishment following starvation and found that they are fully reversible after 30 min of Schneider's addition **(Figure 2F, F')**. Last, we show that heat stress (**Figure 2G, G'**) and arsenate treatment (not shown) do not elicit a GFP-MAD pattern, confirming the specificity of MARylation to amino-acid starvation.

Taken together, we demonstrate that GFP-MAD detects localized MARylation events that are specifically triggered by amino-acid starvation.

dPARP16 activity controls MARylation events upon amino-acid starvation.

In order to identify whether and which PARPs are involved the amino-acid starvation driven MARylation events, we searched for Drosophila PARPs using psi BLAST and HHpred with the canonical dPARP1/CG40441 as query. In line with (Hottiger et al., 2010), we identified 3 additional ORFs: CG4719 is homologous to human Tankyrase, CG15925 is homologous to human PARP16, and CG18812 is homologous to human GDAP2, a macrodomain, not a PARP (Rack et al., 2016). It was therefore not considered here.

We tested these PARPs for their role in GFP-MAD spot formation upon amino-acid starvation and showed that MAD spot formation strictly depends on dPARP16. First, dPARP16 depletion completely prevents their formation upon amino-acid starvation and GFP-MAD remains diffuse in the cytoplasm (**Figure 3A, A'**). In comparison, the depletion of the other PARPs has no effect and GFP-MAD spots form as in mock-depleted cells *(Figure 3, figure supplement 1)*. Second, the overexpression of dPARP16 under growing conditions induces the robust formation of GFP-MAD spots in most of the cells (**Figure 3B, B', E).** Importantly, 84 ± 6% of GFP-MAD spots formed upon dPARP16 overexpression partially or completely co-localize with the enzyme (**Figure 3B, B'**). These results suggest that dPARP16 mediates the MARylation response to amino-acid starvation.

dPARP16 is the closest homolog of human PARP16 as shown by building a

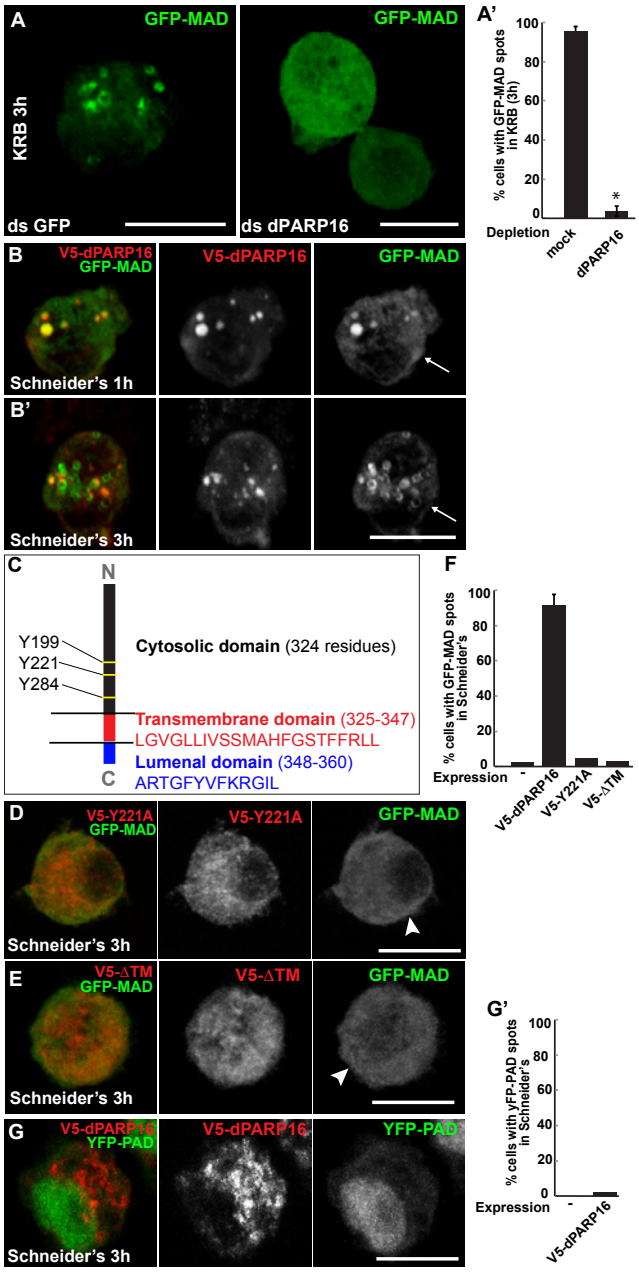

Figure 3: Amino-acid starvation triggered MARylation events are dPARP16 dependent. A, A': Visualization of GFP-MAD in mock and dPARP16 depleted cells upon amino-acid starvation (KRB) (A). Note that dPARP16 depleted cells do not exhibit GFP-MAD spots (quantified in A'). **B, B'**: Visualization of GFP-MAD in S2 cells expressing V5-dPARP16 in growing conditions. Note that the enzyme expression drives the formation of GFP-MAD spots in the absence of stress and that MAD spot strongly co-localize with the enzyme (quantified in F) **C**: dPARP16 has 359 residues including a transmembrane domain of 22 (in red) and a luminal domain of 12 (in blue). The TM has been predicted

using the TMHMM server V.2.0 (http://www.cbs.dtu.dk/services/TMHMM-2.0/). The three tyrosines making up the catalytic sites are marked. **D-F**: Visualization of GFP-MAD in S2 cells expressing Y221A V5-dPARP16 catalytic mutant (E) and ΔTM V5-dPARP16 (F) in growing conditions. Note that none of the mutated form of dPARP16 elicits GFP-MAD spot formation (arrowheads) (quantified in F). **G, G'**: Visualization of YFP-PAD in S2 cells expressing V5-dPARP16 in growing conditions. Note that the PAD localization does not change (quantified in G'). Scale bars: 10 μm Error bars: SEM.

phylogenetic tree containing dPARP16 and all human PARPs *(Figure 3, figure supplement 2)*. Both enzymes are of similar length and they have similar catalytic domain. Human PARP16 has a catalytic site comprising the triad HYY (Hottiger et al., 2010) and using HHpred, we predicted that the catalytic site of dPARP16 consists of the YYY triad (Y199, Y221, Y284) *(Figure 3, figure supplement 3)*. Of note, flies are the outliers as PARP16 in C.elegans and Xenopus do have a HYY site. Last, as hPARP16, dPARP16 is also predicted to be membrane anchored with catalytic domain facing the cytoplasm (Di Paola et al., 2012; Jwa and Chang, 2012) (**Figure 3C**). Accordingly, we find that dPARP16 localizes to ER (*Figure 3, figure supplement 4).* In support of this localization, overexpression of dPARP16 remodels the ER (as shown with KDEL receptor and calnexin) in a very similar fashion as amino-acid starvation does *Figure 3, figure supplement 5).* This phenotype strengthens the notion that dPARP16 is localized at the ER and that the ER remodeling is a result of its activation.

To address the role of dPARP16 catalytic activity in GFP-MAD detected MARylation, we generated the dPARP16 catalytic mutant Y221A. We showed that its expression does not lead to the formation of GFP-MAD spot (**Figure 3D, F)**, whereas expression of the wild type dPARP16 does **(Figure 3B, B', F)**. This indicates that the integrity of dPARP16 catalytic site is required for its MARylation activity.

We then addressed the role of membrane anchoring in dPARP16 function by expressing the dPARP16 cytoplasmic domain (ΔTM dPARP16). Unlike the wild type protein (**Figure 3B', F**), expression of the ΔTM dPARP16 does not induce the formation of GFP-MAD spots (arrowheads **in Figure 3E, F**), indicating that dPARP16 membrane anchoring is required for its MARylation activity.
Last, we show expression of dPARP16 does not elicit a PARylation pattern using YFP-PAD **(Figure 3G, G').**

Taken together, these results show that upon amino-acid starvation, membrane bound dPARP16 catalyzes localized MARylation events that are detected by GFP-MAD. This makes MAD a sensor detecting dPARP16 catalytic activity *in vivo.*

dPARP16 is necessary and sufficient for Sec body formation.

We have recently shown that amino-acid starvation drives the formation of a novel stress assembly related to the early secretory pathway, the Sec body. Sec bodies are pro-survival cytoplasmic stress assembly that incorporate and protect COPII subunits and ERES components from degradation (Zacharogianni et al., 2014) **(Figure 4A')**.

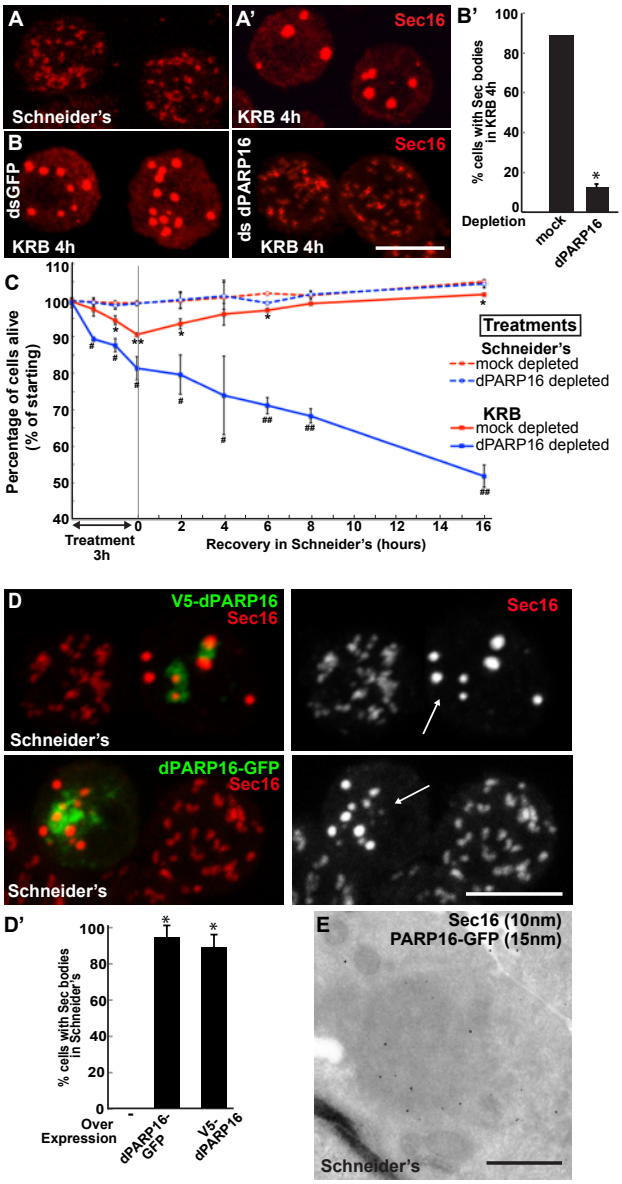

Figure 4: dPARP16 is required for amino-acid starvation driven Sec body formation. A: Immunofluorescence (IF) visualization of endogenous Sec16 (red) at the ERES in growing Drosophila S2 cells (Schneider's) and in Sec bodies upon amino-acid starvation (KRB). **B-B'**: IF visualization of endogenous Sec16 (red) in mock and dPARP16 depleted S2 cells upon amino-acid starvation (KRB) (B). Note that dPARP16 depletion inhibits Sec body formation (quantified in B'). **C**: Graph of cell viability (expressed as percentage of alive cells) upon "treatments" as indicated and recovery. The number of starting cells at t=0, mock- (dsGFP, red lines) and dPARP16 depleted (blue lines) is set at 100%. These cells are incubated in Schneider's (dashed lines) and KRB (solid lines) for 3 h followed by further incubation in Schneider's for 16 h. Note that the dPARP16 cells are more sensitive to starvation than controls and do not recover, whereas their viability not affected when grown in full medium. For each time point, p-values were calculated between mock-depleted cells incubated in Schneider's and in KRB.

* marks p-values higher the 10^{-2} and **, p-values higher than 10^{-5}. p-values were also calculated between mock and dPARP16 depleted incubated in KRB. # marks p-values higher the 10^{-2} and ##, p-values higher than 10^{-4}. **D-D'**: IF visualization of endogenous Sec16 (red) in cells) over-expressing dPARP16-GFP and V5-dPARP16 in growing cells (Schneider's) (C). Note that it drives the robust formation of Sec bodies (arrows in C) (quantified in D'). **E**: Immuno-electron microscopy (IEM) visualization of endogenous Sec16 (10 nm gold) in dPARP16-GFP overexpressing cells (15 nm). Scale bars: 10 μm (A, B, D); 500 nm (E). Error bars: SEM (A, D') and SD (C).

By immunofluorescence, Sec bodies appear as bright circular structures of 700 ± 100 nm in diameter (confirmed by immuno-electron microscopy, IEM) and there are typically 7 ± 3 Sec bodies per starved cells (Zacharogianni et al., 2014). They are distinct from ERES that are more numerous (about 15 ± 7), appear fainter and have a more irregular shape (**Figure 4A, A'**).

We assessed whether amino-acid starvation driven dPARP16 dependent MARylation events are linked to Sec body formation by testing the role of this enzyme in their formation. We found that dPARP16 depletion completely prevents Sec body formation upon amino-acid starvation (**Figure 4B, B'**). We had shown that inhibition of Sec body formation strongly affects cell survival (Zacharogianni et al., 2014). In agreement with this, dPARP16 depletion also strongly affects cell survival upon amino-acid starvation as well as cell recovery upon stress relief (**Figure 4C**). In contrast, in dPARP16 depleted cells during growing conditions cell survival is unaffected, indicating that dPARP16 plays a crucial role exclusively upon starvation. These results together demonstrated that dPARP16 is a key factor in the survival response to amino-acid starvation.

Furthermore, expression of dPARP16 quantitatively drives the specific formation of Sec bodies under growing conditions (**Figure 4D,** arrows**, Figure 4D'**). This was confirmed by immuno-EM (**Figure 4E**). dPARP16 is therefore necessary and sufficient for Sec body formation as it is for GFP-MAD spot formation. Accordingly, depletion *(Figure 4, figure supplement 1)* and overexpression *(Figure 4, figure supplement 2)* of dPARP1 and dTNK do not affect Sec body formation.

We further tested whether dPARP16 catalytic activity is required for Sec body formation. Whereas expression of wild type PARP16 leads to Sec body formation, the expression of dPARP16 catalytic mutants (Y199A and Y221A) do not (**Figure 5A, A'**). To confirm this result, we show that the expression of Y199A dPARP16 does not rescue Sec body formation in starved dPARP16 depleted cells, whereas the expression of wild type dPARP16 does (**Figure 5B, B')**. We also tested the role of membrane anchoring in dPARP16 function in Sec body formation by expressing the dPARP16 cytoplasmic domain (ΔTM dPARP16). We show that unlike the wild type protein, it does not induce Sec body formation (**Figure 5C, A',** arrowheads).

These results show that dPARP16 coordinates the response to amino-acid starvation, i.e. the MARylation events and Sec body formation. In support of this, we found that dPARP16 localizes near or around Sec bodies **(Figure 5C, D,** small green arrows**)**, suggesting that Sec body components could be dPARP16 MARylated substrates.

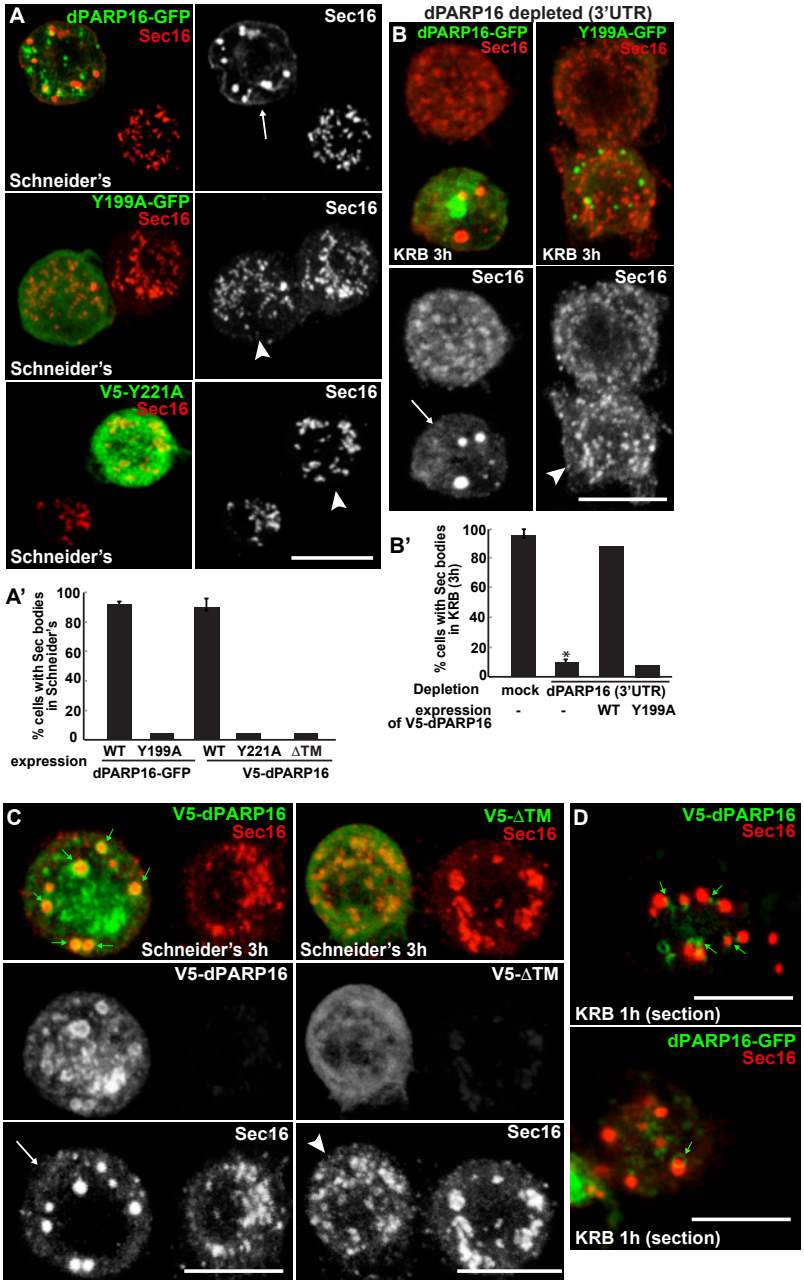

Figure 5: dPARP16 catalytic activity and membrane anchoring is required for Sec body formation. **A, A'**: IF visualization of Sec body formation (Sec16, red) in growing S2 cells (Schneider's) expressing wild type and catalytic mutant dPARP16 (Y199A and Y221A) (green) (B). Note that the expression of the catalytic mutants does not drive Sec body formation (arrowhead in B) whereas the wild type dPARP16 does (arrow in A) (quantified in A'). **B, B'**: IF visualization of Sec body formation (Sec16, red) in amino-acid starved S2 cells depleted of dPARP16 (3'UTR) and expressing wild type dPARP16 and Y199A dPARP16 catalytic mutant (B). Note that the mutant does not rescue Sec body

formation (arrowhead in C) whereas the wild type dPARP16 does (arrow in B) (quantified in B'). **C:** IF visualization of Sec16 (red) upon wild type V5-dPARP16 and ΔTM V5-dPARP16 expression (green) for 3 h in Schneider's. Note that wild type dPARP16 leads to the formation of dPARP16 rings (green arrows) and Sec bodies (while arrows) whereas the ΔTM form does not (arrowheads) (quantified in A'). **D:** IF visualization in confocal sections of V5-dPARP16 and dPARP16-GFP (green) and Sec16 (red) after 1 h incubation in KRB. Note that the forming Sec bodies localize closely to dPARP16. Scale bars: 10 μm. Error bars: SEM.

Sec16 is MARylated upon amino-acid starvation.

To address whether Sec body components are dPARP16 substrates, we first visualized GFP-MAD kinetics during amino-acid starvation with respect to Sec body formation. We found that a large proportion of MAD spots that form after 1 and 2 incubation in KRB overlap with, or are in close proximity to, ERES and small forming Sec bodies, respectively (**Figure 6A, A'**), suggesting that ERES components could be MARylated prior to Sec body formation.

Furthermore, we found that a significant number of Sec bodies (up to 40% after 3h incubation in KRB) are formed adjacent to, or overlapping with, MAD spots (**Figure 6B, B',** arrowheads). In agreement, a small but consistent pool of Sec16 is observed within the MAD spots (**Figure 6C, D**). We also found a small pool of GFP-MAD within Sec bodies (**Figure 6D'**), but overall GFP-MAD presence within Sec bodies is weak. Together, this suggests that MARylation of ERES components is linked to Sec body formation.

To strengthen the notion that Sec body components are MARylated upon amino-acid starvation, we focused on Sec16, a key Sec body component (Zacharogianni et al., 2014). We set up an in vivo MARylation assay as an alternative to the classical *in vitro* one that uses purified components. To do this, we designed anchoring-away strategy where Sec16 is tagged at its C-terminus with the CAAX motif of Ras that efficiently anchors it to the plasma membrane (Hancock et al., 1991), and is co-expressed with cherry-MAD. Given that this probe specifically binds MARylated substrates (**Figure 2C**), the reasoning is that if Sec16-CAAX is MARylated upon amino-acid starvation, it will recruit cherry-MAD to the plasma membrane.

First, we verified that Sec16-GFP-CAAX expression results in its localization to the plasma membrane. From there, it is able to recruit other Sec body components specifically upon amino-acid starvation (such as Sec23, *Figure 7, figure supplement 1,* arrows). As a result, Sec bodies are no longer formed in the cytoplasm *(Figure 7, figure supplement 1).* When cherry-MAD and Sec16-GFP-CAAX are co-transfected in S2 cells in growing conditions, the probe remains diffuse (**Figure 7A**). However, it strongly co-localizes with Sec16-GFP-CAAX at the plasma membrane upon amino-acid starvation (**Figure 7A', E**). These results suggest that Sec16 is likely MARylated. Interestingly, cherry-MAD is not recruited to the plasma membrane by Sec23-GFP-CAAX (**Figure 7B, E**) upon amino-acid starvation, suggesting substrate specificity.

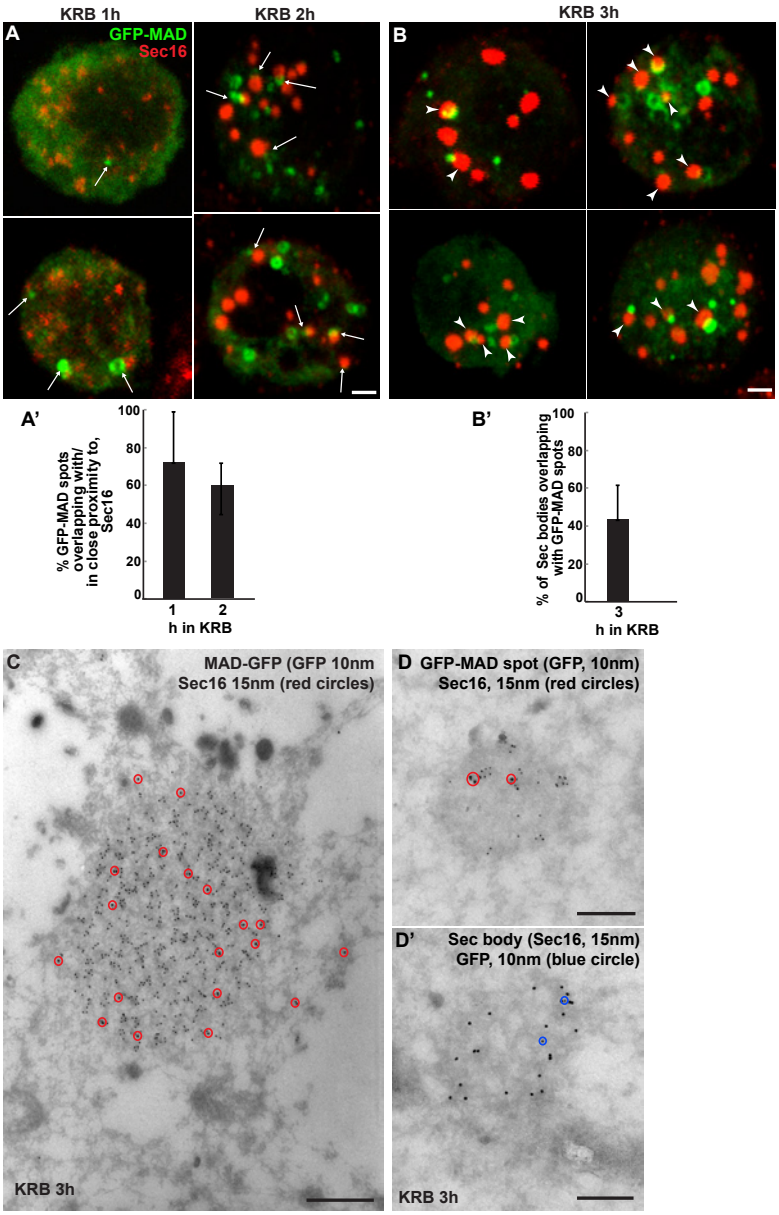

Figure 6: Sec bodies are formed in close proximity to GFP-MAD spots. **A, A'**: Visualization of GFP-MAD and Sec16 (red) upon 1-2h incubation in KRB. The formed MAD spot are closed to, or overlap with, ERES (1 h) and small Sec bodies (2 h) (arrows) (quantified in A'). **B, B'**: Visualization of GFP-MAD and Sec16 (red) upon 3 h incubation in KRB. The forming/formed Sec bodies are adjacent to MAD spots (arrowheads) (quantified in B'). **C**: IEM of a GFP-MAD spot (GFP, 10 nm gold) and Sec16 (15 nm) in cells incubated in KRB for 3 h. Note that a small pool of Sec16 is present within the MAD spots.**D-D'**: IEM of GFP-MAD (10 nm gold) and Sec16 (15 nm). A small fraction of Sec16 is found in a MAD spot (D) and conversely, a small fraction of GFP-MAD is present in Sec bodies (both of the presented structures are found in the same cell). Scale bars: 1 μm (A,B) and 200 nm (C-D'). Error bars: SEM.

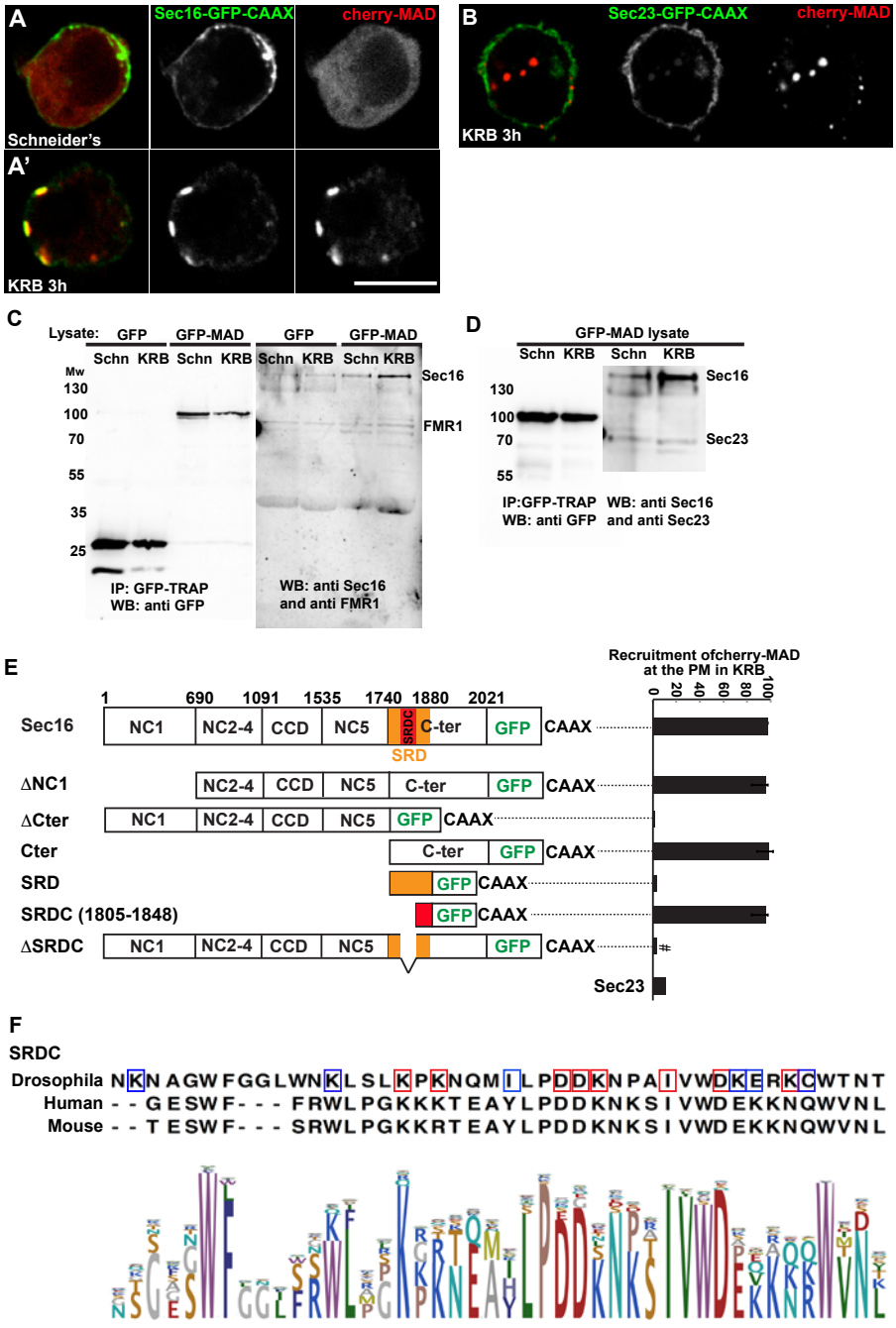

Figure 7: Sec16 SRCD is MARylated. A, A': Co-visualization of full length Sec16-GFP-CAAX and Cherry-MAD in growing (Schneider's) S2 cells (A) and upon amino-acid starvation (KRB) (A'). Note that Sec16-GFP-CAAX localizes to the plasma membrane where cherry-MAD is recruited upon amino-acid starvation (KRB), whereas in Schneider's, it remains cytoplasmic. **B**: Co-visualization of full length Sec23-GFP-CAAX (B) and cherry-MAD upon amino-acid starvation (KRB). Note that cherry-MAD

is not recruited to the plasma membrane and forms spots in the cytoplasm. **C**: WB (using anti GFP, anti Sec16, anti FMR1) of GFP-MAD immuno-precipitation (IP) using GFP-Trap from stable S2 cell lines expressing GFP-MAD and GFP, either in growing conditions (Schneider's) or upon amino-acid starvation (KRB 3 h). **D**: WB (using anti GFP, anti Sec16, anti Sec23) of GFP-MAD IP from stable S2 cells expressing GFP-MAD, either in growing conditions (Schneider's) or upon amino-acid starvation (KRB 3 h). Note that Sec23 pull-down by GFP-MAD is very weak when compared to Sec16. **E:** Map of all Sec16-GFP-CAAX constructs used and the quantitation of cherry-MAD recruitment to the plasma membrane. Note that Sec16-ΔSRDC-GFP-CAAX transfection was performed in Sec16 depleted cells (marked by #) to avoid oligomerization with endogenous Sec16. **F:** Muscle sequence alignment of Drosophila, human and mouse Sec16 SRDC (1805-1848) and presentation of logo sequence outlining the degree of sequence conservation among all eukaryotes (defined using CLC Main Workbench 6.7.1 using the full length Sec16 sequence against all eukaryote sequences from the non-redundant protein database using standard settings). The red squares indicate the conserved residues that are potentially MARylated and the blue squares the non-conserved ones.

To confirm this result, we used GFP-trap to immuno-precipitate GFP-MAD from cell lysates prepared from growing and amino-acid starved S2 cells. Cells expressing GFP were used as control. GFP-MAD binds Sec16 significantly more upon amino-acid starvation than under growing conditions and more than GFP (**Figure 7C, D**). To further test the specificity of the GFP-MAD/Sec16 interaction, we investigated whether Sec23 (**Figure 7D**) and RNA binding proteins (FMR1, Caprin and Rasputin) (**Figure 7C** and not shown) are also pulled down by GFP-MAD upon amino-acid starvation. We found that neither of them is. These results show that Sec16 is likely MARylated upon amino-acid starvation, although we cannot rule out that Sec16 could also bind a MARylated substrate that is bound by MAD.

dPARP16 dependent Sec16-SRDC MARylation is a key event in Sec body formation.

To identify the region of Sec16 that is recognized by MAD upon amino-acid starvation (and that is likely MARylated), we employed the same CAAX anchoring-away strategy as above on Sec16 truncations. Removing the N-terminus of Sec16 (ΔNC1-GFP-CAAX*)* does not alter cherry-MAD recruitment to the plasma membrane upon starvation **(Figure 7E)**. In contrast, truncation of Sec16 C-terminus (ΔCter-GFP-CAAX) completely abolishes cherry-MAD recruitment to the plasma membrane upon starvation (**Figure 7E)**. Instead, cherry-MAD form spots in the cytoplasm (red arrows *Figure 7, figure supplement 2A*)**.** Accordingly, co-expression of Cter-GFP-CAAX with cherry-MAD results in the strong recruitment of cherry-MAD to the plasma membrane (**Figure 7E;** *Figure 7, figure supplement 2B***)**. Taken together, these results show that upon amino-acid starvation, cherry-MAD binds the MARylated C-terminus of Sec16.

To narrow down the MARylated sequence of the Sec16 C-terminus, we focused on a region of 140 amino-acids that we previously identified as required for the response to serum starvation ("Starvation Response Domain", SRD, 1740-1880) (Zacharogianni et al., 2011) *(***Figure 7E***).* However, expression of SRD-GFP-CAAX

in amino-acid starved cells does not lead to the recruitment of cherry-MAD to the plasma membrane (**Figure 7E;** *Figure 7, figure supplement 2C*).

Upon comparison of the SRD sequence in all eukaryotes, we noticed a conserved sequence of 44 amino-acids (1805-1848), that we called SRDC (**Figure 7F**). Strikingly, expression of SRDC-GFP-CAAX leads to the robust recruitment of cherry-MAD to the plasma membrane upon amino-acid starvation (**Figure 7E;** *Figure 7, figure supplement 2D*). In agreement, Sec16 lacking SRDC (ΔSRDC-GFP-CAAX) in Sec16 depleted cells (to prevent oligomerization with endogenous Sec16) is unable to recruit cherry-MAD to the plasma membrane (**Figure 7E;** *Figure 7, figure supplement 2E*). This shows that this sequence is MARylated upon amino-acid starvation.

To begin to show the functionality of SRDC in Sec body formation, we expressed SRDC-GFP in growing Drosophila cells. Strikingly, this results in the efficient formation of the Sec bodies in the absence of stress (**Figure 8A, D**), a phenotype strongly reminiscent of dPARP16 overexpression (**Figure 4D**). Accordingly, we found that dPARP16 is critically necessary for SRDC induced Sec body formation, since they were not formed in dPARP16 depleted cells (**Figure 8B, D**). Importantly, SRD-GFP expression does not induced Sec body formation **(Figure 8C, D).** We propose that dPARP16 SRDC MARylation is one of the events that initiate/drive Sec body formation.

To confirm this, we performed a rescue experiment in cells depleted of Sec16. As expected, Sec16 depleted cells do not form Sec bodies (here marked by Sec23) upon amino-acid starvation (**Figure 8H**), and transfection of Sec16-GFP (**Figure 8E, H**) and SRDC-GFP (**Figure 8F, H**) significantly rescues this formation. However, transfection of ΔSRDC-GFP does not, demonstrating the direct role of SRDC in Sec body formation.

Taken together, using the MAD probe, we show a strong MARylation response upon amino-acid starvation, as Sec16 SRDC is MARylated in a dPARP16 dependent manner, a key event that initiates Sec body formation.

Discussion

MAD, a specific probe to detect MARylation *in vivo* and *in vitro*.

By using biological modules known as macrodomains that do not posses any hydrolase activity, we built and optimized a specific and stable Mono-ADP-ribosylation detection probe (MAD) that has important specifications: First, MAD specifically detects and binds Mono-ADP-ribose. This specificity is sustained by 3 arguments: i) MAD is designed and built using PARP14 macrodomains 1-3. Crystallography and calorimetric assays show that each macrodomain has a conserved fold with high binding affinity for mono-ADP-ribose (particularly macrodomains 2 and 3) and the affinity required for *in vivo* visualization is provided by the 3 macrodomains

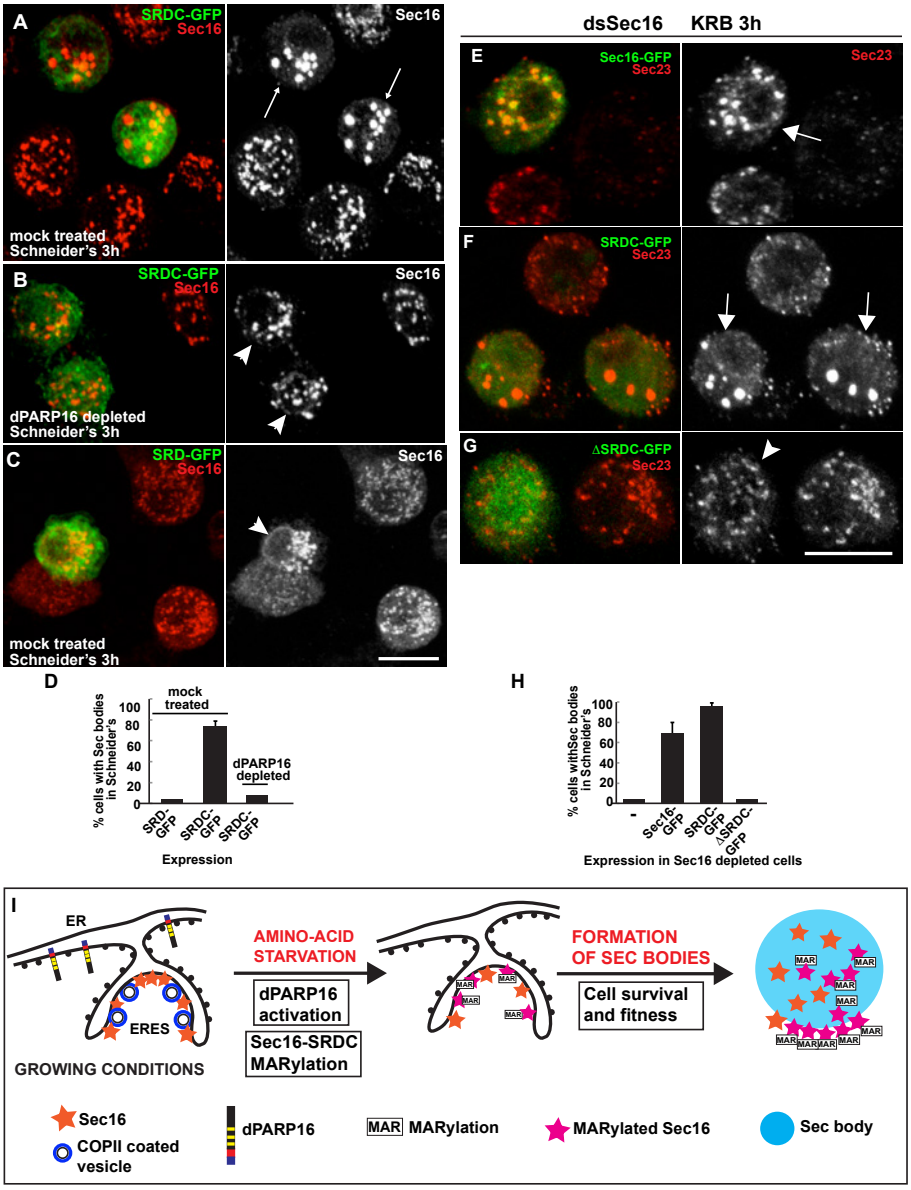

Figure 8: Sec16 SRDC MARylation is critical for Sec body formation. **A-D:** Visualization of endogenous Sec16 (red) in mock treated (A,C) and dPARP16 depleted S2 cells (B) in Schneider's transfected with SRDC-GFP (A,C) and SRD-GFP (B). Note that expression of SRDC leads to the formation of Sec bodies, similar to dPARP16 overexpression and that dPARP16 depletion prevents this formation (quantified in D). **E-H**: Visualization of endogenous Sec23 in starved Sec16 depleted cells (ds Sec16) transfected with Sec16-GFP (E), SRDC-GFP (F) and ΔSRDC-GFP (G). Note that Sec16 depletion prevent cells to form Sec bodies, that both full length Sec16 and SRDC transfection rescue Sec body formation, but not Sec16 lacking SRDC. Arrows point to cells where Sec bodies have formed and arrowheads where they haven't. **I**: Model of Sec16 SRDC MARylation by dPARP16 that is activated by amino-acid starvation leading to Sec body formation and cell survival and fitness. Scale bars: 10 μm. Error bars: SEM.

together in a cooperative manner. ii) We show that the mutated G1055E probe (affecting the binding pocket of macrodomain 2 in such as way that it does not bind mono-ADP-ribose any longer) does not elicit a pattern upon amino-acid starvation in vivo. iii) The amino-acid starvation MAD pattern is abrogated upon depletion of dPARP16, the closest homologue of an established human MARylation enzyme PARP16. Conversely, overexpression of dPARP16 elicits MAD spot formation (but not PAD spots, which rule out PARylation events). This is confirmed by the use of a PARylation detection probe YFP-PAD. It visualizes PARylation events consistent with those reported to occur to RNA binding proteins upon arsenate treatment leading to stress granule formation (Gagne et al., 2008; Leung et al., 2011). However, YFP-PAD is not remodeled during amino-acid starvation suggesting that PARylation is not prominent during this stress. Taken together, these evidences demonstrate the specificity of MAD in binding mono-ADP-ribose and detecting MARylation events.

Second, MAD can be used in cells to follow MARylation in real time. In this regard, MAD allows the visualization of an unprecedented display of MARylation events upon amino-acid starvation (but not heat shock or arsenite poisoning) under the form of non-membrane bound, reversible spots/rings in the cytoplasm. To the best of our knowledge, this is the first time that MARylation response is visualized in real time during stress.

Third, MAD has also allowed us to identify dPARP16 as the enzyme catalyzing these events in defined regions of the cytoplasm in a dynamic manner. We propose that MAD spots represent a concentration of MARylated substrates reflecting local dPARP16 activation. This is supported by their co-localization upon expression of both enzyme and probe. This makes MAD, an efficient activity sensor of the nutrient stress response and dPARP16 the key MARylation enzyme eliciting this response and a survival factor upon amino-acid starvation (see below).

Fourth, MAD can be used for *in vitro* approaches such as IP and this allowed the identification of Sec16 as a potential substrate. Furthermore, MAD can be used *in vivo* in an anchor-away MARylation assay as an alternative to *in vitro* approaches using purified components. This has allowed us to map the MARylated region of Sec16.

dPARP16, Sec16 and Sec body formation.

dPARP16 is necessary and sufficient for Sec body formation upon amino-acid starvation and this creates an unprecedented link between MARylation, metabolic stress and the formation of stress assembly. PARP16 is necessary for cell survival during amino-acid starvation and recovery. This makes dPARP16 a key enzyme for the cells to specifically cope with amino-acid starvation, as the viability of dPARP16 depleted cells kept in full medium is not compromised.

Nutrient starvation in yeast also leads to storage of metabolic enzymes in reversible assemblies (Narayanaswamy et al., 2009), such as glutamine synthetase (Petrovska

et al., 2014) or proteasome subunits (Peters et al., 2013). Although no PARPs have been identified in *Saccharomyces cerevisiae*, the regulation of their organization might be controlled by SIRT, another class of NAD+ dependent protein that also display ADP-ribosylation activity (Butepage et al., 2015). Conversely, given the abundance of PARPs with predicted MARylation activity in the mammalian genome, it is likely that additional ones, will be required and/or involved in the formation of stress assemblies upon different biological processes, including metabolic stress as described here. We have reported that large Sec bodies did not form in mammalian cells upon conditions used for Drosophila cells, although a remodeling of the early secretory pathway was observed (Zacharogianni et al., 2014). Therefore, the fine dissection of the signaling pathways involved in Sec body formation will allow us to recapitulate conditions to trigger their formation in mammalian cells and tissues.

According to our RNA-seq data of S2 cells in growing conditions and upon amino-acid starvation conditions (unpublished), dPARP16 has a very low transcriptional level when compared to most genes, suggesting that its protein level is also low. Because dPARP16 moderate overexpression in growing cells leads the detection of MARylation events, it suggests that dPARP16 overexpression leads to its activation. This also suggests that dPARP16 level needs to be kept low in basal conditions to avoid its activation, challenging the detection of its activity in basal conditions. Conversely, dPARP16 is essential during stress, at least amino-acid starvation as depletion of dPARP16 affects the viability of cells during the stress period. How is PARP16 activated upon amino-acid starvation remains to be elucidated. Given the nature of the stress, TORC1 activation would be an ideal pathway but we have shown that it is not involved in Sec body formation (Zacharogianni et al., 2014). Another possibility is the fluctuation in the intracellular pH as this occurring in yeast upon energy deprivation that results in the formation of macromolecular assemblies (Munder et al., 2016). However, the time scale is very different (minutes for the drop in pH fluctuation versus hours of starvation for Sec body formation). Furthermore, the assemblies formed upon pH fluctuation do not appear to be mediated by a signalling pathway. This remains to be investigated.

In mammalian cells, PARP16 is activated via auto-MARylation triggered by ER stress (Jwa and Chang, 2012). As a result, it MARylates two key kinases of the ER stress response UPR, Ire1 and PERK (Gardner et al., 2013), leading to their activation (Jwa and Chang, 2012) and the unfolded Protein Response. As dPARP16 shares many features with its human counterpart, ER stress could in principle lead to Sec body formation. However, we have previously shown (Zacharogianni et al., 2014) and our unpublished results) that inducing ER stress does not lead to Sec body formation. Although ER stress might be involved in the amino-acid starvation stress response, it is not sufficient to trigger it. This result is reinforced by the demonstration that cell survival is significantly more affected by amino-acid starvation than by ER stress *(Figure 8, Figure supplement 1).* As a result, dPARP16 appears to be more critical for amino-acid starvation than for ER stress *(Figure 8,*

Figure supplement 1).

This suggests that additional signals are generated during amino-acid starvation. These are under investigation. Another substrate of mammalian PARP16 is karyopherin (Di Paola et al., 2012), a component required for nuclear export. However, our unpublished results shows that the pharmacological inhibition of nuclear export does not inhibit Sec body formation (not shown), suggesting that at least during amino-acid starvation, karyopherin might not play a prominent role and that dPARP16 has different substrates.

One of these substrates is the ERES/Sec body component Sec16 and more specifically a conserved 44 amino-acid sequence (SRDC) in its C-terminus. Indeed, The CAAX version of SRDC recruits cherry MAD to the plasma membrane. Overexpression of SRDC leads to the formation of Sec bodies in a dPARP16 dependent manner, and SRCD rescues Sec body formation in Sec16 depleted cells. This suggests that Sec16-SRDC MARylation is a triggering event in Sec body formation.

The discovery of a short peptide required for the formation of Sec bodies is reminiscent to the existence of an Amyloid Converting Peptide in proteins found in nuclear amyloid bodies in cells upon several stress (Audas et al., 2016). Interestingly, amyloidogenesis is mediated by this motif binding a long non-coding RNA that could be equivalent or comparable to the SRDC MARylation during Sec body formation. Whether the SRCD sequence is also present in other proteins recruited to Sec bodies remains to be investigated.

In the context of the full-length endogenous protein, SRDC MARylation could act as both a signaling and structural event allowing the recruitment of Sec16 and other ERES components into Sec bodies. However, SRCD on its own is not recruited to Sec bodies, and our interpretation is that it may act only as a signaling event for Sec body formation. The nature of this signaling need to be further investigated. This is in line with the fact that MAD is not readily observed within the Sec body core. MAD appears as a ring at the basis of Sec bodies. Although this is consistent with the protein packing and competing binding that takes place during the formation of stress assemblies (that most likely would exclude MAD), it might also suggest that MARylated Sec16 forms a signaling platform. This would lead to the modifications of other Sec body components allowing their incorporation (**Figure 8J**).

Interestingly, PARylation has been proposed to preferentially occur on LCSs (Low complexity sequences, that is, region of poor amino-acid diversity) (Leung, 2014). These are normally thought to correspond to disordered regions. Sec16 is rich in LCSs (Zacharogianni et al., 2014) and SRDC is intrinsically disordered, therefore accessible to be modified by dPARP16 . Taken together, this makes Sec16 a stress response protein and a new substrate for the pro-survival dPARP16 in amino-acid starvation.

Experimental procedures

Cell culture, amino acid starvation, depletions (RNAi) and transfections
Drosophila S2 cells were cultured in Schneider's medium supplemented with 10% insect tested foetal bovine serum at 26°C as described in (Kondylis and Rabouille, 2003; Kondylis et al., 2007). Amino acid starvation of cells for 3 or 4 h was performed using Krebs Ringer's Bicarbonate buffer (10 mM D(+) Glucose; 0.5 mM $MgCl_2$; 4.5 mM KCl; 121 mM NaCl; 0.7 mM Na_2HPO_4; 1.5 mM NaH_2PO_4 and 15 mM sodium bicarbonate) at pH 7.4 (Zacharogianni et al., 2014).

Wild type Drosophila S2 cells were depleted by dsRNAi, as previously described (Kondylis and Rabouille, 2003; Kondylis et al., 2007). Cells were analysed after incubation with dsRNAs for 5 days typically leading to depletion in more than 90% of the cells.

Transient transfections of PMT constructs (see below) were performed using Effectene transfection reagent (301425; Qiagen, Germany) according to manufactures instructions. Expression was induced 48 h after transfection with 1 mM $CuSO_4$ for 1.5 h (Zacharogianni and Rabouille, 2013).
Stable cell lines expressing GFP-MAD and GFP are maintained in Schneider's supplemented medium with 300 ug/ml Hygromycin B. Plasmid expression is induced with 1 mM $CuSO_4$.

Antibodies
The following antibodies were used: Rabbit polyclonal anti-Sec16 (Ivan et al., 2008) 1:800 IF, 1:2500 WB; Rabbit polyclonal anti-Sec23 (Thermo scientific), 1:200 IF, 1:500 WB; Mouse monoclonal anti-V5 (Invitrogen 46-0705) 1:500 IF; Rabbit polyclonal anti-V5 (Sigma V8137); Mouse monoclonal anti-ATP5A (Abcam 15H4C4) 1:1000 IF; Mouse monoclonal anti-KDEL receptor (Abcam ab69659) 1:500 IF; Mouse monoclonal anti-calnexin 99A (Gift fom Sean Munro) 1:10 IF; Mouse monoclonal anti-FMR1(DSHB supernatant clone 5A11) 1:800 IF 1:2000 WB; Rabbit polyclonal anti-GFP WB 1: 5000 (Acris antibodies); Rabbit polyclonal anti-GFP 1:100 IEM; polyclonal FMR1-c 1:20 IF 1:500 WB (DSHB), anti-Rabbit HRP 1:2000 (GE healthcare) and anti-Mouse HRP 1:2000 (GE Healthcare).

PMT-DNA constructs and dsRNAs
All the primers used for generating the DNA constructs and RNAi probes are listed in *Figure 1-figure supplement 1*. To generate the pMT-sfGFP vector, super folder (sf) GFP was amplified and cloned into pMT-V5 using *SacII* and *PmeI* restriction sites replacing the V5 tag with sfGFP.

The sequence corresponding to the ORFs of CG40441 (dARTD1/PARP1), CG4719(dTankyrase) and CG15925(dPARP16) were amplified from a cDNA library made from Drosophila S2 cells and clone into pMT-sfGFP using *KpnI* and *ApaI*.

To generate pMT-V5-dPARP16, dPARP16 was amplified from dPARP16-GFP and cloned into pMT-V5 using *AgeI* and *PmeI*. To generate the mutant pMT-Y199A-dPARP16-GFP, dPARP16 was amplified using primers harboring a mutation at position Y199A and cloned into pMT-GFP using *KpnI* and *ApaI*.

To generate the mutant PMT-V5 Y221A-dPARP16, dPARP16 was amplified using primers harboring a mutation at position Y221A and cloned into pMT-V5 using *AgeI* and *PmeI*.

To generate the truncated pMT-ΔTM-V5-dPARP16, dPARP16 was amplified and cloned into pMT-V5 using *AgeI* and *PmeI*.

To generate the pMT-CAAX-sfGFP vector, the sequence corresponding to C-terminus CAAX motif of Ras (SGLRSRAQASNSRVKMSKDGKKKKKKSKTKCVIM) was amplified and cloned into pMT-sfGFP using *AgeI* and *PmeI*. The Sec16 truncations: ΔNC1, ΔCter; Cter, SRD and SRDC were cloned into pMT-CAAX-sfGFP using *EcoI* and *ApaI*.

To generate the pMT-Sec16ΔSRDC-sfGFP and the pMT-CAAX-Sec16-ΔSRDC-sfGFP the SRDC deleted version was cross-amplified using fusion primers (***Figure 1,*** *figure supplement 1*) and cloned into pMT-Sec16Fl-sfGFP and pMT-CAAX-Sec16Fl-sfGFP respectively using *EcoRvI* and *SacII*.

The dsRNAs used for RNAi of dARTD1, dARTD9, dARTD5-6 and dPARP16 were amplified using primers harbouring T7 promoters in their sequence and used for in vitro transcription using the T7 Megascript Kit (AMBION) to generate the dsRNAs.

To generate GFP-MAD, the macrodomains 1-3 of human ARDT8 were amplified from cDNA of human HEK293 cells and cloned into pMT-GFP using *AgeI* and *PmeI* followed by the insertion of a Hex-HIS-TEV-linker using *AgeI*. To generate the GFP-MAD-Macro2 mutant, the macrodomains 1-3 of MAD were amplified using primers harbouring the G1995A mutation followed by the insertion of a Hex-HIS-TEV linker as described above.

To generate YFP-PAD, YFP was amplified from a YFP-plasmid and cloned into pMT-sfGFP with *AgeI* and *ApaI* replacing sf-GFP with SYFP. H2A1.1 was amplified from a pUCIDT plasmid synthesized by (IDT) and cloned into pMT-SYFP with *AgeI* and *PmeI*, followed by the insertion of a Hex-HIS-TEV linker as described above.

Immunofluorescence (IF)
Drosophila S2 cells were plated on glass coverslips, treated as described, fixed in 4% PFA in PBS for 20 min and processed for inmunofluorescence as previously described (Kondylis and Rabouille, 2003; Zacharogianni and Rabouille, 2013). Samples were viewed under a Leica SPE confocal microscope using a 63x oil lens and 2-4x zoom. 14 to 20 planes were projected to capture the whole cell that is displayed unless indicated otherwise.

Immuno-electron microscopy (IEM) and correlative GFP fluorescence/IEM

IEM of dPARP16 was performed as described previously (Kondylis et al., 2007; van Donselaar et al., 2007). The correlative Fluorescence/IEM method (Hassink et al., 2012) is adapted from (Vicidomini et al., 2010). Briefly, S2 cells stably expressing GFP-MAD were incubated in KRB for 1 and 3 h, fixed with 4% PFA (in 0.1M PB) for 3h followed by 1% PFA overnight. Ultrathin sections were cut, picked up on electron microscopy copper formvar coated grids, labeled with a goat anti-GFP antibody coupled to biotin followed by a rabbit anti-biotin antibody and Protein A Gold (10 nm), followed or not by labeling with a rabbit anti Sec16 antibody followed by protein A Gold 15 nm.

Sections were visualized on a Delta vision fluorescence microscope to detect the fluorescence signal corresponding to GFP. Cell profiles were recorded. The same grid was then viewed in the electron microscope (Jeol) and the ROI was photographed.

Live imaging experiments
Live imaging of GFP-MAD was performed using S2 cells stably expressing GFP-MAD at 26°C in Schneider's medium (t=0) and incubated in KRB up to 3 h. Cells were filmed using a Leica SPE confocal microscope using a 63x lens at 4x zoom. 10 z-planes with a z-step of 0.5 um were recorded every 10 minutes.

Immuno-precipitation and Western blot
$200x10^6$ and $150x10^6$ S2 cells stably expressing GFP-MAD and GFP were incubated for 3 h at 26°C in KRB and in Schneider's, respectively. Cells were harvested, placed immediately on ice and washed with ice cold PBS by mild centrifugation (1100 rpm, 4min at 4°C). Cells were lysed in 600 ul lysis buffer (10% glycerol; 1% Triton X100; 50 mM Tris-HCl pH 7.5; 150 mM NaCl; 50 mM NaF; 25 mM Na_2gP; 1 mM Na_2VO_3; 5 mM EDTA and 1 tablet Roche protease inhibitor/100 ml) for 30 min upon rotation at 4°C. The cell lysate was then centrifuged at 14,000 rpm for 20 min at 4°C. Protein concentration was determined by using BCA protein assay. The cell lysate was added to 20ul GFP-Trap (R) beads (Chromotek) washed in lysis buffer and incubated by rotation at 4°C. The GFP-Trap beads were then washed 3x for 5 min at 4°C with 1ml lysis buffer (at 2000 rpm, 2 min at 4°C). The supernatant was collected and boiled for 5 min in 50 ul 2 x sample buffer with DTT. Samples (15 mg of protein) were fractionated on a 10% SDS-PAGE gel, proteins transferred to a nitrocellulose membrane. Blotting was done in blocking buffer (PBST with milk), after which the antibodies were added in the concentrations as described above.

Heat stress and Arsenite treatment
Heat stress was performed on $2x10^6$ Drosophila S2 cells in 3 cm dish in a oven at 37°C (Thermo Electron) for 3 h as described in (Jevtov et al., 2015). Treatment with 0.5 mM $NaAsO_2$ was performed at 26°C for 3 h.

Cell survival and fitness upon and after amino-acid starvation and ER stress. 0.75 million cells were mock- (dsGFP) and dPARP16 depleted. After 5 days of depletion the cells proliferated to reach 3.0 million respectively. This was set at 100% (t=0). For the treatments, cells were either kept in Schneider's, or amino-acid starved in KRB for 3 h or treated with Schneider's supplemented with 2.0 mM DTT for 3 h (ER stress). The cells were then washed, and the medium changed to Schneider's allowing recovery for up to 16 h.

Cell viability was determined by exclusion of Trypan Blue. For each time point, 0.1 ml of cell suspension was mixed with 0.1 ml of 0.4% Trypan. The number of living cells were counted using a hemocytometer. The cell number was monitored and expressed as a percentage of t=0.

Experiments were performed in at least 3 biological replicates each consisting of three technical replications. All technical replicates were averaged.

The error bars in the graphs are standard deviation (SD) calculated over all biological replicates.

Quantification and statistics
Two/three biological replicates were performed per experiment. For IF of depleted or treated cells, at least 4 fields per experiment were analyzed comprising at least 50 cells. For transfected cells, at least 30 cells were analyzed. Results are expressed as standard deviations.

Author contributions

A. Aguilera Gomez designed and performed most of the experiments described in this manuscript. The results were discussed and analyzed with C. Rabouille. M.van Oorschot performed the IP, and the IEM (and correlative method) was performed by T. Veenendal. CR and AAG wrote the ms.

Acknowledgements

We thank the Rabouille's lab members and Fulvio Reggiori, Adam Grieve and Tim Levine for critically reading the manuscript as well as Geert Kops and Puck

Knipscheer for helpful comments. We thank Anko de Graaff and the Hubrecht Imaging Center for supporting the imaging. The work is supported by NWO grant to CR (822-020-016).

Supplemental figures

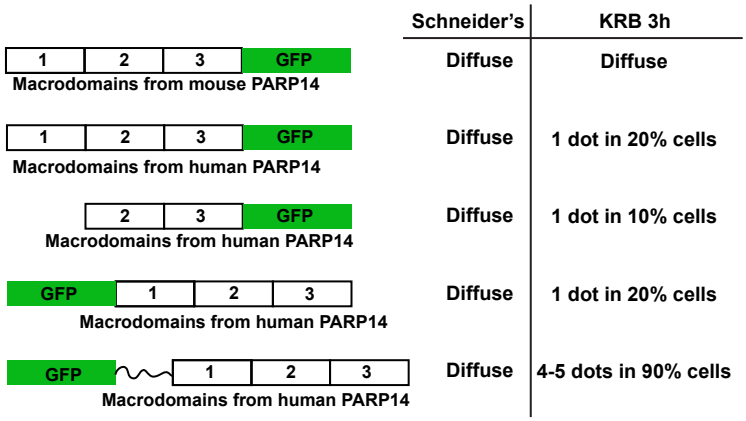

Figure 2- figure supplement 1: GFP-MAD design and optimization. Schematics representation of several version of GFP-MAD based upon macrodomains 1-3 of PARP14. Note that the macrodomains of human PARP14 are more efficient at detecting MARylation in S2 cells than those from mouse PARP14 that were originally used by (Forst et al., 2013). Furthermore, the insertion of a linker greatly improved the probe sensitivity and/or efficiency.

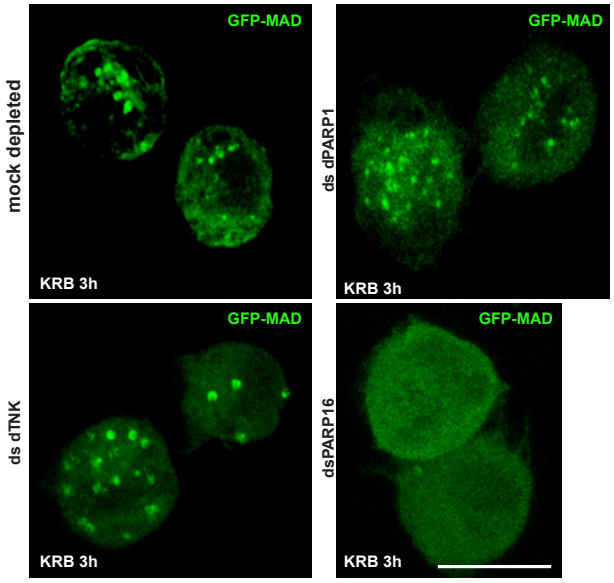

Figure 3- figure supplement 1: Screen for PARPs in MAD spot formation. IF visualization of GFP-MAD spots in amino-acid starved (KRB) mock, dPARP1, dTNK and dPARP16 depleted S2 cells. Note that, with exception of dPARP16 depletion, MAD spots formation is not affected by dPARP1 and dTNK depletions. Scale bar: 10 μm.

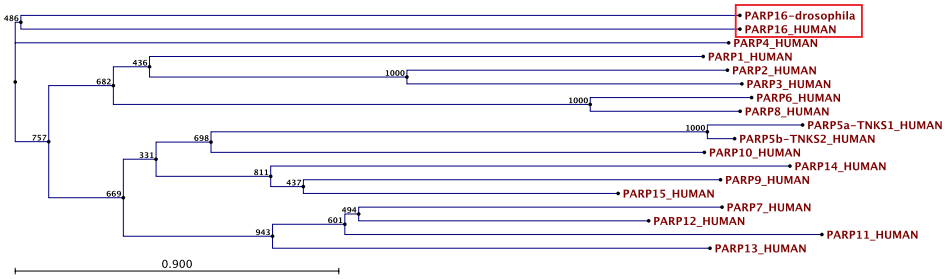

Figure 3- figure supplement 2: Drosophila PARP16 is the homologue of human PARP16. Bootstrap analysis of the Drosophila PARP16 against all human PARPs. Note that dPARP16 clusters with hPARP16 (red box).

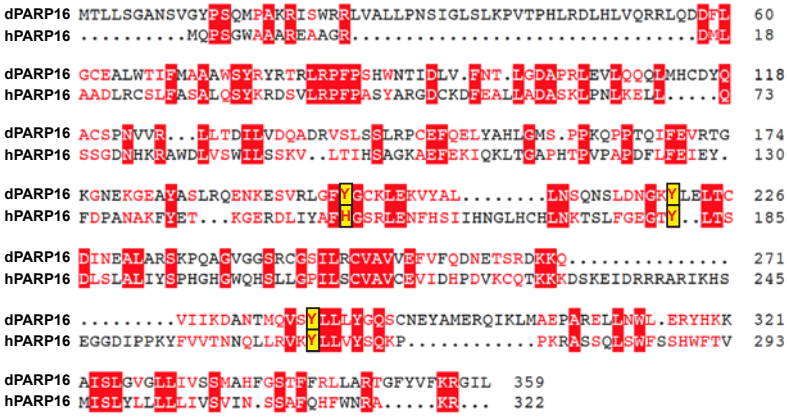

Figure 3- figure supplement 3: Comparison between Drosophila and human PARP16 catalytic site. Muscle Sequence alignment of human (h) and Drosophila (d) PARP16. The yellow boxes outlines the 3 key amino acids that form the PARP16 catalytic site. Note that they are conserved.

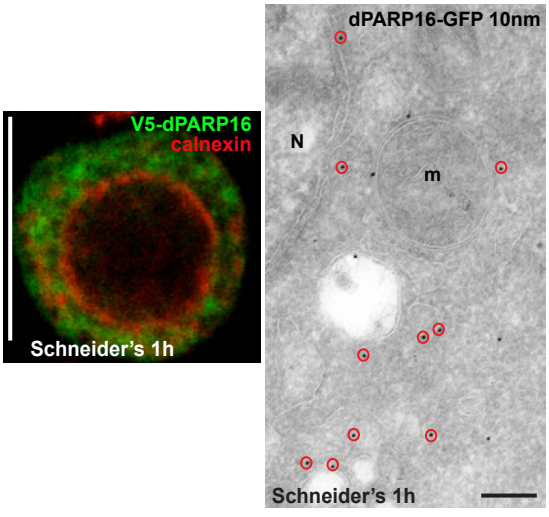

Figure 3-figure supplement 4: dPARP16 is anchored at the ER. IF visualization of V5-dPARP16 (green) with respect to the ER marker Calnexin (red) after 1 h expression in growing S2 cells (Schneider's). Although PARP16 only partially co-localizes with calnexin, the ER localization was confirmed by IEM (red circles). N; Nucleus. Scale bar: 10 µm (left) and 200 nm (right).

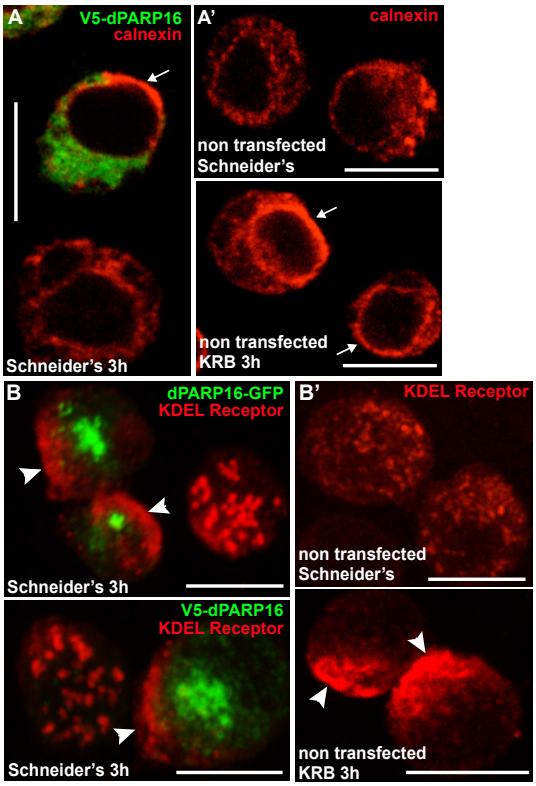

Figure 3-figure supplement 5: dPARP16 is anchored at the ER. A-B': Overexpression of dPARP16 leads to a strong re-arrangement of the ER marked by calnexin (A) that appears to accumulate at the nuclear envelop (arrows) and KDEL receptor that appears to concentrate near the cell cortex (B, arrowheads). Interestingly, the same ER re-arrangements are observed upon starvation for both markers (A' and B'). Scale bars: 10 μm.

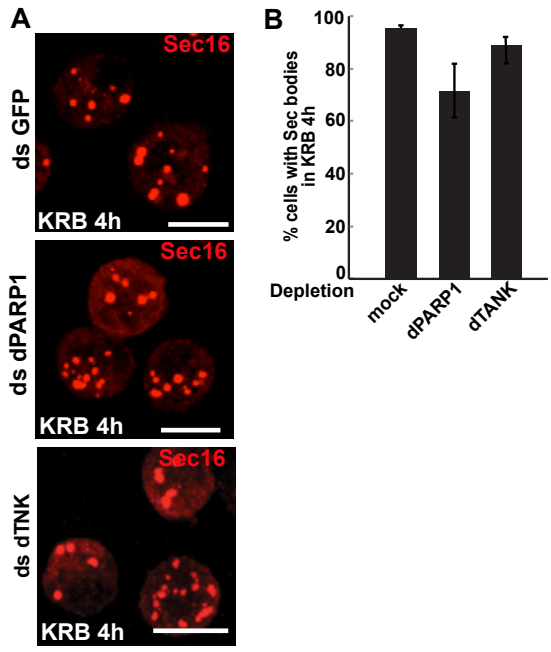

Figure 4- figure supplement 1: dPARP1 and dTNK depletion does not affect Sec body formation upon amino-acid starvation. A, B: IF visualization of endogenous Sec16 (red) in amino-acid starved (KRB) S2 cells that are mock, dPARP1 and dTNK depleted. Note that Sec body formation is not affected as they form as efficiently in all conditions (quantified in B). Scale bars: 10 μm Error bars: SEM.

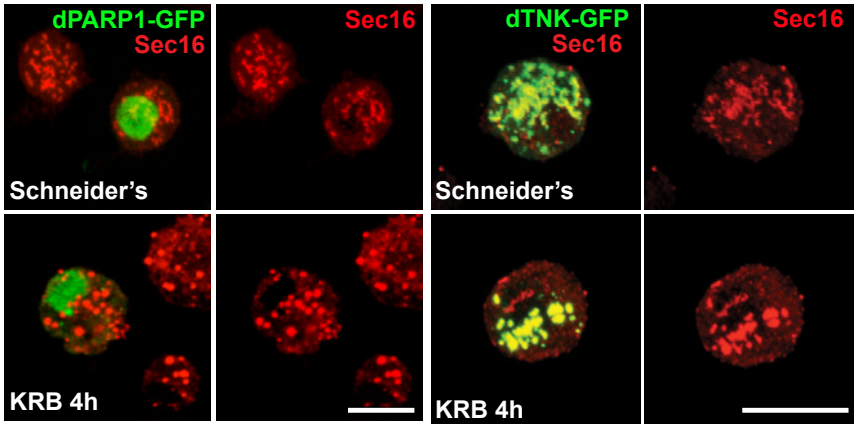

Figure 4- figure supplement 2: dPARP1 and dTNK overexpression does not lead to Sec body formation in growing conditions. IF visualization of endogenous Sec16 (red) in S2 cells expressing dPARP1 and dTNK in Schneider's and KRB. Note that the overexpression of any of these enzymes neither leads to Sec body formation in Schneider's nor affects their formation in KRB. Scale bars: 10 μm. Of note: dTNK, a cytoplasmic predicted MARylation enzyme, co-localizes robustly with ERES in S2 cells, both under growing conditions and upon amino-acid starvation. Furthermore, its overexpression leads to the remodeling of the ERES. Yet, neither its overexpression nor its depletion has an effect on Sec body formation. This shows that the localization of MARylation enzymes at/near ERES is not sufficient to displace Sec16 and elicit a stress response, and that dARDT15 MARylation activity is substrate (and stress) specific.

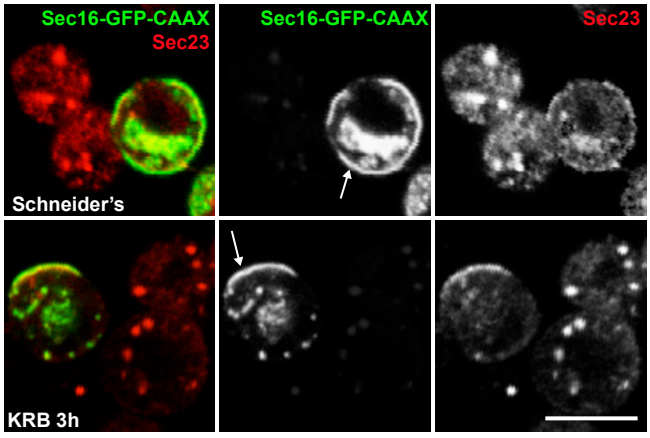

Figure 7- figure supplement 1: Sec16-CAAX recruits Sec23 to the PM upon AA starvation. Co-visualization of full length Sec16 (Sec16-GFP-CAAX) and Sec23 in growing (Schneider's) and upon amino-acid starvation (KRB). Note that Sec16-GFP-CAAX localizes at the plasma membrane in Schneider's and KRB but that Sec23 is only recruited in KRB, whereas in Schneider's, it localizes at ERES. Note also that Sec bodies do not form in the CAAX transfected cells. Scale bars: 10 μm.

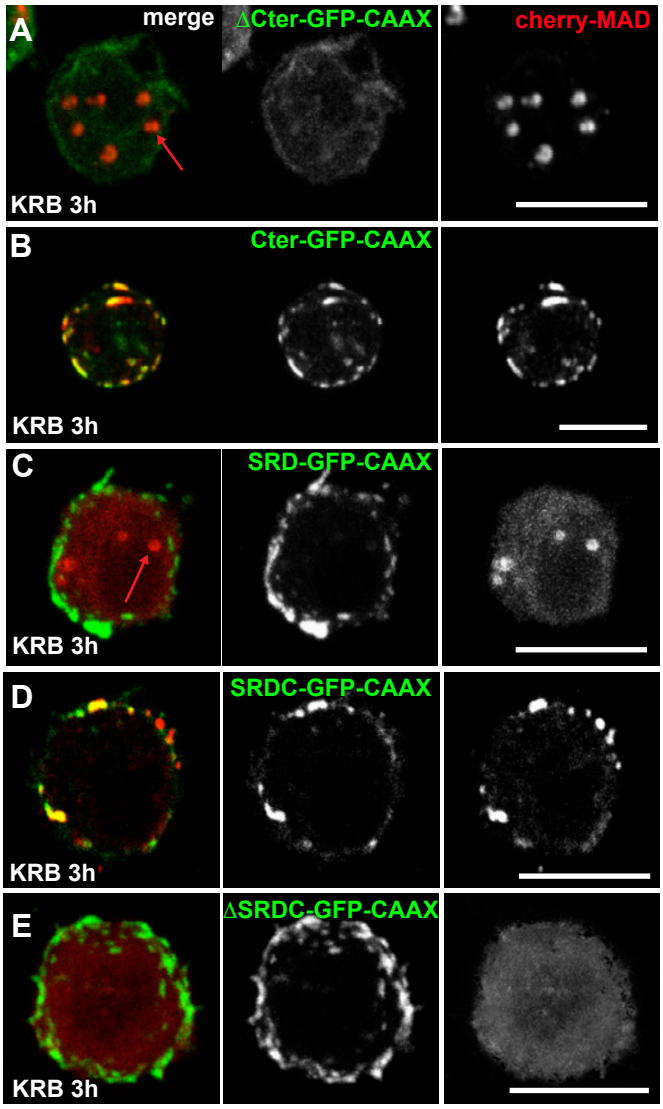

Figure 7- figure supplement 2. A-C: Co-visualization of Sec16 ΔCter-GFP-CAAX (A), Sec16 Cter-GFP-CAAX (B), SRD-GFP-CAAX (C) co-transfected with cherry-MAD in wild type cells in KRB **D-E:** Co-visualization of SRDC-GFP-CAAX (D) and Sec16-ΔSRDC-GFP-CAAX (E) co-transfected with cherry-MAD in KRB (quantified in **Figure 7E'**). Note that although SRD does not recruit cherry-MAD, SRDC does. Scale bars: 10 μm.

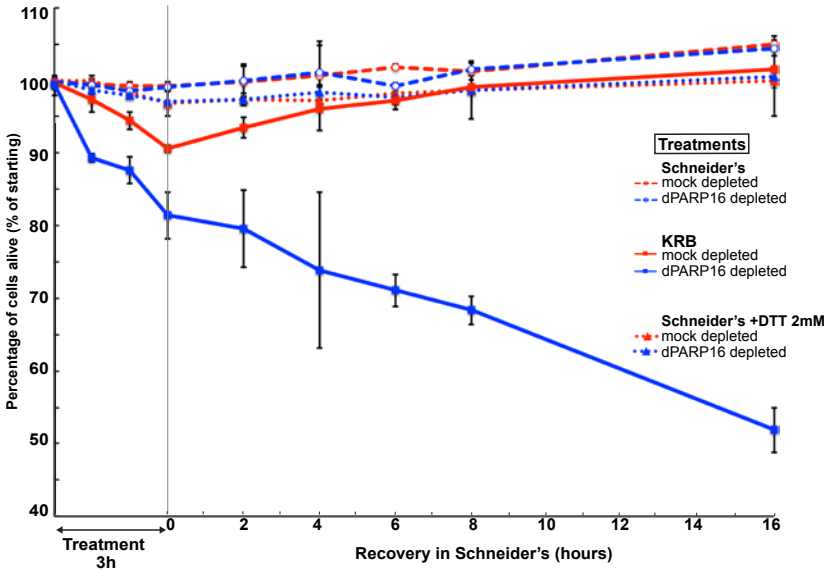

Figure 8- figure supplement 1: Comparison of cell viability upon amino-acid starvation and ER stress. Graph of cell viability (expressed as percentage of alive cells) upon "treatments" as indicated and recovery. The number of starting cells at t=0, mock- (dsGFP, red lines) and dPARP16 depleted (blue lines) is set at 100%. These cells are incubated in Schneider's (dashed lines) KRB (solid lines) and Schneider's supplemented by 2 mM DTT (ER stress)(dotted lines) for 3h followed by further incubation in Schneider's for 16 h. For each time point, p-values were calculated between cells incubated in Schneider's alone and Schneider's +DTT. Green asterisks marks p-values higher than 0.02. p-values were calculated between mock depleted cells incubated in Schneider's and in KRB. Orange* marks p-values higher the 10^{-2} and **, p-values higher than 10^{-5} (See F Fig.4C). The cells are therefore more sensitive to amino-acid starvation than ER stress that does not affect their survival and their recovery significantly. There were no significant difference between mock and dPARP16 depleted cells treated with DTT. Therefore, dPARP16 depletion does not make the cells more sensitive to ER stress.

Figure 2- figure supplement 2: GFP-MAD time-lapse movie of 1 cells incubated in KRB. This movie is available in the online version of this manuscript.

Primers used for cloning and RNAi	
sfGFP-F	ggccgcggatggtgagcaagggcgagga
sfGFP-R	gggtttaaacttacttgtacagctcgtccatg
dARTD1/PARP1-F	cagtggtaccatggatattgaattaccttatcttgctgagtatgc
dARTD1/PARP1-R	cagtgggccctcataagaatacttgaattccatacgaaacaaatattgaatatt
ARTD5-6/Tankyrase-F	gtcaggtaccatggccaacagcagccgaagtcg
ARTD5-6/Tankyrase-R	gtcagggccctctcttgtatcctccgttcc
ARTD15/PARP16-F	gtcaggtaccatgactctgctttcgggcgccaac
ARTD15/PARP16-R	gtcagggccctccaaaatacctcgcttgaatacgtagaatacgtagaagcc
pMT-V5-PARP16-F	gtcaggtaccatgactctgctttcgggcgccaac
pMT-V5-PARP16-R	gaatccgttcgcctgggcttcgctggcygcaagctagagaagg
pMT-Y199>A-PARP16-sfGFP	ccttctctagcttgcagccagcgaagcccaggcgaacggattc
pMT-V5-Y221>A-PARP16-F	caaaattccctggacaatggaaaggctctggagctaacctgcgatatc
pMT-V5-Y221>A-PARP16-R	gatatcgcaggttagctccagagcctttccattgtccagggaattttg
pMT-V5-ΔTM-PARP16	gtcagggccctcggatatggccttcttgtggtatctttcc
dARTD1/PARP1-RNAi-F	ctaatacgactcactatagggcgaaggaaattaacggatcttgtgga
dARTD1/PARP1-RNAi-R	ctaatacgactcactatagggcgaagattttattggtggtatggcg
ARTD5-6/Tankyrase-RNAi-F	taatacgactcactatagggcgagctgaggtccaccacaggcattg
ARTD5-6/Tankyrase-RNAi-R	taatacgactcactatagggcgatcttgtatcctccgttccactactgc
ARTD15/PARP16-RNAi-F	taatacgactcactatagggcgaatgactctgctttcgggcgccaac
ARTD15/PARP16-RNAi-R	taatacgactcactatagggcgacaaaatacctcgcttgaatacgtagaagcc
ARTD15/PARP16-RNAi-3utr-F	taatacgactcactatagggcgacttttactatccatatcctgtgacc
ARTD15/PARP16-RNAi-3utr-R	taatacgactcactatagggcgattcacacattacagatgcct
ARDT8-Macro1-3-F	cagtaccggtgggcagaagtgcttctctcggac
ARDT8-Macro1-3-R	cagtgtttaaaccccttctcttttcttcatgttggcataaaacac
Hex-HIS-TEV-F	5Phos/ccggtcatcatcaccatcaccatgagaacctgtacttccaatccata
Hex-HIS-TEV-R	5Phos/ccggtattggattggaagtacaggttctcatggtgatggtgatgatga
GFP-MAD-MutMacro2-F	ctaagtccctcttggaaaaagctgaaccagagctccaggaggaattg
GFP-MAD-MutMacro2-R	caattcctcctggagctctggttcagctttttccaagagggacttag
YFP-F	gactgggcccgcggttcgaaatggtgtctaaaggggaagagctcttta
YFP-R	gactaccggtcttatacagctcatccatgcccaggg
H2A1.1-F	cagtaccggtcagggtgaagtcagtaaggcagcc
H2A1.1-R	cagtgtttaaacgttggcgtccagcttggccatttc
CAAX-RAS-F	cagtaccggttccggactcagatctcgagctc
CAAX-RAS-R	cagtgtttaaacttacataattacacactttgtctttgacttctttttc
SEC16>NC1-F	cagtactagtatgcattcaaccactcagcaggagaagaa
SEC16-R	ccaccggtaatggggctgccatacgtttgc
SEC16>CT-R	gtcaccgcggaaatgagacacgattaatgagaatgggatcatg
SEC16-CT-F	cagtggtaccatggcgagtcctccgaatgccactag
SEC16-SRD-F	cagtggtaccatgctgcagcaacagacgcgccc
SEC16-SRD-R	gtcaccgcggaatggggctgccatacgtttgcg
SEC16-SRD-C-F	cagtggtaccatgaataaaaatgcgggctggtttggcg
SEC16-SRD-C-R	gtcaccgcggggtgtttgtccagcatttgcgctc
SEC16 ΔSRD-C-fusion-F	cgcacctggggaaggcaacggcgacgaggctgaaag
SEC16 ΔSRD-C-fusion-R	cgttgccttccccaggtgcgccaagatcgctgcc
SEC16 ΔSRD-C-F	gcgcccggcgatatccatgcccaag
SEC16 ΔSRD-C-R	gtcaccgcggctgctggggtacaaagtaaccgc

Figure 1- figure supplement 1: List of primers used.

References

Amodio, G., Renna, M., Paladino, S., Venturi, C., Tacchetti, C., et al., 2009. Endoplasmic reticulum stress reduces the export from the ER and alters the architecture of post-ER compartments. Int J Biochem Cell Biol 41, 2511-2521.

Audas, T.E., Audas, D.E., Jacob, M.D., Ho, J.J., Khacho, M., et al., 2016. Adaptation to Stressors by Systemic Protein Amyloidogenesis. Dev Cell 39, 155-168.

Butepage, M., Eckei, L., Verheugd, P., Luscher, B., 2015. Intracellular Mono-ADP-Ribosylation in Signaling and Disease. Cells 4, 569-595.

Carter-O'Connell, I., Jin, H., Morgan, R.K., Zaja, R., David, L.L., et al., 2016. Identifying Family-Member-Specific Targets of Mono-ARTDs by Using a Chemical Genetics Approach. Cell Rep 14, 621-631.

Cosi, C., Marien, M., 1999. Implication of poly (ADP-ribose) polymerase (PARP) in neurodegeneration and brain

energy metabolism. Decreases in mouse brain NAD+ and ATP caused by MPTP are prevented by the PARP inhibitor benzamide. Ann N Y Acad Sci 890, 227-239.
Dani, N., Stilla, A., Marchegiani, A., Tamburro, A., Till, S., et al., 2009. Combining affinity purification by ADP-ribose-binding macro domains with mass spectrometry to define the mammalian ADP-ribosyl proteome. Proc Natl Acad Sci U S A 106, 4243-4248.
Di Paola, S., Micaroni, M., Di Tullio, G., Buccione, R., Di Girolamo, M., 2012. PARP16/ARTD15 is a novel endoplasmic-reticulum-associated mono-ADP-ribosyltransferase that interacts with, and modifies karyopherin-ss1. PLoS One 7, e37352.
Forst, A.H., Karlberg, T., Herzog, N., Thorsell, A.G., Gross, A., et al., 2013. Recognition of mono-ADP-ribosylated ARTD10 substrates by ARTD8 macrodomains. Structure 21, 462-475.
Fujimori, H., Shikanai, M., Teraoka, H., Masutani, M., Yoshioka, K., 2012. Induction of cancerous stem cells during embryonic stem cell differentiation. J Biol Chem 287, 36777-36791.
Gagne, J.P., Isabelle, M., Lo, K.S., Bourassa, S., Hendzel, M.J., et al., 2008. Proteome-wide identification of poly(ADP-ribose) binding proteins and poly(ADP-ribose)-associated protein complexes. Nucleic Acids Res 36, 6959-6976.
Gardner, B.M., Pincus, D., Gotthardt, K., Gallagher, C.M., Walter, P., 2013. Endoplasmic reticulum stress sensing in the unfolded protein response. Cold Spring Harb Perspect Biol 5, a013169.
Gibbs-Seymour, I., Fontana, P., Rack, J.G., Ahel, I., 2016. HPF1/C4orf27 Is a PARP-1-Interacting Protein that Regulates PARP-1 ADP-Ribosylation Activity. Mol Cell 62, 432-442.
Gibson, B.A., Kraus, W.L., 2012. New insights into the molecular and cellular functions of poly(ADP-ribose) and PARPs. Nat Rev Mol Cell Biol 13, 411-424.
Hancock, J.F., Cadwallader, K., Paterson, H., Marshall, C.J., 1991. A CAAX or a CAAL motif and a second signal are sufficient for plasma membrane targeting of ras proteins. EMBO J 10, 4033-4039.
Hassink, G., Slotman, J., Oorschot, V., Van Der Reijden, B.A., Monteferrario, D., et al., 2012. Identification of the ubiquitin ligase Triad1 as a regulator of endosomal transport. Biol Open 1, 607-614.
Hottiger, M.O., Hassa, P.O., Luscher, B., Schuler, H., Koch-Nolte, F., 2010. Toward a unified nomenclature for mammalian ADP-ribosyltransferases. Trends Biochem Sci 35, 208-219.
Hu, B., Wu, Z., Hergert, P., Henke, C.A., Bitterman, P.B., et al., 2013. Regulation of myofibroblast differentiation by poly(ADP-ribose) polymerase 1. Am J Pathol 182, 71-83.
Ivan, V., de Voer, G., Xanthakis, D., Spoorendonk, K.M., Kondylis, V., et al., 2008. Drosophila Sec16 mediates the biogenesis of tER sites upstream of Sar1 through an arginine-rich motif. Mol Biol Cell 19, 4352-4365.
Jankevicius, G., Hassler, M., Golia, B., Rybin, V., Zacharias, M., et al., 2013. A family of macrodomain proteins reverses cellular mono-ADP-ribosylation. Nat Struct Mol Biol 20, 508-514.
Jevtov, I., Zacharogianni, M., van Oorschot, M.M., van Zadelhoff, G., Aguilera-Gomez, A., et al., 2015. TORC2 mediates the heat stress response in Drosophila by promoting the formation of stress granules. J Cell Sci 128, 2497-2508.
Jwa, M., Chang, P., 2012. PARP16 is a tail-anchored endoplasmic reticulum protein required for the PERK- and IRE1alpha-mediated unfolded protein response. Nat Cell Biol 14, 1223-1230.
Karras, G.I., Kustatscher, G., Buhecha, H.R., Allen, M.D., Pugieux, C., et al., 2005. The macro domain is an ADP-ribose binding module. EMBO J 24, 1911-1920.
Kondylis, V., Rabouille, C., 2003. A novel role for dp115 in the organization of tER sites in Drosophila. J Cell Biol 162, 185-198.
Kondylis, V., van Nispen tot Pannerden, H.E., Herpers, B., Friggi-Grelin, F., Rabouille, C., 2007. The golgi comprises a paired stack that is separated at G2 by modulation of the actin cytoskeleton through Abi and Scar/WAVE. Dev Cell 12, 901-915.
Krishnakumar, R., Kraus, W.L., 2010. The PARP side of the nucleus: molecular actions, physiological outcomes, and clinical targets. Mol Cell 39, 8-24.
Kustatscher, G., Hothorn, M., Pugieux, C., Scheffzek, K., Ladurner, A.G., 2005. Splicing regulates NAD metabolite binding to histone macroH2A. Nat Struct Mol Biol 12, 624-625.
Leung, A.K., 2014. Poly(ADP-ribose): an organizer of cellular architecture. J Cell Biol 205, 613-619.
Leung, A.K., Vyas, S., Rood, J.E., Bhutkar, A., Sharp, P.A., et al., 2011. Poly(ADP-ribose) regulates stress responses and microRNA activity in the cytoplasm. Mol Cell 42, 489-499.
Miller, E.A., Schekman, R., 2013. COPII - a flexible vesicle formation system. Curr Opin Cell Biol 25, 420-427.
Munder, M.C., Midtvedt, D., Franzmann, T., Nuske, E., Otto, O., et al., 2016. A pH-driven transition of the cytoplasm from a fluid- to a solid-like state promotes entry into dormancy. Elife 5.
Narayanaswamy, R., Levy, M., Tsechansky, M., Stovall, G.M., O'Connell, J.D., et al., 2009. Widespread reorganization of metabolic enzymes into reversible assemblies upon nutrient starvation. Proc Natl Acad Sci U S A 106, 10147-10152.
Peters, L.Z., Hazan, R., Breker, M., Schuldiner, M., Ben-Aroya, S., 2013. Formation and dissociation of proteasome storage granules are regulated by cytosolic pH. J Cell Biol 201, 663-671.
Petrovska, I., Nuske, E., Munder, M.C., Kulasegaran, G., Malinovska, L., et al., 2014. Filament formation by metabolic enzymes is a specific adaptation to an advanced state of cellular starvation. Elife.
Rack, J.G., Perina, D., Ahel, I., 2016. Macrodomains: Structure, Function, Evolution, and Catalytic Activities. Annu Rev Biochem.
Rosenthal, F., Feijs, K.L., Frugier, E., Bonalli, M., Forst, A.H., et al., 2013. Macrodomain-containing proteins are new mono-ADP-ribosylhydrolases. Nat Struct Mol Biol 20, 502-507.
Sprangers, J., Rabouille, C., 2015. SEC16 in COPII coat dynamics at ER exit sites. Biochem Soc Trans 43, 97-103.
Timinszky, G., Till, S., Hassa, P.O., Hothorn, M., Kustatscher, G., et al., 2009. A macrodomain-containing histone rearranges chromatin upon sensing PARP1 activation. Nat Struct Mol Biol 16, 923-929.

van Donselaar, E., Posthuma, G., Zeuschner, D., Humbel, B.M., Slot, J.W., 2007. Immunogold labeling of cryosections from high-pressure frozen cells. Traffic 8, 471-485.
Vicidomini, G., Gagliani, M.C., Cortese, K., Krieger, J., Buescher, P., et al., 2010. A novel approach for correlative light electron microscopy analysis. Microsc Res Tech 73, 215-224.
Vivelo, C.A., Leung, A.K., 2015. Proteomics approaches to identify mono-(ADP-ribosyl)ated and poly(ADP-ribosyl)ated proteins. Proteomics 15, 203-217.
Watanabe, Y., Papoutsoglou, P., Maturi, V., Tsubakihara, Y., Hottiger, M.O., et al., 2016. Regulation of Bone Morphogenetic Protein Signaling by ADP-ribosylation. J Biol Chem 291, 12706-12723.
Zacharogianni, M., Aguilera Gomez, A., Veenendaal, T., Smout, J., Rabouille, C., 2014. A stress assembly that confers cell viability by preserving ERES components during amino-acid starvation. Elife 3.
Zacharogianni, M., Kondylis, V., Tang, Y., Farhan, H., Xanthakis, D., et al., 2011. ERK7 is a negative regulator of protein secretion in response to amino-acid starvation by modulating Sec16 membrane association. EMBO J 30, 3684-3700.
Zacharogianni, M., Rabouille, C., 2013. Trafficking along the secretory pathway in Drosophila cell line and tissues: a light and electron microscopy approach. Methods Cell Biol 118, 35-49.

Chapter 4

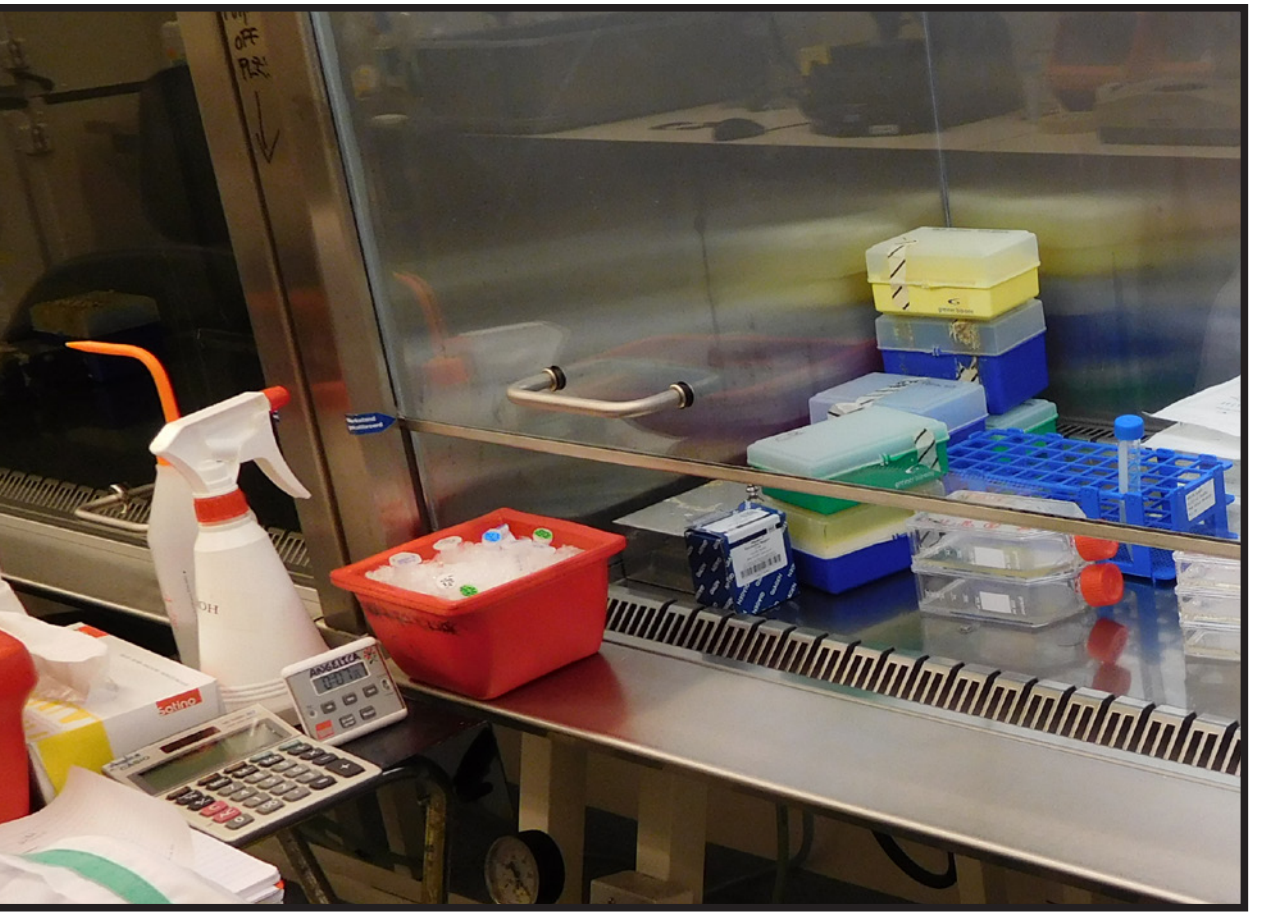

PARP1 nuclear export is essential for stress granule formation upon amino acid starvation

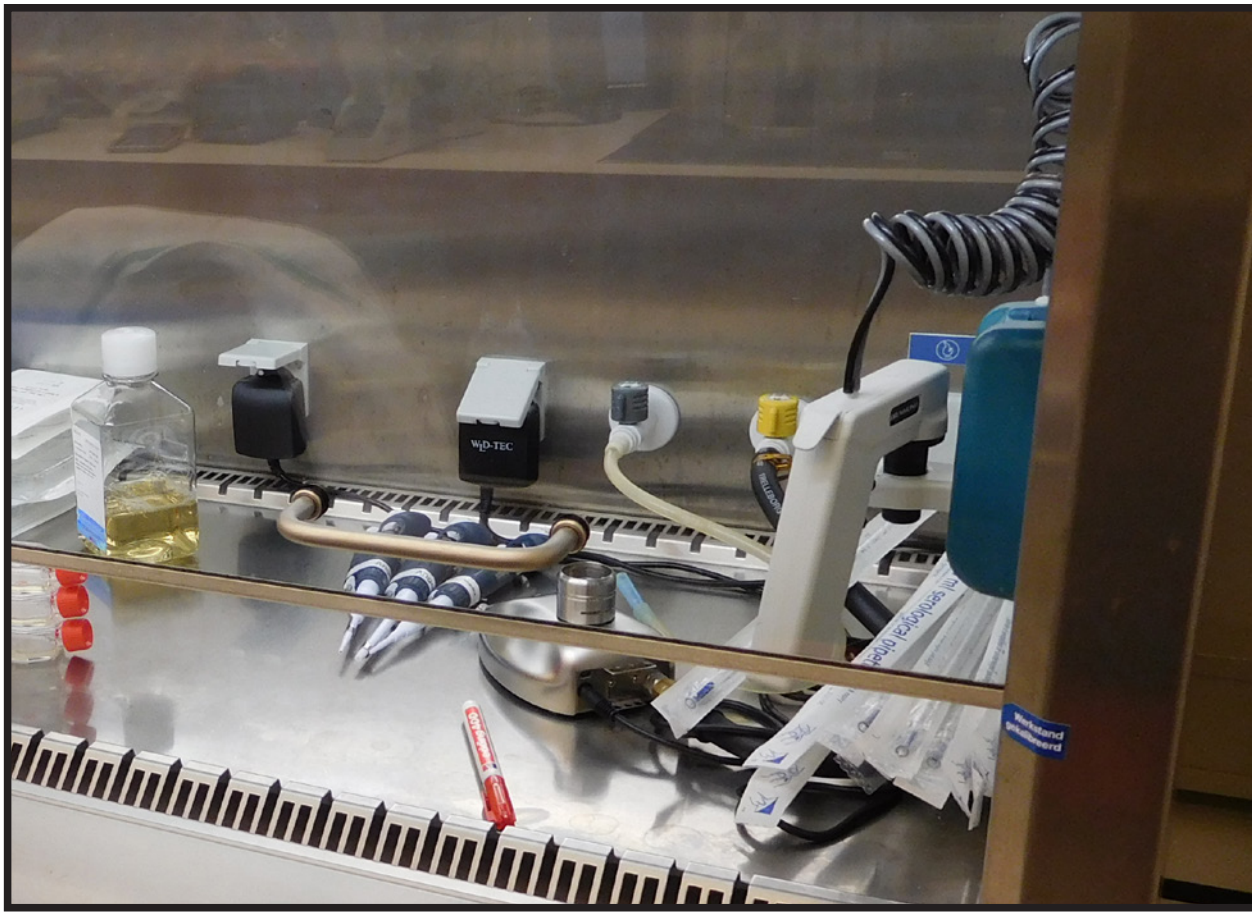

Angelica Aguilera-Gomez and Catherine Rabouille (2017)
In preparation

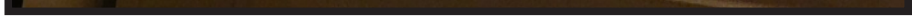

PARP1 nuclear export is essential for stress granule formation upon amino acid starvation

Abstract

Amino-acid starvation of Drosophila S2 cells induces stress granule assembly. Here, we investigate the role of ADP-ribosylation in their formation. We have found that the mono-ADP-ribose dPARP16 is necessary but not sufficient for stress granule formation. In addition, the use of the poly-ADP-ribosylation inhibitor 3 aminobenzamide, and overexpression of the poly-ADP-ribose glycohydrolase PARG inhibit their assembly, pointing also towards a role for Poly-ADP-ribosylation. In this regard, we show that the nuclear resident, poly-ADP-ribose dPARP1 plays a crucial role. Interestingly, we demonstrate that in order to induce stress granule formation, it has to localize at the cytoplasm. In line with this, both Leptomycin B treatment and the depletion of the nuclear export factor Karyopherin beta 3 inhibit stress granule formation upon amino-acid starvation. Critically, dPARP1 localization out of the nucleus depends of dPARP16, possibly through the mono-ADP-ribosylation of Karyopherin beta 3.

Taken together, this provides a novel layer of complexity for the cellular mechanisms involved in the response to amino acid starvation. Furthermore, it provides a link between the stress responses exerted at the secretory pathway, nuclear export and the translation turnover upon this nutrient stress.

Introduction

Stress granules are formed from accumulating mRNAs that are stalled in translation initiation. Translation initiation can be inhibited by treatment with several drugs or a variety of stresses (Anderson and Kedersha, 2009). Stress granules contain initiation factors as well as RNA and non-RNA binding proteins (Anderson and Kedersha, 2009; Jain et al., 2016; Parker and Sheth, 2007). Recently, the research into stress granules has become a subject of broader interest for several reasons: first, their assembly and dynamics can dramatically affect several cellular responses, such as mRNA localization, degradation, translation as well as multiple signaling pathways (Bhattacharyya et al., 2006; Buchan et al., 2013). Also mutations in genes encoding TDP-43 and FUS can drive an increase in stress granule formation or limit their clearance originating some neurodegenerative diseases (Li et al., 2013; Ramaswami et al., 2013). The last reason is that stress granules are a major representative of non-membrane bound compartments, and understanding the mechanism behind their formation and cellular function opens up exciting areas of study in cell biology.

Stress granules are assembled through the interactions between untranslated mRNAs, RNA-binding proteins and translation inhibition factors (Protter and

Parker, 2016). In mammalian cell lines some factors that are essential for their formation have been identified, among others, the well characterized Ras GTPase-activating protein-binding protein 1 (G3BP1) (Kedersha et al., 2016; Tourriere et al., 2003) and cytotoxic granule-associated RNA binding protein 1 (Tia-1) (Gilks et al., 2004; Kedersha et al., 1999). However, these studies have mostly focused on heat and oxidative stress responses (Anderson and Kedersha, 2002). With Drosophila S2 cell lines, we have shown that stress granules are also assembled upon other stresses such as amino-acid starvation (Zacharogianni et al., 2014) **Chapter 4)**. Interestingly, amino-acid starvation leads to the formation of another stress assembly, the Sec body. As stress granules, Sec bodies are non-membrane bound and pro-survival stress assemblies with liquid droplets properties. However, instead of mRNAs, they store and protect ER exit sites (ERES) components. Sec bodies and stress granules are formed approximately in the same time frame, and even though they have similar properties they do not fuse together at the cytoplasm (Aguilera-Gomez et al., 2016; Zacharogianni et al., 2014).

Recently, it has been proposed that ADP-ribosylation and more specifically poly-ADP-ribosylation is involved in the formation of cytoplasmic mRNP granules upon oxidative stress and viral infections (Leung, 2014). This post-translational modification consists out of the addition of an ADP-ribose group from NAD+ to target proteins (Daniels et al., 2015). The modification can occur by the addition of a single unit, mono-ADP ribose (MARylation), or in polymeric chains, as poly-ADP ribose (PARylation). These modifications are executed by the active members of the ADP-ribosyltransferases (ARTs), also known as poly-ADP-ribose polymerases (PARPs) (Hottiger et al., 2010; Vyas et al., 2014). These enzymes have been associated with many cellular functions, such as cell cycle progression, DNA repair, apoptosis, genome integrity, and stress responses (Aguilera-Gomez et al., 2016; Aredia and Scovassi, 2014; Daniels et al., 2015; Feijs et al., 2013).

In this regard, we have recently demonstrated that MARylation plays a crucial role in Sec body formation. The formation of this stress assembly is driven by the activation of the ER localized MARylation enzyme dPARP16 that MARylates Sec16 on a conserved sequence close to its C-terminus (Aguilera-Gomez et al., 2016). Importantly, the sole MARylation of Sec16 is sufficient to drive Sec body formation, even in the absence of stress. Whether MARylation is also involved in stress granule formation upon amino acid starvation remains to be investigated.

Interestingly, several substrates of human PARP16 have been identified, such as PERK and IRE1 (Jwa and Chang, 2012). Furthermore, it has been demonstrated that human PARP16 MARylates and interacts with Karyopherin beta1 (Di Paola et al., 2012). Karyopherin beta1 plays a crucial role in shuttling proteins containing nuclear localization signals between the cytosol and the nucleus through the nuclear pore complex (Conti and Izaurralde, 2001; Fried and Kutay, 2003; Gorlich et al., 1995). It has been suggested that Karyopherin beta1 may exhibit a functional role

at the ER due to its association with the ER associated protein degradation (ERAD) transmembrane components (Moss et al., 1997). Mass spectrometry data revealed that the ERES component Sec16 interacts with Karyopherin beta3 upon amino-acid starvation **(Chapter 4)**. Karyopherin beta3 is widely conserved from yeast to mammals (Chung et al., 2008). Furthermore, depletion of PSE1, the yeast ortholog of mammalian Karyopherin beta3, has been shown to cause specific blockage of mRNA export from the nucleus (Seedorf et al., 1999; Seedorf and Silver, 1997).

The founding member of the PARP family is the PARylation enzyme PARP1, and its main role is to act as a sensor for DNA breaks. As such, it plays a key role in their repair by catalyzing auto and hetero-modifications of histones and other proteins involved in DNA synthesis and repair (Hassa and Hottiger, 2008; Schreiber et al., 2006). PARP1 is highly conserved, very abundant in mammalian tissues and is mostly nuclear localized. PARP1 also PARylates itself, which inhibits its activity allowing a negative feedback for auto-regulation (Krishnakumar and Kraus, 2010). PARylation is reversible, and the primary enzyme involved in PARPs degradation is the Poly ADP-ribose glycohydrolase PARG (Hatakeyama et al., 1986). Interestingly, PARG can efficiently remove ribose bonds in a chain but it cannot remove the terminal ADP-ribose unit, resulting in mono-ADP-ribosylated proteins (Slade et al., 2011). It has been shown that during heat shock or viral infection, stress granules are enriched with PARPs and PARGs (Leung et al., 2011). Furthermore, overexpression of PARG isoforms leads to the inhibition of stress granule formation (Leung et al., 2011).

Interestingly, the results presented in this manuscript point towards the cellular use of both MARylation and PARylation upon amino-acid starvation in the context of stress granule formation. Here, we report that dPARP16 MARylation activity is necessary for stress granule formation, but in contrast to Sec body formation, its role for stress granules appears to be indirect. Instead, the critical modification for stress granule formation is PARylation. This is supported by the fact that either treatment with the PARylation inhibitor 3-aminobenzamide and PARG overexpression inhibit their assembly. In addition, we demonstrate that the nuclear Poly-ADP-ribose dPARP1 is necessary for stress granule formation and for this, it needs to be trans located outside of the nucleus.

Importantly, we show that dPARP16 is required for dPARP1 nuclear export. In the absence of dPARP16, dPARP1 remains strictly nuclear and stress granule formation is inhibited. We propose that dPARP16 modification of Karyopherin beta3 facilitates dPARP1 nuclear export upon amino-acid starvation. In this regard, we show that Karyopherin beta3 depletion inhibits stress granule formation. Thus, we provide a preliminary but solid link between nuclear export and protein translation. This enriches the scarce knowledge of the function of PARPs and their mechanism of action in the context of amino-acid starvation.

RESULTS

dPARP16 is necessary but not sufficient for stress granule formation upon amino-acid starvation.

It has been previously demonstrated that amino-acid starvation leads to the formation of two pro-survival stress assemblies, stress granules (**Suppl**. **Figure 1A**), and Sec bodies (**Suppl. Figure 1B**) where respectively, untranslated mRNAs and ERES components are stored and protected, while this nutrient stress is taking place. Stress granules and Sec bodies are formed in close proximity to each other and approximately at the same time frame, although stress granule formation is consistently delayed by 30-60 minutes when compared to Sec bodies formation (Suppl. Figure 1C, C') (Zacharogianni et al., 2014)**.**

We have recently shown that dPARP16 is necessary and sufficient for Sec body assembly (Aguilera-Gomez et al., 2016). Indeed, dPARP16 overexpression leads to Sec body formation in the absence of stress **(Figure 1A, A")**, and conversely, dPARP16 depletion inhibits Sec body formation upon amino-acid starvation **(Figure 1B, B')**.

Here, we investigated whether dPARP16 is also required for stress granule formation. To approach this, dPARP16 was depleted and stress granule formation monitored. We observed that dPARP16 depletion also abrogates stress granule assembly **(Figure 1B, B')**, suggesting that dPARP16 is necessary for their formation. However, overexpression of dPARP16 under growing conditions (in the absence of stress) does not lead to stress granule formation **(Figure 1A', A").** Taken together, these results demonstrate that dPARP16 and presumably its MARylation activity, is necessary but not sufficient for stress granule formation upon amino-acid starvation.

Poly-ADP ribosylation is involved in stress granule formation.

As mentioned in the introduction, it has been suggested that PARylation plays a role in the formation of cytoplasmic structures, like mRNP granules (Leung et al., 2011). Therefore we investigated whether PARylation plays a role in stress granule formation upon amino-acid starvation in Drosophila S2 cells using 3-aminobenzamide, a well-known PARylation inhibitor. Application of this PARylation inhibitor abrogates stress granule formation upon this nutrient stress **(Figure 2A, A').** Importantly, 3-aminobenzamide treatment does not affect Sec body formation under the same conditions **(Figure 2A, A')**. This is expected, as PARylation inhibitors do not affect mono-ADP-ribosylation, the modification required for Sec bodies formation (Aguilera-Gomez et al., 2016). Taken together, these results suggest that Poly- and not mono-ADP ribosylation is involved in stress granule formation upon amino acid starvation.

To strengthen the notion that PARylation is required for stress granule formation,

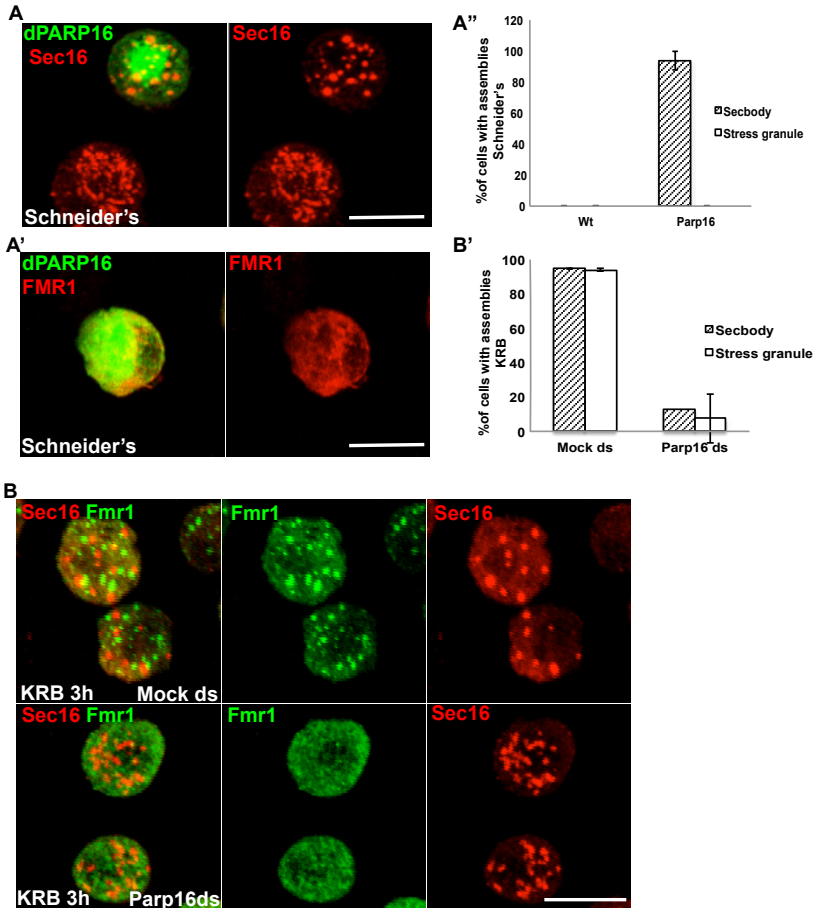

Figure 1: dPARP16 is necessary but not sufficient for stress granule formation upon amino-acid starvation. A: (IF) visualization of endogenous Sec16 (in red) in S2 cells transfected with dPARP16 and incubated in Schneider's for 3 h. Note that sec bodies are formed in dPARP16 transfected cells under growing conditions. **A':** (IF) visualization of endogenous Fmr1 (in red) in S2 cells transfected with dPARP16 and incubated in Schneider's for 3 h. Note that stress granules do not form in dPARP16-transfected cells under growing conditions. **A":** Quantification of stress granule/sec bodies formation in S2 cells incubated in Schneider's and transfected with dPARP16, expressed as the percentage of cells exhibiting stress assemblies. **B:** (IF) visualization of endogenous Sec16 (in red) and Fmr1 (green) in mock and dPARP16 depleted S2 cells incubated in KRB for 3 h. Note that neither stress granules/sec bodies do form in dPARP16 depleted cells. **B':** Quantification of stress granule/sec bodies formation in Mock and dPARP16 depleted S2 cells incubated in KRB for 3 h, expressed as the percentage of cells exhibiting the formation of the stress assemblies. Scale bars: 10 μm, error bars: SEM.

we investigated whether the Poly-ADP ribose glycohydrolase (dPARG; CG2864) is involved in stress granule dynamics. This enzyme removes ribose bonds in a chain but it cannot remove terminal ADP-riboses (Slade et al., 2011). Overexpression of dPARG in cells under amino-acid starvation prevented stress granule formation **(Figure 2B, B').** Importantly, and as expected, dPARG overexpression does not affect Sec body formation **(Figure 2C, B').** Strengthening the notion that PARylation and

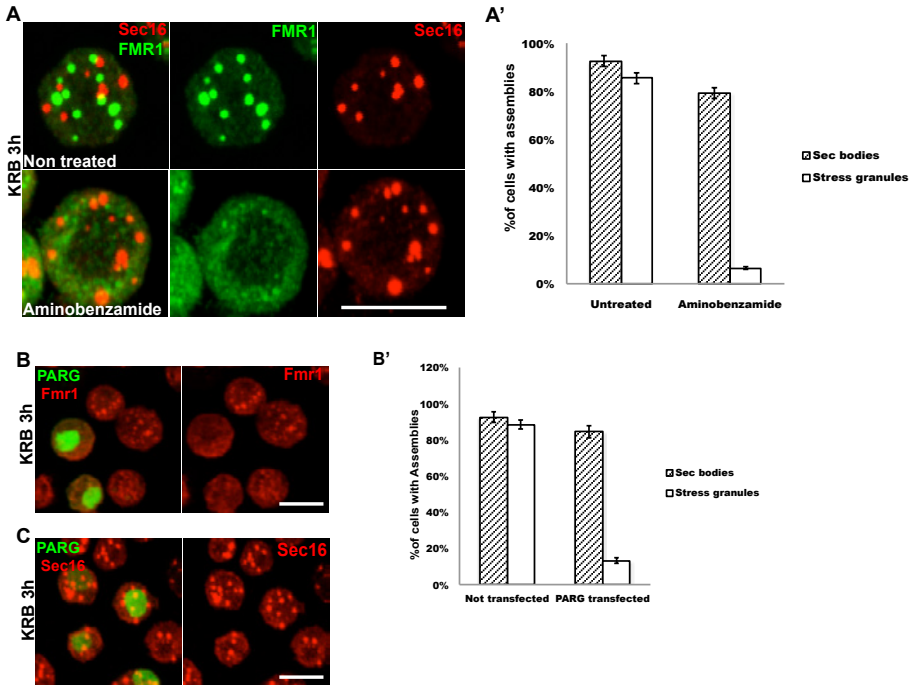

Figure 2: Poly-ADP ribosylation is involved in stress granules formation. A: (IF) visualization of endogenous Fmr1 (green) and Sec16 (red) in S2 cells non-treated and treated with 3 aminobenzamide and incubated in KRB for 3 h. Note that stress granules do not form in 3 aminobenzamide treated cells. **A':** Quantification of stress granule/sec body formation in S2 cells non-treated and treated with 3 aminobenzamide and incubated in KRB for 3 h, expressed as the percentage of cells exhibiting the stress assemblies formation. **B:** (IF) visualization of endogenous Fmr1 (red) in dPARG transfected S2 cells (green) in KRB for 3 h. Note that stress granules do not form in dPARG transfected cells. **B':** Quantification of stress granule/sec body formation in dPARG transfected S2 cells incubated in KRB for 3 h, expressed as the percentage of cells exhibiting stress granules/sec body formation. **C:** (IF) visualization of endogenous Sec16 (red) in dPARG transfected S2 cells (green) in KRB for 3 h. Note that sec bodies do form in dPARG transfected cells. Scale bars: 10 μm, error bars: SEM.

not MARylation is the post-translational modification directly involved in stress granule formation.

dPARP1 is necessary but not sufficient for stress granule formation upon amino-acid starvation.

To identify which PARP is required for stress granule formation, the other two PARPs present in the Drosophila genome, dPARP1 (CG40441) and dTank (CG15626), were tested. We find that dTank depletion or overexpression has no effect on stress granule formation upon amino-acid starvation (data not shown).

However, dPARP1 is clearly involved in stress granules formation. As, dPARP1 depletion completely inhibits stress granule formation upon amino-acid starvation (**Figure 3A, A').** Importantly, as reported before in (Aguilera-Gomez et al., 2016),

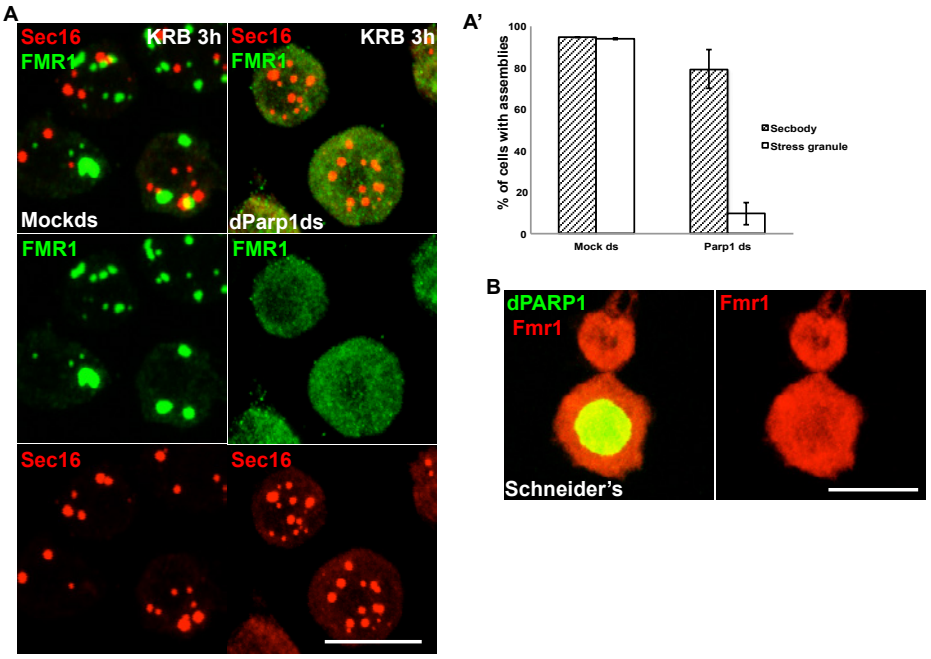

Figure 3: PARP1 is essential but not sufficient for stress granule formation upon amino-acid starvation. A: (IF) visualization of endogenous Fmr1 (green) and Sec16 (red) in dPARP1 depleted S2 cell incubated in KRB for 3 h. Note that stress granules do not form in dPARP1 depleted cells. **A':** Quantification of stress granule/sec body formation in dPARP1 depleted S2 cells incubated in KRB for 3 h, expressed as the percentage of cells exhibiting stress assembly formation. **B:** (IF) visualization of endogenous Fmr1 (red) in dPARP1 transfected S2 cells (green) incubated in Schneider's for 3 h. Note that stress granules do not form in dPARP1 transfected cells. Scale bars: 10 μm, error bars: SEM.

its depletion does not affect Sec body formation (**Figure 3A, A'**)**.** This reinforces the specificity of the enzyme for stress granule formation upon this nutrient stress. However, dPARP1 overexpression does not lead to the formation of stress granules under growing conditions (**Figure 3B**).

Taken together these results suggest that the nuclear resident dPARP1 is necessary but not sufficient for stress granule formation upon amino-acid starvation. This result is in line with the role of human PARP1 during the formation of cytoplasmic structures upon heat shock and viral infections (Leung et al., 2012).

dPARP1 nuclear export is necessary and sufficient for stress granule formation.

As expected, dPARP1 in Drosophila cells is a nuclear protein (**Figure 4A**), which raises the question of how it can be involved in a cytoplasmic event. In this respect, we noticed that upon amino-acid starvation, a small amount of dPARP1 is localized in the cytoplasm (**Figure 4B**). Therefore, we asked whether nuclear export of dPARP1 is important for stress granule assembly. To test this, nuclear export was

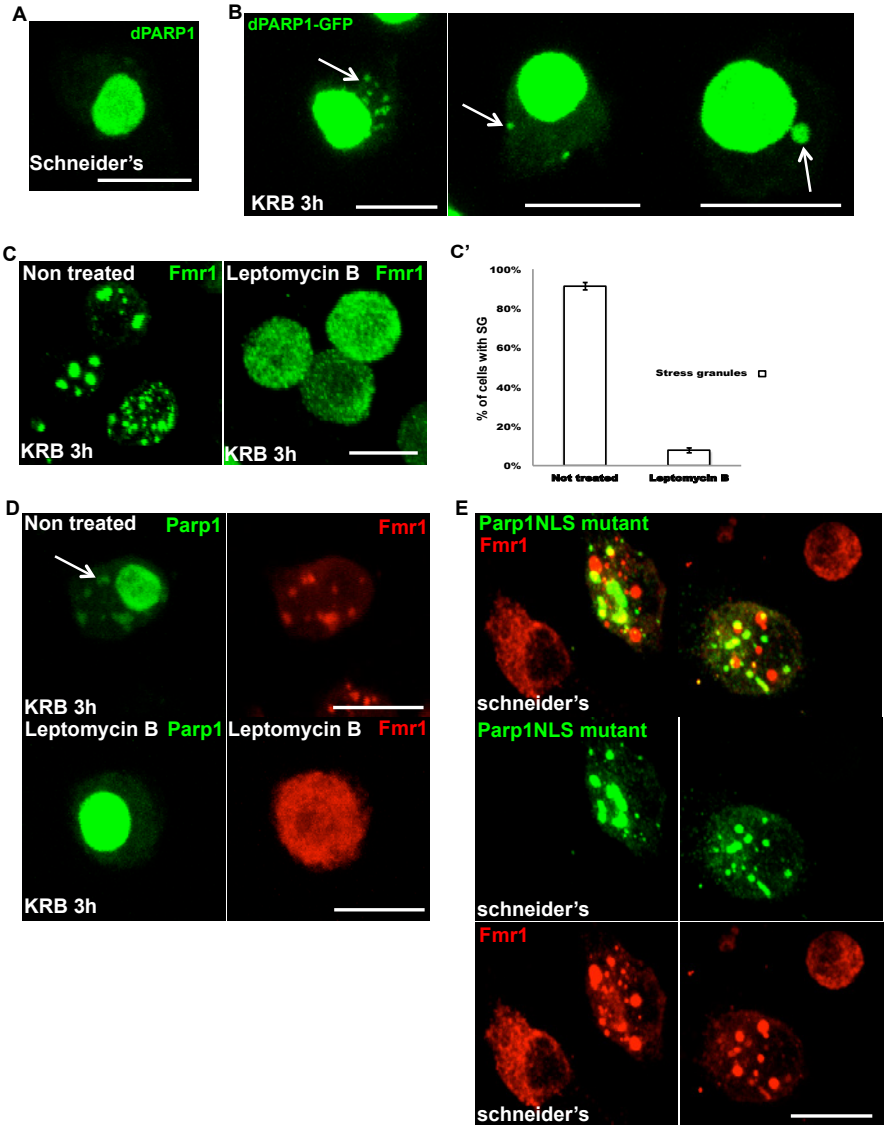

Figure 4: PARP1 nuclear export is necessary and sufficient for stress granule formation. A: (IF) visualization of dPARP1 transfected S2 cell (green) incubated in Schneider's for 3 h. Note that dPARP1 is a nuclear resident. **B:** (IF) visualization of dPARP1 transfected S2 cell (green) incubated in KRB for 3 h. Note that dPARP1 is found in the cytoplasm. **C:** (IF) visualization of endogenous Fmr1 (green) in S2 cells incubated in KRB and treated or non-treated with Leptomycin B for 3 h. Note that the Leptomycin B treated cells do not form stress granules. **C':** Quantification of stress granule formation in Leptomycin B treated S2 cells incubated in KRB for 3 h, expressed as the percentage of cells exhibiting stress granules formation. **D:** (IF) visualization of endogenous Fmr1 (red) in dPARP1 transfected S2 cells, treated or non-treated with Leptomycin B incubated in KRB for 3 h. Note that in Leptomycin B treated cells stress granules do not form stress granules and dPARP1 does not go out of the nucleus. **E:** (IF) visualization of endogenous Fmr1 (red) in dPARP1-NLS-mutant transfected S2 cells (green) incubated in Schneider's for 3 h. Note that stress granules formation is induced in dPARP1 transfected cells under growing conditions. Scale bars: 10 µm, error bars: SEM.

blocked using Leptomycin B. Treatment of cells with Leptomycin B completely abrogates stress granule formation upon amino-acid starvation **(Figure 4C, C')**, and as expected dPARP1 is no longer observed in the cytoplasm (**Figure 4D**).

In order to confirm that the cytoplasmic localization of dPARP1 is indeed driving stress granule assembly, a rescue approach was performed by transfecting a dPARP1-NLS-mutant (a mutant that is entirely cytoplasmic) in Leptomycin B treated S2 cells (to prevent endogenous dPARP1 movement out of the nucleus). Expression of the dPARP1-NLS-mutant rescues stress granule formation in amino-acid starved Leptomycin B treated cells. Importantly, it also leads to the formation of stress granules in cells under growing conditions (**Figure 4E**). Taken together these results show that dPARP1 nuclear export or cytoplasmic localization is necessary and sufficient to drive stress granule formation.

dPARP16 is required for dPARP1 nuclear export.

As shown above, dPARP16 depletion negatively affects stress granule assembly upon amino acid starvation. Therefore we investigated whether dPARP16 plays a role in dPARP1 dynamics out of the nucleus. To test this, dPARP1 was overexpressed in dPARP16 depleted cells upon amino-acid starvation. Depletion of dPARP16 prevents dPARP1 nuclear export, suggesting that dPARP16 is involved in dPARP1 translocation out of the nucleus (**Figure 5A**). Furthermore, whereas dPARP1 overexpression leads to the formation of very large stress granules upon amino-acid starvation **(Figure 5A**), we find that dPARP16 depletion prevent stress granule formation **(Figure 5A)**. This strongly suggests that dPARP16 most likely mediates dPARP1 nucleus cytoplasmic transport upon amino-acid starvation.

We then asked how dPARP16 modulates dPARP1 nuclear export upon amino-acid starvation. Interestingly, the nuclear export factor Karyopherin beta1 is a substrate of human PARP16 (Di Paola et al., 2012). Furthermore, we have recently identified Sec16 as a novel dPARP16 substrate (Aguilera-Gomez et al., 2016), and strikingly, our mass-spec data indicated that Sec16 interacts with the nuclear export factor Karyopherin beta3. To assess the role of Karyopherin beta3 in stress granule formation upon amino acid starvation, we depleted it from S2 cells. Consistent with our hypothesis, we found that Karyopherin beta3 depletion inhibits stress granule formation upon amino acid starvation. (**Figure 5B, B').** Taken together, these results suggest that dPARP16 plays an essential role in stress granule formation, possibly through the MARylation of Karyopherin beta 3, which in turn would regulates dPARP1 nuclear export, resulting in stress granule assembly.

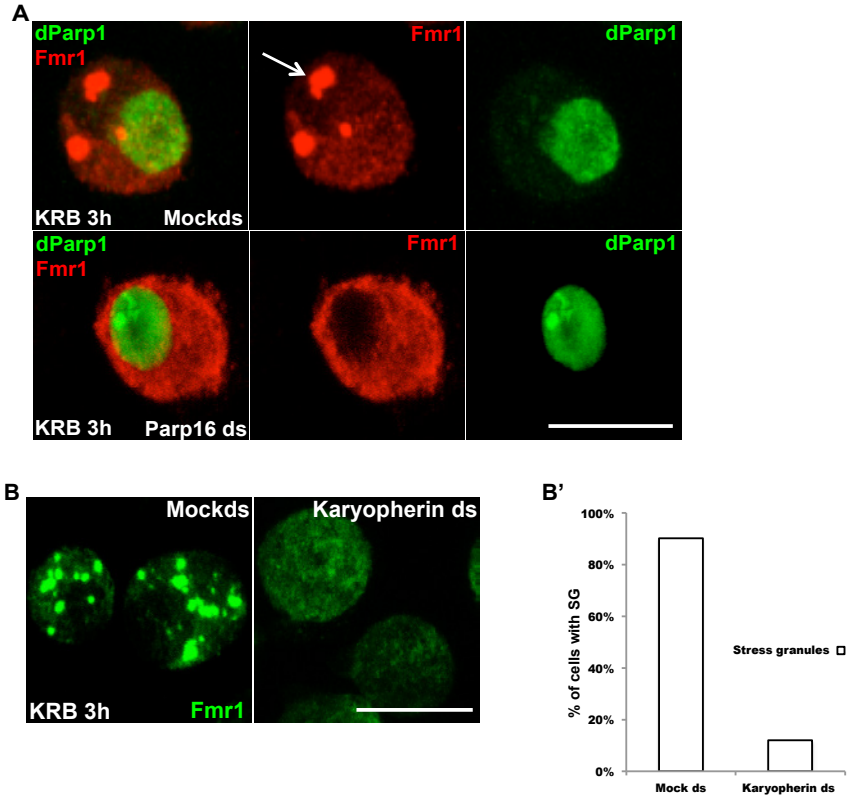

Figure 5: Karyopherin beta 3 plays a role in dPARP1 nuclear export. A: (IF) visualization of endogenous Fmr1 (red) in dPARP1 transfected S2 cells, either Mock or dPARP16 depleted incubated in KRB for 3 h. Note that in dPARP16 depleted cells stress granules do not form and dPARP1 does not localize outside of the nucleus. **B:** (IF) visualization of endogenous Fmr1 (green) in Mock and Karyopherin beta 3 depleted S2 cells incubated in KRB. Note that in Karyopherin beta 3 cells stress granules do not form. **B':** Quantification of stress granule formation in Mock and Karyopherin beta 3 incubated in KRB for 3 h, expressed as the percentage of cells exhibiting stress granules formation.

Discussion

Stress granules seem to follow Sec bodies formation.

We have previously reported the simultaneous formation of two pro-survival stress assemblies with liquid droplets properties upon the stress of amino acid starvation, the Sec body and the stress granule (Zacharogianni et al., 2014). It is well described that upon a given stress, the first cellular survival strategy is to stall or slow down major anabolic pathways (Buchan and Parker, 2009; Kedersha et al., 2013; Wheeler et al., 2016), and this is often follow by the formation of stress assemblies in order to save key components that would ensure a quick, efficient recovery once the stress condition is relieved (Jevtov et al., 2015; Zacharogianni et al., 2014).

Here, we report that upon amino-acid starvation, stress granules seem to follow Sec body formation by a time lapse of approximately 30 to 60 minutes (**See Suppl. Figure 1 C'**). This kinetics suggests that the response to protein transport inhibition is followed by the response to protein translation inhibition. Although, this also may suggest that Sec body initiation is a necessary step for stress granule formation. Whether upon stress relief, both pathways are simultaneously activated or whether protein transport is more promptly resumed remains to be investigated.

Stress granules and Sec bodies often overlap. Do they communicate?

Recently, it has been shown that mammalian stress granules are formed by two different layers. One layer at the outer shell that behaves mostly as liquid-liquid phase separation droplets and is formed by weak interactions, and an inner more dense core layer formed by stronger interactions (Jain et al., 2016; Wheeler et al., 2016).

In this regard, we propose that stress granules may share components with Sec bodies, but mostly at the outer layer. This notion is strengthened by the fact that stress granules and Sec bodies often localize in close proximity and/or partly overlap, particularly at the edges. This suggests a close relationship and/or communication between these assemblies. We have shown that this communication largely depends on the ERES component Sec16 (Aguilera-Gomez et al., 2016; Connerly et al., 2005; Ivan et al., 2008; Watson et al., 2005). In line with this, the depletion of Sec16 abolishes stress assembly formation **(Chapter 5)**. Importantly, the Sec body component Sec16 has been found inside stress granules, and this is most likely due to its interaction with the RNA binding protein and other stress granule component, Rasputin **(Chapter 5)**. Whether Sec16 interacts with other stress granule components remains to be elucidated.

Furthermore, mass spectrometry data shows that Sec16 also interacts with Karyopherin beta3, a nuclear exporter which broad evidence points towards its association with the protein transport pathway (Deane et al., 1997; Deng et al., 2006; Dynes et al., 2004; Jakel and Gorlich, 1998). The relevance of this interaction upon amino acid starvation remains to be investigated. However, our results suggest that it may be crucial for stress granule formation, as Karyopherin beta3 depletion inhibits their formation (the possible role of Karyopherin in stress granules formation is further addressed below).

MARylation and PARylation a cross-link for stress granule formation.

Non-membrane bound cytoplasmic assemblies are formed and maintained because their components cannot diffuse freely (Hyman et al., 2014). The way these components are assembled together is via RNA-Protein and protein-protein interactions (Anderson and Kedersha, 2009; Jain et al., 2016; Parker and Sheth,

2007). In addition, it has been proposed that the post-translational modification PARylation plays a role in the formation and maintenance of mRNP granules by keeping the proteins together via interaction with the poly ADP-ribose bonds (Leung, 2014).

In this regard, we have previously reported that the MARylation activity of dPARP16 is necessary and sufficient for Sec body assembly, via mono-ADP-ribosylation of Sec16 (Aguilera-Gomez et al., 2016). However, in the case of stress granules dPARP16 activity is necessary but not sufficient. Additionally, here we report that PARylation also has a role, as stress granule formation is specifically inhibited by the use of a PARylation inhibitor and overexpression of PARG. Importantly, we show that the PARylation enzyme dPARP1 is necessary for stress granule assembly. However, to exert this role, it has to be localized at the cytoplasm. How a nuclear resident like dPARP1 shuttles out of the nucleus remains to be elucidated.

Importantly, we have shown that dPARP16 is necessary for dPARP1 cytoplasmic localization upon amino-acid starvation. As mentioned above, the exporting Karyopherin beta 3 interacts with Sec16 upon amino acid starvation. Interestingly, It has been shown that Karyopherin beta1 is a substrate of human PARP16 (Di Paola et al., 2012). Therefore, we propose that Karyopherin beta 3 is also a dPARP16 substrate, and that the MARylation of both Sec16 and possibly Karyopherin beta 3 are upstream signaling events orchestrating the response to amino acid starvation. Taken together, we propose a model, whereby upon amino-acid starvation the ER localized dPARP16 MARylates Karyopherin beta3, which in turn induces a tightly regulated cytosolic export of dPARP1 through the nuclear pore where it drives via PARylation the formation of cytoplasmic stress granules **(Figure 6)**.

Furthermore, we propose an interesting cross-link between MARylation and PARylation for stress granule formation as our results strongly suggest that both processes are required for the response upon this nutrient stress.

Materials and methods

Cell culture, amino acid starvation, depletions (RNAi) and transfections

Drosophila S2 cells (mycoplasma free) were cultured in Schneider's medium (Sigma) supplemented with 10% insect tested fetal bovine serum at 26ºC as described in (Kondylis and Rabouille, 2003; Kondylis et al., 2007). Amino acid starvation of cells for 3 or 4 h was performed using Krebs Ringer's Bicarbonate buffer (10 mM D(+) Glucose; 0.5 mM $MgCl_2$; 4.5 mM KCl; 121 mM NaCl; 0.7 mM Na_2HPO_4; 1.5 mM NaH_2PO_4 and 15 mM sodium bicarbonate) at pH 7.4 (Aguilera-Gomez et al., 2016; Zacharogianni et al., 2014).

Wild type Drosophila S2 cells were depleted by dsRNAi, as previously described (Aguilera-Gomez et al., 2016). Cells were analyzed after incubation with dsRNAs for five days typically leading to depletion in more than 90% of the cells.

Transient transfections of PMT constructs (see below) were performed using Effectene transfection reagent (301425; Qiagen, Germany) according to manufactures instructions. Expression was induced 48 h after transfection with 1 mM CuSO4 for 1.5 h (Zacharogianni and Rabouille, 2013).

Antibodies

The following antibodies were used:

Rabbit polyclonal anti-Sec16 (Ivan et al., 2008) 1:800 IF, Mouse monoclonal anti-FMR1 (RRID:AB_528251, DSHB supernatant clone 5A11, 1:800 IF).

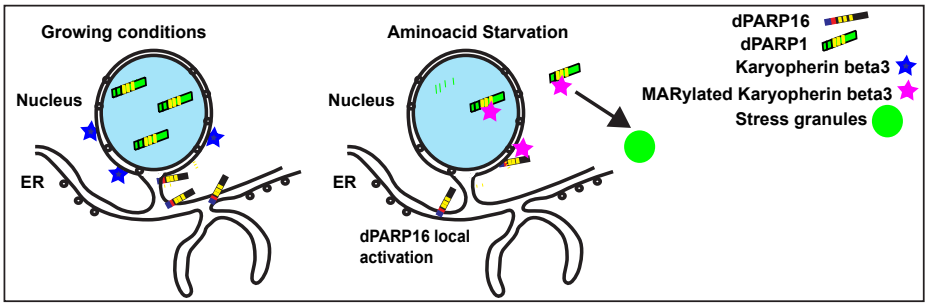

Figure 6: Model for stress granules formation upon amino-acid starvation. Upon amino-acid starvation the ER localized dPARP16 MARylates Karyopherin beta 3, which in turn induces a tightly regulated cytosolic export of dPARP1 through the nuclear pore where it drives via PARylation the formation of cytoplasmic stress granules.

PMT-DNA constructs and dsRNAs
All the primers used for generating the DNA constructs and RNAi probes are listed in Suppl. Table 1. To generate the pMT-sfGFP vector, the ORF of super folder (sf) GFP was amplified and cloned into pMT-V5 using *SacII* and *PmeI* restriction sites replacing the V5 tag with sfGFP. The sequence corresponding to the ORFs of CG40441 (dPARP1), CG15925 (dPARP16), CG2864 (PARG), dTank were amplified from a cDNA library made from Drosophila S2 cells and cloned into pMT-sfGFP using *KpnI* and *ApaI* To generate pMT-dPARP1-NLS-mutant-sfGFP, The mutant was amplified using *AgeI* and *PmeI*

The dsRNAs used for RNAi of dPARP16, dPARP1, Sec16 and Karyopherin were amplified using primers harboring T7 promoters in their sequence and used for in vitro transcription using the T7 Megascript Kit (AMBION) to generate the dsRNAs (see Suppl. Table S1)

Immunofluorescence (IF)
Drosophila S2 cells were plated on glass coverslips, treated as described, fixed in 4% PFA in PBS for 20 min and processed for imunofluorescence as previously described (Kondylis and Rabouille, 2003; Zacharogianni and Rabouille, 2013). Samples were viewed under a Leica SPE confocal microscope using a 63x oil lens and 2-4x zoom. 14 to 20 planes were projected to capture the whole cell that is displayed unless indicated otherwise.

Immuno-electron microscopy (IEM)
IEM was performed as described previously (Kondylis et al., 2007; van Donselaar et al., 2007).

3 Aminobenzamide and Leptomycin B treatments
3-Aminobenzamide and Leptomycin B treatments were performed using S2 cells incubated in Schneider's and KRB at a concentration of 2 mM and 20 nM respectively for 3 h.

Quantification and statistics
2-5 biological replicates were performed per experiment. For IF of depleted or treated cells, at least four fields per experiment were analyzed comprising at least 50 cells. For transfected cells, at least 30 cells were analyzed. Results are expressed as standard deviations.

Acknowledgements

We thank the Rabouille's group lab members. Financial support for this paper is provided by the Hubrecht Institute of the KNAW and grant from NWO to CR (822-020-016). We thank Anko de Graaff and the Hubrecht imaging center for supporting the imaging.

Supplemental figures

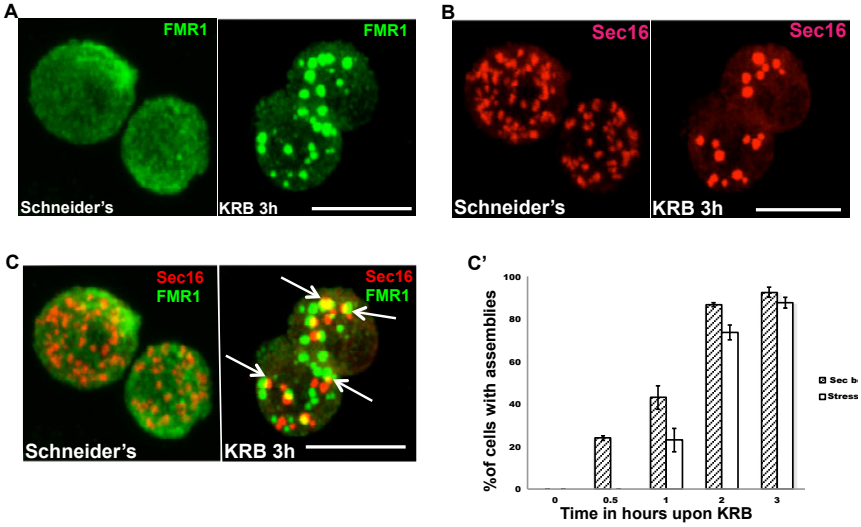

Suppl. Figure 1: Amino-acid starvation leads to stress granules formation. A: Immuno-fluorescence (IF) visualization of endogenous Fmr1 in cells incubated in Schneider's and KRB for 3 hours. Stress granules are formed upon KRB treatment. **B**: (IF) visualization of endogenous Sec16 in cells incubated in Schneider's and KRB for 3 hours. Sec bodies are formed upon KRB treatment. **C**: (IF) visualization of endogenous Fmr1 and Sec 16 in cells incubated in Schneider's and KRB for 3 hours. Note that stress granules and Sec bodies are formed upon KRB treatment. **C'**: Kinetics of stress granule and sec bodies formation) in S2 cells incubated in KRB over indicated time (up to 3 h) expressed as the percentage of cells exhibiting Sec bodies and stress granules. Scale bars: 10 μm, error bars: SEM.

Suppl. Table S1:

Primers used for cloning and RNAi	
sfGFP-F	ggccgcggatggtgagcaagggcgagga
sfGFP-R	gggtttaaacttacttgtacagctcgtccatg
dARTD1/PARP1-F	cagtggtaccatggatattgaattaccttatcttgctgagtatgc
dARTD1/PARP1-R	cagtgggccctcataagaatacttgaattccatacgaaacaaatattgaatatt
ARTD5-6/Tankyrase-F	gtcaggtaccatggccaacagcagccgaagtcg
ARTD5-6/Tankyrase-R	gtcagggccctctcttgtatcctccgttcc
ARTD15/PARP16-F	gtcaggtaccatgactctgctttcgggcgccaac
ARTD15/PARP16-R	gtcagggccctccaaaatacctcgcttgaatacgtagaatacgtagaagcc
dPARG-F	gatatcgcaggttagctccagagcctttccattgtccagggaattttg
dPARG-R	gtcagggccctcggatatggccttcttgtggtatctttcc
dARTD1/PARP1-RNAi-F	ctaatacgactcactatagggcgaaggaaattaacggatcttgtgga
dARTD1/PARP1-RNAi-R	ctaatacgactcactatagggcgaagattttattggtggtatggcg
ARTD5-6/Tankyrase-RNAi-F	taatacgactcactatagggcgagctgaggtccaccacaggcattg
ARTD5-6/Tankyrase-RNAi-R	taatacgactcactatagggcgatcttgtatcctccgttccactactgc
ARTD15/PARP16-RNAi-F	taatacgactcactatagggcgaatgactctgctttcgggcgccaac
ARTD15/PARP16-RNAi-R	taatacgactcactatagggcgacaaaatacctcgcttgaatacgtagaagcc
dPARG-RNAi-F	gcgcccggcgatatccatgcccaag
dPARG-RNAi-R	gtcaccgcggctgctggggtacaaagtaaccgc

References

Aguilera-Gomez, A., van Oorschot, M.M., Veenendaal, T., Rabouille, C., 2016. In vivo vizualisation of mono-ADP-ribosylation by dPARP16 upon amino-acid starvation. Elife 5.

Anderson, P., Kedersha, N., 2002. Stressful initiations. J Cell Sci 115, 3227-3234.

Anderson, P., Kedersha, N., 2009. Stress granules. Curr Biol 19, R397-398.

Aredia, F., Scovassi, A.I., 2014. Poly(ADP-ribose): a signaling molecule in different paradigms of cell death. Biochem Pharmacol 92, 157-163.

Bhattacharyya, S.N., Habermacher, R., Martine, U., Closs, E.I., Filipowicz, W., 2006. Relief of microRNA-mediated translational repression in human cells subjected to stress. Cell 125, 1111-1124.

Buchan, J.R., Kolaitis, R.M., Taylor, J.P., Parker, R., 2013. Eukaryotic stress granules are cleared by autophagy and Cdc48/VCP function. Cell 153, 1461-1474.

Buchan, J.R., Parker, R., 2009. Eukaryotic stress granules: the ins and outs of translation. Mol Cell 36, 932-941.

Chung, K.M., Cha, S.S., Jang, S.K., 2008. A novel function of karyopherin beta3 associated with apolipoprotein A-I secretion. Mol Cells 26, 291-298.

Connerly, P.L., Esaki, M., Montegna, E.A., Strongin, D.E., Levi, S., et al., 2005. Sec16 is a determinant of transitional ER organization. Curr Biol 15, 1439-1447.

Conti, E., Izaurralde, E., 2001. Nucleocytoplasmic transport enters the atomic age. Curr Opin Cell Biol 13, 310-319.

Daniels, C.M., Ong, S.E., Leung, A.K., 2015. The Promise of Proteomics for the Study of ADP-Ribosylation. Mol Cell 58, 911-924.

Deane, R., Schafer, W., Zimmermann, H.P., Mueller, L., Gorlich, D., et al., 1997. Ran-binding protein 5 (RanBP5) is related to the nuclear transport factor importin-beta but interacts differently with RanBP1. Mol Cell Biol 17, 5087-5096.

Deng, T., Engelhardt, O.G., Thomas, B., Akoulitchev, A.V., Brownlee, G.G., et al., 2006. Role of ran binding protein 5 in nuclear import and assembly of the influenza virus RNA polymerase complex. J Virol 80, 11911-11919.

Di Paola, S., Micaroni, M., Di Tullio, G., Buccione, R., Di Girolamo, M., 2012. PARP16/ARTD15 is a novel endoplasmic-reticulum-associated mono-ADP-ribosyltransferase that interacts with, and modifies karyopherin-ss1. PLoS One 7, e37352.

Dynes, J.L., Xu, S., Bothner, S., Lahti, J.M., Hori, R.T., 2004. The carboxyl-terminus directs TAF(I)48 to the nucleus and nucleolus and associates with multiple nuclear import receptors. J Biochem 135, 429-438.

Feijs, K.L., Forst, A.H., Verheugd, P., Luscher, B., 2013. Macrodomain-containing proteins: regulating new intracellular functions of mono(ADP-ribosyl)ation. Nat Rev Mol Cell Biol 14, 443-451.

Fried, H., Kutay, U., 2003. Nucleocytoplasmic transport: taking an inventory. Cell Mol Life Sci 60, 1659-1688.

Gilks, N., Kedersha, N., Ayodele, M., Shen, L., Stoecklin, G., et al., 2004. Stress granule assembly is mediated by prion-like aggregation of TIA-1. Mol Biol Cell 15, 5383-5398.

Gorlich, D., Kostka, S., Kraft, R., Dingwall, C., Laskey, R.A., et al., 1995. Two different subunits of importin cooperate to recognize nuclear localization signals and bind them to the nuclear envelope. Curr Biol 5, 383-392.

Hassa, P.O., Hottiger, M.O., 2008. The diverse biological roles of mammalian PARPS, a small but powerful family of poly-ADP-ribose polymerases. Front Biosci 13, 3046-3082.

Hatakeyama, K., Nemoto, Y., Ueda, K., Hayaishi, O., 1986. Purification and characterization of poly(ADP-ribose) glycohydrolase. Different modes of action on large and small poly(ADP-ribose). J Biol Chem 261, 14902-14911.

Hottiger, M.O., Hassa, P.O., Luscher, B., Schuler, H., Koch-Nolte, F., 2010. Toward a unified nomenclature for mammalian ADP-ribosyltransferases. Trends Biochem Sci 35, 208-219.

Hyman, A.A., Weber, C.A., Julicher, F., 2014. Liquid-liquid phase separation in biology. Annu Rev Cell Dev Biol 30, 39-58.

Ivan, V., de Voer, G., Xanthakis, D., Spoorendonk, K.M., Kondylis, V., et al., 2008. Drosophila Sec16 mediates the biogenesis of tER sites upstream of Sar1 through an arginine-rich motif. Mol Biol Cell 19, 4352-4365.

Jain, S., Wheeler, J.R., Walters, R.W., Agrawal, A., Barsic, A., et al., 2016. ATPase-Modulated Stress Granules Contain a Diverse Proteome and Substructure. Cell 164, 487-498.

Jakel, S., Gorlich, D., 1998. Importin beta, transportin, RanBP5 and RanBP7 mediate nuclear import of ribosomal proteins in mammalian cells. EMBO J 17, 4491-4502.

Jevtov, I., Zacharogianni, M., van Oorschot, M.M., van Zadelhoff, G., Aguilera-Gomez, A., et al., 2015. TORC2 mediates the heat stress response in Drosophila by promoting the formation of stress granules. J Cell Sci 128, 2497-2508.

Jwa, M., Chang, P., 2012. PARP16 is a tail-anchored endoplasmic reticulum protein required for the PERK- and IRE1alpha-mediated unfolded protein response. Nat Cell Biol 14, 1223-1230.

Kedersha, N., Ivanov, P., Anderson, P., 2013. Stress granules and cell signaling: more than just a passing phase? Trends Biochem Sci 38, 494-506.

Kedersha, N., Panas, M.D., Achorn, C.A., Lyons, S., Tisdale, S., et al., 2016. G3BP-Caprin1-USP10 complexes mediate stress granule condensation and associate with 40S subunits. J Cell Biol 212, 845-860.

Kedersha, N.L., Gupta, M., Li, W., Miller, I., Anderson, P., 1999. RNA-binding proteins TIA-1 and TIAR link the phosphorylation of eIF-2 alpha to the assembly of mammalian stress granules. J Cell Biol 147, 1431-1442.

Kondylis, V., Rabouille, C., 2003. A novel role for dp115 in the organization of tER sites in Drosophila. J Cell Biol 162, 185-198.

Kondylis, V., van Nispen tot Pannerden, H.E., Herpers, B., Friggi-Grelin, F., Rabouille, C., 2007. The golgi

comprises a paired stack that is separated at G2 by modulation of the actin cytoskeleton through Abi and Scar/WAVE. Dev Cell 12, 901-915.
Krishnakumar, R., Kraus, W.L., 2010. The PARP side of the nucleus: molecular actions, physiological outcomes, and clinical targets. Mol Cell 39, 8-24.
Leung, A., Todorova, T., Ando, Y., Chang, P., 2012. Poly(ADP-ribose) regulates post-transcriptional gene regulation in the cytoplasm. RNA Biol 9, 542-548.
Leung, A.K., 2014. Poly(ADP-ribose): an organizer of cellular architecture. J Cell Biol 205, 613-619.
Leung, A.K., Vyas, S., Rood, J.E., Bhutkar, A., Sharp, P.A., et al., 2011. Poly(ADP-ribose) regulates stress responses and microRNA activity in the cytoplasm. Mol Cell 42, 489-499.
Li, Y.R., King, O.D., Shorter, J., Gitler, A.D., 2013. Stress granules as crucibles of ALS pathogenesis. J Cell Biol 201, 361-372.
Moss, J., Zolkiewska, A., Okazaki, I., 1997. ADP-ribosylarginine hydrolases and ADP-ribosyltransferases. Partners in ADP-ribosylation cycles. Adv Exp Med Biol 419, 25-33.
Parker, R., Sheth, U., 2007. P bodies and the control of mRNA translation and degradation. Mol Cell 25, 635-646.
Protter, D.S., Parker, R., 2016. Principles and Properties of Stress Granules. Trends Cell Biol 26, 668-679.
Ramaswami, M., Taylor, J.P., Parker, R., 2013. Altered ribostasis: RNA-protein granules in degenerative disorders. Cell 154, 727-736.
Schreiber, V., Dantzer, F., Ame, J.C., de Murcia, G., 2006. Poly(ADP-ribose): novel functions for an old molecule. Nat Rev Mol Cell Biol 7, 517-528.
Seedorf, M., Damelin, M., Kahana, J., Taura, T., Silver, P.A., 1999. Interactions between a nuclear transporter and a subset of nuclear pore complex proteins depend on Ran GTPase. Mol Cell Biol 19, 1547-1557.
Seedorf, M., Silver, P.A., 1997. Importin/karyopherin protein family members required for mRNA export from the nucleus. Proc Natl Acad Sci U S A 94, 8590-8595.
Slade, D., Dunstan, M.S., Barkauskaite, E., Weston, R., Lafite, P., et al., 2011. The structure and catalytic mechanism of a poly(ADP-ribose) glycohydrolase. Nature 477, 616-620.
Tourriere, H., Chebli, K., Zekri, L., Courselaud, B., Blanchard, J.M., et al., 2003. The RasGAP-associated endoribonuclease G3BP assembles stress granules. J Cell Biol 160, 823-831.
van Donselaar, E., Posthuma, G., Zeuschner, D., Humbel, B.M., Slot, J.W., 2007. Immunogold labeling of cryosections from high-pressure frozen cells. Traffic 8, 471-485.
Vyas, S., Matic, I., Uchima, L., Rood, J., Zaja, R., et al., 2014. Family-wide analysis of poly(ADP-ribose) polymerase activity. Nat Commun 5, 4426.
Watson, P., Forster, R., Palmer, K.J., Pepperkok, R., Stephens, D.J., 2005. Coupling of ER exit to microtubules through direct interaction of COPII with dynactin. Nat Cell Biol 7, 48-55.
Wheeler, J.R., Matheny, T., Jain, S., Abrisch, R., Parker, R., 2016. Distinct stages in stress granule assembly and disassembly. Elife 5.
Zacharogianni, M., Aguilera Gomez, A., Veenendaal, T., Smout, J., Rabouille, C., 2014. A stress assembly that confers cell viability by preserving ERES components during amino-acid starvation. Elife 3.
Zacharogianni, M., Rabouille, C., 2013. Trafficking along the secretory pathway in Drosophila cell line and tissues: a light and electron microscopy approach. Methods Cell Biol 118, 35-49.

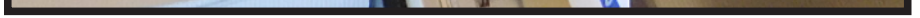

Chapter 5

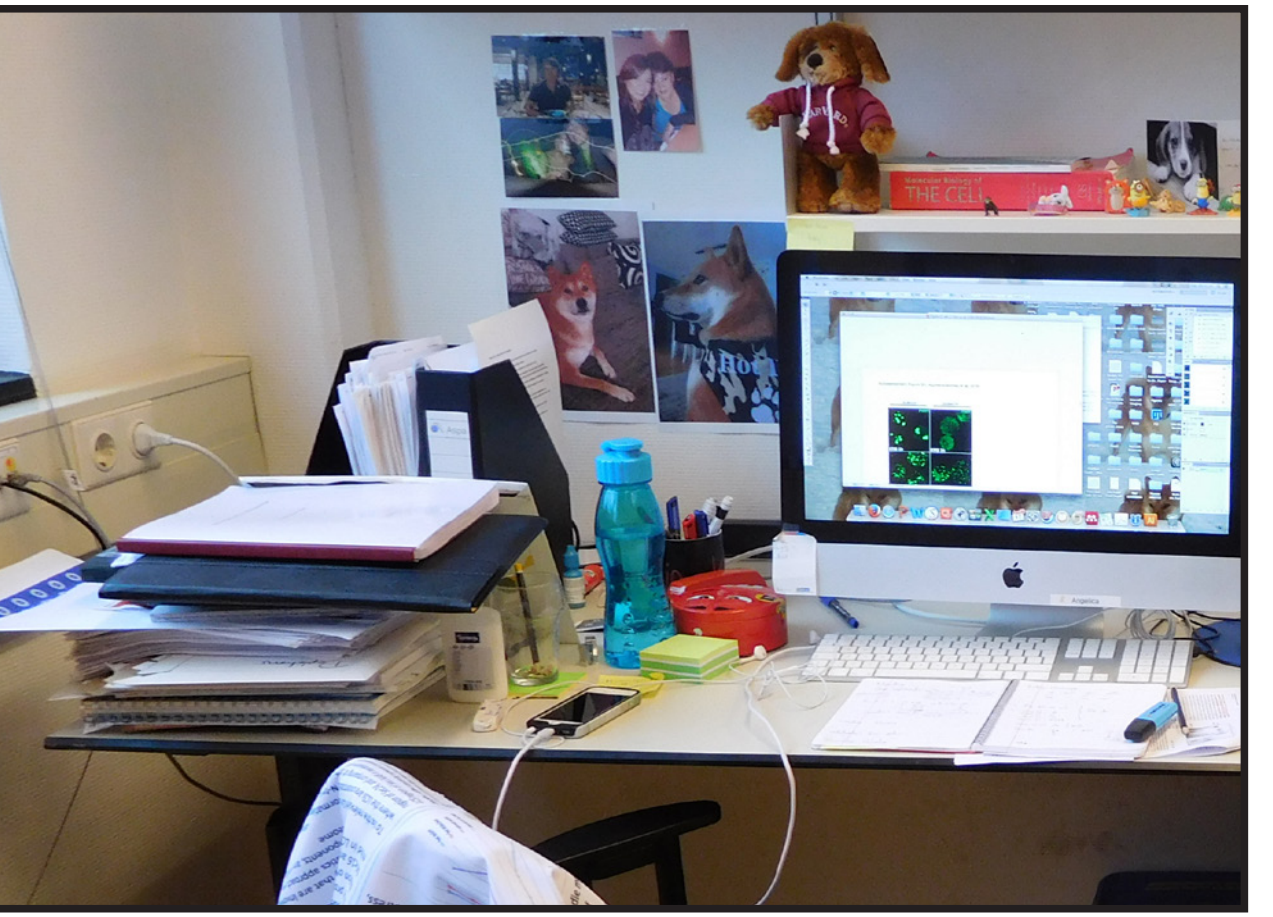

Phospho-Rasputin stabilization by Sec16 is required for stress granules formation upon amino-acid starvation

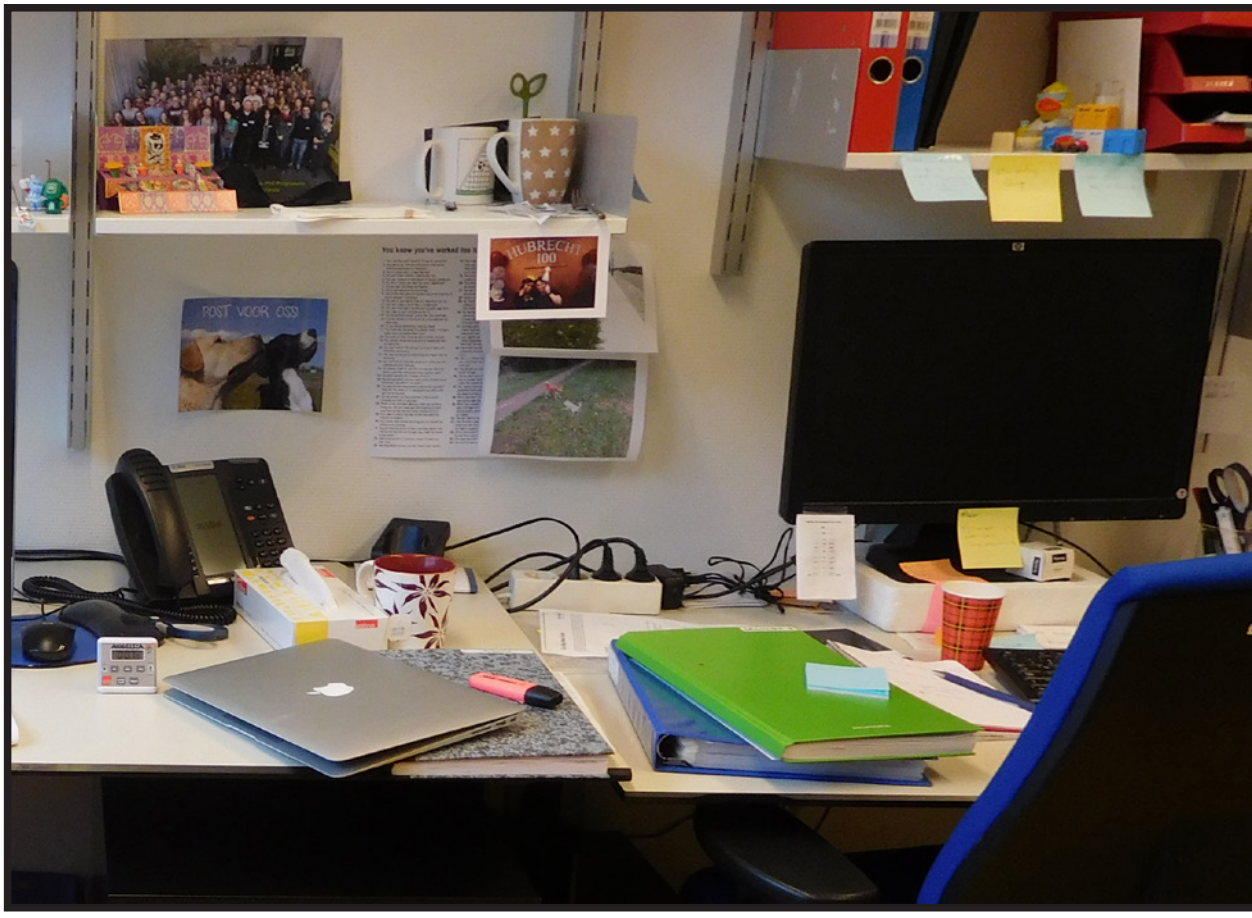

Angelica Aguilera-Gomez, Margarita Zacharogianni, Marinke M. van Oorschot, Heide Genau, Tineke Veenendaal, Kristina S. Sinsimer, Elisabeth A. Gavis, Christian Behrends and Catherine Rabouille (2016)
Submitted to Cell reports

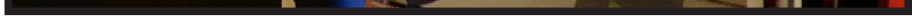

Phospho-Rasputin stabilization by Sec16 is required for stress granules formation upon amino-acid starvation

Abstract

Most cellular stresses induce protein translation inhibition and stress granules formation. Here, using Drosophila S2 cells, we investigate the role of G3BP/Rasputin in this process. In contrast to arsenite treatment where dephosphorylated-Ser142 Rasputin is recruited to stress granules, we find that upon amino-acid starvation, only the phosphorylated-Ser142 form is recruited. Furthermore, we identify the ERES component Sec16 as a Rasputin interactor and stabilizer. Sec16 depletion results in Rasputin degradation and inhibition of stress granule formation. However, in the absence of Sec16, pharmacological stabilization of Rasputin is not enough to rescue stress granules assembly. This is most likely because Sec16 specifically interacts with phosphorylated-Ser142-Rasputin, the form required for stress granule formation upon amino-acid starvation. Taken together, we demonstrate that stress granule formation is fine-tuned by specific signaling clues that are unique to each stress. These results also expand the role of Sec16 as a stress response protein.

Introduction

Stress granules are well-studied cytoplasmic reversible, pro-survival stress assemblies where untranslated free RNAs (resulting from protein translation inhibition) are stored and protected together with RNA binding proteins, translation initiation factors and the 40S ribosomal subunits (Anderson and Kedersha, 2008; Protter and Parker, 2016). Stress granule formation has been best investigated in mammalian cells upon different types of stress, among which heat and oxidative stress (Anderson and Kedersha, 2002). This has lead to the identification of a number of factors that are essential for their formation, such as the case for Tia-1 (Gilks et al., 2004; Kedersha et al., 1999) and G3BP1/2 (referred to as G3BP thereafter, Ras-GAP SH3 domain binding protein) (Tourriere et al., 2003).

G3BP was first identified in human cells through co-immunoprecipitation with the SH3 domain of RasGAP. However, it has a RNA recognition motif (RRM domain) towards the C-terminus, suggesting that it binds mRNAs. In growing cells, G3BP is normally cytoplasmic, but after stress induction (especially stress leading to eIF2α phosphorylation (McEwen et al., 2005), it is not only readily recruited to stress granules but is also necessary for their formation (Kedersha et al., 2016; Tourriere et al., 2003). Furthermore, it drives stress granule formation when overexpressed in the absence of stress (Tourriere et al., 2003). Importantly, G3BP is phosphorylated on Serine 149 during basal conditions but needs to be dephosphorylated to drive stress granule assembly triggered by arsenite treatment (Kedersha et al., 2016; Tourriere

et al., 2003). Taken together, G3BP is critical for stress granule formation when its Serine 149 is dephosphorylated and through the binding to Caprin and the 40S ribosomal subunit. Conversely, it is inhibited when binding to peptidase USP10 (Kedersha et al., 2016).

G3BP also appears to have an important role in disease. First, some viruses can exploit G3BP to assemble replication complexes (Kim et al., 2016) and regulate PKR activation (Reineke et al., 2015). Other viral infections can lead to its cleavage, making it unable to form cyto-protective stress granules (Dougherty et al., 2015) while few viral proteins can bind G3BP and inhibit it (Panas et al., 2015) (reviewed in (Tsai and Lloyd, 2014)). However, G3BP also appears to slow down HIV replication by leading to the sequestration of viral mRNA (Cobos Jimenez et al., 2015). Second, G3BP is overexpressed in gastric cancer (Min et al., 2015) bone and lung sarcomas (Somasekharan et al., 2015) where it is considered as a marker for poor survival. Strikingly, down regulation of G3BP in cells and *in vivo* reduces stress granule formation as expected but also tumor invasion and metastasis, showing a clear role for stress granule formation in cancer. Last, G3BP is a target of TDP-43 that is often mutated, misplace and mis-accumulated in ALS (Aulas et al., 2012). Affected stress granule dynamics is a common feature of this disease (Li et al., 2013). Stress granules are also formed in Drosophila, for instance upon heat stress and arsenite (Farny et al., 2009) and upon amino-acid starvation of Drosophila S2 cells (Zacharogianni et al., 2014), but the mechanism for their formation is not completely understood. Interestingly, amino-acid starvation leads to the formation of another recently described stress assembly, the Sec body that stores and protects most of the COPII subunits and the ERES component Sec16 (Zacharogianni et al., 2014).

Sec16 is a conserved peripheral membrane protein that localizes and concentrates to ERES (Connerly et al., 2005) (Watson et al., 2006) via a domain that has been mapped to the conserved central domain coupled to a small arginine rich region upstream (Hughes et al., 2009; Ivan et al., 2008). It binds nearly all COPII subunits and controls at least two aspects of COPII coated vesicle dynamics (Sprangers and Rabouille, 2015). Sec16 is essential for ER to Golgi transport *in vivo*, especially in Drosophila where absence of Sec16 results in a severe inhibition of anterograde transport (Ivan et al., 2008). Sec16 also responds to nutrient stress. We have recently shown that Sec16 is a key factor driving Sec bodies formation upon amino-acid starvation that activates the ER localized dPARP16. In turn, it mono-ADP-ribosylates Sec16 on a conserved sequence close to its C-terminus (Aguilera-Gomez et al., 2016) and Sec16 modification by dPARP16 is enough to elicit Sec body formation. This demonstrates that Sec16 is a stress response protein that plays an important role in the response to amino-acid starvation.

Here, we show that the phosphorylation state of the G3BP Drosophila ortholog Rasputin is differentially required for the formation of stress granules upon arsenite and amino-acid starvation. Whereas stress granule formation upon arsenite treatment

requires the non-phosphorylated form of Rasputin, amino-acid starvation requires the phosphorylated form. Furthermore, we show that Sec16 that specifically binds to phosphorylated Rasputin mediates this differential requirement.

All together, these results provide a novel link between the protein transport from the ER and protein translation. It also explains the specific requirement of Sec16 for stress granule formation upon amino acid starvation but no other stress. Furthermore, it enlarges the scope of Sec16 function at the ER by unraveling new functions as a stress response protein specifically upon amino-acid starvation.

Results

Amino-acid starvation induces stress granule formation.

Amino-acid starvation induces the inhibition of protein translation (**Figure 1A**), the phosphorylation of eIF2α (**Figure 1B**) as strongly as arsenite treatment, and the subsequent formation of stress granules marked by three RNA binding proteins, FMR1, Caprin and Rasputin (**Figure 1C**) as well as the initiation factor elF4E (**Figure 1D**). We also found that stress granules that form upon this stress contain P-bodies components, such as Tral (**Figure 1E)** and begin to form after 1 hour of starvation with their number reaching their maximum after 3 hours (**Figure 1F**).

Rasputin Ser142E, not Ser142A is required for SG formation upon AA starvation.

As mentioned in the introduction, Rasputin is the Drosophila ortholog of G3BP and their molecular organization is largely conserved (Suppl. Fig. S1). They show high sequence similarity in the NFT2 domain, the RNA binding domain (RRM), and G3BP Ser149 is conserved in Rasputin (Ser142). Furthermore, both proteins harbor a proline-rich intrinsically disordered domain and a glycine rich-domain at the C-terminus (Kedersha et al., 2016). Interestingly, as G3BP, Rasputin overexpression in mammalian cells leads to the formation of stress granules in the absence of stress (Tourriere et al., 2003).

To test the role of Rasputin in stress granule formation in amino-acid starved Drosophila cells, we first depleted it. In the absence of Rasputin, stress granules (marked by FMR1) do not form (**Figure 2A, A'**). We then investigated whether Rasputin overexpression drives stress granule formation in S2 cells in the absence of stress, but this does not appear to be the case (**Figure 2B, B'**). Taken together, this suggests that Rasputin is necessary, but not sufficient, to drive the assembly of stress granule. Of note, cells overexpressing Rasputin-V5 upon starvation display stress granules that are 1.5 fold less numerous and 1.3 ± 0.2 fold larger that in non-transfected cells. This suggests that the Rasputin overexpression enhances stress granules formation and/or dynamics.

As hinted in the introduction, Ser149A but not Ser149E G3BP rescues arsenate

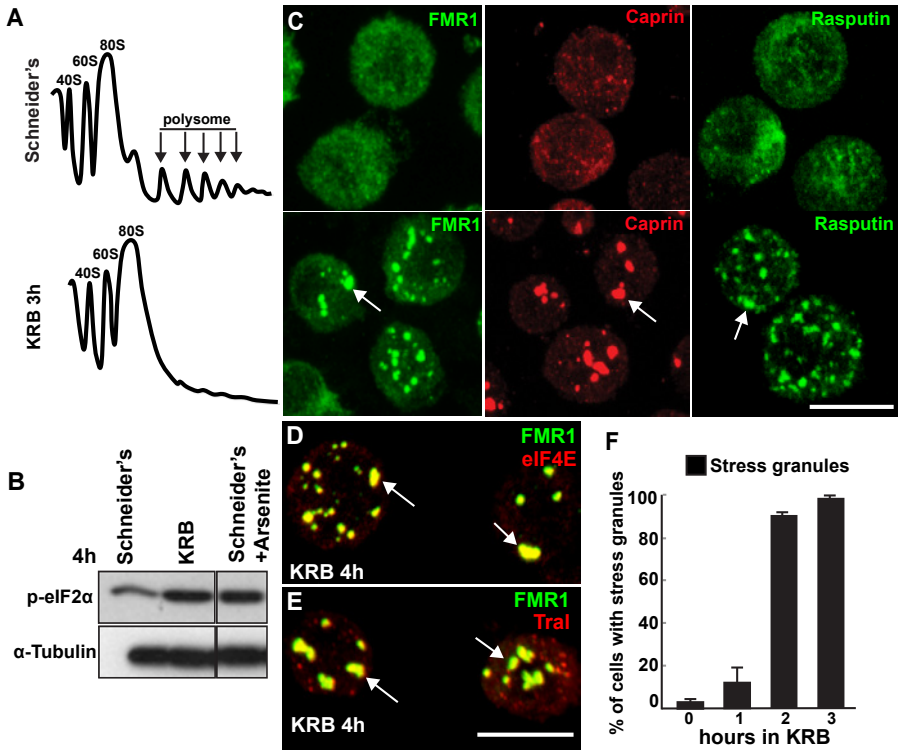

Figure 1: Amino-acid starvation leads to the formation of stress granules. A: Polysome profiles of S2 cells grown in Schneider's and incubated 4h in KRB. **B**: Western blot visualization of eIF2alpha-phosphorylation upon growing, KRB and arsenite treated cells. Note that eIF2alpha is as strongly phosphorylated upon both KRB as upon arsenite treatments. **C**: Immuno-fluorescence (IF) visualization of endogenous FMR1, caprin and Rasputin in cells incubated in Schneider's and KRB for 3 h. Note that stress granules form (arrows) **D, E**: IF visualization of FMR1 and the translation initiation marker eIF4E (**D**) and the P-body marker Tral (E). Note that they co-localize in stress granules upon amino-acid starvation (arrows). **F**: Kinetics of stress granule formation (marked by FMR1) in S2 cells incubated in KRB over indicated time (up to 3 h) expressed as the percentage of cells exhibiting. Scale bars: 10 μm Error bar: SEM.

triggered stress granule formation in G3BP depleted **(Tourriere et al., 2003)** and mutant **(Kedersha et al., 2016)** mammalian cells. This shows that that upon arsenite treatment, the stress granule formation competent form of G3BP is the dephosphorylated form.

To confirm that Rasputin behaves similarly in S2 cells, we generated phospho-mimetic S142E-V5 and non-phosphorylatable S142A-V5 Rasputin mutants and tested them for their ability to be incorporated to stress granules upon arsenite treatment. In agreement with the mammalian results, only Ser142A Rasputin is incorporated in stress granules, whereas Ser142E is completed excluded and remains cytoplasmic **(Figure 2C, C').** However, in striking contrast, upon amino-acid starvation, Ser142A remains cytosolic, whereas Ser142E Rasputin is readily incorporated to stress granules as efficiently as the WT Rasputin (**Figure 2D, D'**).

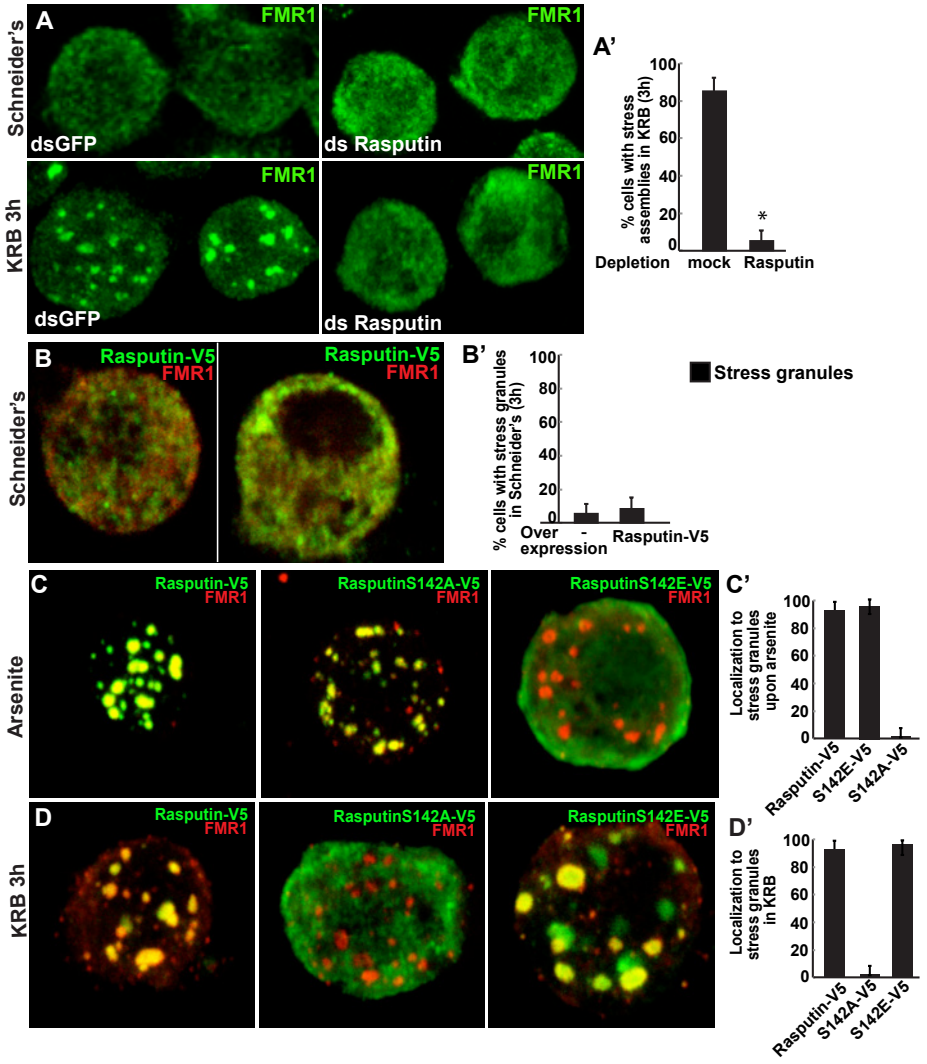

Figure 2: Rin Ser142E, not Ser142A is incorporated in stress granules upon AA starvation. A, A': IF visualization of FMR1 in mock (ds GFP)- and Rasputin (ds Rasputin) depleted cells (A). Note that in Rasputin depleted cells stress granules do not form. Quantified in A'. **B, B'**: IF visualization of cells expressing Rasputin-V5 and endogenous FMR1 in growing cells (B). Note that Rasputin-V5 overexpression does not induce stress granule formation. Quantified in B'. **C, C'**: IF visualization of cells expressing Rasputin-V5, non-phosphorylatable (Ser142A) Rin-V5 and phospho-mimetic (Ser142E) Rin-V5 upon arsenite treatment (C). Note that Ser142A Rasputin-V5 is steadily recruited into stress granule, while Ser142E mutant is not. Quantified in C'. **D, D'**: IF visualization of cells expressing wildtype Rasputin-V5, non-phosphorylatable (Ser142A) Rasputin-V5 and phospho-mimetic (Ser142E) Rasputin-V5 upon amino acid starvation (D). Note that Ser142E Rasputin-V5 is steadily recruited into stress granule, while Ser142A is not. Quantified in D'. Scale bars: 10 μm. Error bar: SD.

Furthermore, it leads to an increase in the size of the stress granules larger than WT Rasputin (2.7 ± 0.3 fold versus 1.3), suggesting that phosphorylated Rasputin is the competent form for stress granule dynamics upon amino-acid starvation.

This suggests that the formation of stress granules upon both arsenite and amino-acid starvation is modulated by different but specific signaling clues. This prompted us to look for factors that are required for stress granule formation specifically upon amino-acid starvation but not upon other stress.

Sec16 interacts with Rin.

Interestingly, in addition to stress granule formation, amino-acid starvation also triggers Sec body formation (Zacharogianni et al., 2014) in the same time frame. Importantly, Sec bodies only form upon amino-acid starvation, not arsenite treatment. Furthermore, although stress granules and Sec bodies are distinct structures, they tend to form in close proximity to one another (**Figure 3A-A")**. In this respect, using immuno-electron microscopy, we found a small pool of Sec16 localized inside stress granules (**asterisk in Figure 3B, B', red circles),** although**,** as published before, its bulk is found in Sec bodies **(Figure 3B,** arrow**)**(Zacharogianni et al., 2014). This led us to investigate whether Sec16 has a role to play in stress granule formation upon amino-acid starvation.

To begin to investigate this, we performed a mass spectrometry analysis of proteins co-immunoprecipitated with endogenous Sec16 from cells upon amino-acid starvation with growing cells as control. 122 candidate interactors passing the selection criteria (see Materials and methods; Suppl Table S1,) were pulled down, 62% of which from both growing and starved cells. They are grouped in 12 GO terms and one of the largest is "Membrane traffic" as expected with interactors such as Sec23. Sec16 also interacts with many other factors that may be functional for stress granule formation, among which RNA binding proteins and Rasputin in particular (Suppl Table S1, **Figure 3C)**.

We confirmed Sec16/Rasputin interaction by western blot (**Figure 3D**) and showed the specificity of this interaction, as Sec16 does not interact with Caprin and FMR1 (Suppl. Fig. S2A**)**. We also used an anchor-away strategy whereby Sec16 tagged with the Ras CAAX motif results into its anchoring to the plasma membrane (Aguilera-Gomez et al., 2016). Using full length Sec16-CAAX, we demonstrated that endogenous Rasputin is very efficiently recruited to the plasma membrane (**Figure 3E, H).** This interaction is also visible in physiological conditions where Rasputin is observed in very close proximity to Sec16 especially at earlier time point of amino-acid starvation **(Suppl. Fig. S3A, B)**.

The C-terminus part of Sec16 has been implicated in stress response (Zacharogianni et al., 2014; Zacharogianni et al., 2011) (Aguilera-Gomez et al., 2016), and we tested whether it is also required for Rasputin binding. To do this, we expressed Sec16-GFP-CAAX lacking its C-terminus but Rasputin is still recruited to the plasma

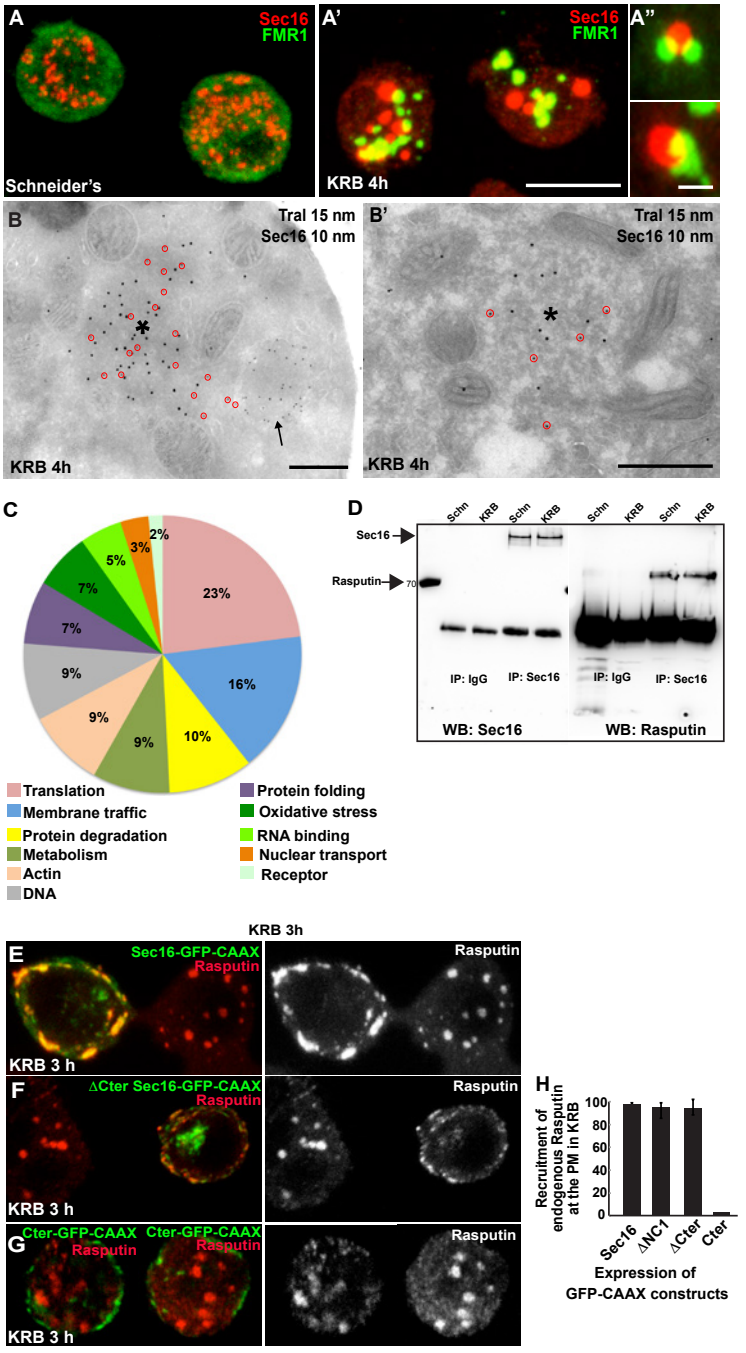

Figure 3: Sec16 interacts with Rasputin. **A-A"**: IF visualization of FMR1 (green) and Sec16 (red) in growing conditions (A) and upon amino-acid starvation (A'). Note that Sec bodies (marked by Sec16) and stress granules form in close proximity to one another (A"). **B, B'**: Immuno-EM localization of Sec16 (10 nm gold) and Tral (15 nm gold) in ultrathin sections of S2 cells incubated in KRB for 4h. Note that

Sec16 is mostly localized to Sec bodies (arrow) but also populates (red circles) stress granules (asterisks, marked by Tral). Note the mitochondria surrounding stress granules. **C**: Pie chart representation of the gene ontology grouping of the 122 interactors of endogenous Sec16 (see Materials and Methods and Suppl. Table S1). **D:** Western blot visualization of Rasputin following the immunoprecipitation of endogenous Sec16 from growing (Schneider's) and amino-acid starved (KRB 3 h) cells. Rasputin co-immunoprecipitates with Sec16 both in growing and amino-acid starvation conditions. **E-H**: Co-visualization of full length Sec16-GFP-CAAX (E), ΔCter Sec16-GFP-CAAX (F) and Cter-GFP-CAAX (G) and endogenous Rasputin (red) upon amino-acid starvation (KRB). Note that Sec16-GFP-CAAX and ΔDcter Sec16-GFP-CAAX localizes at the plasma membrane and efficiently recruits Rasputin. Cter-GFP-CAAX also localizes to the plasma membrane but does not recruit Rasputin that forms stress granules in the cytoplasm. Quantified in H. Scale bars: 10 μm. Error bar: SD.

membrane (**Figure 3F, H**). Accordingly, expression the Sec16 Cter-CAAX does not recruit Rasputin (**Figure 3G, H**) and Rasputin is able to form stress granules in the cytoplasm. This suggests that the C-terminal part of Sec16 is not required for Rasputin binding in line with the fact that Rasputin interacts with Sec16 both in growing and starved conditions. The N-ter of Sec16 is also not required for Rasputin binding (Suppl. Figure S2B, **Figure 3H).**

Sec16, but not active secretion, is required for stress granule formation specifically upon AA starvation.

We then examined whether Sec16 could have a role to play in stress granule formation specifically induced by amino-acid starvation. We starved Sec16 depleted cells and found that stress granules form 75% less than in mock depleted cells, as monitored using Rasputin (**Figure 4A**) and FMR1 (**Figure 4C**). Caprin (not shown). elF4E and Tral behave like FMR1 (**Figure 4B**). This indicates that Sec16 is a novel factor required in stress granule formation.

To investigate the specificity of Sec16 upon amino acid starvation, we treated Sec16 depleted cells with arsenite for 3 h and monitored stress granule formation that was found to be as efficient as in mock depleted cells (**Figure 4D, E**). The same was also true for heat stress and ER stress with DTT **(Suppl. Fig. S4A**, **Figure 4E)**. This shows that Sec16 is required for stress granule formation specifically upon amino-acid starvation.

Last, we addressed whether the role of Sec16 in stress granule formation is linked to its role in protein exit from the ER or COPII coated vesicle dynamics. To test this, we inhibit COPII vesicle formation by depleting Sar1, but this does not prevent stress granule formation upon amino-acid starvation **(Suppl. Fig. S4B, Figure 4E)**. Similarly, COPI coated vesicle formation and retrograde transport from the Golgi to the ER are also not required as stress granule formation is insensitive to incubation with BFA **(Suppl. Fig. S4B, Figure 4E)**. Taken together, transport through the early secretory pathway is not required for stress granule formation upon amino-acid starvation and the role for Sec16 in their formation lies somewhere else.

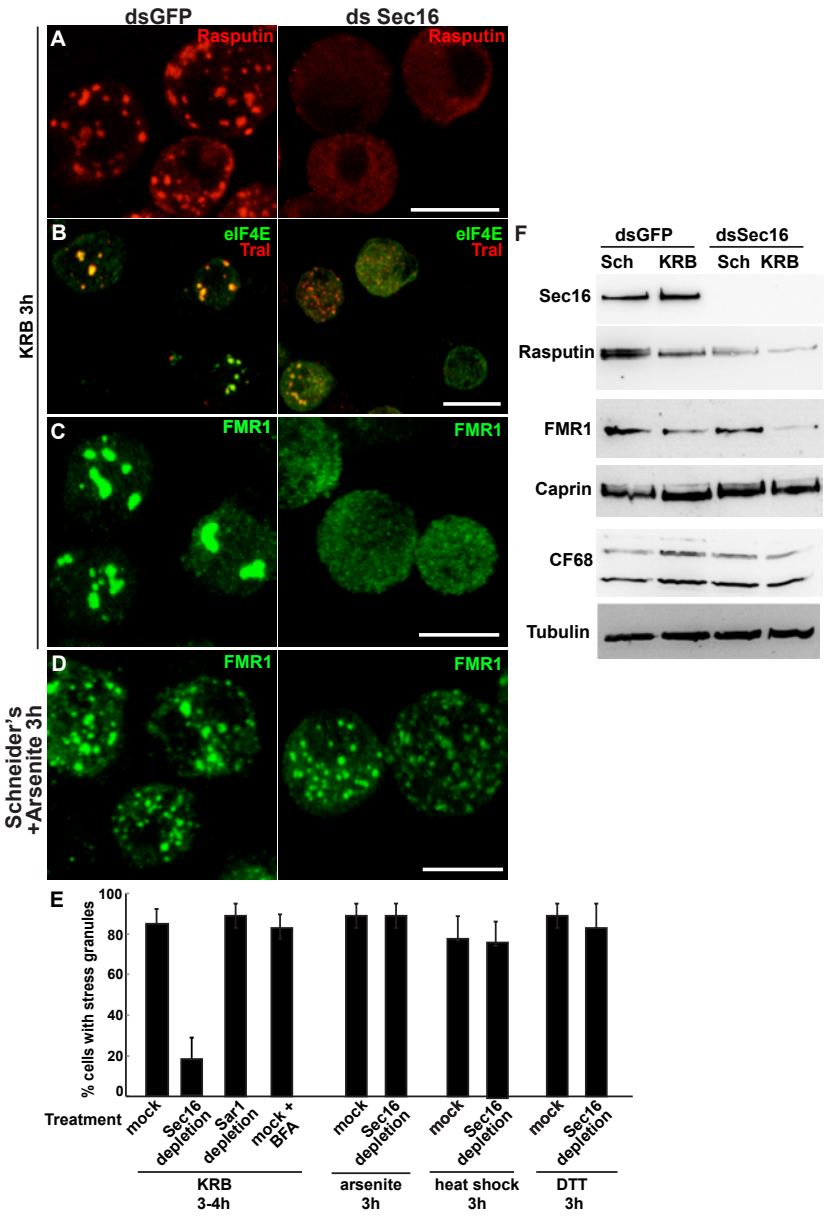

Figure 4: Sec16 is required for stress granule formation specifically upon AA starvation. A-C: IF visualization of endogenous Rasputin (A), Tral and eIF4E (B) and FMR1 (C) in mock (dsGFP) and Sec16 (ds Sec16) depleted cells upon 3 h of incubation in KRB. Note that in the absence of Sec16, stress granules do not form and that Rasputin fluorescence is very weak in Sec16 depleted cells, when compared to the mock depleted. **D**: IF visualization of endogenous FMR1 in mock and Sec16 depleted cells upon arsenite treatment (3 h). Note that stress granules form as efficiently in mock and Sec16 depleted cells. **E**: Quantification of Sec16 depleted cells treated with KRB, arsenite, heat shock and DTT, expressed in percentage of cell with stress granules. **F:** Western blot of Sec16, Rasputin, FMR1, Caprin, CF68 and tubulin in mock and Sec16 depleted cells. Scale bars: 10 μm. Error bars: SEM.

Sec16 is required for Rasputin stability.

We noticed that the fluorescence level of Rasputin in Sec16 depleted cells was very low (**Figure 4A**), and this was confirmed by Western blot (**Figure 4F**). In the absence of Sec16, Rasputin level in amino-acid starved cells is reduced by about 80% when compared to control cells. This seems to be specific because Caprin, as well as another Sec16 interactor CF68, are not affected, whereas FMR1 is partly affected. This result suggests that Sec16 depletion mimics Rasputin depletion, which, we have shown above (**Figure 2A**), results in a strong inhibition of stress granule formation.

There are at least three manners by which Sec16 can contribute to the maintenance of Rasputin level. It could stabilize its mRNA; it could promote its translation; and it could stabilize the Rasputin protein. To test the latter hypothesis, we transfected mock- or Sec16 depleted cells with Rasputin-V5 and treated them with or without the proteasome inhibitor MG132. This allows us to trigger Rasputin acute expression for a short period of time and monitor its level. If the reduced level of Rasputin observed upon Sec 16 depletion is due to protein degradation, addition of MG132 should rescue it.

We first confirmed that Rasputin-V5 level is also very low in Sec16 depleted cells (**Figure 5A and B,** compare lanes 1 and 2). In the presence of MG132, however, Rasputin-V5 level was restored to nearly the level of mock-depleted cells (**Figure 5A, B,** compare lanes 3 and 4). This shows that Sec16 stabilizes Rasputin protein and protects it against degradation through the proteasome. Furthermore, whereas stress granule formation was inhibited in Sec16 depleted starved cells as reported above, MG132 treatment significantly rescued stress granule formation in cells expressing Rasputin-V5 (**Figure 5B, arrow; Figure 5E**) (also positive for FMR1, not shown). This demonstrates that the role of Sec16 is in the stabilization of Rasputin that can then act as a driver for stress granule formation in amino-acid starved cells.

Sec16 interacts specifically with phospho-Rasputin.

However, although the level of endogenous Rasputin was also largely recovered upon MG132 incubation of Sec16 depleted cells **(Figure 5C),** stress granule formation was not rescued (**Figure 5D, arrowhead; Figure 5E**). This suggests that maintaining the level of endogenous Rin is not enough to form stress granules when Sec16 is absent.

As Sec16 is specifically required for stress granule formation upon amino-acid starvation but not upon arsenite (**Figure 4C and D**) and the phosphorylated form of Rasputin is specifically recruited to stress granule upon amino-acid starvation, we reasoned that Sec16 may interact and stabilize with Rasputin phosphorylated on Ser142. To test this, we anchored-away Sec16 to the plasma membrane using a CAAX motif of Ras, and expressed the two Rasputin mutants Ser142A and Ser142E

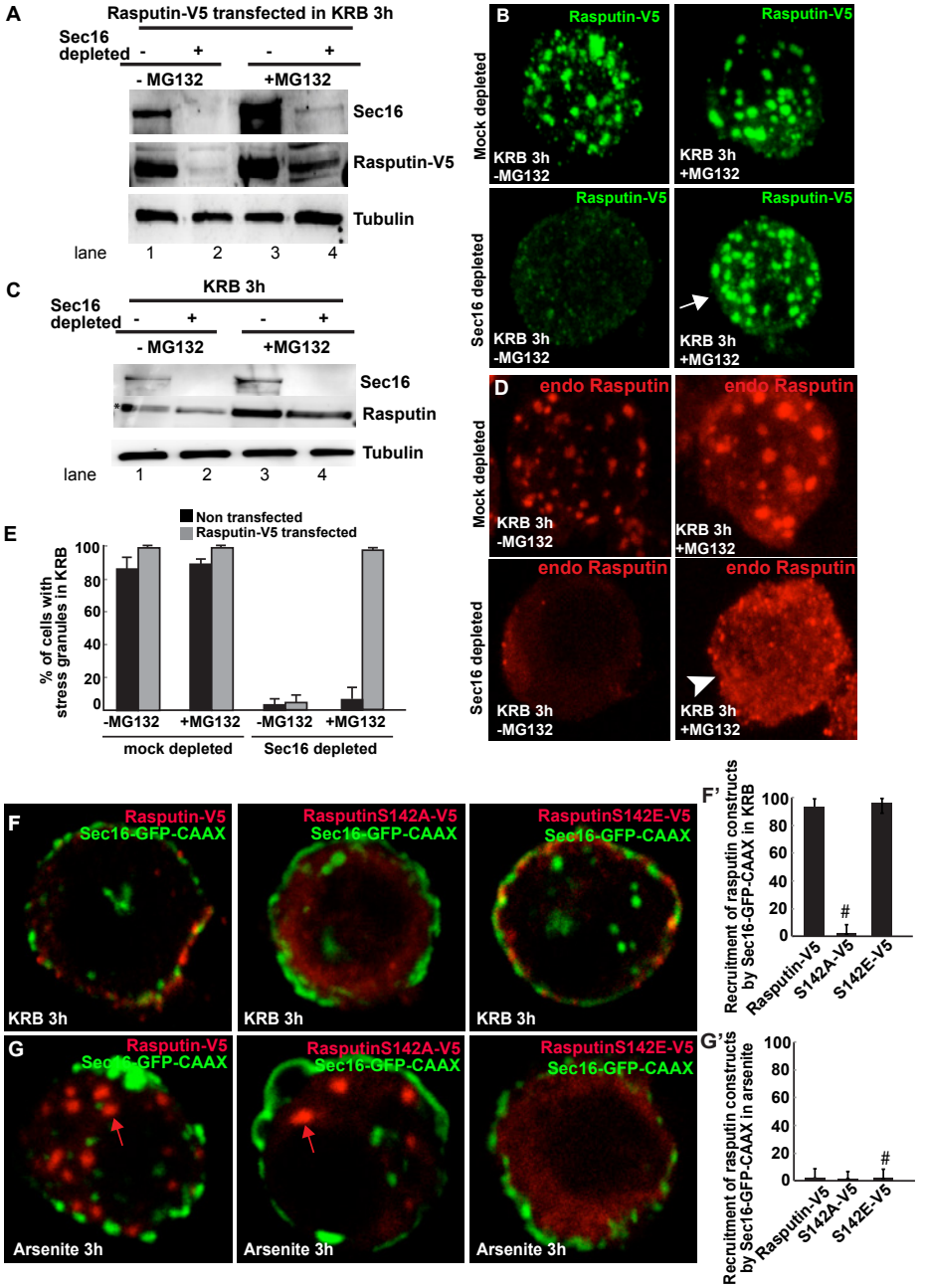

Figure 5: Sec16 prevents Rasputin degradation by the proteasome A: Western blot visualization of Rasputin-V5 (using an anti V5 antibody) transfected in mock- and Sec16 depleted cells incubated in Schneider's and KRB (3 h) supplemented or not by MG132. Note that MG132 incubation largely rescues Rasputin-V5 protein level. **B:** IF visualization of Rasputin-V5 transfected in mock- and Sec16 depleted cells in KRB supplemented or not with MG132. Note that MG132 incubation rescues Rasputin-V5 level and stress granule formation in Sec16 depleted cells. **C**: Western blot visualization

of endogenous Rasputin in mock and Sec16 depleted cells in KRB supplemented or not with MG132. Note that MG132 incubation rescues endogenous Rasputin protein level. **D**: IF visualization of endogenous Rasputin in mock and Sec16 depleted cells in KRB supplemented or not with MG132. Note that MG132 incubation rescues endogenous Rasputin protein level, but does not rescue stress granules formation. **E**: Quantification of stress granule formation in Rasputin-V5 transfected and non-transfected cells in mock and Sec16 depleted cells incubated in KRB supplemented or not with MG132. Expressed in percentage of cell with stress granules. **F, F':** IF Co-visualization of full length Sec16-GFP-CAAX in cells expressing Rasputin-V5, Ser142A-V5 and Ser142E-V5 Rasputin mutants upon amino-acid starvation (KRB) (F). Note that both Rasputin-V5 and Ser142E-V5 steadily localizes at the plasma membrane in cells expressing Sec16-GFP-CAAX, whereas Ser142A remains dispersed in the cytoplasm (marked by # in F'). Quantified in F' (expressed as percentage of Sec16-GFP-CAAX transfected cells). **G, G'**: IF Co-visualization of full length Sec16-GFP-CAAX in cells expressing Rasputin-V5, Ser142A-V5 and Ser142E-V5 Rasputin mutants, upon arsenite treatment (G). Note that none of the Rasputin forms are recruited by Sec16-GFP-CAAX. Furthermore, in agreement with Figure 2E, F, Rasputin-V5 and Ser142E form stress granules (red arrows). In contrast, Ser142E remains diffuse in the cytoplasm (marked by # in G'). Quantified in G' (expressed as percentage of Sec16-GFP-CAAX transfected cells). Scale bar: 10 μm. Error bar: SD.

upon amino-acid starvation. In agreement with above, Ser142E strongly co-localizes to Sec16 whereas Ser142A does not (**Figure 5F and F').** In striking contrast, none of the Rasputin forms are recruited to the plasma membrane by Sec16-GFP-CAAX upon arsenite stress (**Figure 5G, G'**). Instead Rasputin-V5 and Ser142A-V5 form stress granules (red arrows), whereas Ser142E remains diffuse in the cytoplasm.

Taken together, we show that Sec16 is required for stress granule formation upon amino-acid starvation by specifically interacting with, and stabilizing phospho-Rin, the form that is incorporated to stress granules upon this type of stress.

Discussion

Rasputin and stress granule formation upon different stresses.

Stress granules are formed when translation initiation is inhibited either by drugs or by a stress response (Anderson and Kedersha, 2006; Kedersha et al., 2016) and their components are thought to be recruited through protein-protein interactions mediated by low and multivalence interactions, sometimes facilitated by posttranslational modifications resulting from activation of signaling pathways. In addition to RNA binding proteins, they also contain metabolic enzymes and signaling pathway components (Jain et al., 2016) (Buchan et al., 2011) (Wippich et al., 2013) (Leung, 2014).

Both heat stress, arsenite treatment (Farny et al., 2009) and amino-acid starvation (this manuscript) of Drosophila S2 cells leads to protein translation inhibition/stalling through the phosphorylation of the initiation factor eIF2α. Furthermore, numerous factors are required for stress granule formation upon several stresses, such a G3BP upon arsenite treatment and heat shock of mammalian cells (Tourriere et al., 2003) and Rasputin upon amino-acid starvation of S2 cells (this manuscript).

However, even when the signal (translation inhibition) and the effector (G3BP/Rasputin) appear to be the same, the mechanism and/or signaling clues inducing

stress granule formation may be different. For instance, even though eIF2alpha is phosphorylated upon heat shock and arsenite, this phosphorylation is not a requirement for stress granule formation upon heat stress, whereas it is upon arsenite (Farny et al., 2009). Remarkably, here, we show that Rasputin is differentially recruited to stress granules upon arsenite and amino-acid starvation, and that this recruitment depends of its phosphorylated status. To the best of our knowledge, this is the first example that clearly demonstrates this phenomenon and this further documents that stress granules are more complex, variable, and not just a temporal storage of stalled mRNPs. This is also reflected by the fact that stress granules contain diverse proteomes (Jain et al., 2016).

Sec16, an ERES component, binds to Rasputin.

Sec16 is required for stress granule formation specifically upon amino-acid starvation
What determines the use for phosphor-Rasputin versus non-phospho-Rasputin in stress granule formation upon different stressors remains unknown. However, one step in this understanding comes from the discovery that the large hydrophilic ERES protein Sec16 binds Rasputin.

Sec16 adds to the lengthening list of factors modulate stress granule formation such as G3BP (YB-1 (Somasekharan et al., 2015), caprin (Kedersha et al., 2016; Solomon et al., 2007), TDP43 (Aulas et al., 2012), usp10 (Panas et al., 2015; Soncini et al., 2001) (Kedersha et al., 2016). However, Sec16 is unique because interacts only with phosphor-Rasputin (on Ser142) upon amino-acid starvation and phosphor-Rasputin is the form that is required for stress granule formation upon amino-acid starvation. As a result, Sec16 is specifically required for stress granule formation upon amino-acid starvation (thus showing the functionality of the interaction), but not upon heat, ER and arsenite treatment. In contrast, Sec16 does not interact with non-phosphorylated Rasputin that is the form required for stress granule formation upon arsenite in Drosophila (our results) and in mammalian cells (Kedersha et al., 2016; Tourriere et al., 2003). As Sec16 is specifically MARylated upon amino-acid starvation by dPARP16 (Aguilera-Gomez et al., 2016), it suggests that this modification may be instrumental in binding phosphor-Rasputin. It is indirect as Sec16 C-terminus (where the MARylation occurs) is not required for Rasputin binding.

Sec16, an ERES component linking inhibition of protein translation and protein transport.
Why does amino-acid starvation requires this specific Sec16/phospho-Rasputin interaction? Why is an ERES component functionally linked to stress granule formation specifically upon this nutrient stress? It is likely that this specific interaction elicit the formation of unique stress granules, perhaps storing mRNAs encoding proteins key for survival upon starvation and fitness upon stress relief. In

this respect, stress granules formed during amino-acid starvation contain the P-body component Tral that is not found in those formed upon heat shock (Jevtov et al, 2015). Interestingly, Tral has been shown to bind mRNAs encoding COPII subunits (Wilhelm et al., 2005). It is also possible that Sec16 interaction to Rasputin may sequester and protect mRNAs encoding or secretory pathway components inside stress granules. Conversely, as ER translated mRNAs (possibly encoding secretory proteins required in stress recovery) are proposed to escape sequestration to stress granules (Unsworth et al., 2010), it is possible that Sec16 interaction with stress granule components restrict stress granule formation to specific sites away from these mRNAs. The spatial restriction could be helped/mediated by Sec bodies that also specifically form upon amino-acid starvation.

In any case, recent evidence and these results strengthen the link between protein translation, RNA metabolism and the secretory pathway. Stress granules are formed in response to ER stress ((McEwen et al., 2005) and our data). P-bodies also localize in close proximity to the ER and increase in number in response to ER homeostasis perturbations and protein transport inhibition in Arf1 yeast mutant (Kilchert et al., 2010). Last, ER resident proteins are now shown to regulate P-body formation in yeast (Weidner et al., 2014).

Sec16 protects Rasputin against degradation

Upon amino-acid starvation Sec16 protects Rasputin again proteasome degradation. It is very often the case that proteins in a complex stabilize each other and when one partner is absent, the other is degraded. However, Rasputin depletion does not affect Sec16 stability. This suggests that Sec16 has an active role in protecting Rasputin. Given that Sec16 interacts specifically with phospho-Rasputin (on Ser142), the protection could happen in two ways. Rasputin phosphorylation could take place in the cytoplasm independently of Sec16 that would recognize phospho-Rasputin and stabilize it. Alternatively, Sec16 could actively contribute to Rasputin phosphorylation acting as a scaffold by binding both Rasputin and the kinase responsible for Rasputin phosphorylation. The involved kinase, which is likely to be activated by amino-acid starvation, remains to be identified.

Given that G3BP is involved in the development of many diseases, it will be interesting to investigate the role of its phosphorylation status as well as the role of Sec16 in the pathology.

Sec16, a versatile protein.

Our results provide further evidences of the versatility of Sec16 both in growing and stress conditions. In growing conditions, mammalian Sec16 exists as two isoforms that are both localized to ERES (Watson et al., 2006) (Bhattacharyya and Glick, 2007). These two isoforms have non-redundant functions in humans. Whereas Sec16A is classically required for the ER exit of proteins destined to the Golgi and the

plasma membrane (Sprangers and Rabouille, 2015), Sec16B in specialized transport to peroxisomes (Budnik et al., 2011) (Yonekawa et al., 2011). Furthermore, Sec16 exons have been shown to be alternatively spliced upon T- cell activation (Martinez et al., 2012) and increased expression of the Sec16 isoform containing exon 29 leads to an increased number of ERES and more efficient COPII transport in activated T cells (Wilhelmi et al., 2016). In this regard, Sec16 is also specifically phosphorylated by ERK2 upon serum stimulation in mammalian cells leading to an increase in the number of ERES and a larger secretory capacity (Farhan et al., 2010). Last, Sec16 interacts with LKKR2 albeit in a kinase activity independent fashion (Cho et al., 2014).

Sec16 also plays key roles in the response to stress, specifically to amino-acid starvation. Amino-acid starvation is an interesting stress as it triggers the formation of two stress assemblies in the same time frame, both requiring Sec16 but in two different manners: The first is Sec16 MARylation on its C-terminus by ER localized dPARP16 that is enough to trigger the formation of Sec bodies (Aguilera-Gomez et al., 2016). The second is that Sec16 interacts with, and stabilizes phospho-Rasputin leading to the formation of stress granules. Interestingly, none of these are linked to Sec16 role in protein exit from the ER or COPII coated vesicle dynamics ((Zacharogianni et al., 2014).

It has been suggested that at least in yeast, stress granules posses a core made of components that exchange slowly and less dynamically (Buchan and Parker, 2009; Jain et al., 2016) whereas the components of the shell can exchange more rapidly. It is tempting to suggest that stress granules and Sec bodies are also organized in this way, mostly because although they often localize in close proximity, they do not mix. Because of this close proximity, a pool of Sec16 can perhaps exchange between the two structures and localize to their shell where it interacts with Rasputin as suggested by immunofluorescence (not shown).

Taken together, this demonstrates the versatility and extensive capacity of the large scaffold protein Sec16 to regulate diverse cellular processes, many of them pro-survival. Therefore more Sec16 crucial interactors remain to be identified and studied.

Experimental Procedures

Cell culture, amino acid starvation, depletions (RNAi) and transfections

Drosophila S2 cells (mycoplasma free) were cultured in Schneider's medium (Sigma) supplemented with 10% insect tested fetal bovine serum at 26ºC as described in (Kondylis and Rabouille, 2003; Kondylis et al., 2007). Amino-acid starvation of cells for 3 or 4 h was performed using Krebs Ringer's Bicarbonate buffer (10 mM D(+) Glucose; 0.5 mM MgCl2; 4.5 mM KCl; 121 mM NaCl; 0.7 mM Na2HPO4; 1.5 mM NaH2PO4 and 15 mM sodium bicarbonate) at pH7.4 (Aguilera-Gomez et al., 2016; Zacharogianni et al., 2014).

Wild type Drosophila S2 cells were depleted by dsRNAi, as previously described (Aguilera-Gomez et al., 2016). Cells were analyzed after incubation with dsRNAs for five days typically leading to depletion in more than 90% of the cells.

Transient transfections of PMT constructs (see below) were performed using Effectene transfection reagent (301425; Qiagen, Germany) according to manufactures instructions. Expression was induced 48 h after transfection with 1 mM CuSO4 for 1.5 h (Zacharogianni and Rabouille, 2013).

Antibodies
Rabbit polyclonal anti-Sec16 (Ivan et al., 2008) 1:800 IF, 1:2500 WB; Mouse monoclonal anti-V5 (ThermoFischer Scientific 46–0705, 1:500 IF); Rabbit polyclonal anti-V5 (RRID:AB_261889, Sigma V8137); Mouse monoclonal anti-FMR1(RRID:AB_528251, DSHB supernatant clone 5A11, 1:800 IF, 1:2000 WB);; Rabbit anti- Caprin 1:500 IF, 1:2000 WB (Reich and Papoulas, 2012), anti-eIF2alpha 1:1000 WB, anti-eIF4G 1:1000 WB, anti-Tral 1:200 IF 1:100 WB, rabbit polyclonal anti-phospho-eIF2α (S51) (Cell signaling 9721s, 1:1000 WB); mouse monoclonal anti-α-tubulin (Sigma T5168, 1:100000 WB); rabbit polyclonal anti CF68 (CG7185; Gift from Zbigniew Dominski).

The Rabbit polyclonal anti-Rasputin was generated as follows: The *rasputin* coding region was PCR amplified from cDNA clone LD31994 (Berkeley *Drosophila* Genome Project) to add an NdeI site at the ATG and a BamHI site immediately following the stop codon. The PCR product was digested with NdeI and BamHI and inserted into the corresponding sites of pET15b. $(His)_6$-Rasputin was expressed in *E. coli* BL21 cells and then resolved by SDS-PAGE. The band corresponding to $(His)_6$-Rasputin was excised from the gel and used as the antigen to generate polyclonal rabbit anti-serum. The specificity of the antiserum was tested by immunoblotting of wild-type or *rasputin*^{2}/*Df* ovary extract and ECL detection. Anti-Rasputin was used at 1:500,000. The blot was re-probed with anti-Khc (1:20,000; Cytoskeleton) as a loading control **(Suppl. Fig. S5)**

PMT-DNA constructs and dsRNAs
All the primers used for generating the DNA constructs and RNAi probes are listed in Suppl. Table S2

To generate pMT-Rin-V5, Rasputin was amplified from S2 cells DNA and cloned into pMT-V5 using *SacII* and *KpnI*. To generate the mutant pMT-Rasputin S142A, Rasputin cross-was amplified using primers harboring a mutation at position S142A and cloned into pMT-V5 using *SacII* and *KpnI*. To generate the mutant PMT-Rasputin S142E Rasputin was cross-amplified using primers harboring a mutation at position S142A and cloned into pMT-V5 using *SacII* and *KpnI*.

To generate the pMT-CAAX-sfGFP vector, the sequence corresponding to C-terminus CAAX motif of Ras (SGLRSRAQASNSRVKMSKDGKKKKKKSKTKCVIM) was amplified and cloned into pMT-sfGFP using *AgeI* and *PmeI*. The Sec16 truncations: ΔNC1, ΔCter; Cter, SRD and Fl were cloned into pMT-CAAX-sfGFP using *EcoI* and *ApaI*.

To generate the pMT-sfGFP vector, super folder (sf) GFP was amplified and cloned into pMT-V5 using *SacII* and *PmeI* restriction sites replacing the V5 tag with sfGFP.

The dsRNAs used for RNAi of Rasputin and Sec16 were amplified using primers harboring T7 promoters in their sequence and used for in vitro transcription using the T7 Megascript Kit (AMBION) to generate the dsRNAs (see Suppl Table S2)

Immunofluorescence and Immuno-electron microscopy (IEM)
Drosophila S2 cells were plated on glass coverslips, treated as described, fixed in 4% PFA in PBS for 20 min and processed for imunofluorescence as previously described (Kondylis et al., 2007; Zacharogianni and Rabouille, 2013). Samples were viewed under a Leica SPE confocal microscope using a 63x oil lens and 2-4x zoom. 14 to 20 planes were projected to capture the whole cell that is displayed unless indicated otherwise.

The IEM of FRM1, TRAL, Sec16 was performed as described previously (Kondylis et al., 2007) (van Donselaar et al., 2007).

Immuno-precipitation and mass spectrometry (MS/MS)
Sec16 immuno-precipitation: 200-300 million S2 cells were grown and starved in KRB for 4 h. Cell lysate was prepared by incubating cells for 20 min on ice in lysis buffer (10% glycerol, 1% TritonX-100, 50 mM TrisHCl pH 7.5, 150 mM NaCl, 50 mM NaF, 25 mM Na_2-glycerophosphate, 1 mM Na_2VO_4, 5 mM EDTA, tablet protease inhibitors tablet (Roche). Protein A beads slurry was washed with lysis buffer and incubated for 1 h at 4^0C with 20 ug of control IgG and anti Sec16 IgG. Subsequently, the beads where incubated for 2 h at 4^0C with cell lysate. After washing with lysis buffer, beads where boiled for 10 min in sample buffer followed by SDS-PAGE and Western blot was performed.

Mass spectrometry
Endogenous Sec16 was immunoprecipitated from growing and starved S2 cells as described above and separated by SDS-PAGE. In-gel-trypsin digestion of the immunoprecipitates was performed as described previously (Shevchenko et al., 2006). Briefly, each lane was cut into five pieces and each piece was dehydrated with acetonitrile, reduced with DTT, alkylated with iodoacetamide and digested overnight with trypsin. Tryptic peptides were extracted with acetonitrile, desalted and analyzed by liquid chromatography tandem mass spectrometry (LC-MS/MS) using an Orbitrap Elite mass spectrometer coupled to a EasyLC nano-HPLC system (both Thermo Fisher Scientific, Dreieich, Germany). Peptide mixtures were loaded on a C18 reverse phase column in Solvent A (0.5% acetic acid) and eluted with a 5%-33% gradient solvent B (80% acetonitril in 0.5% acetic acid) running at a constant flow rate of 200 nl/min. Full-scan MS spectra were acquired in a mass range from m/z 300 to 2,000 with a resolution of 120.000 without lock mass. The 20 most intense precursor ions were sequentially CID fragmented in each scan cycle. In all measurements, up to 500 sequenced precursor masses were excluded from further analysis for 90 s. The target values of the mass analyzers were 1 million charges (MS) and 5,000 charges (MS/MS). The MS data was processed using default parameters of the MaxQuant software (1.2.5.5) (Cox and Mann, 2008). The peak lists were queried against the Drosophila UniProt database (2012_12). Full tryptic specificity was required, and up to two missed cleavages were allowed. Carbamidomethylation of cysteine was set as fixed modification. Protein N-terminal acetylation and oxidation of methionine were set as variable modifications. Initial precursor mass tolerance was set to 20 ppm and 0.5 Da at the fragment ion level. False discovery rates were set to 1% at peptide and protein group level.

Criteria for selecting the candidates: 5 mass spec experiments were performed as described above. For each, candidates for which more than 3 peptides were specifically recovered (not present in the IgG IP) and for which the number of recovered peptides were 3 times more than the IgG control were considered.

When such a candidate was present in at least 3 independent mass spec experiments and analysis, it is listed in bold (For instance, Rin appears in all 4 of the 5 mass spec). The strongest candidate is Sec16 itself and 122 additional candidates were selected in total.

Heat stress, Arsenate, and DTT treatments

Heat stress was performed on 2 × 10^6 Drosophila S2 cells in an oven at 37°C (Thermo Electron) for 3 h as described in (Jevtov et al., 2015). Treatment with 0.5 mM NaAsO2 was performed at 26°C for 3 h, treatment with DTT at a concentration of 2.0 mM at 26°C for 3 h.

Polysome profiles

Polysome profiles were generated as described in (Pereboom et al., 2011).

Quantification and statistics

2-5 biological replicates were performed per experiment. For IF of depleted or treated cells, at least four fields per experiment were analysed comprising at least 50 cells. For transfected cells, at least 30 cells were analysed. Results are expressed as SD and SEM.

Acknowledgements

The polysomes profiles were generated by the group of Alyson McInnes.
Financial support for this paper is provided by the Hubrecht Institute of the KNAW and grant from NWO 822-020-016 to CR. Work in the CB's lab is supported by the Deutsche Forschungsgemeinschaft (German Research Foundation) within the framework of the Munich Cluster for Systems Neurology (EXC 1010 SyNergy) and of the Collaborative Research Centre on Autophagy (SFB1177).

Supplemental figures

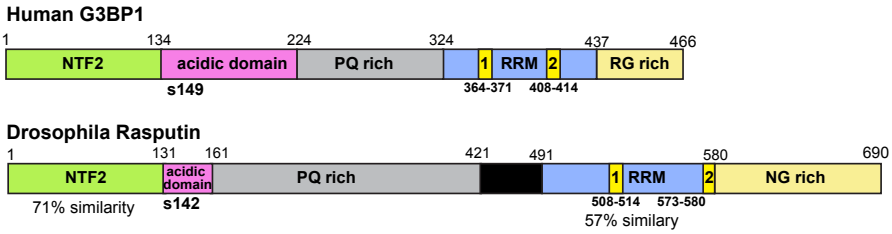

Suppl. Figure S1: Domain comparison of G3BP and Rin.

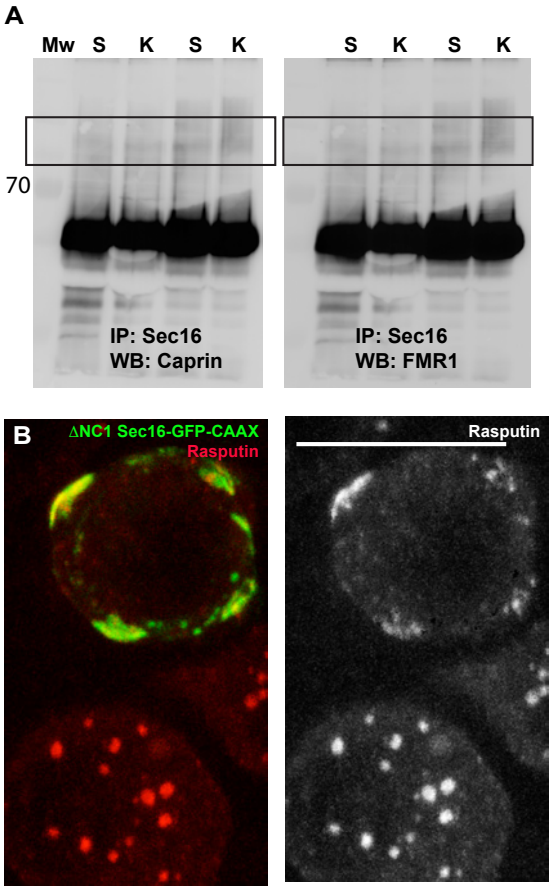

Suppl. Figure S2: **Specificity of Sec16 binding to Rasputin. A**: Co-IP of FRM1 and Caprin with Sec16. FMR1 and Caprin do not co-immunoprecipitate with Sec16 both in growing and amino-acid starvation conditions. **B:** Co-visualization of ΔNC1Sec16-GFP-CAAX with endogenous Rasputin. Note that Rasputin is still recruited to the plasma membrane, albeit to a smaller extent than full length Sec 16.

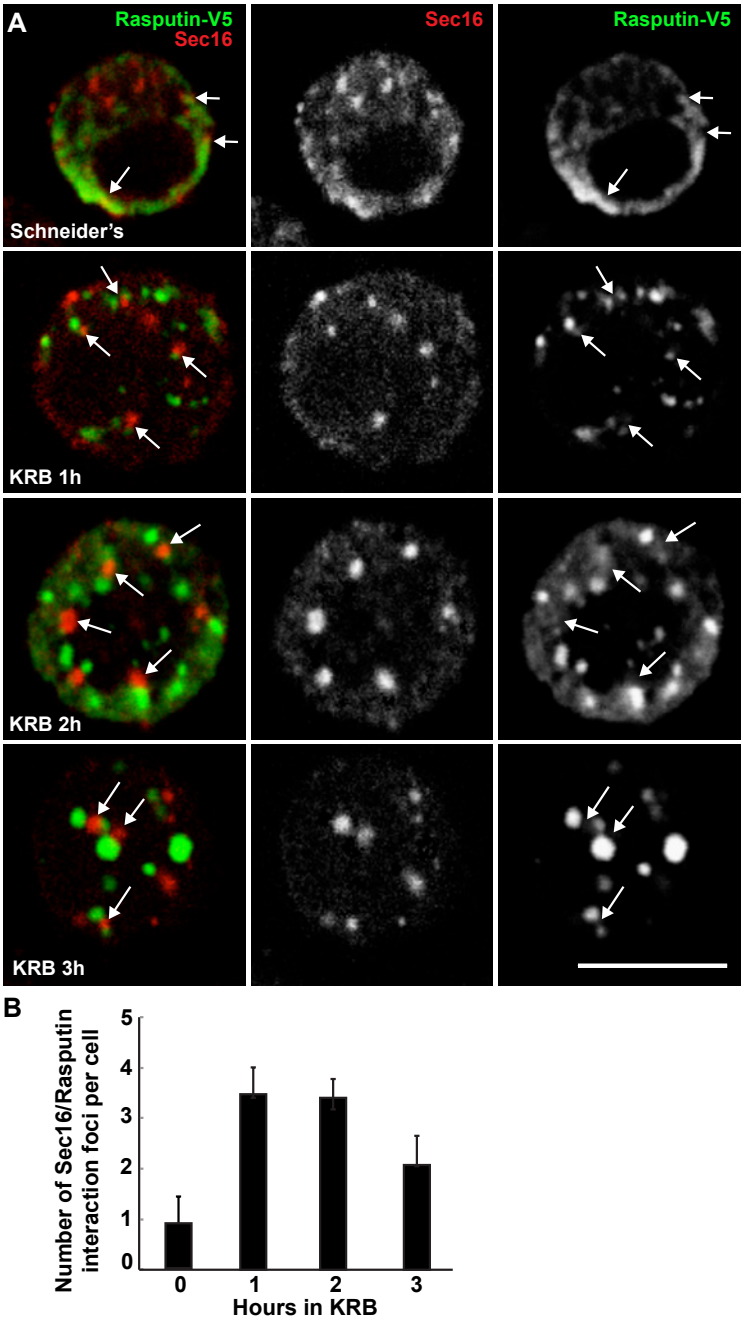

Suppl. Figure S3: Sec16/Rasputin interaction kinetics upon amino acid starvation. A: IF visualization of Rasputin-V5 (green) and Sec16 (red) after 0, 1, 2 h of amino-acid starvation. Sec16 and Rasputin increasingly appears to be in close proximity or overlapping. This interaction reaches its maximum at 2 h. Arrows point at Sec16 that is close to Rasputin. **B:** Quantification of the interaction foci per cell (from panel A).

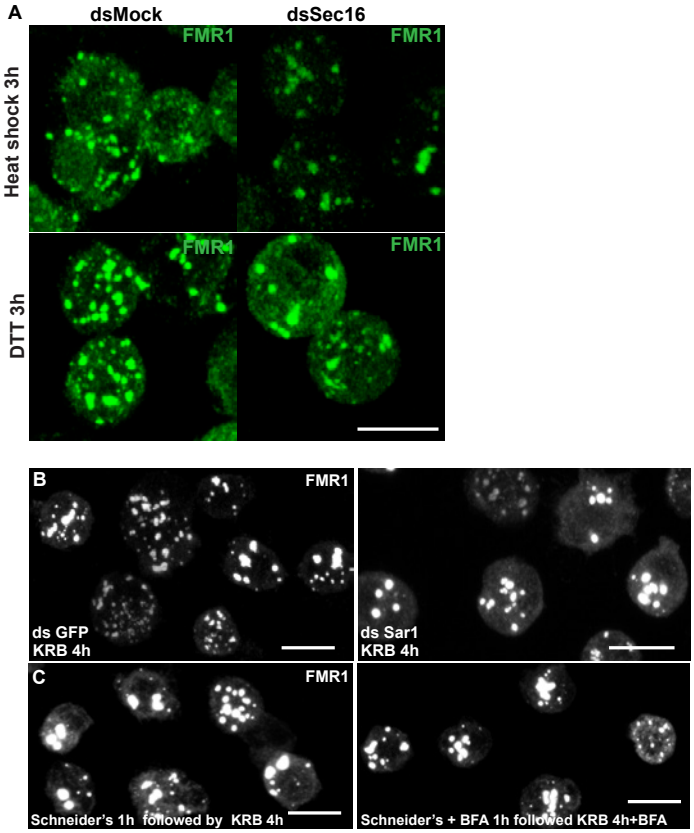

Suppl. Figure S4: stress granule in arsenite and heat shock. **A**: IF visualization of endogenous FMR1 in mock- and Sec16 depleted cells upon heat shock (3 h) and DTT (3 h). Note that stress granules form as efficiently in mock and Sec16 depleted cells. **B:** IF visualization of FMR1 in mock- and Sar1 depleted cells incubated in KRB for 4 h. Note that stress granule formation is as efficient in both depletions. Note that the Sar1 depletion was evidenced by the typical enlargement of the ERES (Ivan et al., 2008). **C:** IF visualization of FMR1 in cells treated or not with BFA. Note that stress granule formation is as efficient in treated and non treated cells. Scale bars: 10 μm.

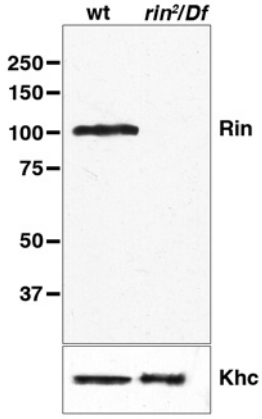

Suppl. Figure S5: Specificity of the rabbit polyclonal anti-Rasputin. The specificity of the antiserum was tested by Western blotting of wild-type and rin²/Df ovary extract and ECL detection. Anti-Rasputin was used at 1:500,000. The blot was re-probed with anti-Khc (1:20,000; Cytoskeleton) as a loading control. Note that the band at 70Kd disappears in the mutant extract.

Suppl. Table S1: List of Sec16 interactors after IP of endogenous Sec16 followed by mass-spec (MS/MS) Interactors are presented as in Figure 3C with the same color coding (see Materials and Methods). This table is available as Excel file upon request.

Suppl. Table S2: List of the primers used in this study.

Suppl. Table S2: Primers used for vector construction and RNAi	
sfGFP-F	ggccgcggatggtgagcaagggcgagga
sfGFP-R	gggtttaaacttacttgtacagctcgtccatg
pMT- Rin -V5-F	cagtggtaccatggtcatggatgcgacccaatcg
pMT- Rin-V5-R	gtcaccgcgggcgacgtccgtagttgccaccac
pMT-Rin-S142A-V5-F	gaggacgagcaggatggcgaggcgcgatcggagaacgatgaggag
pMT-Rin-S142A-V5-R	ctcctcatcgttctccgatcgcgcctcgccatcctgctcgtcctc
pMT-Rin-S142E-V5-F	gaggacgagcaggatggcgaggagcgatcggagaacgatgaggag
pMT-Rin-S142E-V5-R	ctcctcatcgttctccgatcgctcctcgccatcctgctcgtcctc
CAAX-RAS-F	cagtaccggttccggactcagatctcgagctc
CAAX-RAS-R	cagtgtttaaacttacataattacacactttgtctttgacttctttttc
CAAX-RAS-Sec16-F	cagtactagtatgttgcacaataatgcgccctggc
CAAX-RAS-Sec16-R	gtcaccgcggttgctggtgttgctgctgcagcg
SEC16>NC1-F	cagtactagtatgcattcaaccactcagcaggagaagaa
SEC16>NC1-R	ccaccggtaatggggctgccatacgtttgc
SEC16>CT-F	gtcaccgcggaaatgagacacgattaatgagaatgggatcatg
SEC16>CT-R	cagtggtaccatggcgagtcctccgaatgccactag
dsGFP-F	gggtttaaacttacttgtacagctcgtccatg
dsGFP-R	ggccgcggatggtgagcaagggcgagga
dsRin-F	taatacgactcactatagggggacagagtggtggtggc
dsRin-R	taatacgactcactatagggggccgagctgaagcttacatt
dsSec16-F	taataccgactcactatagggcgagagaaggaggaagtcagtgatgttgg
dsSec16-R	taatacgactcactatagggcgaccacaatccctgaactacaataac

References

Aguilera-Gomez, A., van Oorschot, M.M., Veenendaal, T., Rabouille, C., 2016. In vivo vizualisation of mono-ADP-ribosylation by dPARP16 upon amino-acid starvation. Elife 5.

Anderson, P., Kedersha, N., 2002. Stressful initiations. J Cell Sci 115, 3227-3234.

Anderson, P., Kedersha, N., 2006. RNA granules. J Cell Biol 172, 803-808.

Anderson, P., Kedersha, N., 2008. Stress granules: the Tao of RNA triage. Trends Biochem Sci 33, 141-150.

Aulas, A., Stabile, S., Vande Velde, C., 2012. Endogenous TDP-43, but not FUS, contributes to stress granule assembly via G3BP. Mol Neurodegener 7, 54.

Bhattacharyya, D., Glick, B.S., 2007. Two mammalian Sec16 homologues have nonredundant functions in endoplasmic reticulum (ER) export and transitional ER organization. Mol Biol Cell 18, 839-849.

Buchan, J.R., Parker, R., 2009. Eukaryotic stress granules: the ins and outs of translation. Mol Cell 36, 932-941.

Buchan, J.R., Yoon, J.H., Parker, R., 2011. Stress-specific composition, assembly and kinetics of stress granules in Saccharomyces cerevisiae. J Cell Sci 124, 228-239.

Budnik, A., Heesom, K.J., Stephens, D.J., 2011. Characterization of human Sec16B: indications of specialized, non-redundant functions. Sci Rep 1, 77.

Cho, H.J., Yu, J., Xie, C., Rudrabhatla, P., Chen, X., et al., 2014. Leucine-rich repeat kinase 2 regulates Sec16A at ER exit sites to allow ER-Golgi export. EMBO J 33, 2314-2331.

Cobos Jimenez, V., Martinez, F.O., Booiman, T., van Dort, K.A., van de Klundert, M.A., et al., 2015. G3BP1 restricts HIV-1 replication in macrophages and T-cells by sequestering viral RNA. Virology 486, 94-104.

Connerly, P.L., Esaki, M., Montegna, E.A., Strongin, D.E., Levi, S., et al., 2005. Sec16 is a determinant of transitional ER organization. Curr Biol 15, 1439-1447.

Cox, J., Mann, M., 2008. MaxQuant enables high peptide identification rates, individualized p.p.b.-range mass accuracies and proteome-wide protein quantification. Nat Biotechnol 26, 1367-1372.

Dougherty, J.D., Tsai, W.C., Lloyd, R.E., 2015. Multiple Poliovirus Proteins Repress Cytoplasmic RNA Granules.

Viruses 7, 6127-6140.
Farhan, H., Wendeler, M.W., Mitrovic, S., Fava, E., Silberberg, Y., et al., 2010. MAPK signaling to the early secretory pathway revealed by kinase/phosphatase functional screening. J Cell Biol 189, 997-1011.
Farny, N.G., Kedersha, N.L., Silver, P.A., 2009. Metazoan stress granule assembly is mediated by P-eIF2alpha-dependent and -independent mechanisms. RNA 15, 1814-1821.
Gilks, N., Kedersha, N., Ayodele, M., Shen, L., Stoecklin, G., et al., 2004. Stress granule assembly is mediated by prion-like aggregation of TIA-1. Mol Biol Cell 15, 5383-5398.
Hughes, H., Budnik, A., Schmidt, K., Palmer, K.J., Mantell, J., et al., 2009. Organisation of human ER-exit sites: requirements for the localisation of Sec16 to transitional ER. J Cell Sci 122, 2924-2934.
Ivan, V., de Voer, G., Xanthakis, D., Spoorendonk, K.M., Kondylis, V., et al., 2008. Drosophila Sec16 mediates the biogenesis of tER sites upstream of Sar1 through an arginine-rich motif. Mol Biol Cell 19, 4352-4365.
Jain, S., Wheeler, J.R., Walters, R.W., Agrawal, A., Barsic, A., et al., 2016. ATPase-Modulated Stress Granules Contain a Diverse Proteome and Substructure. Cell 164, 487-498.
Jevtov, I., Zacharogianni, M., van Oorschot, M.M., van Zadelhoff, G., Aguilera-Gomez, A., et al., 2015. TORC2 mediates the heat stress response in Drosophila by promoting the formation of stress granules. J Cell Sci 128, 2497-2508.
Kedersha, N., Panas, M.D., Achorn, C.A., Lyons, S., Tisdale, S., et al., 2016. G3BP-Caprin1-USP10 complexes mediate stress granule condensation and associate with 40S subunits. J Cell Biol 212, 845-860.
Kedersha, N.L., Gupta, M., Li, W., Miller, I., Anderson, P., 1999. RNA-binding proteins TIA-1 and TIAR link the phosphorylation of eIF-2 alpha to the assembly of mammalian stress granules. J Cell Biol 147, 1431-1442.
Kilchert, C., Weidner, J., Prescianotto-Baschong, C., Spang, A., 2010. Defects in the secretory pathway and high Ca2+ induce multiple P-bodies. Mol Biol Cell 21, 2624-2638.
Kim, D.Y., Reynaud, J.M., Rasalouskaya, A., Akhrymuk, I., Mobley, J.A., et al., 2016. New World and Old World Alphaviruses Have Evolved to Exploit Different Components of Stress Granules, FXR and G3BP Proteins, for Assembly of Viral Replication Complexes. PLoS Pathog 12, e1005810.
Kondylis, V., Rabouille, C., 2003. A novel role for dp115 in the organization of tER sites in Drosophila. J Cell Biol 162, 185-198.
Kondylis, V., van Nispen tot Pannerden, H.E., Herpers, B., Friggi-Grelin, F., Rabouille, C., 2007. The golgi comprises a paired stack that is separated at G2 by modulation of the actin cytoskeleton through Abi and Scar/WAVE. Dev Cell 12, 901-915.
Leung, A.K., 2014. Poly(ADP-ribose): an organizer of cellular architecture. J Cell Biol 205, 613-619.
Li, Y.R., King, O.D., Shorter, J., Gitler, A.D., 2013. Stress granules as crucibles of ALS pathogenesis. J Cell Biol 201, 361-372.
Martinez, N.M., Pan, Q., Cole, B.S., Yarosh, C.A., Babcock, G.A., et al., 2012. Alternative splicing networks regulated by signaling in human T cells. RNA 18, 1029-1040.
McEwen, E., Kedersha, N., Song, B., Scheuner, D., Gilks, N., et al., 2005. Heme-regulated inhibitor kinase-mediated phosphorylation of eukaryotic translation initiation factor 2 inhibits translation, induces stress granule formation, and mediates survival upon arsenite exposure. J Biol Chem 280, 16925-16933.
Min, L., Ruan, Y., Shen, Z., Jia, D., Wang, X., et al., 2015. Overexpression of Ras-GTPase-activating protein SH3 domain-binding protein 1 correlates with poor prognosis in gastric cancer patients. Histopathology 67, 677-688.
Panas, M.D., Schulte, T., Thaa, B., Sandalova, T., Kedersha, N., et al., 2015. Viral and cellular proteins containing FGDF motifs bind G3BP to block stress granule formation. PLoS Pathog 11, e1004659.
Pereboom, T.C., van Weele, L.J., Bondt, A., MacInnes, A.W., 2011. A zebrafish model of dyskeratosis congenita reveals hematopoietic stem cell formation failure resulting from ribosomal protein-mediated p53 stabilization. Blood 118, 5458-5465.
Protter, D.S., Parker, R., 2016. Principles and Properties of Stress Granules. Trends Cell Biol 26, 668-679.
Reich, J., Papoulas, O., 2012. Caprin controls follicle stem cell fate in the Drosophila ovary. PLoS One 7, e35365.
Reineke, L.C., Kedersha, N., Langereis, M.A., van Kuppeveld, F.J., Lloyd, R.E., 2015. Stress granules regulate double-stranded RNA-dependent protein kinase activation through a complex containing G3BP1 and Caprin1. MBio 6, e02486.
Shevchenko, A., Tomas, H., Havlis, J., Olsen, J.V., Mann, M., 2006. In-gel digestion for mass spectrometric characterization of proteins and proteomes. Nature protocols 1, 2856-2860.
Solomon, S., Xu, Y., Wang, B., David, M.D., Schubert, P., et al., 2007. Distinct structural features of caprin-1 mediate its interaction with G3BP-1 and its induction of phosphorylation of eukaryotic translation initiation factor 2alpha, entry to cytoplasmic stress granules, and selective interaction with a subset of mRNAs. Mol Cell Biol 27, 2324-2342.
Somasekharan, S.P., El-Naggar, A., Leprivier, G., Cheng, H., Hajee, S., et al., 2015. YB-1 regulates stress granule formation and tumor progression by translationally activating G3BP1. J Cell Biol 208, 913-929.
Soncini, C., Berdo, I., Draetta, G., 2001. Ras-GAP SH3 domain binding protein (G3BP) is a modulator of USP10, a novel human ubiquitin specific protease. Oncogene 20, 3869-3879.
Sprangers, J., Rabouille, C., 2015. SEC16 in COPII coat dynamics at ER exit sites. Biochem Soc Trans 43, 97-103.
Tourriere, H., Chebli, K., Zekri, L., Courselaud, B., Blanchard, J.M., et al., 2003. The RasGAP-associated endoribonuclease G3BP assembles stress granules. J Cell Biol 160, 823-831.
Tsai, W.C., Lloyd, R.E., 2014. Cytoplasmic RNA Granules and Viral Infection. Annu Rev Virol 1, 147-170.
Unsworth, H., Raguz, S., Edwards, H.J., Higgins, C.F., Yague, E., 2010. mRNA escape from stress granule sequestration is dictated by localization to the endoplasmic reticulum. FASEB J 24, 3370-3380.
van Donselaar, E., Posthuma, G., Zeuschner, D., Humbel, B.M., Slot, J.W., 2007. Immunogold labeling of cryosections from high-pressure frozen cells. Traffic 8, 471-485.
Watson, P., Townley, A.K., Koka, P., Palmer, K.J., Stephens, D.J., 2006. Sec16 defines endoplasmic reticulum exit

sites and is required for secretory cargo export in mammalian cells. Traffic 7, 1678-1687.
Weidner, J., Wang, C., Prescianotto-Baschong, C., Estrada, A.F., Spang, A., 2014. The polysome-associated proteins Scp160 and Bfr1 prevent P body formation under normal growth conditions. J Cell Sci 127, 1992-2004.
Wilhelm, J.E., Buszczak, M., Sayles, S., 2005. Efficient protein trafficking requires trailer hitch, a component of a ribonucleoprotein complex localized to the ER in Drosophila. Dev Cell 9, 675-685.
Wilhelmi, I., Kanski, R., Neumann, A., Herdt, O., Hoff, F., et al., 2016. Sec16 alternative splicing dynamically controls COPII transport efficiency. Nat Commun 7, 12347.
Wippich, F., Bodenmiller, B., Trajkovska, M.G., Wanka, S., Aebersold, R., et al., 2013. Dual specificity kinase DYRK3 couples stress granule condensation/dissolution to mTORC1 signaling. Cell 152, 791-805.
Yonekawa, S., Furuno, A., Baba, T., Fujiki, Y., Ogasawara, Y., et al., 2011. Sec16B is involved in the endoplasmic reticulum export of the peroxisomal membrane biogenesis factor peroxin 16 (Pex16) in mammalian cells. Proc Natl Acad Sci U S A 108, 12746-12751.
Zacharogianni, M., Aguilera Gomez, A., Veenendaal, T., Smout, J., Rabouille, C., 2014. A stress assembly that confers cell viability by preserving ERES components during amino-acid starvation. Elife 3.
Zacharogianni, M., Kondylis, V., Tang, Y., Farhan, H., Xanthakis, D., et al., 2011. ERK7 is a negative regulator of protein secretion in response to amino-acid starvation by modulating Sec16 membrane association. EMBO J 30, 3684-3700.
Zacharogianni, M., Rabouille, C., 2013. Trafficking along the secretory pathway in Drosophila cell line and tissues: a light and electron microscopy approach. Methods Cell Biol 118, 35-49.

Chapter 6

Intra Golgi transport

Angelica Aguilera-Gomez and Catherine Rabouille (2014)
Encyclopedia of Cell Biology, Elsevier, Article ID: Intra-Golgi Transport/20034

Intra Golgi transport

Abstract

Anterograde transport through the secretory pathway is critical for the delivery of most of the integral plasma membrane and secreted proteins. Although enormous progress has been made in the identification of the transport machinery between the different organelles of the secretory pathway, there are still no clear consensus on how newly synthesized proteins traverse the Golgi apparatus in a manner that allows their processing and sorting while keeping the structural integrity of the organelle. In this chapter, we outline the different models currently proposed in the field.

Introduction

Cell survival and communication largely depends on the secretion of circulating protein ligands (such as insulin and epithelial growth factor among many others) and plasma membrane receptors that bind these ligands, thus eliciting appropriate signaling pathways triggering growth, differentiation, proliferation, release of biological materials etc (Farhan and Rabouille, 2011).

Although these ligands and receptors are usually synthesized in different cell types, they have in common to have reached their final destination by trafficking through the secretory pathway. This pathway is made of discrete membrane bound organelles. The secretory cargo (proteins to be transported through the secretory pathway) are *de novo* synthesized in the endoplasmic reticulum (ER), packaged into COPII coated carriers at ER exit sites, and transported to the Golgi complex, the central sorting and processing station of secretory cargo proteins of the secretory pathway. The passage through the Golgi ensures that they become biologically active after they are properly glycosylated and processed before being packaged for transport to their final destinations. Of note, these destinations are not only the plasma membrane but also the multiple internal membrane-bound compartments, including these of the secretory pathway itself. The Golgi has the capacity of processing grams of proteins per day, such as a digestive enzymes secreted by the exocrine pancreas.

Despite this enormous protein trafficking, the Golgi complex keeps its structural integrity. At the structural level, the most basic organization of the Golgi complex found in most organisms comprises three sub-compartments, the *cis*, medial and *trans* cisternae, flattened membrane bound compartments. In mammalian cells, they are of 1 μm cross-sectional diameter and stacked to form a polarized compact structure, the Golgi stack (**Figure 1**). A noticeable exception to the stacked organization is the Golgi in S. cerevisiae, which displays only single cisternae, at least in normal lab conditions (Rambourg et al., 1993).

This Golgi stack is flanked on each side by a tubular membrane network: The *cis*

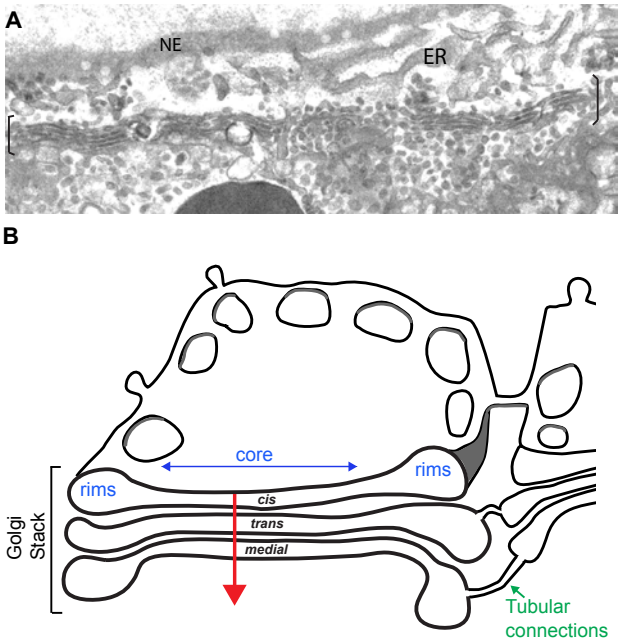

Figure 1: The Golgi complex. A. Electron micrograph of a Golgi stack of a mouse epithelial fibroblast. A portion of the Golgi ribbon is displayed between brackets. NE, nuclear envelope; ER, endoplasmic reticulum. **B**. Cartoon representation of a Golgi stack comprising 3 stacked cisternae (cis, medial and trans), each with a core (center) and more dilated (and fenestrated) rims. Each cisterna is also laterally linked to an equivalent cisterna by tubular connections, thus forming the Golgi ribbon.

Golgi Network (CGN) at the *cis* side of the stack where proteins that have just exited the ER enter the Golgi complex, and the *trans* Golgi Network (TGN), where they exit. In mammalian cells, the stacks are connected together by tubules to form the so-called mammalian Golgi ribbon capping the nucleus (**Figure 1**). In non-mammalian species, the Golgi stacks are not connected and remain discrete in the cytoplasm, for instance in Drosophila (Kondylis and Rabouille, 2009). In addition to the stack' *cis* to *trans* polarity and to the 3D ribbon organization, there is also lateral anisotropy within each cisterna: the cisterna thin core seems to be functionally different from its rims that are often dilated and highly fenestrated (Weidman et al., 1993) (**Figure 1**).

Recognized 50 years ago by Nobel Prize winner George Palade (Palade, 1975), *cis* to *trans* anterograde transport through the Golgi is a prerequisite for almost all proteins that reach the plasma membrane and the extracellular medium. There is now a consensus about the molecular machinery mediating intra-Golgi transport, as recognized by the Nobel Prize awarded to James E. Rothman this year, a prize that also recognized Randy W. Schekman and Thomas S. Südhof for the elucidation of the machinery required for ER exit and neurotransmitter release, respectively. However, a general agreement on how intra-Golgi transport is mechanistically sustained is yet to be reached. We are now down to 6 models and not closer to reach a consensus,

as groups using almost identical technology continue to reach opposite conclusions.

I: A crash course in the machinery involved in intra Golgi transport.

In order to provide a framework to place the different models by which proteins are thought to undergo intra-Golgi transport, we briefly mention here a number of key molecules required in the process (reviewed in Mellman and Warren, 2000).

COPI coated vesicles

Net forward movement of proteins through the secretory pathway is mediated by formation of small membrane carriers that specifically fuse with receptor compartments. One type that buds at the Golgi are COPI (Coatomer Protein Complex I) coated vesicles that were identified in the late 80ies by the group of Jim Rothman (Malhotra et al., 1989). COPI is a cytosolic 700-kDa protein complex comprising seven stoichiometric subunits, α, β, β', γ, δ, ε, and ζ-COP conserved from yeast to mammals (Gaynor et al., 1998) and pre-assembled into 2 cytoplasmic sub-complexes in the cytoplasm (β, γ, δ and ζ-COP subunits on one hand, and α, β and ε-COP subunits, on the second hand) (Watson et al., 2004). Recruited upon activation of the activated small GTPase ADP-Ribosylation Factor 1 (Arf1), the coatomer complex is sufficient for COPI coated vesicle formation (reviewed in Hsu and Yang, 2009).

Note that in addition to COPI coated vesicles, two (and perhaps more) other types of coated vesicles are present in the secretory pathway. COPII coated vesicles bud from the ER and form ER exit sites (reviewed in Lee and Schekman, 2004), whereas clathrin coated vesicles bud from the TGN to mediate transport of newly synthesized lysosomal hydrolases to the lysosomes (as well as from the plasma membrane to mediate endocytosis of transmembrane receptors).

Tethers and Rabs

The fusion of small carriers to their receptor compartment requires at least two types of complexes. The first is made of tethering factors and their associated small Rab GTPases. In the Golgi, there are two types of tethers: i) long coiled-coil peripheral proteins called golgins, except Giantin that spans the membrane, and GRASP65/55 that are not coiled-coils. ii) multimeric complexes, such as the COG (Conserved Oligomeric Golgi) (Lees et al., 2010) and TRAPP (Transport protein particle) (Hughson and Reinisch, 2010). All specifically associate to one (or more) of the 60 small Rab GTPases (reviewed in Pfeffer, 2013a; Ramirez and Lowe, 2009; Short et al., 2005; Sinka et al., 2008 for the golgins and GRASPs; Cottam and Ungar, 2012 for the COG; and Barrowman et al., 2010 for the TRAPP).

SNARE complexes

The second complex required for the fusion of small carriers to their receptor

compartment is made of SNARE complexes and their "recycling/priming" machinery (trimeric triple ATPase NSF and its SNARE adaptor SNAP). SNAREs are type II transmembrane proteins with most of their mass in the cytoplasm. They are functionally divided into v-SNAREs for the SNARES associated with the vesicle and t-SNAREs for those at target compartments (Fasshauer et al., 1998). Overlapping this functional definition, SNARES are also classified as Qa, Qb, Qc and R subfamilies. For intra-Golgi transport, the Qa t-SNARE is Syntaxin 5, Qb v-SNARE, Gos28, the Qc t-SNARE Gs15 and the R-tSNARE, Ykt6, that are assembled, as other SNAREs complexes in a parallel helical bundle (Malsam and Sollner, 2011; Sollner et al., 1993; Sudhof and Rothman, 2009).

Upon budding, a coated vesicle incorporates a v-SNARE, a tether and a Rab. When the coat is shed, the vesicle is captured near the target membrane via the interaction of tethers at their surface and tether at the surface of the target compartment. This allows the formation of functional SNARE complexes and mediates bilayer fusion. When fusion is achieved, the SNARE complex must disassemble to recycle the SNARE molecules, and this is mediated by NSF and SNAP (for details, see excellent review by (Malsam and Sollner, 2011).

II: The vesicular anterograde transport model.

At the beginning of the 80ies, the group of Jim Rothman at Stanford University, CA, designed a biochemical assay aimed to dissect the different steps of intra-Golgi transport. The concept behind this assay was to follow the acquisition of endoglycosidase H (endoH) resistance of a sensitive VSV-G protein contained in a "donor" Golgi fraction enriched from the mutant CHO cell line that lacks the N-acetylglucosaminyltransferase. This fraction was mixed with an acceptor Golgi fraction from wild type CHO cells. Vesicles deriving from the donor Golgi fraction (thus encapsulating endoH sensitive VSVG) would fuse with wild type acceptor Golgi, allowing the VSVG oligosaccharide chain to be processed and become endoH resistant (Balch et al., 1984; Fries and Rothman, 1980). This assay allowed the identification of key molecules, such as NSF (Malhotra et al., 1988), SNAP (Clary et al., 1990) and COPI (Malhotra et al., 1989; Orci et al., 1989; Waters et al., 1991) and SNAREs (Sollner et al., 1993).

Of note, at the same time and only few miles away, at the University of Berkeley, CA, the Schekman's group designed a forward genetic screen in yeast (Novick and Schekman, 1979) that identified 23 genes required for secretion, including the COPII components (Barlowe et al., 1994; Novick et al., 1980). Both breakthroughs rang the advent of molecular membrane traffic.

The "vesicular anterograde transport model" was the first attempt to make sense of the molecular data obtained with the Golgi transport assay, and has paved the first roadmap of intra-Golgi transport. In this model, the 2-4 cisternae of the Golgi stack

(each defined by a set of Golgi resident enzymes, such as glycosylation enzymes and proteases) are proposed to be static over the time scale of protein flow across it (typically 5–25 min, depending on the cargo). In this model, what moves is the secretory cargo. Upon delivery from the ER to the *cis* most cisterna, the cargo undergoes a series of modifications specific to this cisterna. The cargo is then re-packaged into COPI coated vesicles that deliver it to the medial cisternae where it is further modified. It is then re-packaged again in COPI coated vesicles to reach the *trans* cisterna where it undergo final modifications before exiting the Golgi (reviewed in (Rothman, 2010) (**Figure 2A**).
This model is very much in line with the general consensus that small vesicular carriers are the means by which proteins reach their destination, as it is the case for the first step of the secretory pathway, the exit of the ER by COPII coated vesicles (Barlowe et al., 1994). Furthermore, the use of vesicles as anterograde vehicles conceptually allows the Golgi to maintain its structural integrity.

III: The cisternal maturation model.

In the mid-late 90, however, the cisternal maturation model, that was prevalent in the pre-Rothman era (Morre et al., 1979) started to re-emerge as an alternative for intra-Golgi transport (Glick et al., 1997). One of the motivations for challenging the vesicular transport model was the size that some of the cargo adopts, such as long algal scales (Becker et al., 1995) and rod shape trimeric collagen complex of 300nm, both way too large to fit into a 50-100 nm COPI coated vesicles.

The cisternal maturation model has two tenets: Tenet 1 proposes that the cargo is static in one membrane compartment that undergoes changes of its identity. In this model, the part that moves is the processing machinery, not the secretory cargo. Exiting the ER, the cargo is present in a compartment at the *cis* side of the most *cis* Golgi cisterna. This compartment acquires *cis* Golgi resident enzymes and therefore becomes a *bonafide cis* cisterna. Tenet 2 proposes that the acquisition of cisternal identity is mediated by the retrograde movement of these enzymes by COPI coated vesicles from the pre-existing *cis* cisterna that becomes devoid of *cis* markers. But in the same time frame, this cisterna acquires medial markers from the pre-existing medial cisterna and becomes a medial cisterna (**Figure 2B**), whereas the medial cisterna becomes a *trans* cisterna by the same retrograde movement of *trans* markers. Overall, the features that best distinguish the two models (cisternal maturation versus vesicular anterograde transport) are the content and directionality of the COPI coated vesicles that bud from the rims of Golgi cisternae. In the vesicular transport model, COPI vesicles carry cargo and move from one Golgi cisterna to the next in an anterograde *cis*>medial>*trans* fashion. In the cisternal maturation model, the COPI coated vesicles move in a retrograde *trans*>medial>*cis* fashion and function as a retrieving device that is used by Golgi enzymes to maintain their specific and differential localization over the Golgi stack (Rabouille and Klumperman, 2005).

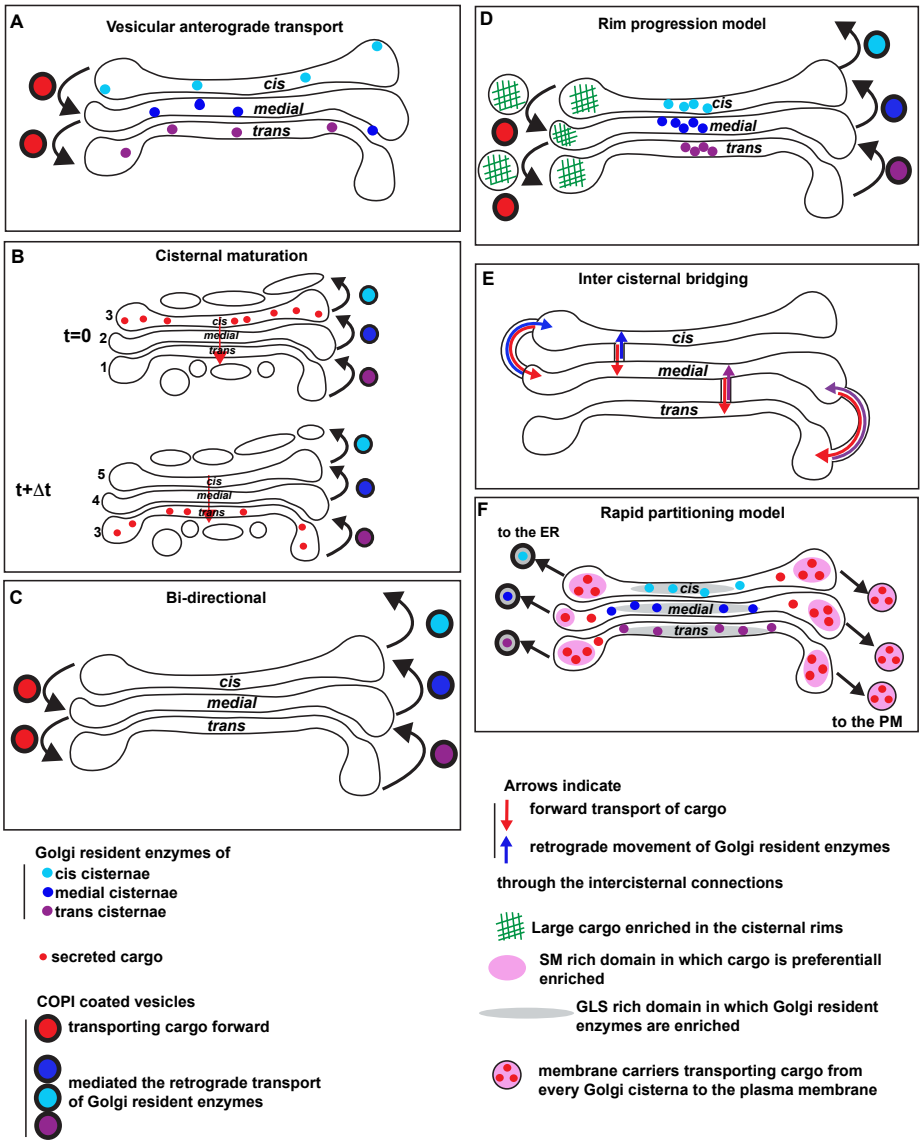

Figure 2: The different models by which proteins are proposed to undergo intra Golgi transport. **A**. Vesicular anterograde transport model: The Golgi stack and its resident proteins are static while the secretory cargo moves through the cisternae in a cis to trans fashion via COPI coated vesicles. **B**. Cisternal maturation model: The cargo remains in one cisterna that acquires in turn cis, medial and trans identity by the COPI coated vesicle mediated retrograde movement of Golgi resident enzymes. **C**. Bi-directional model: COPI coated vesicles mediate the anterograde transport of cargo and the retrograde transport of Golgi enzymes. **D**. Rim progression model: Large cargo is transported forward by re-arrangement/budding of one cisternal rim and fusion to the next. In this model, the Golgi enzymes are proposed to remain in the cisternal core. **E**. Intercisternal continuities: Vesicles are not involved in the cargo anterograde transport that is mediated by intercisternal tubular bridges. Golgi resident enzymes are also moving through the tubules as well as in COPI coated vesicles. **F**. Rapid partitioning model. The cargo is able to leave the Golgi from any cisternae after being enriched in sphingolipid domains whereas the Golgi enzymes are retained in the stack in glycerophospholipids.

The evidence for the cisternal maturation model is to be found in four separate sets of results:

- Large cargo, such as collagen has been shown to move through the Golgi stack without entering vesicular structures (Bonfanti et al., 1998; Mironov et al., 2001).
- Purified COPI coated vesicles are shown to contain a higher concentration of Golgi enzymes/proteins than secretory cargo (Lanoix et al., 1999; Lanoix et al., 2001), supporting the role of COPI vesicles in cisternal maturation (Gannon et al., 2011; Gilchrist et al., 2006). Conversely, abundant cargo, such as albumin appears depleted in these vesicles when compared to the Golgi stack (Gilchrist et al., 2006).
- COPI coated vesicles observed in vivo by immuno-electron microscopy are shown to have 1.5 fold more Mannosidase II, a medial Golgi resident enzyme, than the adjacent cisternae (Martinez-Menarguez et al., 2001). Furthermore, GFP tagged GalNAc-Tranferase 2 is shown to be present in COPI coated vesicles identified by 3D-electron tomography after GFP triggered DAB-precipitation following illumination (Grabenbauer et al., 2005).
- State of the art live cell imaging techniques in yeast has shown the conversion of a *cis* cisterna into a *trans* one as predicted by the model (Losev et al., 2006; Matsuura-Tokita et al., 2006).

IV: The COPI mediated bi-directional transport model.

Although many compelling evidence (listed above) has been gathered in support of cisternal maturation, the debate remained open. The first strategy to support the vesicular transport model has been to get evidence that COPI coated vesicles also contain secretory cargo (moving in an anterograde manner) in addition to Golgi enzymes (moving in a retrograde manner) **(Figure 2C)** (tenet 2). Using the same technique of immuno-electron microsocopy as the Klumperman's group (Martinez-Menarguez et al., 2001), the Orci's group showed that in insulin producing cells, COPI coated vesicles budding at every level of the Golgi stack contain both the KDEL receptor (retrograde-directed) and pro-insulin (anterograde-directed) (Orci et al., 1997).

The Warren's group then showed the co-existence of 2 classes of COPI coated vesicles; The first class contains Golgin 84 and CASP, lacks cargo receptor of the p24 family and is enriched in Golgi enzymes. Manipulation of these golgins inhibits the delivery of Golgi enzymes to the ER, supporting the role of these first class of COPI vesicles in retrograde transport The second class of COPI coated vesicles contains p115 and giantin, and uses GM130 and Rab1 to be tethered to the CGN in an anterograde manner (Malsam et al., 2005). These results suggest that COPI coated vesicles can mediate the differential retrograde and anterograde movement of two different types of molecules. Whether this is related to the existence of multiple

coatomer complexes isolated by the group F. Wieland (Wegmann et al., 2004) remains to be established.

Recently, an study aiming to monitor Golgi transport by live cell imaging in mammalian cells supported the ability of COPI coated vesicles to move both secretory cargo and Golgi resident enzymes. This study uses fused cells containing two types of Golgi, one marked by a small secretory cargo coupled to a fluorophore and the other marked by a Golgi resident enzyme coupled to a different fluorophore. Both cargo and Golgi enzymes are transported in small carriers with properties consistent with COPI coated vesicles, suggesting that these vesicles have the ability to incorporate both types of molecules (Pellett et al., 2013). However, this assay monitors material exchange between two Golgis (inter Golgi), not intra-Golgi transport. It is therefore possible that COPI delivers cargo (and Golgi enzymes) from one given cisterna in one Golgi to an equivalent cisterna in the second Golgi. It does not directly address how cargo progresses through the stack.

In summary, COPI coated vesicles may contain anterograde cargo as well as Golgi enzymes, and they might mediate anterograde as well as retrograde transport.

The second strategy to support the vesicular transport model has been to directly test and disprove one critical prediction of the cisternal maturation model, according to which, once a cargo is trapped in a given Golgi cisterna, it progresses forward without leaving this cisterna (tenet 1). The group of Rothman at Yale developed a new method (Lavieu et al., 2013) exactly designed to follow forward movement of cargo of different size within the Golgi stack. The first cargo used in this study is a chimeric type I membrane protein made of CD8 fused to 4 copies of the dimerization motif FM at its N-terminal luminal domain (4FM-CD8). The presence of these FM domains makes this protein to spontaneously self-oligomerize. Conversely, addition to a specific small molecule (AP21998) triggers the release of monomers (Rollins et al., 2000). When expressed in any compartments of the secretory pathway, the self-aggregated protein is trapped. For instance in the ER, it forms small aggregates (staples) that spans and compacts the width of the ER tubules, as if "stapled".

By manipulating the culture conditions in the presence and absence of the disaggregating drug, staples were allowed to form either in the *cis* or in the *trans* cisternae of the Golgi stack. Once formed, for instance in the *cis* cisterna, the staples were found not to move, and therefore did not traverse the Golgi stack. As controls, monomeric 4FM-CD8 moved to the cell surface **(Lavieu et al., 2013)**. The fact that 4FM-CD8 staples remain where they are generated supports a model in which Golgi compartments are static.

Staple technology has nevertheless limitations that are subjected to interpretation. Indeed, A. Luini's group (Napoli, Italy) used an almost identical staple strategy and reached opposite results (Rizzo et al., 2013). In this study, instead of 4FM-CD8 (see above), the type II protein Golgi mannosidase I was appended by 3 FM domains at the C-terminal (MannI-3FM). Again it self-aggregates and forms plaques in the

cis Golgi cisterna as expected, but the main difference is that these plaques are later found in the *trans* cisterna. This suggests that they have moved forward, contrary to the 4FM-CD8 staples, but in agreement with the prediction of the cisternal maturation model.

Whether the sharp difference in these results arises from using a cargo (CD8) instead of a resident enzyme (MannI), a type I instead of the type II protein, 3 FM domains instead of 4, at high or low expression, is not elucidated, and we are left with no clearer answers (Morriswood and Warren, 2013).

V: The Rim progression model specifically addresses large cargo transport.

As mentioned above, the original motivation to challenge the vesicular anterograde transport model was that large cargo could not fit into the small 50-70nm COPI coated vesicles. So, the third strategy to validate this model was to explain how large cargo moves from cisterna to cisterna across the Golgi stack. The existence of mega vesicles moving large cargo forward (Volchuk et al., 2000) has recently been re-investigated using the staple technology (see above). Indeed, large aggregates of a cargo can be generated, but this time with the distinct difference that these aggregates are not attached to the Golgi membrane by a transmembrane domain as in the case of 4FM-CD8 (Lavieu et al., 2013). Remarkably, these aggregates move through the Golgi stacks through cisternal rims. This has led to the so-called "Rim progression model" that proposes that large cargo are enriched at the cisternal rims and that the rims progress forward by re-arrangement/budding from one cisterna and fusion to the next, very much alike what is proposed for COPI vesicles enriched in small cargo (that is independently packaged) **(Figure 2D).**

There are, however, two major difference with the COPI coated vesicles. The fission of COPI coated vesicles is well documented and largely depends on the coat itself (Adolf et al., 2013), whereas nothing is known on the fission of these rim-derived mega vesicles. Second, it appears that a Golgi ribbon is necessary for the intra-Golgi transport of large cargo. When the mammalian Golgi ribbon is broken into mini-stacks, the transport of large cargo is significantly slowed down whereas small cargo (such as VSV-G) is unaffected (Lavieu et al., 2014). This suggests that large vesicles generated from one cisterna in one given Golgi stack cannot fuse with the next cisterna of the same stack (see below VI for a possible mechanism).

The rim progression model also proposes that Golgi resident enzymes are enriched in the cisternal core (Cosson et al., 2002) and that they do not diffuse to the rims. How the Golgi enzymes are retained in the cisterna core in a manner that also allows their dynamic incorporation in COPI coated vesicles for recycling to the ER but not their diffusion in the rims remains to be investigated. In this regard, the kin-oligomerisation model proposed by the Warren's group (Nilsson et al., 1994) could be useful in explaining both the retention/localization and the dynamics of Golgi resident enzymes. The stalks and transmembrane domains of Golgi enzymes

localizing in the same set of cisternae have been shown to form oligomers (kin-oligomer), helping in their retention. Modulation of the size of this oligomer (through mechanisms that are still to be defined) could allow the enzyme recycling to the ER (between 5 and 10%) via COPI coated vesicles.

VI: The cisternal progenitor model.

How can rims participate in forward movement large cargo and more generally of secretory cargo?

The first consideration put forward by the Pfefer' group (Pfeffer, 2013a) is that in mammalian cells, the rims are very dynamics and the site of many lateral fusion/fission events. For instance, the depolymerisation of microtubules, the depletion of Golgin 84 (Diao et al., 2003), and the double depletion of GRASP65 and 55 (Jarvela and Linstedt, 2014) leads to the dispersion of Golgi ribbon in ministacks. Second, it is now well established from research in the endocytic field that transport vectoriality is provided by small Rab GTPases. They decorate the surfaces of almost all membrane compartments (including the Golgi) where they catalyze the formation of membrane microdomains (particularly clear on the endosomal system (Sonnichsen et al., 2000). The vectoriality is provided by Rab cascade of Rab activation by specific GEFs and inactivation by specific GAPs (Chesneau et al., 2012; Pfeffer, 2013b; Poteryaev et al., 2010; Rink et al., 2005; Rivera-Molina and Novick, 2009).

Applied to the Golgi, this Rab cascade has led to the following model: A Golgi stack comprises three tightly stacked cisternae. The *cis* cisterna is marked by RabA, the medial by RabB, and the *trans* by RabC. RabA defines a domain containing the machinery facilitating homologous fusion between RabA containing cisterna. RabB and RabC would have the same property for the medial and *trans* cisterna. This would account for, for instance, the fusion of ministacks into a Golgi ribbon.

RabA can also recruit the GEF for RabB. As a result, a RabA domain leads to the formation of an adjacent RabB domain but because of the ministack dynamics, the two domains could be separated. This new RabB compartment deriving for the *cis* cisterna can then fuse with the compartment in which RabB is the most enriched, the medial cisterna. If this new RabB compartment is a rim enriched with large cargo, it would essentially equate with the fusion of the *cis* cisterna's rim with the medial cisterna, exactly what the rim progression proposes.

At the same time, RabB could recruit the GEF for RabC and the same scenario could repeat itself so that a new RabC compartment deriving from the medial cisterna would fuse with the trans cisterna **(Pfeffer, 2013b)**. In conclusion, one or several Rab cascades could in principle explain the forward progression of the cisternal rims. It would also explain why a Golgi ribbon is conducive for rim progression and (see above).

In conclusion, many evidence have been gathered to support either the cisternal maturation model or the vesicular anterograde transport model in its extended

version that includes rim progression. As stated above, the issue is, however, not settled and is further complicated by the description of two new models.

VII: Intercisternal continuities. Is COPI no longer involved?

At the beginning of the new century, in what seemed a complete departure from the involvement of COPI coated vesicle in intra-Golgi transport, a new model emerged. This was based on observations of intercisternal bridges that seemed to form under high cargo loading, such as VSV-G transfection of HeLa cells (Trucco et al., 2004) or glucose stimulation of pancreatic islets (Marsh et al., 2004). Till this time, the Golgi cisternae were considered to be discrete sub-compartments of the Golgi stack, and although each cisterna is linked laterally to an equivalent adjacent cisterna to form the Golgi ribbon (at least in mammalian cells, see Figure 1), intercisternal bridges were not readily (to almost never) observed.

This lack of evidence might be due to the fact that these bridges cannot be resolved by light microscopy. Furthermore, due to their small size and tubular nature, they would mostly be missed in EM using ultrathin sections. In this regard, 3D-electron tomography and its application on cellular structures provided the first evidence for their existence. In the pancreatic islet, few T-shaped tubules are found to connect the flat core part of two cisternae (Marsh et al., 2004). In VSV-G expressing HeLa cells, the tubules are reported to be more numerous and tended to preferentially connect the rims (Trucco et al., 2004).

The relevance of these tubules has become topical to Golgi transport as they are shown to play a role during intra-Golgi trafficking of several secretory cargo (**Figure 2E**). This would therefore suggest that COPI coated vesicles are no longer involved in transport. Indeed, intra-Golgi tubulation (as well inter-Golgi tubulation generating the Golgi ribbon) appears to be induced by the enzyme cPLA2 (San Pietro et al., 2009). cPLA2 inhibition prevents both types of Golgi tubulation and results in the inhibition of anterograde transport (San Pietro et al., 2009). A recent article from the same group now reports that albumin uses these intercisternal continuities for its secretion, but not pro-collagen, suggesting that multiple types of transport might occur in the same stack (Beznoussenko et al., 2014). Golgi enzymes also seem to also move from cisterna to cisterna via these tubules (Yang et al, 2011).

Is the COPI coat out of the equation with the involvement of intercisternal continuities in intra-Golgi transport? A membrane bud coated with COPI is meant to become a COPI coated vesicle but under certain circumstances, it can also become an intercisternal tubule. This bud fate decision is mediated by the interplay between two enzymes. When Lysophosphatidic acid (LPA) acytransferase type γ (LPAAT–γ) that promotes COPI coated vesicle formation is inhibited, tubules grow. cPLA2 inhibits LPAAT–γ, thus promoting tubule growth at the expense of vesicles. As expected, the COPI complex is necessary for the formation of the vesicles (that according to the authors carry Golgi enzymes in the retrograde fashion), but unexpectedly, also the

tubules through which small secretory cargo and enzymes move (Yang et al., 2011).

In conclusion, the role for COPI vesicles in anterograde is put under scrutiny but not the role of the COPI coat itself that is here shown to be instrumental in the formation of intercisternal continuities.

VIII: The rapid partitioning model.

The last model described here has been put forward in 2008 by the group of J. Lippincott-Schwartz (NIH, Bethesda) (Patterson et al., 2008). This group studied the dynamics of small secretory cargo (VSV-G-GFP) through the secretory pathway and got results that did not fit the cisternal maturation model. This model predicts that once a cargo enters the Golgi, it would remain in this organelle a given time to allow the maturation to take place, and leave the Golgi at the TGN with a linear kinetics, in line with the consumption of a single compartment. Instead, the Lippincott-Schwarz's group found no lag time and an exponential kinetics. From this, they concluded that a cargo is able to leave the Golgi from any cisterna, not only from the TGN. Their second observation was that Golgi resident enzymes and cargo did not completely overlap within a single Golgi cisterna, suggesting the existence of domains within cisternae.

In an attempt to integrate the kinetic data mentioned above and the existence of these two domains, lipid-trafficking pathways were introduced as the driving force for protein trafficking. The Golgi contains two major lipids, the glycerophospholipids (GPLs) and sphingolipids (SLs) that have significantly different synthetic and trafficking routes. On one hand, GPLs are synthesised in the ER and are transported to the Golgi in vesicles together with proteins. On the other hand, SLs are uniquely synthesized in the Golgi (Levine et al., 2000; van Meer et al., 2008) from ceramide that is itself produced in the ER but transferred directly to the trans Golgi by a lipid carrier protein, CERT (D'Angelo et al., 2007; Halter et al., 2007).

The rapid partitioning model proposes that each cisterna (whether *cis*, medial or *trans*) contains two domains: The first is enriched in SLs, and a large proportion of secretory cargo (that has a higher affinity for this lipid) partitions in this domain. This is consistent with observations that SLs are delivered to the PM from the Golgi by transport carriers that are formed at all levels of the Golgi (Helms and Zurzolo, 2004; Rodriguez-Boulan et al., 2005; van Meer et al., 2008) and preferably at the rims. The second domain is enriched in GPLs in which Golgi processing enzymes (that have a higher affinity for this lipid) partition. This has been proposed to be part of the localization/retention of glycosylation enzymes within the Golgi by S. Munro's group (Bretscher and Munro, 1993).

Thus, a SM rich domain containing the partitioned cargo could be incorporated in transport carriers, the nature of which needs to be determined. Concomitantly, the glycosylation enzymes would be retained in the GLM domain of the Golgi, thus both retained and retrieved back to the ER in GLM rich carriers (**Figure 2F**),

possibly in COPI coated vesicles.

How mechanisms of Golgi enzyme retention in the Golgi that have been proposed in the past (Nilsson et al., 1994; Opat et al., 2001; Schmitz et al., 2008; Tu et al., 2008) fit in the rapid partitioning is, however, not addressed. For instance, could kin-oligomerisation of Golgi enzymes (see above, Nilsson et al, 1994) be modulated by GLM?

Conclusions/perspectives

The journey ends here with an entire library of evidences in support of each model, ranging from live cell imaging to EM to 3D electron tomography, transport assays, biochemical assays, mathematical modeling, mass spectrometry, in yeast and in several mammalian cells. In 2009, the community agrees to disagree in an amiable fashion (Emr et al., 2009).

Whether this reflects fundamental biological differences in cargo types, cell types, growth conditions, tissue cultured conditions versus in vivo, is starting to be addressed. In particular, the departure from VSV-G as a typical anterograde secretory cargo has been initiated, for instance in the flow cytometry-based assay for measuring constitutive secretion from the Peden' lab (Gordon et al., 2010), and the RUSH system from the Perez's lab (Boncompain et al., 2012). The latter allows controlled studies of different cargo molecule trafficking and might reveal interesting differences that might reconcile aspects of the proposed models. The next step will be to study intra-Golgi transport in vivo with endogenous proteins tagged in the genome.

Acknowledgment

We thank the entire Golgi community for stimulating discussions and we apologize for any omissions. AA is supported by an open ALW-NWO grant (822-020-016).

References

Adolf, F., Herrmann, A., Hellwig, A., Beck, R., Brugger, B., et al., 2013. Scission of COPI and COPII vesicles is independent of GTP hydrolysis. Traffic 14, 922-932.

Balch, W.E., Dunphy, W.G., Braell, W.A., Rothman, J.E., 1984. Reconstitution of the transport of protein between successive compartments of the Golgi measured by the coupled incorporation of N-acetylglucosamine. Cell 39, 405-416.

Barlowe, C., Orci, L., Yeung, T., Hosobuchi, M., Hamamoto, S., et al., 1994. COPII: a membrane coat formed by Sec proteins that drive vesicle budding from the endoplasmic reticulum. Cell 77, 895-907.

Barrowman, J., Bhandari, D., Reinisch, K., Ferro-Novick, S., 2010. TRAPP complexes in membrane traffic: convergence through a common Rab. Nature reviews. Molecular cell biology 11, 759-763.

Becker, B., Bolinger, B., Melkonian, M., 1995. Anterograde transport of algal scales through the Golgi complex is not mediated by vesicles. Trends in cell biology 5, 305-307.

Beznoussenko, G.V., Parashuraman, S., Rizzo, R., Polishchuk, R., Martella, O., et al., 2014. Transport of soluble proteins through the Golgi occurs by diffusion via continuities across cisternae. eLife, e02009.

Boncompain, G., Divoux, S., Gareil, N., de Forges, H., Lescure, A., et al., 2012. Synchronization of secretory protein traffic in populations of cells. Nature methods 9, 493-498.

Bonfanti, L., Mironov, A.A., Jr., Martinez-Menarguez, J.A., Martella, O., Fusella, A., et al., 1998. Procollagen

traverses the Golgi stack without leaving the lumen of cisternae: evidence for cisternal maturation. Cell 95, 993-1003.
Bretscher, M.S., Munro, S., 1993. Cholesterol and the Golgi apparatus. Science 261, 1280-1281.
Chesneau, L., Dambournet, D., Machicoane, M., Kouranti, I., Fukuda, M., et al., 2012. An ARF6/Rab35 GTPase cascade for endocytic recycling and successful cytokinesis. Current biology : CB 22, 147-153.
Clary, D.O., Griff, I.C., Rothman, J.E., 1990. SNAPs, a family of NSF attachment proteins involved in intracellular membrane fusion in animals and yeast. Cell 61, 709-721.
Cosson, P., Amherdt, M., Rothman, J.E., Orci, L., 2002. A resident Golgi protein is excluded from peri-Golgi vesicles in NRK cells. Proc Natl Acad Sci U S A 99, 12831-12834.
Cottam, N.P., Ungar, D., 2012. Retrograde vesicle transport in the Golgi. Protoplasma 249, 943-955.
D'Angelo, G., Polishchuk, E., Di Tullio, G., Santoro, M., Di Campli, A., et al., 2007. Glycosphingolipid synthesis requires FAPP2 transfer of glucosylceramide. Nature 449, 62-67.
Diao, A., Rahman, D., Pappin, D.J., Lucocq, J., Lowe, M., 2003. The coiled-coil membrane protein golgin-84 is a novel rab effector required for Golgi ribbon formation. J Cell Biol 160, 201-212.
Emr, S., Glick, B.S., Linstedt, A.D., Lippincott-Schwartz, J., Luini, A., et al., 2009. Journeys through the Golgi--taking stock in a new era. J Cell Biol 187, 449-453.
Farhan, H., Rabouille, C., 2011. Signalling to and from the secretory pathway. J Cell Sci 124, 171-180.
Fasshauer, D., Sutton, R.B., Brunger, A.T., Jahn, R., 1998. Conserved structural features of the synaptic fusion complex: SNARE proteins reclassified as Q- and R-SNAREs. Proceedings of the National Academy of Sciences of the United States of America 95, 15781-15786.
Fries, E., Rothman, J.E., 1980. Transport of vesicular stomatitis virus glycoprotein in a cell-free extract. Proceedings of the National Academy of Sciences of the United States of America 77, 3870-3874.
Gannon, J., Bergeron, J.J., Nilsson, T., 2011. Golgi and related vesicle proteomics: simplify to identify. Cold Spring Harb Perspect Biol 3.
Gaynor, E.C., Graham, T.R., Emr, S.D., 1998. COPI in ER/Golgi and intra-Golgi transport: do yeast COPI mutants point the way? Biochimica et biophysica acta 1404, 33-51.
Gilchrist, A., Au, C.E., Hiding, J., Bell, A.W., Fernandez-Rodriguez, J., et al., 2006. Quantitative proteomics analysis of the secretory pathway. Cell 127, 1265-1281.
Glick, B.S., Elston, T., Oster, G., 1997. A cisternal maturation mechanism can explain the asymmetry of the Golgi stack. FEBS letters 414, 177-181.
Gordon, D.E., Bond, L.M., Sahlender, D.A., Peden, A.A., 2010. A targeted siRNA screen to identify SNAREs required for constitutive secretion in mammalian cells. Traffic 11, 1191-1204.
Grabenbauer, M., Geerts, W.J., Fernadez-Rodriguez, J., Hoenger, A., Koster, A.J., et al., 2005. Correlative microscopy and electron tomography of GFP through photooxidation. Nat Methods 2, 857-862.
Halter, D., Neumann, S., van Dijk, S.M., Wolthoorn, J., de Maziere, A.M., et al., 2007. Pre- and post-Golgi translocation of glucosylceramide in glycosphingolipid synthesis. The Journal of cell biology 179, 101-115.
Helms, J.B., Zurzolo, C., 2004. Lipids as targeting signals: lipid rafts and intracellular trafficking. Traffic 5, 247-254.
Hsu, V.W., Yang, J.S., 2009. Mechanisms of COPI vesicle formation. FEBS letters 583, 3758-3763.
Hughson, F.M., Reinisch, K.M., 2010. Structure and mechanism in membrane trafficking. Current opinion in cell biology 22, 454-460.
Jarvela, T., Linstedt, A.D., 2014. Isoform-specific tethering links the Golgi ribbon to maintain compartmentalization. Molecular biology of the cell 25, 133-144.
Kondylis, V., Rabouille, C., 2009. The Golgi apparatus: lessons from Drosophila. FEBS Lett 583, 3827-3838.
Lanoix, J., Ouwendijk, J., Lin, C.C., Stark, A., Love, H.D., et al., 1999. GTP hydrolysis by arf-1 mediates sorting and concentration of Golgi resident enzymes into functional COP I vesicles. The EMBO journal 18, 4935-4948.
Lanoix, J., Ouwendijk, J., Stark, A., Szafer, E., Cassel, D., et al., 2001. Sorting of Golgi resident proteins into different subpopulations of COPI vesicles: a role for ArfGAP1. The Journal of cell biology 155, 1199-1212.
Lavieu, G., Dunlop, M.H., Lerich, A., Zheng, H., Bottanelli, F., et al., 2014. The Golgi-Ribbon Structure Facilitates Anterograde Transport of Large Cargoes. Molecular biology of the cell.
Lavieu, G., Zheng, H., Rothman, J.E., 2013. Stapled Golgi cisternae remain in place as cargo passes through the stack. eLife 2, e00558.
Lee, M.C.S., Schekman, R., 2004. Cell biology. BAR domains go on a bender. Science (New York, N Y) 303, 479-480.
Lees, J.A., Yip, C.K., Walz, T., Hughson, F.M., 2010. Molecular organization of the COG vesicle tethering complex. Nature structural & molecular biology 17, 1292-1297.
Levine, T.P., Wiggins, C.A., Munro, S., 2000. Inositol phosphorylceramide synthase is located in the Golgi apparatus of Saccharomyces cerevisiae. Mol Biol Cell 11, 2267-2281.
Losev, E., Reinke, C.A., Jellen, J., Strongin, D.E., Bevis, B.J., et al., 2006. Golgi maturation visualized in living yeast. Nature 441, 1002-1006.
Malhotra, V., Orci, L., Glick, B.S., Block, M.R., Rothman, J.E., 1988. Role of an N-ethylmaleimide-sensitive transport component in promoting fusion of transport vesicles with cisternae of the Golgi stack. Cell 54, 221-227.
Malhotra, V., Serafini, T., Orci, L., Shepherd, J.C., Rothman, J.E., 1989. Purification of a novel class of coated vesicles mediating biosynthetic protein transport through the Golgi stack. Cell 58, 329-336.
Malsam, J., Satoh, A., Pelletier, L., Warren, G., 2005. Golgin tethers define subpopulations of COPI vesicles. Science 307, 1095-1098.
Malsam, J., Sollner, T.H., 2011. Organization of SNAREs within the Golgi stack. Cold Spring Harb Perspect Biol 3, a005249.
Marsh, B.J., Volkmann, N., McIntosh, J.R., Howell, K.E., 2004. Direct continuities between cisternae at different

levels of the Golgi complex in glucose-stimulated mouse islet beta cells. Proc Natl Acad Sci U S A 101, 5565-5570.
Martinez-Menarguez, J.A., Prekeris, R., Oorschot, V.M., Scheller, R., Slot, J.W., et al., 2001. Peri-Golgi vesicles contain retrograde but not anterograde proteins consistent with the cisternal progression model of intra-Golgi transport. J Cell Biol 155, 1213-1224.
Matsuura-Tokita, K., Takeuchi, M., Ichihara, A., Mikuriya, K., Nakano, A., 2006. Live imaging of yeast Golgi cisternal maturation. Nature 441, 1007-1010.
Mellman, I., Warren, G., 2000. The road taken: past and future foundations of membrane traffic. Cell 100, 99-112.
Mironov, A.A., Beznoussenko, G.V., Nicoziani, P., Martella, O., Trucco, A., et al., 2001. Small cargo proteins and large aggregates can traverse the Golgi by a common mechanism without leaving the lumen of cisternae. The Journal of cell biology 155, 1225-1238.
Morre, D.J., Kartenbeck, J., Franke, W.W., 1979. Membrane flow and intercoversions among endomembranes. Biochimica et biophysica acta 559, 71-52.
Morriswood, B., Warren, G., 2013. Cell biology. Stalemate in the Golgi battle. Science 341, 1465-1466.
Nilsson, T., Hoe, M.H., Slusarewicz, P., Rabouille, C., Watson, R., et al., 1994. Kin recognition between medial Golgi enzymes in HeLa cells. EMBO J 13, 562-574.
Novick, P., Field, C., Schekman, R., 1980. Identification of 23 complementation groups required for post-translational events in the yeast secretory pathway. Cell 21, 205-215.
Novick, P., Schekman, R., 1979. Secretion and cell-surface growth are blocked in a temperature-sensitive mutant of Saccharomyces cerevisiae. Proceedings of the National Academy of Sciences of the United States of America 76, 1858-1862.
Opat, A.S., Houghton, F., Gleeson, P.A., 2001. Steady-state localization of a medial-Golgi glycosyltransferase involves transit through the trans-Golgi network. Biochem J 358, 33-40.
Orci, L., Malhotra, V., Amherdt, M., Serafini, T., Rothman, J.E., 1989. Dissection of a single round of vesicular transport: sequential intermediates for intercisternal movement in the Golgi stack. Cell 56, 357-368.
Orci, L., Stamnes, M., Ravazzola, M., Amherdt, M., Perrelet, A., et al., 1997. Bidirectional transport by distinct populations of COPI-coated vesicles. Cell 90, 335-349.
Palade, G., 1975. Intracellular aspects of the process of protein synthesis. Science 189, 867.
Patterson, G.H., Hirschberg, K., Polishchuk, R.S., Gerlich, D., Phair, R.D., et al., 2008. Transport through the Golgi apparatus by rapid partitioning within a two-phase membrane system. Cell 133, 1055-1067.
Pellett, P.A., Dietrich, F., Bewersdorf, J., Rothman, J.E., Lavieu, G., 2013. Inter-Golgi transport mediated by COPI-containing vesicles carrying small cargoes. eLife 2, e01296.
Pfeffer, S.R., 2013a. Hopping rim to rim through the Golgi. Elife 2, e00903.
Pfeffer, S.R., 2013b. Rab GTPase regulation of membrane identity. Current opinion in cell biology 25, 414-419.
Poteryaev, D., Datta, S., Ackema, K., Zerial, M., Spang, A., 2010. Identification of the switch in early-to-late endosome transition. Cell 141, 497-508.
Rabouille, C., Klumperman, J., 2005. Opinion: The maturing role of COPI vesicles in intra-Golgi transport. Nat Rev Mol Cell Biol 6, 812-817.
Rambourg, A., Clermont, Y., Kepes, F., 1993. Modulation of the Golgi apparatus in Saccharomyces cerevisiae sec7 mutants as seen by three-dimensional electron microscopy. Anat Rec 237, 441-452.
Ramirez, I.B., Lowe, M., 2009. Golgins and GRASPs: holding the Golgi together. Semin Cell Dev Biol 20, 770-779.
Rink, J., Ghigo, E., Kalaidzidis, Y., Zerial, M., 2005. Rab conversion as a mechanism of progression from early to late endosomes. Cell 122, 735-749.
Rivera-Molina, F.E., Novick, P.J., 2009. A Rab GAP cascade defines the boundary between two Rab GTPases on the secretory pathway. Proceedings of the National Academy of Sciences of the United States of America 106, 14408-14413.
Rizzo, R., Parashuraman, S., Mirabelli, P., Puri, C., Lucocq, J., et al., 2013. The dynamics of engineered resident proteins in the mammalian Golgi complex relies on cisternal maturation. The Journal of cell biology 201, 1027-1036.
Rodriguez-Boulan, E., Kreitzer, G., Musch, A., 2005. Organization of vesicular trafficking in epithelia. Nature reviews. Molecular cell biology 6, 233-247.
Rollins, C.T., Rivera, V.M., Woolfson, D.N., Keenan, T., Hatada, M., et al., 2000. A ligand-reversible dimerization system for controlling protein-protein interactions. Proceedings of the National Academy of Sciences of the United States of America 97, 7096-7101.
Rothman, J.E., 2010. The future of Golgi research. Mol Biol Cell 21, 3776-3780.
San Pietro, E., Capestrano, M., Polishchuk, E.V., DiPentima, A., Trucco, A., et al., 2009. Group IV phospholipase A(2)alpha controls the formation of inter-cisternal continuities involved in intra-Golgi transport. PLoS Biol 7, e1000194.
Schmitz, K.R., Liu, J., Li, S., Setty, T.G., Wood, C.S., et al., 2008. Golgi localization of glycosyltransferases requires a Vps74p oligomer. Dev Cell 14, 523-534.
Short, B., Haas, A., Barr, F.A., 2005. Golgins and GTPases, giving identity and structure to the Golgi apparatus. Biochim Biophys Acta 1744, 383-395.
Sinka, R., Gillingham, A.K., Kondylis, V., Munro, S., 2008. Golgi coiled-coil proteins contain multiple binding sites for Rab family G proteins. J Cell Biol 183, 607-615.
Sollner, T., Whiteheart, S.W., Brunner, M., Erdjument-Bromage, H., Geromanos, S., et al., 1993. SNAP receptors implicated in vesicle targeting and fusion. Nature 362, 318-324.
Sonnichsen, B., De Renzis, S., Nielsen, E., Rietdorf, J., Zerial, M., 2000. Distinct membrane domains on endosomes in the recycling pathway visualized by multicolor imaging of Rab4, Rab5, and Rab11. The Journal of cell biology

149, 901-914.
Sudhof, T.C., Rothman, J.E., 2009. Membrane fusion: grappling with SNARE and SM proteins. Science 323, 474-477.
Trucco, A., Polishchuk, R.S., Martella, O., Di Pentima, A., Fusella, A., et al., 2004. Secretory traffic triggers the formation of tubular continuities across Golgi sub-compartments. Nat Cell Biol 6, 1071-1081.
Tu, L., Tai, W.C., Chen, L., Banfield, D.K., 2008. Signal-mediated dynamic retention of glycosyltransferases in the Golgi. Science 321, 404-407.
van Meer, G., Voelker, D.R., Feigenson, G.W., 2008. Membrane lipids: where they are and how they behave. Nature reviews. Molecular cell biology 9, 112-124.
Volchuk, A., Amherdt, M., Ravazzola, M., Brugger, B., Rivera, V.M., et al., 2000. Megavesicles implicated in the rapid transport of intracisternal aggregates across the Golgi stack. Cell 102, 335-348.
Waters, M.G., Serafini, T., Rothman, J.E., 1991. 'Coatomer': a cytosolic protein complex containing subunits of non-clathrin-coated Golgi transport vesicles. Nature 349, 248-251.
Watson, P.J., Frigerio, G., Collins, B.M., Duden, R., Owen, D.J., 2004. Gamma-COP appendage domain - structure and function. Traffic 5, 79-88.
Wegmann, D., Hess, P., Baier, C., Wieland, F.T., Reinhard, C., 2004. Novel Isotypic / Subunits Reveal Three Coatomer Complexes in Mammals. Mol Cell Biol 24, 1070-1080.
Weidman, P., Roth, R., Heuser, J., 1993. Golgi membrane dynamics imaged by freeze-etch electron microscopy: views of different membrane coatings involved in tubulation versus vesiculation. Cell 75, 123-133.
Yang, J.S., Valente, C., Polishchuk, R.S., Turacchio, G., Layre, E., et al., 2011. COPI acts in both vesicular and tubular transport. Nat Cell Biol 13, 996-1003.

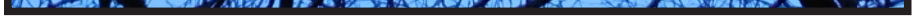

Chapter 7

Summary, general discussion and concluding remarks

Summary, general discussion and concluding remarks

Summary

In this thesis, we have mainly addressed the stress response to amino-acid starvation using Drosophila S2 cells. This response results in major changes of the cellular architecture; among them a dramatic remodeling of the ERES into a novel non-membrane bound cytoplasmic stress assemblies with liquid droplets properties, the Sec body (**Chapter 2**). In **Chapter 3**, we have identified the mono ADP-ribose dPARP16 as an essential component of the signaling cascade stimulated by amino-acid starvation. dPARP16, mono-ADP-ribosylates the key ERES component Sec16, an event necessary and sufficient to induce Sec body formation.

Amino-acid starvation leads to the simultaneous formation of another stress assembly, the stress granule (**Chapter 4**). Here we show that the concerted activity of both the mono-ADP-ribose dPARP16 and the poly-ADP-ribose dPARP1 are needed to elicit stress granule formation, with the remarkable finding that dPARP1 localizes at the cytoplasm upon amino-acid starvation and that this localization depends on dPARP16.

Furthermore, in **Chapter 5** we find that surprisingly, Sec16 is also necessary for stress granule formation upon amino-acid starvation. This is because it interacts and stabilizes the RNA-binding protein and G3BP ortholog Rasputin. G3BP and Rasputin are essential for stress granule formation in mammalian and Drosophila cells respectively. However, upon many stresses such as heat shock or arsenite, it is the de-phosphorylated form that is active in stress granule formation. In contrast, upon amino-acid starvation the active form is the phosphorylated.

Mesoscale protein assembly formation such as Stress Granules, P-bodies or Sec bodies, among others (see introduction) is emerging as a general response to stress, and is gaining increasing attention (Hyman and Brangwynne, 2011; Wilson and Gitai, 2013).

On one hand, in this thesis, we have unraveled novel mechanisms required for the formation of stress assemblies upon amino-acid starvation. On the other hand, we have also unveiled some similarities and differences for the formation of these assemblies depending of their content and the given stress.

Stress assemblies: good or noxious?

Non-membrane bound protein assemblies can confer rapid compartmentalization, giving an advantage in order to maintain cellular homeostasis upon challenging conditions. In this regard, in **Chapter 2,** we demonstrated that Sec bodies confer a fitness advantage to the starved cells by preserving ERES components. This

preservation ensures that the secretory pathway can resume its function once the stress is relieved, in order to support and continue cell growth and proliferation. However, some stress assemblies can become dysfunctional as they become irreversible and therefore toxic for the cell, leading to pathologies such as many neurodegenerative diseases including ALS and laminopathies (Monahan et al., 2016; Ramaswami et al., 2013). So far Sec bodies have not been linked to pathologies or toxicity, but further investigation needs to be done in this aspect.

Amino-acid starvation of Drosophila S2 cells is an acute and atypical stress.

Amino-acid starvation of Drosophila S2 cells appears to result in an acute and atypical stress response. Not only does it lead to the dramatic cytoplasmic re-arrangements we have reported, but also it displays two additional remarkable features.

First, these cytoplasmic re-arrangements are not under the control of mammalian target of rapamycin complex I (mTORC1). This is surprising as mTORC1 has been established as the major pathway that is controlled by the scarcity of essential nutrients, like amino-acids. Usually nutrient scarcity is sensed by mTORC1 leading to its inactivation (Wek et al., 2006). Consequently, suppressed mTORC1 signaling triggers activation of the autophagy pathway (He and Klionsky, 2009) which helps to recycle amino-acids and re-supply the cell.

In contrast, we have observed that during the formation of Sec bodies and stress granules upon amino-acid starvation in Drosophila, TORC1 inhibition does not play any role. As expected, autophagy is activated but this response precedes the formation of stress assemblies. We have also shown that pharmacological inhibition of autophagy leads to the premature formation of Sec bodies. This suggests that the two responses are separated in time and are under the control of different pathways (**Chapter 2**).

The second special feature is the activation of dPARP16 by amino-acid starvation that we have shown is essential for Sec body formation (**Chapter 3**). In mammalian cells, PARP16 is activated via auto-MARylation that is triggered by ER stress using DTT and Thapsigargin (Jwa and Chang, 2012). As a result of its activation, PARP16 MARylates two kinases at the ER, Ire1 and PERK (Gardner et al., 2013; Jwa and Chang, 2012), leading to the full activation of the unfolded Protein Response (UPR). As dPARP16 shares many features with its human counterpart, in principle ER stress on its own should lead to Sec body formation. However, we have previously shown (Zacharogianni et al., 2014) (and our unpublished results) that inducing ER stress does not lead to Sec body formation, and it does not affect cell survival as much as amino-acid starvation does **(Chapter 3, Suppl. Figures)**.

However, amino-acid starvation seems to lead to ER stress. As, we have observed some of the typical ER stress features such as, XBP1 splicing (van Schadewijk et al., 2012) (and our unpublished results). This therefore suggests that additional stress

signals are generated during amino-acid starvation making it a very complex stress. Alternatively, this nutrient stress could represent an acute version of the typical ER stress response. These hypothesis are under investigation.

Is dPARP16 Marylation just the tip of the iceberg?

Several liquid droplets have been described to form through weak protein-RNA interactions. However, to the best of our investigations, Sec bodies do not contain RNAs, suggesting that their components may establish protein-protein interactions, probably assisted by molecular modifications, such as MARylation. In **Chapter 3,** we have monitored MARylation in real time by using a specific MARylation detection probe (MAD) that we have designed and built. This probe allows the visualization of an unprecedented display of MARylation events upon amino-acid starvation. Interestingly, the amino-acid starvation driven MAD pattern is abrogated upon depletion of dPARP16.

Furthermore, we have demonstrated that dPARP16 is necessary and sufficient for Sec body formation and cell survival upon amino-acid starvation. This makes dPARP16 a key enzyme to specifically cope with amino-acid starvation, as the viability of dPARP16-depleted cells kept in full medium is not compromised.

Interestingly, dPARP16 is lowly expressed, at least at the transcriptional level, suggesting that its protein level is also low. In line with this, dPARP16 moderate overexpression in growing cells elicit MARylation events that are detected by the probe MAD, suggesting that dPARP16 overexpression leads to its activation **(Chapter 3)**.

However, if dPARP16 transcription levels are so low, why do we observe such a strong activation of MARylation events upon amino-acid starvation? Three possibilities rise to address this question. The first is that once dPARP16 is activated, its catalytic activity is very high. Second, in addition to Sec16, it probably has many more substrates. The third possibility is that dPARP16 is an upstream initiator triggering MARylation events that activate downstream mono-ADP-ribosylation enzymes such as SIRT proteins that are also present in Drosophila. This remains to be investigated.

MARylation and Parylation: a cross-link path for stress granule assembly.

Furthermore **in Chapter 4,** we add a layer of complexity to stress granule formation as we propose an interesting cross-link between MARylation and PARylation. In this regard, our results strongly suggest that both processes are required for stress granule formation upon amino-acid starvation. We demonstrate that both the mono-ADP-ribosylation enzyme dPARP16 and the poly-ADP-ribosylation enzyme dPARP1 are necessary for stress granule formation.

dPARP1 is strictly nuclear due to its NLS. However, we have observe that to exert its role in stress granule formation upon amino-acid starvation, dPARP1 has to be localized in the cytoplasm. How a nuclear resident like dPARP1 shuttles out of the nucleus remains to be elucidated. One possibility is that dPARP1 is exported out of the nucleus assisted by a nuclear exporter such as Karyopherin beta 3. This is a strong candidate for dPARP1 export, as it is possibly a dPARP16 substrate, linking both processes. Furthermore, Karyopherin beta 3 also seems to interact with Sec16.

What about Sec bodies in mammals?

Overall, PARPs with predicted MARylation activity are very abundant in the mammalian genome (14 out of the 17 PARPs are predicted to be MARylation enzymes). Therefore it is possible that many of them are involved in the formation of stress assemblies upon different stresses, during specific biological processes and substrates. However, so far, we have not observed large Sec bodies in mammalian cells upon similar conditions used for Drosophila, although a remodeling of the early secretory pathway was observed **(Chapter 2)**. Therefore, further studies of the signaling pathways involved in Sec body formation need to be performed. This would allow us to modulate the necessary conditions to trigger their formation to identified and study the enzymes and pathways involved in this stress response in mammalian cells.

Sec16, an intrinsically disordered protein with versatile function in stress.

Sec16 is a known factor in organizing ERES (Sprangers and Rabouille, 2015). Remarkably, Sec16 is largely disordered, especially at its N and C terminus, leaving only the central domain (about 1/3 of the protein) typically folded. Intrinsically disorder proteins (IDPs) can function without having an ordered 3D-structure (Dunker et al., 2001; Wright and Dyson, 1999), and have been described as evolved proteins that are capable to fold and function within a highly crowded medium, in a very limited available space (Zimmerman and Minton, 1993; Zimmerman and Trach, 1991). Numerous studies have analyzed the behavior of IDPs in natural or artificially crowded environments, and based on their response they have been grouped into two classes, foldable and non-foldable (Kuznetsova et al., 2014). Crowding-foldable IDPs can gain structure in a crowded environment, probably via a hydrophobic core, whereas crowding non-foldable IDPs remain mostly unstructured (or even become more disordered) under crowded conditions (Uversky, 2017). Which of these is the case for Sec16 remains to be elucidated.

IDPs have been shown to be prone to aggregation, especially upon stress conditions (Uversky, 2017). This is the case for Tia1, a key IDP necessary and sufficient for stress granule formation in mammalian cells (Gilks et al., 2004). As mentioned above,

Sec bodies are comprise of COPII subunits, and Sec16 that acts as the upstream ERES organizer. However, the small GTPase Sar1 is not incorporated. Interestingly, in contrast with the other ERES components and particularly Sec24 and Sec16 (**Chapter 2**), Sar1 is not an IDP.

In this regard, we have shown that the intrinsically disorder domain of Sec24 is sufficient and necessary to induce Sec body incorporation upon amino-acid starvation (**Chapter 2**). Nonetheless, it is not sufficient to induce Sec body formation in steady conditions, indicating, that Sec body formation requires additional layers of regulation such as post-translational protein modifications (see MARylation above). Whether Sec24 is also MArylated remains to be investigated.

During the response to amino-acid starvation, we have observed a high degree of functional versatility in Sec16. First, it is a key element in Sec body formation **(Chapters 2 and 3**) especially as a substrate of dPARP16 on its starvation response conserved domain.

The versatility of this protein is further demonstrated with its role in stress granules formation specifically upon amino-acid starvation. As, it interacts with the phosphorylated form of Rasputin (on Ser142) and stabilizes it. Phospho-Rasputin is the form that is required for stress granule formation specifically upon amino-acid starvation. In contrast, Sec16 does not interact with non-phosphorylated-Rasputin that is the form required for stress granule formation upon arsenate in Drosophila **(Chapter 5)** and in mammalian cells (Kedersha et al., 2016; Tourriere et al., 2003). As Sec16 is specifically MARylated upon amino-acid starvation by dPARP16 (Aguilera-Gomez et al., 2016), it is well possible that this modification is instrumental in the binding of Sec16 to phosphor-Rasputin. However this remains to be further investigated.

Remarkably, we show that Rasputin is differentially recruited to stress granules upon arsenate and amino-acid starvation, and that this recruitment depends of its phosphorylation state. This further demonstrates that stress granules are more complex, variable, and not just a temporal storage of stalled mRNPs. This is also reflected by the fact that stress granules contain diverse proteomes and RNAs (Jain et al., 2016). What determines the use for phosphor-Rasputin versus non-phospho-Rasputin in stress granule formation upon different stresses remains unknown. However, it is possible that stress granule components are differentially recruited accordingly to the protective necessities dictated by the type of stress. If this is the case, Sec16 interaction with phosphor-Rasputin could lead to the sequestration and protection inside amino-acid starvation triggered stress granules of mRNAs encoding secretory pathway components and/or ER translated mRNAs (possibly encoding secretory proteins required in stress recovery). Another possibility is that Sec16 interaction with stress granule components restricts stress granule formation to specific cellular sites. This remains to be investigated.

Intra-Golgi transport: a long term paradigm.

In **chapter 6**, we offer a view of the current models that have been proposed for intra-Golgi transport. Over the period of several decades, a lot of work has been done aiming to understand how cells transport newly synthesized proteins from the endoplasmic reticulum to their final cellular destinations. However, although microscopy and technological progress has been made and more experiments in several cellular models performed, a general consensus is still far from being achieved. One of the reasons for this excess of scenarios (each of them supported by strong experimental evidence), can be the fundamental biological differences and needs for each experimental model as they may require different cargo types and growing conditions. Another reason is that morpho-functional questions have proven to be very difficult to address technically and experimentally.

One alternative to approach difficult questions could be the development of assays to deliver polypeptides, such a dominant negative mutants or specific protein domains, onto intracellular targets (Wadia and Dowdy, 2002). This would allow the study of traffic molecules *in vivo*. Interestingly, post-genomic methods are starting to gain a major role (Drees et al., 2001; Wu et al., 2004), allowing the identification of traffic-associated molecules, as well as their maps of physical and functional interactions. Therefore, the integration between such genomic methods and new morphological assays will provide a great advance over the next decade towards a more coherent representation of the *in vivo* physiology of secretory transport.

At last, since all the models of intra-Golgi transport are center on the COPI machinery and the role of COPI coated vesicles. It would be interesting to address how COPI subunits react upon stress and whether they are as well as COPII subunits protected into stress assemblies.

References

Aguilera-Gomez, A., van Oorschot, M.M., Veenendaal, T., Rabouille, C., 2016. In vivo vizualisation of mono-ADP-ribosylation by dPARP16 upon amino-acid starvation. Elife 5.
Drees, B.L., Sundin, B., Brazeau, E., Caviston, J.P., Chen, G.C., et al., 2001. A protein interaction map for cell polarity development. J Cell Biol 154, 549-571.
Dunker, A.K., Lawson, J.D., Brown, C.J., Williams, R.M., Romero, P., et al., 2001. Intrinsically disordered protein. J Mol Graph Model 19, 26-59.
Gardner, B.M., Pincus, D., Gotthardt, K., Gallagher, C.M., Walter, P., 2013. Endoplasmic reticulum stress sensing in the unfolded protein response. Cold Spring Harb Perspect Biol 5, a013169.
Gilks, N., Kedersha, N., Ayodele, M., Shen, L., Stoecklin, G., et al., 2004. Stress granule assembly is mediated by prion-like aggregation of TIA-1. Mol Biol Cell 15, 5383-5398.
He, C., Klionsky, D.J., 2009. Regulation mechanisms and signaling pathways of autophagy. Annu Rev Genet 43, 67-93.
Hyman, A.A., Brangwynne, C.P., 2011. Beyond stereospecificity: liquids and mesoscale organization of cytoplasm. Dev Cell 21, 14-16.
Jain, S., Wheeler, J.R., Walters, R.W., Agrawal, A., Barsic, A., et al., 2016. ATPase-Modulated Stress Granules Contain a Diverse Proteome and Substructure. Cell 164, 487-498.

Jwa, M., Chang, P., 2012. PARP16 is a tail-anchored endoplasmic reticulum protein required for the PERK- and IRE1alpha-mediated unfolded protein response. Nat Cell Biol 14, 1223-1230.
Kedersha, N., Panas, M.D., Achorn, C.A., Lyons, S., Tisdale, S., et al., 2016. G3BP-Caprin1-USP10 complexes mediate stress granule condensation and associate with 40S subunits. J Cell Biol 212, 845-860.
Kuznetsova, I.M., Turoverov, K.K., Uversky, V.N., 2014. What macromolecular crowding can do to a protein. Int J Mol Sci 15, 23090-23140.
Monahan, Z., Shewmaker, F., Pandey, U.B., 2016. Stress granules at the intersection of autophagy and ALS. Brain Res 1649, 189-200.
Ramaswami, M., Taylor, J.P., Parker, R., 2013. Altered ribostasis: RNA-protein granules in degenerative disorders. Cell 154, 727-736.
Sprangers, J., Rabouille, C., 2015. SEC16 in COPII coat dynamics at ER exit sites. Biochem Soc Trans 43, 97-103.
Tourriere, H., Chebli, K., Zekri, L., Courselaud, B., Blanchard, J.M., et al., 2003. The RasGAP-associated endoribonuclease G3BP assembles stress granules. J Cell Biol 160, 823-831.
Uversky, V.N., 2017. How to Predict Disorder in a Protein of Interest. Methods Mol Biol 1484, 137-158.
van Schadewijk, A., van't Wout, E.F., Stolk, J., Hiemstra, P.S., 2012. A quantitative method for detection of spliced X-box binding protein-1 (XBP1) mRNA as a measure of endoplasmic reticulum (ER) stress. Cell Stress Chaperones 17, 275-279.
Wadia, J.S., Dowdy, S.F., 2002. Protein transduction technology. Curr Opin Biotechnol 13, 52-56.
Wek, R.C., Jiang, H.Y., Anthony, T.G., 2006. Coping with stress: eIF2 kinases and translational control. Biochem Soc Trans 34, 7-11.
Wilson, M.Z., Gitai, Z., 2013. Beyond the cytoskeleton: mesoscale assemblies and their function in spatial organization. Curr Opin Microbiol 16, 177-183.
Wright, P.E., Dyson, H.J., 1999. Intrinsically unstructured proteins: re-assessing the protein structure-function paradigm. J Mol Biol 293, 321-331.
Wu, C.C., MacCoss, M.J., Mardones, G., Finnigan, C., Mogelsvang, S., et al., 2004. Organellar proteomics reveals Golgi arginine dimethylation. Mol Biol Cell 15, 2907-2919.
Zacharogianni, M., Aguilera Gomez, A., Veenendaal, T., Smout, J., Rabouille, C., 2014. A stress assembly that confers cell viability by preserving ERES components during amino-acid starvation. Elife 3.
Zimmerman, S.B., Minton, A.P., 1993. Macromolecular crowding: biochemical, biophysical, and physiological consequences. Annu Rev Biophys Biomol Struct 22, 27-65.
Zimmerman, S.B., Trach, S.O., 1991. Estimation of macromolecule concentrations and excluded volume effects for the cytoplasm of Escherichia coli. J Mol Biol 222, 599-620.

Chapter 8

Addendum

Nederlandse samenvatting

Organel membraan-compartimentalisatie is een belangrijke karakteristiek van cellen, daar dit bijdraagt om ze georganiseerd te houden. Recent is er een nieuw concept met betrekking tot compartimentalisatie geïntroduceerd betreffende niet membraan gebonden complexen. Deze complexen zonder membraan zijn in de meeste gevallen het resultaat van diverse stres condities. In dit proefschrift worden de effecten van stres responses tot een tekort aan aminozuren in de cel op de secretie route beschreven. Opmerkelijk is dat deze nutriënten stres resulteert in de vorming van twee complexen zonder membranen, de Sec aggregaten en de Stres korrels.

In **hoofdstuk 1** wordt een overzicht gegeven van de opbouw en het functioneren van de eiwitsecretie route, waarbij we extra aandacht besteden aan de vorming van COPII structuren bij de ER uitgangslocaties. Deze vorming wordt georganiseerd door het scaffolding eiwit Sec16 wat interacteert met de meeste COPII componenten. Tevens wordt het effect van verschillende vormen van stres in de cel en de daarbij behorende regulering beschreven, gevolgd door een overzicht van een aantal stres aggregaten.

In **hoofdstuk 2** bestuderen we de ERES componenten onder een tekort aan aminozuren in de cel. Deze vorm van nutriënten stres zorgt voor halt van eiwitsecretie en resulteert in vorming van een nieuw type stres assemblage, het Sec aggregaat. Dit assemblage slaat ERES componenten zoals COPII eiwitten en Sec16 op, en beschermt deze voor afbraak. Belangrijk hier te vermelden is dat het Sec aggregaat kan worden teruggedraaid als de stres voorbij is wat ervoor zorgt dat de cel door de snelle herinitiatie van de eiwitsecretie betere overlevingskansen heeft.

In **hoofdstuk 3** worden de post-translationele modificaties; Mono en Poly-ADP-ribosilatie *in vivo* bestuurd. Hiervoor hebben wij specifieke fluorescerende probes ontworpen en gemaakt voor het detecteren van MARylatie (MAD) en PARylatie (PAD). Door gebruik te maken van MAD hebben wij aangetoond dat MARylatie door mono-ADP-ribose dPARP16 een cruciale rol speelt bij het vormen van Sec aggregaten, dit door modificatie van het Sec aggregaat component Sec16 op een specifieke sequentie in zijn C-terminus. Modificatie van Sec16 door dPARP16 is essentieel en voldoende om het vormen van Sec aggregaten te initiëren en het verhoogd de overlevingskansen van de cel onder een tekort aan aminozuren.

In **hoofdstuk 4** worden de mechanismen achter de vorming van stres korrels onder een tekort aan aminozuren in de cel bestudeerd. Hier vinden wij dat mono-ADP-ribosilatie door dPARP16 essentieel is maar op zichzelf niet voldoende om de vorming te initiëren. Onze data suggereert ook een rol voor poly-ADP-ribosilatie,

waarbij interessant genoeg, lokalisatie van dPARP1 in het cytoplasma vereist is. Een mogelijke link met dPARP16 is tevens beschreven waarbij lokalisatie van dPARP1 in het cytoplasma afhankelijk is van dPARP16. Mogelijk speelt in dit proces de mono-ADP-ribosilatie van het kern export eiwit Karyopherin beta 3 door dPARP16 een rol. Deze resultaten geven een link aan tussen de stres respons van het eiwit secretie mechanisme, export uit de kern en de translatie turnover tijdens een tekort aan aminozuren in de cel.

In **hoofdstuk 5** bestuderen we de rol van Sec16 in de vorming van stres korrels tijdens een tekort aan aminozuren in de cel. Met behulp van massaspectrometrie en een plasmamembraan "anchor-away" techniek tonen we aan dat Sec16 specifiek interacteert met de gephosphoryleerde Ser-142 van het RNA bindingseiwit en stres korrel component Rasputin. Verder demonstreren wij dat Ser-142 phosphorylering van Rasputin exclusief noodzakelijk is voor stres korrel formatie tijdens een tekort aan aminozuren in de cel. Deze resultaten bekrachtigen de essentie van Sec16 als een stres responsief eiwit onder een tekort aan aminozuren.

Als laatste gaan we in **hoofdstuk 6** dieper in op het onderzoek aan de secretie route. We geven een overzicht van de meeste recente modellen uit het veld die de anterograad secretie route door de secretie route beschrijven. Echter is er nog steeds geen overeenstemming over hoe nieuw gesynthetiseerde eiwitten door het Golgi apparaat worden vervoerd en dit tevens met behoud van de structurele integriteit van het organel.

In **hoofdstuk 7** bediscussiëren we onze bevindingen en suggereren directies voor toekomstig onderzoek.

List of publications

Zacharogianni M, **Aguilera-Gomez A**, Veenendaal T, Smout J, Rabouille C. 2014. A stress assembly that confers cell viability by preserving ERES components during amino-acid starvation. **eLife.** 3:e04132.

Jevtov I, Zacharogianni M, van Oorschot MM, van Zadelhoff G, **Aguilera-Gomez A**, Vuillez I, Braakman I, Hafen E, Stocker H, Rabouille C. 2015. TORC2 mediates the heat stress response in Drosophila by promoting the formation of stress granules. **J Cell Sci**. 128:2497-508. doi: 10.1242/jcs.168724.

Aguilera-Gomez A and Rabouille C. 2016. Intra-Golgi Transport. In: Ralph A Bradshaw and Philip D Stahl (Editors-in-Chief), **Encyclopedia of Cell Biology**, Vol 2, Waltham, MA: Academic Press, pp. 354-362.

Aguilera-Gomez A, van Oorschot MM, Veenendaal T, Rabouille C. 2016. *In vivo* visualization of Mono-ADP-ribosylation by dPARP16 upon amino-acid starvation. **eLife**. 5:e21475.

Aguilera-Gomez A, Zacharogianni M, Oorschot MM, Genau H, Veenendaal T, Sinsimer KS, Gavis EA, Behrends C and Rabouille C. 2017. Phospho-Rasputin stabilization by Sec16 is required for stress granule formation upon amino-acid starvation. **Submitted to Cell reports.**

Aguilera-Gomez A and Rabouille C. 2017. Membrane-less compartments and the control of anabolic pathways. Review. **Developmental Biology.**

Acknowledgements

After these four years of doing a PhD I believe I have truly succeeded. Yes indeed what a great success I am ;). I have struggled for a while and was in denial when confronting the face of my raw reality. Not only because I realized (in a hard way) how few I actually know, but also because I am leaving with a really big dossier of questions for which I would need more than a great imagination to even formulate a possible answer.

Fortunately, one of those good days in between the insufferable ones (and luckily it happened sooner than later) I got hit by the sudden realization and almost almighty experience that this PhD venture has presented me a precious opportunity: "the gift of Wonder", so from then on and disentangled of all guiltiness, I have proclaimed myself "a professional wonderer"…. Isn't this truly exciting? What else could I have wished for?

This journey I have made accompanied by many people that in all humbleness I would like to acknowledge.

Thanks a lot to my promotor **Prof. A. van Oudenaarden** for his really useful remarks during the PhD evaluation meetings. Thanks to all the members of the assessment committee **Prof. M. Maurice**, **Prof. G. Kops**, **Prof. R. Korswagen**, **Prof. F. Reggiori**, **Dr. G.J.T.Zwartkruis** and **Dr. P. van der Sluijs** for taking the time to read and comment upon my thesis. Thanks to **Annemiek van Rooijen** for helping me with the arrangements around my thesis preparation and defense.

To my supervisor **Catherine Rabouille**, I am grateful for the attention and time you have invested in helping me to build and materialize my research goals. Working in your lab has been a very challenging experience that for sure has provided me with several tools to continue my professional growth. I wish you lots of moments of mind stillness and fulfilling happiness. And of course, in the rare case you get to miss my "stratospheric ideas" I will always be happy to provide one or two.

I still remember the early members of the Rabouille group that welcomed and introduced me to the lab and Hubrecht life in their unique way: **Adam** with your dark and smart sense of humor that made me laugh and kept me distracted, the funny, intelligent twins **Fabrizio** and **Gulianno** with your graceful choreographies always stealing the show, **Margarita** with your little lab dictatorship trying to keep us in line and the generous **Tineke** always willing to listen and help; many thanks to you all guys. **Nerys** and **Pili** thank you for all the good moments we spend in preparation of the weddings and also for the fruitful conversations we have shared.

Marinke, I especially want to thank for sharing the lab with me during the last three years with your characteristic kindness and caring and overall thank you just for your presence that brought a sort of stillness in my everyday as a remainder of the humanity and compassion that many people tend to forget in their frantic of doing. So, dear friend let's keep sharing our love for dogs and walks **:)**.

To the students **Jan**, **Joep**, **Alexandro** and **Marloes** thanks for being brave, enthusiastic, bringing into the lab fresh ideas and doing always the best you could. To the newest members of the group **Amalia** and **Rianne**, I wish you a lot of strength and success to achieve your goals.

Thanks a lot to all the members of the Van Rooij group particularly, **Charlotte**, **Hesther**, **Marta**, **Brian**… dear **Bas,** keep going, you are a very smart genuine guy (and again NOT I DON'T have and never will have the white stuff you seem so interested in!!). My dear friend **Moniii,** we have shared so many childish, crazy fun moments and ridiculous laughs, I always enjoy to have you around, I also admire you a lot …but please it is also good to learn decent Spanish words!

Ciao **Roberto** thanks a lot for all the conversations about the present, future and off course science. **Juni** always gentle and open ears, you know I only have the best wishes for this new stage in your life "being a mommy" **Zunamys** que refrescante conocerte y tenerte alrededor, eres una persona muy inteligente y valiente, estoy segura que vas a conseguir todo lo que te propones, sigue adelante con positivismo, ya veras como todo se te dara de la mejor manera.

Orale! Christian gracias por ser tan buena persona, siempre atento a escuchar y ayudar, eres un trabajador incansable y mereces toda mi admiracion, sigue adelante, no tengo dudas de que vas a cumplir todas tus metas, tambien te pido disculpas por todos los chistes malos del chavo pero es que se me "chispotean".

Jelmer Thank you for all your "do the little dance", at the end I never knew the rhythm but anyway I never care, it just looks gracious. Please keep up this good vibe you have. I am so glad you and Marloes found each other just because of the tremendous affinity you both share for orange candies… what an epical love story! Wish you both lots of happiness, take care of each other!

Well I really could go on filling pages of acknowledgments since this institute is packed with amazingly nice people… Thanks to all my neighbors with whom I could not resist to have a halfway chat about life, science, past, present or future Particularly in the Den Hertog group **Alexander** and **Sasja**, the Bakkers group, **Fabian**, **Federico** and **Melanie** long afternoons at the microscope with **Laurence,** at the Laat group, **Erica**, **Carien**, in the Knipscheer group, **Nerea** and **Alice** and at the

Korswagen group, ciao **Lorenzo**, **Euclides** and **Annabel. Kim** I hope you get to have a dog soon, believe me you are missing lots of fun **:)**. Thanks a lot **Joris** and **Shilu** for sharing so many lunches, chats and laughs.

Of course among my Hubrecht most favorite people my charming paranimf **Roel**, thanks you for decorating my world everyday with your gentle smile and always super positive energy, it has been a real pleasure to have you around. I admire your passion for science and I am sure you will continue achieving everything you wish for at the professional level; at the personal level I wish you from the bottom of my heart a life full of happiness together with your beautiful family **Anne**, **Hanna and Mathieu**.

Dankbaar ben ik om het geluk te hebben om verwelkomt en opgenomen te zijn door de familie **van Verk**. Dank jullie allemaal voor het delen van zo vele belangrijke en mooie momenten gedurende al deze jaren. Speciaal wil ik bedanken mijn beste **oma Mol**, nu later in mijn leven heb ik eindelijk de warmte en liefde ervaren van een Oma… nouja beter laat dan nooit ;).

A mi **Padre**, quiero darle las gracias por haberme ensenado a dibujar, por haberme inculcado amor por la lectura, los libros y curiosidad por la cultura. A mi querida **Madre** quiero darle las gracias por haberme dado la libertad de ser y hacer todo lo que he querido. A mi **Tia** nene quiero darte las gracias por haberme cuidado, brindado atencion y ternura cuando tal vez mas lo necesite, tambien mil gracias por mostratrme como ser creativa, recursiva y trabajadora. A mi amado **hermano Raul** quiero decirle que lo extrano mucho cada hora del dia todos los dias.

And at last, but the best, my beloved husband **Marcel.** I have not enough words to express my gratitude. You are my home, my rock, we have grown so much together through these years that now I tend to believe when you tell me "the sky is the limit" …I just feel so blessed to have you in my life.

Thanks to life, for giving me **our treasured Son.** Yes, you have come to my life to fill it up with strength, joy and inspiration in a moment of most need… I cannot wait for the day I will get to kiss you and hold you in my arms… the most exciting blind date ever!!!

With love,

Angelica

Curriculum vitae

Her dog, Ossi

Angelica Aguilera Gomez enrolled in 2001 at the Military University "Nueva Granada" in Bogota Colombia. Besides her studies in biology and military disciplines she performed an in depth three-year training at the department of biotechnology. After her BSc graduation as biologist in 2007 she moved in 2009 to the Netherlands to join the master program molecular and cellular biosciences at Leiden University where she received her Master's degree in 2012.

In April 2013 she started her PhD research on the early secretory pathway under stress and during development in the laboratory of Catherine Rabouille at the Hubrecht Institute. The results of her research are described in this thesis.